

GEOCHEMICAL CYCLES OF THE ATMOPHILE ELEMENTS

ARSENIC AND ANTIMONY

by

Laurence Stuart Austin

B.Sc (Hons), M.Sc

Submitted to the Council for National Academic Awards in partial
fulfilment of the requirements for the degree of Doctor of Philosophy

Submitted August 1984

Department of Marine Science
Faculty of Maritime Studies
Plymouth Polytechnic
Plymouth
Devon
United Kingdom

In collaboration with:
School of Environmental Sciences
University of East Anglia
Norwich
East Anglia
United Kingdom

PLYMOUTH POLYTECHNIC
LIBRARY

Accn.
No.

5500186

Class.
No.

T 574.584 AUS"

Contl
No.

X 7005655.06

ACKNOWLEDGEMENTS

I gratefully acknowledge the assistance rendered by all those who have contributed to this project, in particular :

My supervisor, Dr G.E. Millward for his untiring encouragement and patience in all aspects of my work. Dr P. O'Neill for his supervision in laboratory work. Dr P.S. Liss for his useful discussions, especially in some aspects of the modelling.

Much of the sampling was carried out on board ship, and I would like to thank those who have contributed in this area : Mr Beshaw of Trinity House, Mr A. Fowler (the master) and crew of the Channel Light-vessel; Capt. Britten of the Meteorological Office, Capt. R. Rankin (the master) and crew of the M.V. "Starella"; Mr I. Butler of the M.B.A., Capt. M. Harding (the master) and crew of the R.V. "Frederick Russell". Technical support was received from the following :

Mr B. Davis and Mr R. Hill kept the sampling equipment in working order; Mr K. Pearson, and fellow technicians in chemistry, were most helpful in the laboratory; Mrs H. Serpell supplied some of the meteorological data; Mr B. Lakey and Mrs C. Tye gave much guidance on the electron microscope; Mr G. Bouch, and fellow members of the Polytechnic computer centre, patiently advised on my programming technique; and Mr R. Hartley of the L.R.C. opened up a vast store of reference material.

I would like to thank Dr D.H. Moreby, Capt. L.W.J. Fifield, and my friends and colleagues in the Faculties of Maritime Studies and Science for their interest and support.

Dr J.G. Marsh and Mr D.A. Russell both helped with hydride generation analyses. Mr J. Cleary and Mrs C. Goodchild made available, and assisted with the use of an SP9 spectrophotometer at IMER. Dr R.M. Harrison of Lancaster University provided useful criticism of the sampling method.

Mrs M. Warland typed the thesis with considerable care and patience.

GEOCHEMICAL CYCLES OF THE ATMOPHILE ELEMENTS ARSENIC AND ANTIMONY

by LAURENCE STUART AUSTIN, B.Sc.(Hons), M.Sc.

ABSTRACT

Atmospheric aerosol samples from coastal and open ocean environments in the North Atlantic were analysed for the atmophile elements arsenic and antimony, and for the marine tracers sodium and magnesium. The aerosol concentrations of sodium and magnesium were similar in both environments, about $2000 \text{ ng Na (SCM)}^{-1}$ and $320 \text{ ng Mg (SCM)}^{-1}$. The atmophiles were more concentrated in the coastal aerosol, $0.67 \text{ ng As (SCM)}^{-1}$ and $0.32 \text{ ng Sb (SCM)}^{-1}$, than in the open ocean aerosol, $0.07 \text{ ng As (SCM)}^{-1}$ and $0.086 \text{ ng Sb (SCM)}^{-1}$, and as continental particles were only observed in the coastal aerosol, this indicates that arsenic and antimony in the marine aerosol are of continental origin.

Total deposition fluxes to the North Atlantic were about 1.4 kt yr^{-1} for arsenic and antimony, and about 12 t As yr^{-1} and 5 t Sb yr^{-1} to the dissolved phase of the English Channel. Coastal deposition was higher than the dissolved element fluxes from the River Tamar.

From the above data, steady state models of the arsenic cycle were developed, and an anthropogenic perturbation rate was calibrated for kinetic analysis, to define the most sensitive areas of the geochemical cycle. Air-sea exchange exerts a major control on the atmospheric transport of pollutant arsenic to the sea, variations in river flow exert a minor influence. The major unknown factor in the biogeochemistry of arsenic is the size of the reservoir for low temperature anthropogenic mobilisation, as this has a larger long term effect than industrial pollutant input. Low temperature mobilisation may lead to a serious increase in the atmospheric arsenic burden.

The modelling technique was extended to quantify a novel tentative model for antimony, which was subject to limited examination by kinetic analysis. Again, air-sea exchange exerts a major influence on the atmospheric transport of pollutant antimony to the oceans, although river flow exerts a larger influence than for arsenic. Low temperature mobilisation may be even more significant for antimony than for arsenic.

CONTENTSPage No.

Title page	i
Acknowledgements	ii
Abstract	iv
Contents	v
List of Plates	viii
CHAPTER ONE. INTRODUCTION	1
1.1 Overview	2
1.2 The role of the atmosphere in geochemical cycles	3
1.2.1 The gaseous phase	3
1.2.2 The aerosol phase	5
1.2.2.1 The crustal aerosol	6
1.2.2.2 The marine aerosol	6
1.2.2.3 The anthropogenic aerosol	8
1.2.3 Trace elements in the atmosphere	9
1.3 The biogeochemistries of arsenic and antimony	12
1.3.1 Arsenic	12
1.3.1.1 Arsenic in the lithosphere	12
1.3.1.2 Arsenic in the hydrosphere	14
1.3.1.3 Arsenic in the atmosphere	17
1.3.1.4 Arsenic in the biosphere	21
1.3.2 Antimony	24
1.3.2.1 Antimony in the lithosphere	24
1.3.2.2 Antimony in the hydrosphere	25
1.3.2.3 Antimony in the atmosphere	26
1.3.2.4 Antimony in the biosphere	29
1.4 Geochemical models	31
1.4.1 The steady state	31
1.4.2 Kinetic modelling	33
1.5 Aims of the research programme	35
CHAPTER TWO. SAMPLING AND ANALYSIS OF THE ATMOSPHERIC AEROSOL	36
2.1 Sampling	37
2.1.1 Sampling methods	37
2.1.2 Sampling locations	40
2.2 Analytical methods	44
2.2.1 Electron microscopy	44
2.2.2 Choice of analytical technique	44
2.2.3 Sample preparation	45
2.2.3.1 Choice of preparative technique	45
2.2.3.2 Standardisation	47
2.2.3.3 Seawater leaching	49
2.2.4 Chemical analysis	50

CONTENTSPage No.

2.3 Analytical results	57
2.3.1 Electron microscopy	57
2.3.2 Chemical analysis	65
2.3.2.1 Environmental analysis	65
2.3.2.2 Seawater leaching	89
2.4 Discussion	95
2.4.1 The atmospheric aerosol	95
2.4.2 Flux calculations	98
2.4.2.1 Deposition from the atmosphere	98
2.4.2.2 Trans-coastal fluxes	105
2.4.2.3 Inter-hemisphere fluxes	106
CHAPTER THREE. MODELLING TECHNIQUES	109
3.1 Steady state modelling	110
3.1.1 Concepts for the basic model	110
3.1.2 Refinements to the basic model	115
3.2 Choice of parameters for modelling	120
3.3 Kinetic modelling	124
3.3.1 The environmental pollutant record	124
3.3.2 Modelling pollutant influences	125
3.3.2.1 High temperature processes	125
3.3.2.2 Low temperature processes	129
3.3.3 Computational techniques	131
CHAPTER FOUR. MODELS OF THE GEOCHEMICAL ARSENIC CYCLE	134
4.1 Steady state models	135
4.1.1 The basic model	135
4.1.1.1 The reservoirs	135
4.1.1.2 The fluxes	137
4.1.2 Subdivision of the ocean particulates	143
4.1.3 A heterogeneous troposphere	146
4.1.3.1 A model with a homogeneous particulate reservoir	146
4.1.3.2 Subdivision of the ocean particulates	150
4.1.4 The biosphere	154
4.1.4.1 The marine biosphere	154
4.1.4.2 The terrestrial biosphere	155
4.2 Kinetic modelling	159
4.2.1 The basic model	159
4.2.1.1 High temperature processes	159
4.2.1.2 Low temperature processes	167

<u>CONTENTS</u>	<u>Page No.</u>
4.2.2 The heterogeneous troposphere	175
4.2.3 The biosphere	184
4.2.3.1 First order kinetics	184
4.2.3.2 The effect of phosphorus	190
 CHAPTER FIVE. MODELS OF THE GEOCHEMICAL ANTIMONY CYCLE	 198
5.1 Steady State Models	199
5.1.1 The basic model	199
5.1.1.1 The reservoirs	199
5.1.1.2 The fluxes	201
5.1.2 The subdivision of the ocean particulates	209
5.1.3 The biospheres	210
5.1.3.1 The marine biosphere	210
5.1.3.2 The terrestrial biosphere	212
5.2 Kinetic modelling	216
5.2.1 The basic model	216
5.2.1.1 High temperature processes	216
5.2.1.2 Low temperature processes	221
5.2.2 The biospheres	229
 CHAPTER SIX. CONCLUSIONS	 232
6.1 General discussion	233
6.1.1 The atmospheric aerosol	233
6.1.1.1 Arsenic and antimony in the marine aerosol	233
6.1.1.2 Arsenic and antimony in the coastal aerosol	237
6.1.2 Models of geochemical cycles	240
6.1.2.1 The arsenic cycle	240
6.1.2.2 The antimony cycle	242
6.1.2.3 Comparison of arsenic with antimony	243
6.1.3 Overall conclusions	245
6.2 Recommendations for further work	247
 REFERENCES	 249
 APPENDICES	 A1
Appendix I Integration mathematics	A2
Appendix II The computer programme	A6

LIST OF PLATES

	<u>Facing page</u>
Plate 2.1 Electron micrographs of a combustion particle	58
Plate 2.2 Field of view shows a high particle density on a filter exposed during a temperature inversion over Plymouth. A number of possible combustion particles are present	58
Plate 2.3 Electron micrograph of a calcium sulphate particle	62
Plate 2.4 Electron micrograph of a potassium sulphate particle	62
Plate 2.5 Electron micrograph of a sodium chloride crystal, sampled over Ocean Station Lima	66
Plate 2.6 Electron micrograph of a particle of "millet-seed" morphology, sampled in the marine atmosphere over the English Channel	66
Plate 2.7 A siliceous test sampled from the aerosol 10 m above the sea surface	70

CHAPTER ONE

INTRODUCTION

1.1 OVERVIEW

Since the industrial revolution, mankind has been increasingly venting noxious substances into the atmosphere, through the growth of industrialisation and use of fossil fuels (Goldberg, 1971). As air-breathing animals cannot select which components of the atmosphere they breathe, such substances are readily incorporated into the biosphere, especially as biological uptake is more efficient via the lungs than via the gut (Natusch et al, 1974; Siegel et al, 1973b). Arsenic has long been recognised as a toxic substance, so its anthropogenic input to the atmosphere is of some concern (NAS, 1977). As antimony is chemically analogous to arsenic it is released to the atmosphere by many of the same industrial processes.

Atmospheric particulate matter is enriched in many trace elements, like arsenic and antimony, compared with tracers for crustal material, such as aluminium, or tracers for marine material, such as sodium. Such anomalously enriched trace elements are termed atmophiles. Pollutant transport of these elements to the atmosphere is usually more significant than pollutant transport by streams or rivers (Mackenzie and Wollast, 1977), so the atmospheric enrichment of these elements may be due to pollution (Hoffman et al, 1972). Indeed, Mackenzie and Wollast (1977) estimated that anthropogenic emissions account for 30% of the global deposition of arsenic from the atmosphere, and almost all the deposition of antimony. However, enrichment in remote pristine environments shows that natural volatilisation processes may also be important (Zoller et al, 1974).

The anthropogenic input of trace elements has been assessed on a local scale (Kowalczyk et al, 1982), but little predictive assessment has been made on a global scale. The aim of this work is to assess the behaviour of the atmophile elements arsenic and antimony, in the form of their biogeochemical cycles, as an aid to predicting the consequences of man's mobilisation of these elements.

1.2 THE ROLE OF THE ATMOSPHERE IN GEOCHEMICAL CYCLES

As this study is concerned with the geochemical cycles of two atmophile elements, the analytical work was concentrated on the assessment of their distribution in the atmospheric environment. The atmosphere is divided into three layers encasing the Earth. Only the innermost layer, the troposphere, will be considered in detail, as exchange between this and the stratosphere above is unimportant (Poet et al, 1972). The upper boundary of the troposphere, the tropopause, lies at a height between 10 km and 15 km, depending on the season (Mason, 1966). Below this, the atmosphere can be considered in terms of its two component phases, the gaseous phase and the aerosol phase.

1.2.1 The Gaseous Phase

The atmosphere consists predominantly of the gases nitrogen and oxygen, with some argon, carbon dioxide and numerous trace gases (table 1.1). To a first approximation, the troposphere is well mixed by convective circulation, although departure from the ratios apparent from table 1.1 may occur at high altitude, where gravity separation by molecular weight is an important influence on atmospheric composition. Many trace gases, however, are poorly mixed in the troposphere, especially if their residence time is shorter than the mixing time of the atmosphere. The concept of residence time (T) was first defined for components of the ocean (Goldberg, 1963) as the mass of a component in a reservoir (A), divided by its rate of removal from that reservoir (dA/dt) :

$$T = \frac{A}{dA/dt} \quad (1.1)$$

This should only be applied under steady state conditions, the rate of removal then being equal to the rate of introduction. A component can only be regarded as well-mixed in a reservoir if its residence time is at least

Table 1.1 Average Composition of the Atmosphere

Gas	Composition by volume (ppm)	Composition by weight (ppm)	Weight fraction (%)
N ₂	780 900	755 100	75.52
O ₂	209 500	231 500	23.15
Ar	9 300	12 800	1.28
CO ₂	300	460	0.05
Ne	18	12.5	< 0.01
He	5.2	0.72	< 0.01
CH ₄	1.5	0.94	< 0.01
Kr	1.0	2.90	< 0.01
N ₂ O	0.5	0.80	< 0.01
H ₂	0.5	0.035	< 0.01
O ₃ *	0.4	0.70	< 0.01
Xe	0.08	0.36	< 0.01

* Variable increases with height

After Mason (1966)

three times longer than the mixing time (Whitfield, 1979). Where multiple fluxes to or from a reservoir are considered, then dA/dt is the total influx rate from all sources, or total efflux rate by all mechanisms.

The removal rate (S) of a gas from the atmosphere is a function of its rate of chemical destruction (S_c), and its rate of removal to other environments (S_f) (Junge, 1974), such that :

$$S = S_c + S_f \quad (1.2)$$

Reactive gases, where the S_c term dominates, have short atmospheric residence times, like hydrogen sulphide, which undergoes oxidation in the atmosphere, and has a residence time of 0.1 yr. Gases which are soluble, as well as being reactive, have even shorter residence times. Such a gas is sulphur dioxide, which has a residence time of about 0.01 yr. In contrast, unreactive gases, where the S_f term dominates, have long atmospheric residence times, like helium with a residence time of about 2×10^6 yr (Horne, 1978). Although the volatile species of antimony in the atmosphere have not been identified, those of arsenic have a very short residence time, their removal dominated by the S_c term in equation 1.2 (Braman, 1984).

1.2.2 The Aerosol Phase

Junge (1963) defined an aerosol as "dispersed solid or liquid matter in a gaseous medium, in our case air. The particle size in the atmosphere ranges from clusters of a few molecules to particles of about 20 μm radius, if we disregard cloud, fog and raindrops, and consider only dry air". Like many trace gases, the aerosol is poorly mixed in the troposphere, decreasing in concentration with altitude (Woodcock, 1953), falling to the background level by 5 km over the continents, and by only 2 km over the oceans (Junge and Jaenicke, 1971). Aerosol material may be of crustal, marine or anthropogenic origin.

1.2.2.1 The crustal aerosol

The main component of the crustal aerosol is fine grained mineral dust of radius below 10 μm , although the distribution amongst particles less than 1 μm radius is poorly known. Particles smaller than 2 μm are composed of quartz, clay minerals and a little dolomite (very similar to the composition of deep sea clays); particles of radius greater than 2 μm are about 95% quartz with some feldspar (Junge, 1972). Larger particles, greater than 20 μm , are biologically derived, such as fungi or wax particles (Junge, 1972; Meszaros, 1977), although small biological particles, between 0.1 μm and 0.5 μm , are released from living vegetation by transpiration processes (Beauford et al, 1975 and 1977), and from vegetation undergoing aerobic decay (Schnell and Vali, 1972 and 1973). Forest fires form another source of biological particles, releasing "cokey spherules", which may enter the marine atmosphere, or fall to land to be ultimately washed to the sea (Griffin and Goldberg, 1975).

Crustal particles may also be derived from volcanism, which is largely responsible for the dust loading of the stratosphere (Bigg et al, 1972). Hammer (1977) suggested that particulate volcanic emissions are largely soluble, consisting primarily of sulphate species, mainly sulphuric acid and ammonium sulphate (Frank et al, 1972). Such sulphate species dominate the background aerosol in areas far removed from any obvious source (Junge, 1972; Junge and Jaenicke, 1971).

1.2.2.2 The marine aerosol

Aerosol concentrations are lower over the oceans than over the continents, the concentration of Aitken nuclei (condensation nuclei) is about 16000 N cm^{-3} (nuclei per cubic centimetre) over land, but only about 300 N cm^{-3} over the oceans (Halter and Robinson, 1977). The composition

of the marine aerosol also differs from that of the crustal aerosol, and is dominated by sodium chloride, with potassium, calcium and magnesium (Chesselet et al, 1972), although the mineral dust that dominates the crustal aerosol is still present in the marine aerosol (Chester, 1971). Potassium and calcium show enrichment in the marine aerosol over bulk seawater (Chesselet et al, 1972), although the evidence for magnesium is conflicting (compare Chesselet et al, 1972 with Duce et al, 1976).

Enrichments and depletions of major ions in the marine aerosol may be explained by fractionation in the aerosol formation process. The marine aerosol is formed by bubble rupture at the sea surface (Liss, 1975; MacIntyre, 1974), with two types of particle thus formed. The innermost layers of the bubble are ejected to form large jet drops, usually larger than 1 μm radius, while the collapse of the bubble film forms small film drops in the submicron range. The enrichments of major ions are due to the retention of the larger, heavier ions in the bubble film (Block and Luecke, 1972; Bloch et al, 1966). Ion enrichments that cannot be explained by this process may be caused by enrichment in the jet drops. Rising bubbles act as scavengers of surface active material, especially organic molecules, like polypeptides and humic acids, so the bubble surface may be enriched in organic matter by a factor of 2000 over bulk seawater (MacIntyre, 1974). Because the jet drops consist of the innermost surface of the bubble, they are enriched in any molecule or ion with surface active properties. The surface layer of the sea, the microlayer, which is also enriched in surfactants, probably acts as the major sink for jet drops and film drops falling back to the sea. The surface activity of the bubble film has been used to sample the surface microlayer material with a bubble microtome system (Duce et al, 1976; Wallace and Duce, 1978).

N.B. The non-marine aerosol is termed the continental aerosol throughout this work.

1.2.2.3 The anthropogenic aerosol

Aerosols of anthropogenic origin are derived from high temperature industrial processes and the burning of fossil fuels. Fossil fuel combustion releases particles of similar morphology to those of forest fires, and these have even been observed in the aerosol over the centre of the North Atlantic Ocean (Griffin, 1980; Parkin et al, 1970). Weiss and co-workers (1971) related a post-1952 increase in the sulphur content of a Greenland glacier to the burning of fossil fuels, and a similar increase in mercury was also attributed to man's activities (Bertine and Goldberg, 1971; Weiss et al, 1975). Patterson and coworkers (1976) attributed high atmospheric concentrations of lead to tetraethyl lead in petrol, and high atmospheric concentrations of vanadium were attributed to the burning of oils containing vanadyl porphyrins (Duce and Hoffman, 1976; Hoffman et al, 1972). Although vanadium has been recommended as a tracer for anthropogenic aerosols in the marine atmosphere, Chester and coworkers (1984a) have suggested the use of magnetic spherules, which are not generated by passing ships, unlike oil combustion products.

Smelters are a major anthropogenic source of atmophile elements like arsenic and antimony (Creceius, 1975), and atmospheric transport of aerosol lead, zinc and cadmium has been observed from a lead smelter at Avonmouth, England (Burkitt et al, 1972). When such aerosol emissions occur, the volatile elements are often concentrated on the particle surface (Linton et al, 1976), suggesting that these elements are adsorbed onto the ambient aerosol from the vapour phase formed by the high temperatures. As a result, there is an increase in atmophile concentration with decreasing particle size (Creceius, 1980). However, the extent to which surface adsorption may be important is still unclear. There is little information on the surface activity of particles, although some may have large surface areas,

like combustion particles that have a honeycombed morphology. If the surface activity of such particles is large, then there is a large capacity for the transport of surface-bound trace elements.

1.2.3 Trace Elements in the Atmosphere

The composition of aerosols collected on land is usually compared with that of crustal rocks, normalising against aluminium, or occasionally iron or scandium; aerosols collected at sea are usually compared with seawater composition, normalising against sodium. The atmophile elements are those that are anomalously enriched compared with their crustal or seawater concentrations. Enrichments are expressed as enrichment factors, either EF_{crust} or EF_{ocean} , which are defined for a trace constituent, X, as :

$$EF_{\text{crust}} = \frac{(\text{Concentration of X/concentration of Al})_{\text{aerosol}}}{(\text{Concentration of X/concentration of Al})_{\text{crust}}} \quad (1.3)$$

and for oceanic enrichment factors :

$$EF_{\text{ocean}} = \frac{(\text{Concentration of X/concentration of Na})_{\text{aerosol}}}{(\text{Concentration of X/concentration of Na})_{\text{seawater}}} \quad (1.4)$$

Some authors (see for example : Liss, 1975; MacIntyre, 1974) refer to the above quantities as the crustal or oceanic fractionation, and then define the enrichment factor as :

$$EF = \text{fractionation} - 1 \quad (1.5)$$

For atmophile elements, with enrichment factors as high as 10^5 , the difference between the enrichment factor and the fractionation is insignificant, but not so for elements such as magnesium, that are not highly enriched in the atmosphere. In this work, oceanic enrichment factors have been determined according to equation 1.4. The use of enrichment factors

has been criticised, as variations in the enrichment factor may be due to variations in the reference element, not variations in the atmosphere element concentration (Adams et al, 1980a). Atmosphere elements may be associated with the background aerosol of small particle size, variations in enrichment factors simply a mixing effect between the background aerosol and reference material. This has given rise to the concept of the C_{min} , the minimum background concentration of an atmosphere element at any sampling site (Adams et al, 1980a; Chester et al, 1983). For this reason, only the average enrichment factor at each site has been extensively discussed in this work, and variability within a site has been given little attention.

High enrichment factors have been observed for atmosphere elements in the continental aerosol (see for example: Adams et al, 1977), the marine aerosol (see for example : Duce et al, 1976), and even in the aerosol in such remote regions as the Antarctic (Zoller et al, 1974). As enrichment factors are high in remote areas, natural processes like volcanic degassing have been evoked to explain atmospheric enrichment (Duce et al, 1975), which is no longer considered to be an effect of pollution alone. The sea surface microlayer also shows high enrichments of atmosphere elements (Barker and Zeitlin, 1972; Duce et al, 1972; Szekiolda et al, 1972). However, it is still unclear whether the microlayer is primarily a sink or a source of anomalously enriched elements in the marine aerosol.

There is an enrichment of primary biota in the sea surface microlayer over bulk seawater (Gallagher, 1975; Hardy, 1973), and some secondary biota have adapted to feeding exclusively on this rich food source (MacIntyre, 1974). The enriched elements in the microlayer are concentrated in the particulate phase (Barker and Zeitlin, 1972; Lion et al, 1982). As zooplankton graze by filtering particulate material (Riley and Chester,

1971), this may provide a route for the atmophile elements into the marine food chain, and provide a transport mechanism from the sea surface microlayer to the sea floor in fecal pellets (Chester, 1971).

Although the general behaviour of atmophile elements has been considered in this section, before a geochemical model can be considered, the detailed behaviour of an element in the total environment must be examined.

1.3 THE BIOGEOCHEMISTRIES OF ARSENIC AND ANTIMONY

A reliable data base is an essential pre-requisite to the construction of a reliable geochemical model. As steady state models of arsenic and antimony are to be considered, appropriate environmental data are summarised in the following sections. Such data bases are prone to numerous inaccuracies, and a general paucity of information, but it is hoped that such errors will be overcome as the reliability and availability of environmental data for trace elements improve. The section on antimony is shorter than on arsenic, as the biogeochemistry of antimony has been less well researched, probably because antimony is both less abundant in the environment and less toxic than arsenic. Units in the following sections have been quoted as reported by their respective authors, and no attempt has been made to standardise between different references.

1.3.1 Arsenic

1.3.1.1 Arsenic in the lithosphere

The crystal chemistry of arsenic is controlled by its outer shell electron configuration of $4s^2 4p^3$. It exhibits two major oxidation states in nature, As (V), which forms arsenates analogous to phosphates, and As (III), which forms arsenites. It may also occur as the less common arsenide, salts of which are generally of undetermined structure. There are over 200 naturally occurring arsenic minerals; 60% are arsenates, 20% sulphides and sulphosalts, the remainder consisting of arsenides, arsenites, oxides, alloys and two polymorphs of native arsenic (Baur, 1978). The most common arsenic mineral is arsenopyrite ($FeAsS$) (Onishi, 1969a).

Estimates for the crustal abundance of arsenic vary; the figure which seems to hold the widest acceptance is 1.8 ppm (Mason, 1966; Kronberg *et al*, 1979). Bowen (1966) quoted the same figure for average igneous rocks, whereas the arsenic content of igneous rocks suggested by Onishi (1969a)

was 1.5 ppm. Chester (1975) quoted a value of 5 ppm for the average crustal concentration, somewhat higher than the other estimates. There seems to be good agreement on the average arsenic content of the major types of sedimentary rock: 13 ppm, 1 ppm and 1 ppm for shales, sandstones and limestones respectively (Bowen, 1966; Mason, 1966; Onishi, 1969a). Arsenic is highly concentrated in shales, which represent about 65% of the outcropping rock on land (Garrels and Mackenzie, 1971), so the high crustal content for arsenic quoted by Chester (v.s.) may refer to the average rock exposed to weathering. There is some evidence to suggest that arsenic is also concentrated in soils. Kronberg and coworkers (1979) reported 7 ppm in Brazilian soils that had undergone intense chemical weathering, and suggested that the clay mineral gibbsite was an important factor in the retention of arsenic. Bennett (1981) quoted 7 ppm as a typical arsenic concentration in soils. Kirkham (1979) quoted an average concentration of 6 ppm for arsenic in soils, 45% of which was extractable; clay soils yielding a lower fraction than sandy soils. The most stable arsenic phases in soils are calcium and manganese arsenates (Sadiq et al, 1983), or irreversibly adsorbed phases on iron and aluminium oxides (Woolson et al, 1973). Arsenic is leached as As(V) from oxic soils, or As(III) from anoxic soils (Sadiq et al, 1983), with a half life of about 6.5 yr (Tammes and de Lint, 1969). Thus, any surface contamination of soil is not rapidly leached to lower soil horizons (Robberecht et al, 1983).

Arsenic data for fresh marine sediments are variable, ranging from 11 ppm in pelagic clays (Onishi, 1969a) to 20 ppm for nearshore sediments (Chester, 1975; Dissanayake et al, 1983). However, all such data show significant enrichment over average crustal rock. About 2% of the annual input to estuarine sediments returns to the water column in pore waters (Carpenter et al, 1978), but comparable data are not available for near shore or pelagic sediments. Neal and coworkers (1979) found a very strong

correlation between arsenic and iron in pelagic sediments, and determined an average arsenic accumulation rate in North Atlantic sediments of $5.6 \mu\text{g cm}^{-2} \text{yr}^{-1}$. Over 90% of the arsenic in this environment was authigenic, indicative of scavenging of arsenic from seawater by authigenic iron oxyhydroxides, which is probably the major removal mechanism of arsenic from the sea (Li, 1981a; Neal et al, 1979). Further evidence for such a mechanism is the increase in arsenic concentration in sediments near mid-oceanic ridges. A similar scavenging mechanism has been observed for phosphate (Froelich et al, 1977); both arsenic and phosphorus show higher enrichments in ferromanganese nodules from shallow water than in those from deep water (Calvert and Price, 1977), and arsenic is highly concentrated in phosphatic rocks, with an average concentration of 21 ppm (Onishi, 1969a). Thus, arsenate may be acting as a phosphate analogue. Strong arsenic-iron associations have also been found in estuarine sediments (Langston, 1980). For unpolluted sediments the typical arsenic to iron ratio is about 11×10^{-4} (Langston, 1980; Neal et al, 1979), but increases to about 32×10^{-4} for estuarine sediments in south-west England, due to the influence of local arsenic bearing mines. In severely polluted sediments, such as the Rhine sediments, arsenic may exhibit up to ten-fold enrichment (Dissanayake et al, 1983). Creclius (1975) noted correlations for both iron and manganese in lacustrine sediments, although the correlation with manganese was not as pronounced as that with iron. There is also some evidence for associations between arsenic and organic matter in coastal sediments (Langston, 1980).

1.3.1.2 Arsenic in the hydrosphere

Most of the arsenic in particulate and dissolved form reaching coastal waters is supplied by river run-off. Turekian (1969) suggested an average dissolved arsenic concentration of about $2 \mu\text{g L}^{-1}$ for river water, which falls well within the range of 0.25 to $25 \mu\text{g L}^{-1}$ quoted by Onishi (1969a),

as does the concentration of $4 \mu\text{g L}^{-1}$ suggested by Bowen (1966) for dissolved arsenic in freshwater. Trefry and Presley (1976) measured a dissolved arsenic load of $3 \mu\text{g L}^{-1}$ in rivers flowing into the Gulf of Mexico, which accounted for 30% of the total arsenic load, most of the remainder being suspended load, with bed load accounting for less than 5% of the total. In contrast, Chester (1975) suggested that 70% of river-borne arsenic was in the dissolved form, which is the most important fraction with respect to global oceanic supply, as most riverine particulate arsenic is deposited in coastal or estuarine sediments. Indeed, riverine suspended matter and associated deltaic sediments exhibit very similar arsenic concentrations (Trefry and Presley, 1976). The most recent data for dissolved riverborne arsenic indicate a lower concentration than suggested above, at $1.7 \mu\text{g L}^{-1}$ (Martin and Meybeck, 1979). The same authors also reported arsenic concentrations of 5 ppm in riverine particulates, and suggested that river supply was a major transport mechanism of dissolved arsenic to the oceans. Using the data from Turekian (1969) for global river discharge and input of suspended matter to the oceans, these recent arsenic data yield a global annual riverine flux of 1.3×10^{11} g arsenic to the oceans, 45% in the dissolved form. This is just under half the global stream flux for arsenic, 3×10^{11} g yr^{-1} , suggested by Lantzy and Mackenzie (1979). Much higher dissolved concentrations, up to $7 \mu\text{g L}^{-1}$, have been observed where there is significant anthropogenic input, such as from smelting operations (Andreas et al, 1983).

Waslenchuk (1979) reported that dissolved arsenic in rivers was exclusively in the form of arsenate. More recently, Howard and coworkers (1982) have shown that this only applies in winter months, biological activity in the summer reducing much of the arsenate to arsenite, methylarsonic acid (MAA) and dimethylarsenic acid (DMAA). Usually, the thermodynamically stable

arsenate is dominant, although where there is a high input of arsenite, and oxidation is retarded by acid waters, such as in the River Carnon, arsenite may account for 90% of the total dissolved arsenic (Marsh, 1983). In stagnant lakes or ponds the proportion of methyl arsenic is higher than in flowing riverine waters (Braman and Foreback, 1973).

Waslenchuk and Windom (1978) noted a correlation between dissolved arsenic and dissolved organic carbon, to which they attributed the observed conservative behaviour of dissolved arsenic in estuaries in the South East United States, despite available removal mechanisms such as adsorption onto iron oxyhydroxide precipitates at the freshwater-brackish water interface. Although dissolved organic carbon may also precipitate out of brackish water, such behaviour is usually confined to the high molecular weight fraction (M.W. greater than 1000), whereas arsenic in the S.E. United States estuaries appears to be associated with the lower molecular weight fraction, which exhibits conservative behaviour in estuaries (Burton, 1983). This protective association may not be effective in high salinity regions (Marsh, 1983) or in estuaries with a high dissolved arsenic load, when adsorption onto iron oxyhydroxides becomes a dominant removal mechanism for arsenate and arsenite (Oscarson et al, 1983), although arsenite may be oxidised and resuspended in anoxic waters due to redox reactions with manganese (Peterson and Carpenter, 1983). Such a mechanism was proposed to account for a resuspension peak in the Tamar estuary, which otherwise exhibited conservative behaviour for arsenic (Marsh, 1983).

As for river water, the most recent data for dissolved arsenic in seawater show a lower concentration than do earlier data. Bowen (1966) and Mason (1966) both quoted an average dissolved arsenic concentration of $3 \mu\text{g L}^{-1}$ for seawater. Onishi (1969a) suggested an average of $2 \mu\text{g L}^{-1}$, and Turekian (1969) an average of $2.6 \mu\text{g L}^{-1}$. According to recent work by

Andreae (1978), a total dissolved arsenic concentration of $1.5 \mu\text{g L}^{-1}$ is typical of both deep and surface ocean waters, although there is much variation of arsenic speciation with depth. Arsenate is dominant, as HAsO_4^{2-} (Riley and Chester, 1971; Turner et al, 1981), although arsenite is detectable in the photic zone at about 10% of the total arsenic concentration, due to biological reduction, which is also the cause of the correlation with depth between reduced arsenic and assimilated carbon (Andreae, 1979). Arsenite usually decreases about five-fold in deep water, although occasionally bacterioplankton blooms may give rise to maxima at about 100 m depth. Organic species, MAA and DMAA, are also detectable in surface waters, but at very low concentration. Waslenchuk (1978) noted a slight enrichment of arsenate at depth, probably due to regeneration from organic detritus. The same author suggested that physical mixing was the predominant control over the distribution of dissolved arsenic in seawater.

Published data for oceanic particulate concentrations of arsenic are very scarce. Mackenzie and coauthors (1979) used the arsenic concentrations in shale and limestone as estimates of arsenic in terrestrial and skeletal particulates respectively. The small amount of available data indicates a particulate arsenic concentration of about 10 ppm in surface waters, with no significant change at depth (P. Buat-Menard, pers. comm., 1982). Adsorption thermodynamics predict that arsenic is ultimately removed from the ocean as a particulate phase adsorbed onto goethite (Li, 1981a), although the same author (Li, 1981b) suggested that arsenic is largely transported to the sediments in fecal material. Therefore, the large organic fraction of arsenic lost to the sediments is probably recycled to the water column.

1.3.1.3 Arsenic in the atmosphere

Atmospheric arsenic is dominated by the particulate phase, the vapour phase

not exceeding about 7% of the atmospheric burden (Walsh et al., 1979a). Several workers have studied atmospheric arsenic concentrations at remote locations, to determine natural background levels. Duce and coworkers (1976) reported a mean particulate arsenic concentration of about 1 ng (SCM)^{-1} (SCM = standard cubic metre) in the atmosphere at Bermuda, much higher than the concentration measured by Walsh and coworkers (1979b), who reported marine atmospheric aerosol concentrations for arsenic of about 0.1 ng m^{-3} for the northern hemisphere, and 0.018 ng m^{-3} for the southern hemisphere. Background concentrations of aerosol arsenic in the continental atmosphere are about 1.5 ng m^{-3} (Adams et al., 1977 and 1980b; Walsh et al., 1979b), but may be as low as 0.2 ng m^{-3} for samples collected at high altitude (Dams and de Jonge, 1976). Bowen (1979) quoted a range of 1.5 to 53 ng m^{-3} for aerosol arsenic concentrations in the atmosphere. The lowest atmospheric data reported to date are about 10 to 30 pg (SCM)^{-1} for aerosol arsenic in the Antarctic atmosphere (Maenhaut et al., 1979), where the volatile enriched elements, including arsenic, correlate with sulphate, indicative of a stratospheric origin. The Greenland ice sheet contains about 1 ng As kg^{-1} of ice (Weiss et al., 1975), and shows pre-industrial enrichment in this environment (Weiss et al., 1978), with a significant pollutant input since 1960 (Li, 1981b). Volcanic activity may be a major source of volatile elements in ice and in the atmosphere in remote areas (Hammer, 1977; Olafsson, 1975; Siegel et al., 1973a), as large quantities of volatiles such as arsenic may be emitted during the early stages of eruption (Lepel et al., 1978). Buat-Menard and Arnold (1978) estimated that Mount Etna may emit up to 0.1 t As d^{-1} into the Mediterranean atmosphere, and enrichment factors up to 2780 have been reported for arsenic in volcanic aerosol emissions (Mikhshenskiy et al., 1979). Arsenic may be volatilised from the land surface by low temperature processes. Goldberg (1976) determined that, under continental background aerosol concentrations,

the average crustal composition would be sufficient to support an As_2O_3 vapour pressure of 3.5×10^{-11} torr at 20°C . However, a surface temperature of 74°C would be required to account for background concentrations of arsenic by physical volatilisation (Brimblecombe and Hunter, 1977). Arsenic may also be biologically volatilised, in the form of methyl arsines. Braman (1975) demonstrated the evolution of dimethyl and trimethyl arsine from soil treated with reduced arsenic, and fungi have been isolated which can effect these transformations (Cox and Alexander, 1973a). The vapour phase has been shown to consist entirely of such alkyl arsenic compounds (Johnson and Braman, 1975a).

Around the British Isles, the background aerosol arsenic concentration is about 2 ng kg^{-1} , but may rise to 24 ng kg^{-1} in industrialised areas (Peirson et al, 1973 and 1974). Salmon and coworkers (1978) measured an average arsenic concentration of about 4 ng m^{-3} in air over Oxfordshire since 1967. Local maritime airmasses over Plymouth contain about $1 \text{ ng As (SCM)}^{-1}$ in the aerosol phase, similar to the average of $1.7 \text{ ng As (SCM)}^{-1}$ measured in the aerosol over the English Channel (this work). Peirson and coworkers (1973) reported arsenic concentrations of $1.6 \text{ } \mu\text{g L}^{-1}$ in rain around Britain, giving a washout factor (rain concentration: atmospheric concentration, both in units of $\text{ } \mu\text{g kg}^{-1}$ determined at 20°C , 760 mm Hg pressure) of 640, and estimated a washout arsenic flux of $0.23 \text{ } \mu\text{g cm}^{-2} \text{ yr}^{-1}$, which yields a global flux of $340 \times 10^9 \text{ g yr}^{-1}$. Turekian (1969) quoted the same figure as an average concentration of arsenic in rain, whereas Onishi (1969a) suggested an average arsenic concentration of $1 \text{ } \mu\text{g L}^{-1}$ in rainwater. However, Walsh and coworkers (1979b) suggested an annual global arsenic flux from the troposphere of $30 \times 10^9 \text{ g}$, and estimated a tropospheric residence time for arsenic of 9 d.

Arsenic has received some attention as an atmospheric pollutant. Walsh and coworkers (1979b) claimed that anthropogenic arsenic emissions are three times the worldwide natural emissions, whilst Lantzy and Mackenzie (1979) suggested that emissions are so high that arsenic exhibits an atmospheric interference factor (total anthropogenic emissions expressed as a percentage of the natural input to the atmosphere) of 2786. Brimblecombe (1979) listed the three most important present day sources of atmospheric arsenic as metal smelting, volcanoes and fossil fuel combustion. The main source of anthropogenic emissions is copper smelting (Brimblecombe, 1979; Carpenter et al, 1978; Crecelius, 1975; Larson et al, 1975; NAS, 1977), although coal burning may be locally important in areas remote from smelting activities (Kowalczyk et al, 1982; Sabbioni et al, 1983). Dethier (1979) attributed 50% of the arsenic input to a lake near Seattle to emissions from a local copper smelter, with a stack dust composition of up to 30% arsenic (Crecelius et al, 1974). Over 99% of arsenic emissions from copper smelters are in the particulate phase (Walsh et al, 1979a). This presents an industrial health hazard, as arsenic is concentrated on respirable particles (Natusch et al, 1974), from which about 20% of the arsenic is water soluble (Breslin and Duedall, 1983; Crecelius, 1980), and is therefore available for uptake across the lung membrane. Of the soluble phase, the highest percentage is leachable from the 0.8 to 0.4 μm diameter fraction (Fisher et al, 1979). The majority of such material falls from the atmosphere within a 60 km radius from the source smelter, although background levels may not be achieved inside a 300 km radius from source (Arafat and Glooschenko, 1982). Jedwab (1975) recognised arsenic-bearing pollutant particles in the marine atmosphere, although Bertine and Goldberg (1971) suggested that fuel combustion was an insignificant source of arsenic to the oceans compared with the river supply to coastal waters.

1.3.1.4 Arsenic in the biosphere

There is a growing body of evidence that arsenate may undergo biologically mediated reduction and methylation in aquatic, sedimentary and terrestrial environments (Andreae, 1978; Baker et al., 1983a and 1983b; Brinckman, et al., 1977; Cox, 1975; Howard, et al., 1982; Wood, 1974). McBride and Wolfe (1971) demonstrated microbial methylation of arsenate to dimethylarsine via MAA and DMAA. Methylcobalamine was suggested as the most likely methyl donor in the presence of adenosine triphosphate, so arsenic methylation probably proceeds along the same biochemical pathway as was described for mercury by Wood and coauthors (1968). This is probably a detoxifying process, as inorganic As(III) is more toxic, by a factor of 5, than methyl arsenic (Hood and Harrison, 1982; Watling and Watling, 1982), although methyl arsenic compounds are often used as selective herbicides (Norris et al., 1983; Wauchope and Yamamoto, 1980). Waslenchuk (1979) suggested that biota played an insignificant role in the arsenic geochemistry of river water, in agreement with Braman and Foreback (1973) who noted a higher concentration of methyl arsenic in lakes and ponds than in river water, although Brooks and coworkers (1982) reported a strong correlation between arsenic in polluted streams and arsenic in the associated biota. Sanders (1980) estimated less than 10% of arsenic dissolved in seawater to be methylated, although this can rise to 90% during plankton blooms (Andreae and Klumpp, 1979).

Arsenic has been determined in plankton by several workers, with variable results. Trefry and Presley (1976) found variations from 3 to 52 ppm arsenic in mixed plankton samples. The range was much narrower for zooplankton alone, which had an average arsenic concentration of about 10 ppm (dry weight). Andreae (1978) reported arsenic concentrations an order magnitude lower for marine algae, which fall into the range of 1-14 ppm quoted by

Chester (1975), except for one high result of 2800 ppm. As these were wet weight concentrations, they may be of a similar order to the dry weight concentrations above, although they are of the same order as the dry weight measurements made by Knauss and Ku (1983). Similar ranges were quoted by Onishi (1969a) and Sanders and Windom (1980). Trefry and Presley (1976) suggested that little planktonic arsenic accumulates in sediments, as they observed no dilution of accumulating organic carbon in nearshore sediments, where inorganic sedimentation is rapid, compared to pelagic sediments.

The biological mediation of arsenic speciation results in a large fraction of organic-bound arsenic within an organism. Andreae (1978) found 20-40% of biotic arsenic in the organic form. Sanders and Windom (1980) reported 55% of biotic arsenic to be organic, and estimated a maximum daily reduction of 140 ng arsenate to arsenite and DMAA per milligram of living phytoplankton carbon. They did not observe the evolution of any volatile arsenic species from marine plankton, nor did Baker and coworkers (1983b), in contrast to observations on terrestrial microbes, which can evolve volatile methyl arsines (Braman, 1975; Cox 1975; Cox and Alexander 1973a). In addition to methyl arsenic, complex organic compounds such as arsenobetaine and arsenocholine have been identified in marine biota (Luten et al, 1983; Norin et al, 1983).

Johnson and Braman (1975b) reported arsenic concentrations between 5 and 20 ppm wet weight, for the marine macroflora, Sargassum, with inorganic arsenic as the dominant form. Arsenic concentrations of 40 - 80 ppm were recorded for the same species by Trefry and Presley (1976). An average dry weight arsenic concentration of about 30 ppm has been suggested for marine macroflora by Bowen (1966).

For marine fauna, Onishi (1969a) quoted a range of 0.0036 to 50 ppm dry weight. Bowen (1966) quoted a narrower range of 0.005 to 0.3 ppm. Although

arsenic exhibits bioaccumulation, with higher concentrations in biota than in the surrounding environment, unlike mercury it does not exhibit biomagnification, showing no increase in concentration up the food chain (Woolson, 1975). Leatherland and coworkers (1973) observed a decrease in arsenic concentration up the trophic scale, from about 20 ppm in plankton to about 10 ppm in fish tissues. A similar trend is evident in the data of Johnson and Braman (1975b). For benthic organisms, arsenic uptake from sediments is important, as arsenic correlates with iron in the benthos, and is usually concentrated in the gut in filter feeders (Langston, 1980), although uptake may also be related to the reproductive state of the organism (La Touche and Mix, 1982). A number of benthic organisms demonstrate marked bioaccumulation of arsenic, and may prove useful as pollution indicators (Bryan et al, 1983; Gibbs et al, 1983).

For freshwater fauna, Onishi (1969a) quoted arsenic concentrations in the range 0.05 to 10 ppm, dry weight. Bowen (1966) suggested an average arsenic concentration of 0.2 ppm for terrestrial flora. Where arsenic sources for plants are dominated by atmospheric input, leaf physiology may be an important factor in arsenic uptake (Arafat and Glooschenko, 1982). Some floral species exhibit marked bioaccumulation of arsenic (Byrne and Tusek - Znidaric, 1983). In terrestrial fauna, arsenic is more concentrated in skeletal material than in soft tissue, but is overall of a similar concentration to arsenic in flora (Bowen, 1979). Mammals, including man, are also capable of detoxifying arsenic by methylation (Crecelius, 1977; Hood et al, 1982; Lakso and Peoples, 1975; Yamauchi and Yamamura, 1983), and excrete the methyl product in urine (Crecelius, 1977) or in milk (Kosta et al, 1983).

1.3.2 Antimony

1.3.2.1 Antimony in the lithosphere

The crystal chemistry of antimony is determined by its outer electron structure of $5s^2 p^3$. It occurs in nature in the two valency states, Sb(III) and Sb(V). Minerals containing antimony may be subdivided into four broad groups: metallic antimony with alloys and antimonides, sulphides and sulphosalts, sulpho-oxides and sulpho-halogenides, and finally oxides (Kupcik, 1974), the most common antimony mineral being stibnite (Sb_2S_3) (Onishi, 1969b).

Mason (1966) suggested a crustal abundance for antimony of 0.2 ppm, whereas Bowen (1966) and Onishi (1969b) both quoted this figure for an average igneous rock. The antimony content of shales is variable; Onishi (1969b) quoted a range of 0.1 to 4 ppm, with an average of 1.5 ppm. Thus, antimony is enriched in shales compared to crustal rocks, in common with many other trace elements (Bowen, 1966; Mason, 1966). Onishi, (1969b) quoted an average concentration of 0.3 ppm for antimony in limestone, and, in agreement with Bowen (1979), suggested an average antimony concentration of 0.05 ppm in sandstones. Like arsenic, antimony is enriched in soils. Onishi, (1969b) quoted a range of antimony concentrations in soil from 1 to 9.5 ppm, similar to the range of 2 to 10 ppm quoted by Kirkham (1979). Concentrations up to 20 ppm were reported for antimony in Brazilian soils taken from an area of intense chemical weathering (Kronberg et al, 1979), due to adsorption onto kaolinite and gibbsite. An average antimony concentration of 1 ppm was proposed by Bowen (1979). Pollutant antimony may have a longer residence time in soil than pollutant arsenic (Crecelius et al, 1974).

Antimony exhibits slight enrichment in recent sediments. Martin and Meybeck (1979) quoted an antimony content of 0.8 ppm for pelagic clays, similar to

the figure of 1 ppm quoted by Onishi (1969b), who also noted 0.2 ppm antimony in Globigerina ooze. Bothner and coworkers (1980) reported an antimony concentration of 0.3 ppm in coastal sediments. However, Strohal and coworkers (1975) found higher antimony concentrations in coastal sediments, about 20 ppm, although these sediments were associated with an abnormally high particulate load in the water column. Antimony may be as high as 100 ppm in polluted riverine sediments (Dissanayake et al., 1983). Crecelius (1975) reported a background concentration of about 1 ppm antimony in lacustrine sediments, and noted weak correlations with organic carbon, iron and aluminium, indicating that antimony may be removed from the water column by biota, or adsorbed onto iron oxyhydroxides or lithogenous particles. In contrast, Bothner and coworkers (1980) found associations in coastal sediments between antimony, chromium and leachable copper, although the reason for this association was unclear.

1.3.2.2 Antimony in the hydrosphere

A concentration range of 0.5 to 0.8 $\mu\text{g L}^{-1}$ was quoted by Onishi (1969b) for dissolved antimony in riverwater, whereas a lower concentration of 0.33 $\mu\text{g L}^{-1}$ was given by Bowen (1966). Martin and Meybeck (1979) reported 1 $\mu\text{g L}^{-1}$ dissolved antimony in river water, in agreement with Turekian (1969), and 2.5 ppm antimony in riverine suspended matter. These recent data yield a global riverine flux of antimony to the oceans of $7.2 \times 10^{10} \text{ g yr}^{-1}$, 50% of which is in the dissolved form. This compares favourably to the flux of $10 \times 10^{10} \text{ g yr}^{-1}$ suggested by Lantzy and Mackenzie (1979).

Like arsenic, dissolved antimony has been determined in natural waters as Sb(V), Sb(III), and two methylated forms : methylstibonic acid (MSA), and dimethylstibinic acid (DMSA) (Andr ae et al., 1981). About 98% of dissolved antimony in river water is in the form of Sb(V), as $\text{Sb}(\text{OH})_6^-$ (Riley and Chester, 1971), but this falls to 90% in seawater. The remainder in river

water is composed of equal proportions of Sb(III) and MSA. About 1% of dissolved antimony in seawater is in the form of DMSA, the remaining 9% again in equal proportions of Sb(III) and MSA (Andreas, 1981).

Turekian (1969) quoted a dissolved antimony concentration of $0.33 \mu\text{g L}^{-1}$ in seawater, similar to the concentration of $0.3 \mu\text{g L}^{-1}$ given by Onishi (1969b), whereas Mason (1966) suggested a higher average value of $0.5 \mu\text{g L}^{-1}$. More recent work, referred to by Bowen (1979), indicated a dissolved concentration of $0.24 \mu\text{g L}^{-1}$. Strohal and coworkers (1975) reported a concentration of $0.31 \mu\text{g L}^{-1}$ for dissolved antimony, but also found an anomalously high particulate load of over $40 \mu\text{g L}^{-1}$. Particulate antimony in seawater is usually less than 0.2ng L^{-1} (Buat-Menard and Chesselet, 1979). Particulate matter taken from deep waters contains about 10 ppm antimony (Buat-Menard and Chesselet, 1979; Martin and Meybeck, 1979). Antimony is removed from seawater on manganese oxides (Crecelius, 1975; Li, 1981a), to give a residence time of 3200 yr for antimony in the oceans (Craig, 1974), about two orders of magnitude shorter than the residence time quoted by Mason (1966). However, some of this may undergo post depositional remobilisation, as deep sea clays are significantly lower in antimony than are riverine particulates (Martin and Meybeck, 1979). There is also a large fraction of antimony transported to the sediments in fecal pellets (Li, 1981b), which must be recycled to the water column if removal on manganese oxides is the ultimate removal mechanism of antimony from the oceans (Li, 1981a). Antimony shows enrichment in the microlayer of 10^5 to 5×10^5 over bulk seawater (Szekielda et al, 1972).

1.3.2.3 Antimony in the atmosphere

Data for antimony in the atmospheric aerosol cover several orders of magnitude, 0.0017 to 63ng m^{-3} (Bowen, 1979). Several workers have determined the background antimony concentration in the Antarctic atmosphere.

Maenhaut and coworkers (1979) reported an average antimony concentration of $0.84 \text{ pg (SCM)}^{-1}$ in the Antarctic aerosol, similar to the $1.7 \text{ pg (SCM)}^{-1}$ reported by Zoller and coworkers (1974). Data published by Weiss and coworkers (1975) indicate an accumulation rate for antimony in the Greenland ice sheet of $0.5 \text{ ng cm}^{-2} \text{ yr}^{-1}$, and later reported considerable pre-industrial enrichment of antimony in Greenland (Weiss et al., 1978). The enrichment factors for antimony in the aerosol at these remote locations, about 2300 (Duce et al., 1975), indicate a possible volcanic origin, falling well within the published range for volcanic emissions. Buat-Menard and Arnold (1978) determined an enrichment factor of 3800 for aerosol antimony in an emission from a hot vent on Mount Etna, although the enrichment factor in the aerosol from the main plume was only 660. Mroz and Zoller (1975) also reported a low antimony enrichment factor, 100, in the aerosol emitted by Heimay on Iceland. However, particulate matter from the Tolbachik volcano had an antimony enrichment factor of 11000 (Mikhshenskiy et al., 1979), which only accounted for 20% of the antimony emission. Ambient temperatures at the ground surface may yield a vapour pressure for Sb_2O_3 of 1.2×10^{-10} torr (Goldberg, 1976), although a temperature of 198°C would be required to yield observed background concentrations by this mechanism (Brimblecombe and Hunter, 1977).

The background continental aerosol has an antimony concentration of 0.7 ng m^{-3} (Adams et al., 1980b), although this is higher in the northern hemisphere, between 1 and 2 ng m^{-3} (Dams et al., 1972). At high altitudes lower concentrations, about 0.2 ng m^{-3} , were observed by Dams and De Jonge (1976). Much lower concentrations were reported for marine aerosols, $0.03 \text{ ng (SCM)}^{-1}$ (Duce et al., 1976) for samples taken at Bermuda, and 5 pg (SCM)^{-1} for aerosols sampled at Enewetak Atoll (Duce, 1982), although a higher concentration, 0.11 ng m^{-3} , was observed by Buat-Menard and

Chesselet (1979) in the marine atmosphere. An enrichment factor of 180 was determined for antimony in the Bermuda aerosol, lower than the enrichment factor reported in the Antarctic. Duce (1982) calculated an atmospheric input to the oceans of $0.24 \text{ ng cm}^{-2} \text{ yr}^{-1}$, an order of magnitude higher than the sediment accumulation rate, and suggested this was indicative of pollution or recycling from the ocean to the atmosphere. However, it may be due to remobilisation of antimony from the sediments to the water column (Li, 1981a; Martin and Meybeck, 1979).

In remote areas of the British Isles, aerosol antimony concentrations in the atmosphere are about 0.5 ng kg^{-1} (Peirson et al, 1973 and 1974), although concentrations up to 6 ng kg^{-1} were observed in industrial areas. The same authors (Peirson et al, 1973) reported concentrations of about $1 \text{ } \mu\text{g L}^{-1}$ in rainwater in Britain, and estimated an antimony washout flux of $0.25 \text{ } \mu\text{g cm}^{-2} \text{ yr}^{-1}$. Salmon and coworkers (1978) found an average aerosol antimony concentration of 2 ng m^{-3} in air over Oxfordshire since 1967, higher than the concentration in Plymouth airmasses, an average of $0.45 \text{ ng (SCM)}^{-1}$, and aerosol concentrations of antimony over the English Channel, about $0.8 \text{ ng (SCM)}^{-1}$ (this work).

Like arsenic, antimony is concentrated on particulate emissions from copper smelters (Creelius, 1975; Larson et al, 1975) and may be mobilised by fossil fuel combustion (Sabbioni et al, 1983). Kowalczyk and coworkers (1982) noted that aerosol antimony correlated well with copper in an urban atmosphere, where an average antimony concentration of 18.8 ng m^{-3} was observed, higher than rural concentrations, but much lower than the concentration of $1.9 \text{ } \mu\text{g m}^{-3}$ observed as an aerosol in an industrial atmosphere (Castillo et al, 1982). Natusch and coworkers (1974) reported concentrations up to 53 ppm for antimony in flyash particles smaller than $2 \text{ } \mu\text{m}$, compared to 17 ppm for particles greater than $11 \text{ } \mu\text{m}$. The highest

concentrations are on the 2 to 0.4 μm fraction (Fisher et al, 1979). Crecelius (1980) found 20% of flyash to be soluble in seawater. Anthropogenic sources of antimony yield an estimate for the antimony interference factor of 3878 (Lantzy and Mackenzie, 1979). Little work has been carried out on the global distribution of vapour phase antimony; however, antimony is probably less volatile than arsenic, as the boiling points of most antimony compounds are higher than those of their arsenic analogues (table 1.2).

1.3.2.4 Antimony in the biosphere

Antimony may be methylated by biota (Andreae et al, 1981) by a mechanism similar to that proposed for arsenic (Wood, 1974). Bowen (1979) quoted a range of 0.02 to 0.9 ppm, dry weight, for marine algae, lower than the concentration of 4 ppm reported by Knauss and Ku (1983), and in an earlier publication (Bowen, 1966) suggested an average antimony concentration of 0.2 ppm, dry weight, in marine fauna, which falls into the range of 0.08 to 24 ppm quoted by Onishi (1969b). Kartin (1983) found 30% of the antimony in Sargassum to be in the form of Sb(III), but did not observe any methyl species. Strohal and coworkers (1975) reported antimony concentrations ranging from 0.07 to 0.9 ppm, dry weight, in benthic fauna in the Adriatic, a similar range to that observed for plankton, 0.07 to 0.22 ppm (Buat-Menard and Chesselet, 1979). Leatherland and coworkers (1973) observed a decrease up the marine trophic scale, from 0.03 ppm at the lowest level to 0.009 ppm in a species of shark. Bowen (1966) quoted a similar trend on land, from 0.06 ppm in terrestrial flora to 0.006 ppm in terrestrial fauna. Concentrations in mammalian tissues are less than 0.1 ppm (Onishi, 1969b).

Table 1.2 Boiling Points of Analogous Arsenic and Antimony Compounds

General formula	Boiling Point, °C	
	X = As	X = Sb
X_2O_3	193(s)	1550(s)
X_2S_3	707	1150
XCl_3	130	283
XH_3	-55	-17
XH_2CH_3	2	?
$XH(CH_3)_2$	37	?
$X(CH_3)_3$	70	81
$X(C_2H_5)_3$	140	160

s : sublimation temperature

Data from Weast (1980)

1.4 GEOCHEMICAL MODELS

After critical assessment of the available data, those that are the most reliable may be selected to quantify a geochemical cycle. Such cycles are usually determined as steady state models, although non-steady state models may also be developed.

1.4.1 The Steady State

The unpolluted environment is not at equilibrium, but may be approximated by a steady state (Broecker, 1971). In this approach, the Earth is conceptually divided into well-defined mixing units, such as the oceans or atmosphere, which are termed reservoirs. The mass of any material in the reservoir can be estimated from the appropriate concentration data, and then exchange between the reservoirs considered. Such inter-reservoir exchanges are termed fluxes. A flux is usually comprised of several transport mechanisms, for example, the land to ocean flux is comprised of streams, glacier flow, groundwater and shore erosion, although streams account for over 90% of the flux, so are usually used to approximate the total transport (Mackenzie and Wollast, 1977). Over geologic time the fluxes are thought to have achieved a steady state, each reservoir maintained at a constant mass by a balance between the total influx and the total efflux. However, the steady state concept is only valid for the long term average, as short term variations, like variability in biological activity on a diel or seasonal basis, will mask the steady state, producing short term oscillations.

In a simple steady state model, the Earth is divided into three reservoirs, land, ocean and atmosphere, so the model is termed a three-box model (figure 1.1). There are six fluxes to consider : land to atmosphere (F1), ocean to atmosphere (F2), atmosphere to land (F3), atmosphere to ocean (F4), land to ocean (F5) and ocean to land (F6). The mass balances for the steady

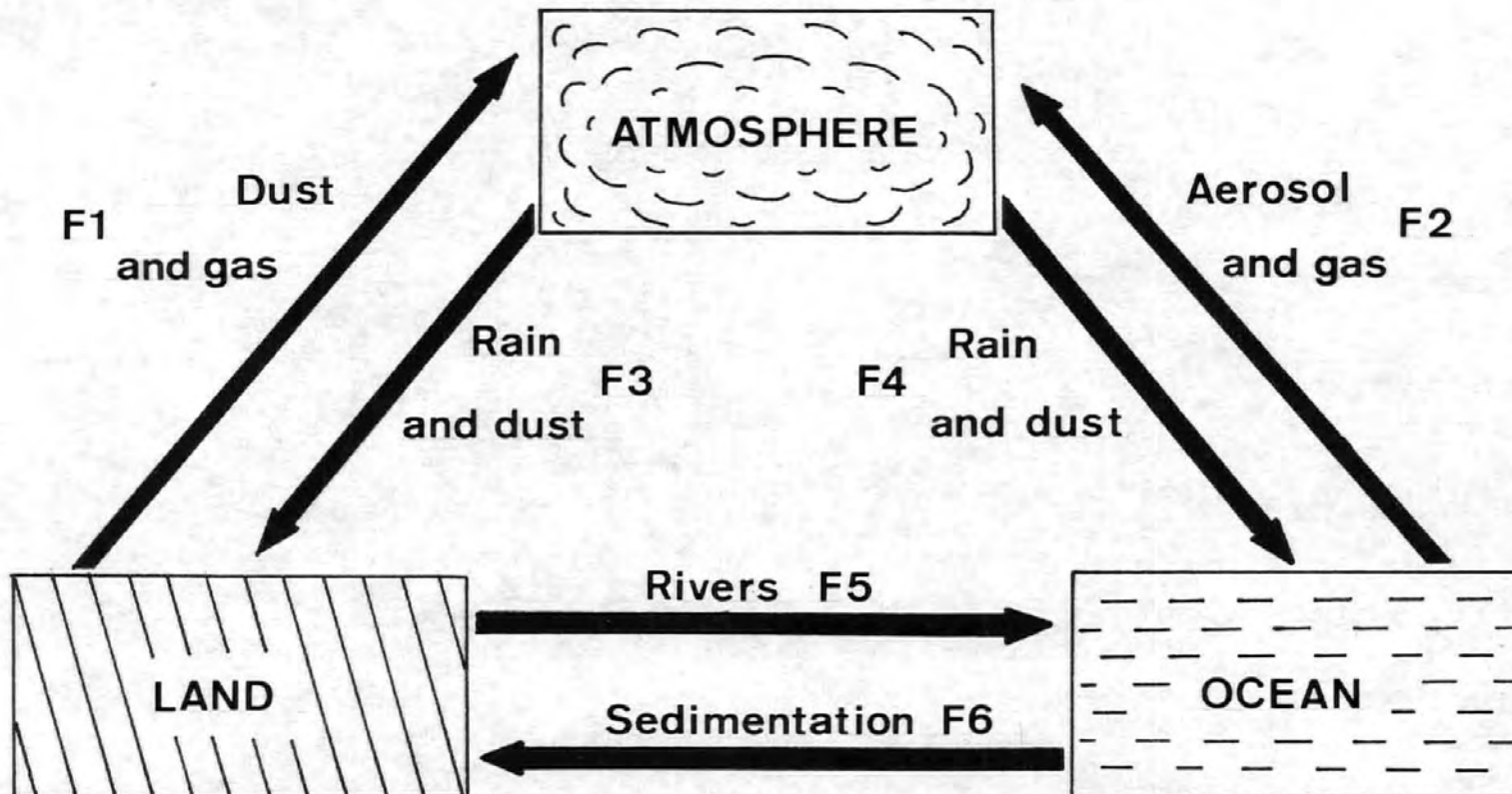


Figure 1.1 A simple three-box model

state are represented by the following equations :

$$\text{Atmosphere} : F_1 + F_2 = F_3 + F_4 \quad (1.6)$$

$$\text{Ocean} : F_4 + F_5 = F_2 + F_6 \quad (1.7)$$

$$\text{Land} : F_3 + F_6 = F_1 + F_5 \quad (1.8)$$

Since the initial development of the three-box model, the complexity of geochemical box models has increased, such as the five-box models by Mackenzie (1975) and Millward (1982). When quantifying complex models, many assumptions are needed to estimate those fluxes for which there are few environmental data. If the aim is to produce a reliable steady state, then the simultaneous modelling of several different tracers may reduce the number of assumptions required, thereby avoiding the choice of cycling parameters that are only supportable for one tracer (Keeling and Bolin, 1967 and 1968).

1.4.2 Kinetic Modelling

The steady state concept is invalid for present day cycles. Man has been observably polluting his environment since the industrial revolution, thereby perturbing the pre-existing steady state. To model the time dependency of a perturbation, the kinetics of global cycling must be considered. If the global cycle is considered as a chemical reactor, and the inter-reservoir fluxes as chemical reactions, then the cycle obeys first order kinetics in the long term (Bennett, 1981; Garrels et al, 1973).

Thus :

$$\frac{dA}{dt} = k.A \quad (1.9)$$

Where A = mass of material in the source reservoir

k = first order rate constant

dA/dt = flux from source reservoir

For trace elements, like arsenic and antimony, reservoir masses are usually in units of kt (kilotonnes), fluxes are in units of kt yr^{-1} , and rate constants are in units of yr^{-1} . The inverse of the rate constant gives the residence time in the source reservoir with respect to the flux in consideration. Thus, each flux is dependant on the mass of its source reservoir. Although this implies that each reservoir is well mixed, first order kinetics can be obeyed by poorly mixed reservoirs (Bolin et al, 1981). There are fixed rate constants for some geochemical processes, independent of the chemistry of the substance under consideration. Such processes are of a physical nature, like the transport of dust to the atmosphere, and individual substances are only passive passengers of the transport mechanism. This is not so for processes such as deep sea scavenging and biological uptake, when the solution chemistry of an element effects its behaviour.

Mackenzie and Wollast (1977) suggested that to increase the number of reservoirs in a model above three is confusing, and further refinement is best treated by subdividing the reservoirs into compartments, with internal cycling. However, if kinetics are to be modelled, then it is important to establish the correct source reservoir for each flux, to determine the appropriate rate constant. For this reason, multi-reservoir models have been considered in this work.

1.5 AIMS OF THE RESEARCH PROGRAMME

The environmental behaviour of many atmophile elements is still poorly understood. The aims of this study were to improve the understanding of this behaviour in the following areas.

1. Aerosol concentrations of arsenic and antimony were to be determined in open ocean and coastal environments, and the importance of aerosol deposition in both environments assessed.
2. Information thus gained was to be used to refine models of the geochemical arsenic cycle.
3. The above models were to be further examined by kinetic analysis, using the atmospheric burdens determined from the environmental analyses above for calibration, and the sensitivity of the models to key parameters assessed. From this, the most important areas for further study could be established.
4. Steady state cycles for antimony were to be established, as this element has not previously been modelled in this manner, and limited sensitivity experiments were to be conducted by kinetic analysis.

CHAPTER TWO
SAMPLING AND ANALYSIS OF THE
ATMOSPHERIC AEROSOL

2.1 SAMPLING

2.1.1 Sampling Methods

Aerosol samples were collected on Millipore aerosol monitors, which consist of a cellulose acetate membrane filter, with an exposed surface of 8 cm^2 , on a cellulose backing pad, housed in a polypropylene assembly. Filters with a nominal pore size of $0.8 \text{ }\mu\text{m}$ were chosen as the optimum compromise between particle retention, 99% efficiency for particles of $0.45 \text{ }\mu\text{m}$ diameter, and gas flow rate through the filter (Dams et al, 1972). From July 1981 to May 1982, an oil-free, carbon bladed, rotary vacuum pump (Lacey-Hulbert Ltd., Model 1361), with a maximum displacement of $8 \text{ m}^3 \text{ hr}^{-1}$, was used to draw air through the filter, via an integrating gas flow meter (U.G.I. (Meters) Ltd.). Since May 1982, a similar pump was used (Lacey-Hulbert Ltd., Model RB. 2506), with a maximum displacement of $20 \text{ m}^3 \text{ hr}^{-1}$. Neither pump was operated at the maximum displacement, due to the pressure drop across the filter assembly, about 630 mbar. The filter assembly, gas flow meter and pump were connected by pressure tubing of about 1.3 cm internal diameter, ensuring air-tight seals. The tubing was attached to the back of the filter housing using an adaptor with a luer fitting.

The gas flow meter measures volume displacement, not mass displacement, so did not completely compensate for the pressure drop. However, the response of the meter is not linear down to such low pressures, so it was not possible to apply a simple correction factor for the pressure drop, determined using a pressure gauge on the inlet of the pump. To determine the appropriate correction factor, the probe from a thermo-anemometer (Wallac Oy, Model Ni-125 ANE), consisting of two fine nickel wires held in a tube of 1.2 cm internal diameter, was mounted in line between the pump and integrating flow meter. Such instruments are essentially thermal transducers, and measure flow rate as the rate of heat

loss from the nickel wires, which is a function of gas density (Perry, 1982). Thus, such instruments measure mass flow, rather than volume flow, and the thermoanemometer reading, in units of m s^{-1} , may be converted to an equivalent s.t.p. volume flow if the diameter of the probe is known. The results for the recalibration are shown in figure 2.1. The overall length of the air column passing through the probe was determined by integrating under the curve in figure 2.1a. This was then converted to volume flow and compared to the equivalent reading from the integrating meter, shown in figure 2.1b. As can be seen from both curves, the pump takes 1 hr to achieve the optimal pumping rate. By comparison of the two methods, the reading from the integrating meter can be corrected to atmospheric pressure by applying a factor of 0.53, not the factor of 0.37 which would result from simply correcting for the pressure drop without recalibrating the integrating meter. Although blockage of the filter may cause an increase in the pressure drop with time in a completely sealed system, a constant pressure drop was achieved using an adjustable pressure release valve on the pump inlet. The system was also tested for leakage before the meter by sealing the open end of a filter. Air flow through the meter due to leakage was less than 1% of the flow through the filter.

During sampling, monitors were mounted in an inverted position, protected by a plastic collar, to avoid fouling or dampening by rain. Also to avoid dampening, the samples were not collected during foggy or misty weather. During ship board sampling, the wind direction was continuously monitored, to ensure the exposed filters were not contaminated by on-board emission sources, such as the ship's funnel or exhaust outlets. Meteorological conditions during sampling were recorded.

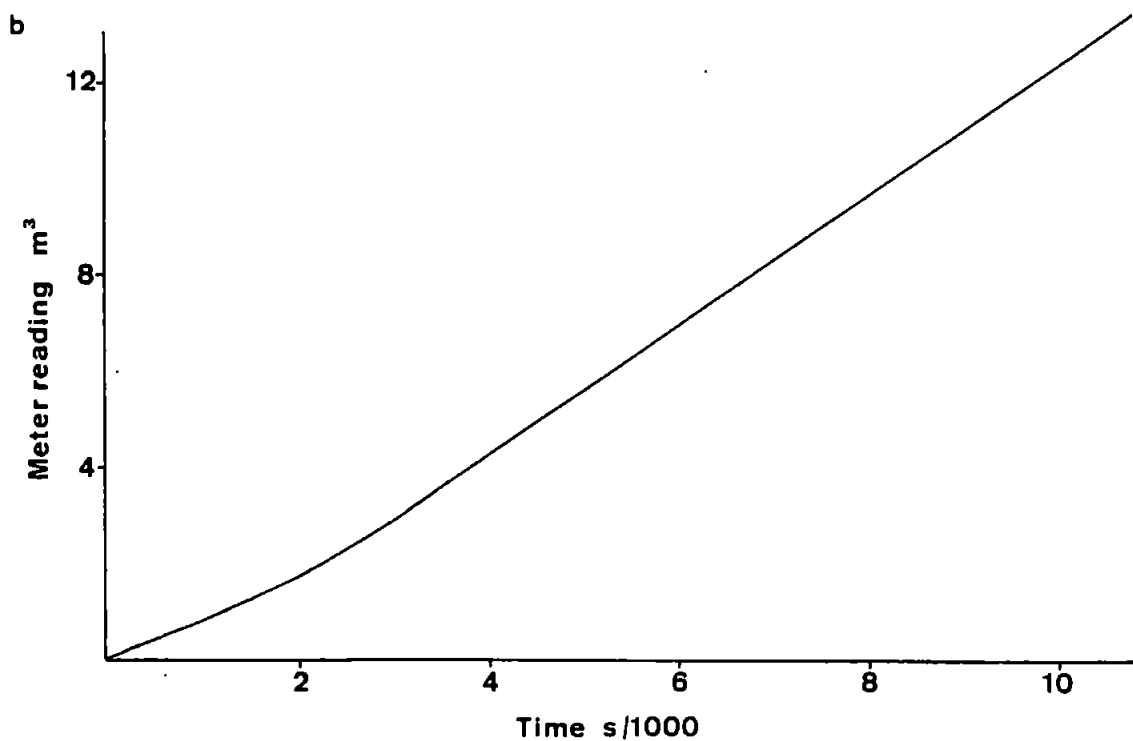
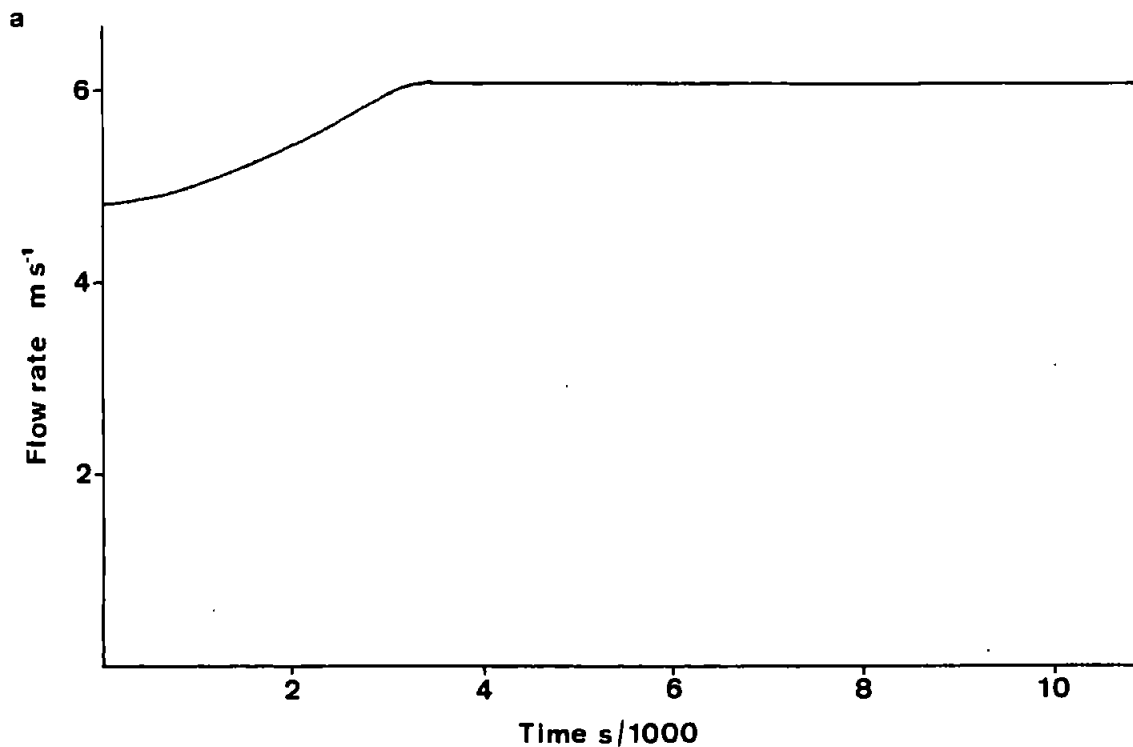


Figure 2.1 Recalibration of the integrating gas meter

a : Area under curve and internal radius of probe, 6 cm, gives a total volume pumped of 7.18 SCM

b : Volume registered on meter in the same period is 13.50 m^3
 Meter reading (m^3) \times 0.53 = volume (SCM)

2.1.2 Sampling Locations

The land-based sampling programme took place at Plymouth Polytechnic, taking both daytime and night time samples at roof level, about 55 m above sea level. The coastal location of Plymouth provided opportunity to sample a variety of airmasses of both continental and marine origin. The occurrence of a temperature inversion over the city in November and December 1982 made it possible to assess the extent to which the city itself was a source of atmospheric arsenic and antimony. Sampling of airmasses at Plymouth usually entailed filtering 10 to 20 m³ of air for one sample.

Samples of the marine aerosol were collected from two stations, the Channel Lightvessel and Ocean Station Lima, with a further research cruise in the English Channel. Sampling on board the lightvessel took place in April 1982. The lightship is moored in the west of the English Channel, between Plymouth and the Channel Islands, to act as a navigation marker for the main shipping routes from Europe and the South of England. The vessel was not under power, so was usually laying into the prevailing current. Therefore, the aerosol monitors were given temporary mountings, to be moved with the prevailing wind to the windward quarter of the vessel. Samples were collected from Ocean Station Lima in March 1983, on board the weather ship, M.V. "Starella". Ocean Station Lima occupies an area about 10,000 km² in the North Atlantic, bounded by latitudes 57° 30' N to the north and 56° 30' N to the south, and longitudes 19° 00' W to the east and 21° 00' W to the west. The "Starella" was usually held into the wind, so aerosol monitors were mounted near the bows of the vessel, above the wheel-house to avoid wetting by spray. Despite the latter precaution, it was not possible to sample in wind speeds above 20 ms⁻¹ (Beaufort Force 9) without the filters becoming waterlogged. The locations of the Plymouth site, the

Channel lightvessel and Ocean Station Lima are shown in figure 2.2.

A final sampling cruise was carried out on board R.V. "Frederick Russell" in September 1983. The vessel sailed from Plymouth, and made six transects of Lyme Bay, before crossing the Channel to Jersey. On the second leg, a voyage was made to the Bay of Biscay, at grid reference $47^{\circ} 30' N$ $11^{\circ} 00' W$, before returning to Plymouth. The route is illustrated in figure 2.3. As the ship's funnel and exhaust ports were on the stern of the vessel, sampling was discontinued if sailing with the wind to stern. For open ocean samples about 50 m^3 of air were filtered per sample.

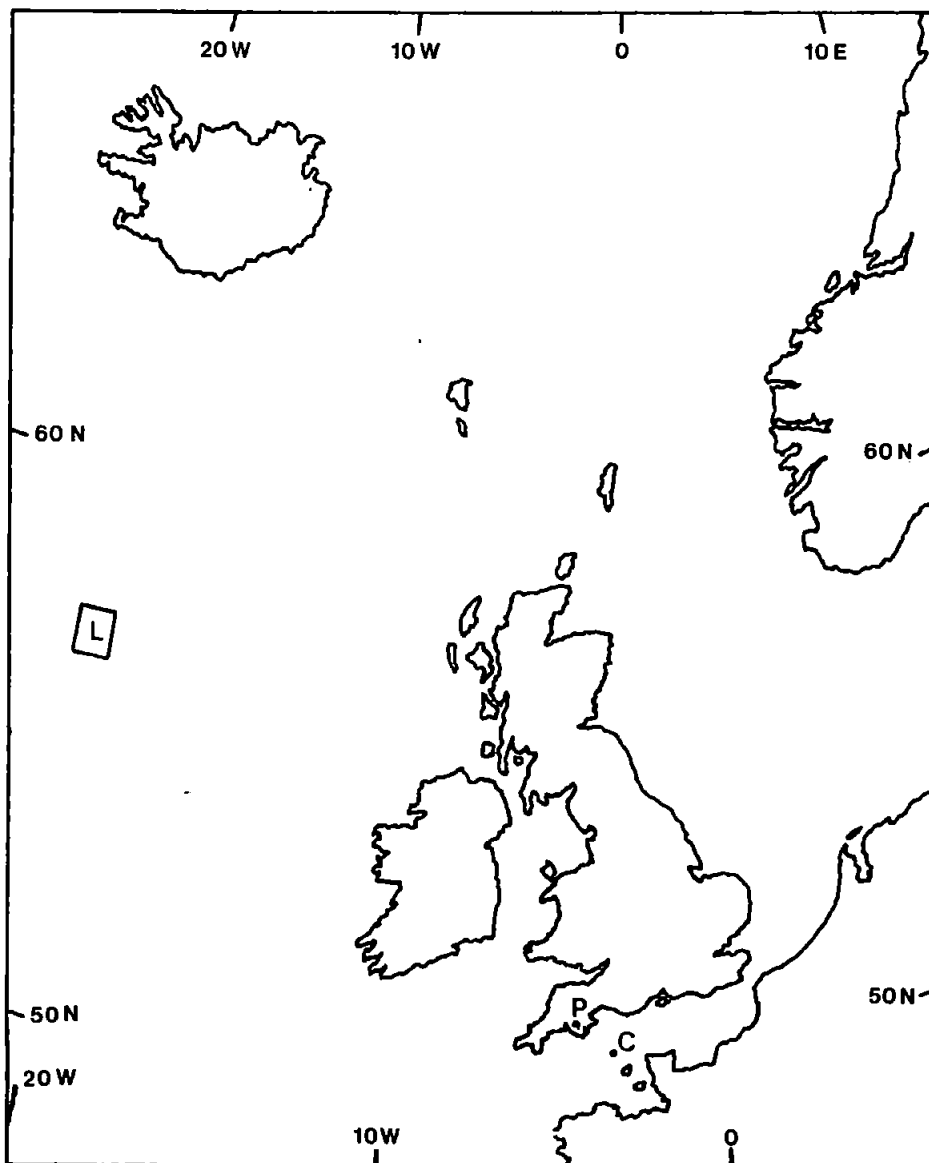


Figure 2.2

Locations of sampling sites.

P = Plymouth
C = Channel Lightvessel
L = Ocean Station Lima

Scale - 1 : 16 000 000

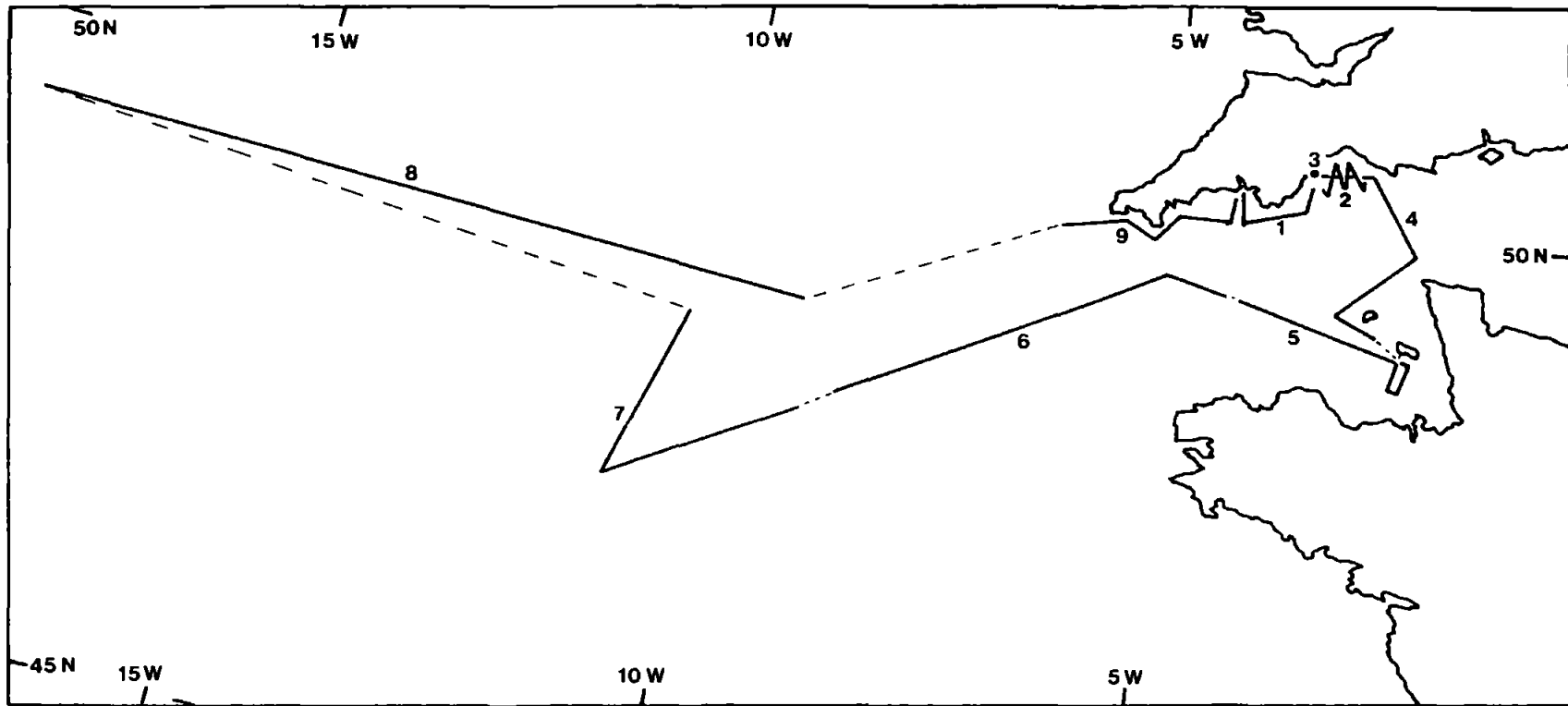


Figure 2.3 Route of R.V. "Frederick Russell" during sampling voyage.
Solid lines indicate filters exposed. Scale - 1 : 6 000 000

2.2 ANALYTICAL METHODS

2.2.1 Electron Microscopy

Some exposed filters were examined under the electron microscope, prior to treatment for chemical analysis. A small section, about 5 mm square, was cut from a filter using a scalpel blade, and attached to an electron microscope stub with double sided adhesive tape. To ensure a good conductivity, thus preventing a charge build-up on the sample whilst in the electron beam, the sample and stub were sputter coated with gold to a thickness of 10 nm. The coated samples were examined in a JEOL JSM 35C Scanning Electron Microscope, fitted with a Link X-Ray Analysis System. X-ray analyses were performed on particles of varying morphology, with the aim of identifying the particle source, in terms of a continental, marine or pollutant origin.

2.2.2 Choice of Analytical Technique

Atomic absorption spectroscopy (AAS) has become one of the most popular techniques for the determination of trace elements such as arsenic or antimony. For such elements, a standard modification to this technique is that of hydride generation, where the analyte is converted to a volatile covalent hydride, which is determined by flame AAS (Castillo et al, 1982; Knudson and Christian, 1974). Although this modification suffers little from spectroscopic interferences, interferences have been observed with the formation of the hydride (Welz and Melcher, 1981). Hydride generation has also been used for speciation, using a temperature gradient to selectively volatilise different hydrides (Andreae et al, 1981; Howard and Arbab-Zavar, 1981). Although atmospheric arsenic and antimony have been determined by hydride generation, coupled with a heated quartz cell to atomise the sample for AAS (Vijan and Wood, 1974), the samples analysed in this work were generally of too low a concentration for reproducible determination by a hydride technique. Instead, aliquots

of each sample were injected into the graphite cuvette of an electro-thermal atomiser, and arsenic and antimony determined by AAS. Graphite furnace atomic absorption spectroscopy (GFAAS) has become the most popular method for the determination of atmospheric arsenic (Bernard and Pinta, 1982; Walsh et al, 1976a, 1976b and 1979a). Colorimetry has been used to determine atmospheric antimony (Morris, 1977). Neutron activation analysis has often been used for multi-element analyses of the atmospheric aerosol (see for example : Adams et al, 1977; Dams et al, 1972; Duce et al, 1976; Peirson et al, 1973; Salmon et al, 1978). Although useful for multi-element analyses, plasma emission has only been used to determine major elements in aerosol samples (Sugimae and Mizoguchi, 1982). In this work, arsenic and antimony were both determined by GFAAS.

2.2.3 Sample Preparation

2.2.3.1 Choice of preparative technique

The published methodology for digestion of filters prior to analysis for arsenic can be divided into two groups, total digest methods and leaching methods. Crock and Lichte (1982) showed that digestion of flyash in hydrofluoric acid was necessary to liberate all arsenic and antimony, other methods losing that fraction bound to silicates. However, as arsenic and antimony are largely bound to sulphides rather than silicates (Onishi, 1969a and 1969b), such losses are not significant. Aristar nitric acid was used for the digests, as sulphate produces a spectral interference with arsenic and antimony (Brooks et al, 1981, and references therein), and chloride is not recommended in GFAAS, as the chloro-complexes thus formed are more readily volatilised during the ashing stages than oxyanion complexes (Fuller, 1977), and may even be formed and lost during the sample digest (Fernandez and Manning, 1971). Simple dissolution in

concentrated nitric acid (70%) was not feasible, as antimony is insoluble in such oxidising conditions (Vogel, 1979). The maximum permissible concentration of nitric acid for use in a graphite cuvette is 10%, although this reduces the cuvette life, so a concentration below 2% is usually preferred. To achieve complete digestion of the filter, the method of Bernard and Pinta (1982) was adapted as follows.

A filter was digested in concentrated Aristar nitric acid (1 ml) overnight at 60°C. The digest was then carefully evaporated to dryness on a hot plate, not exceeding 60°C. The residue was then taken up in 3% nitric acid (1 ml) by ultra-sonic agitation for 30 min. and diluted to 2 ml with distilled water. Although Bernard and Pinta (v.s.) claimed a 95% recovery for arsenic, evaporating at 80°C, the maximum recovery of a 50 ng addition of arsenic in this study was only 35%. The addition of nickel (about 2 µg) prior to digestion enhanced recovery to a maximum of 60%, but the recovery was not reproducible, varying from 40 to 60%. In addition, the filter matrix reduced the sensitivity of the analytical signal five-fold. For these reasons a leachate method was adopted.

Janssens and Dams (1973) used a leachate method to determine atmospheric lead, and Vijan and Wood (1974) used a similar method to determine atmospheric arsenic and antimony. The filters from the monitor assemblies were peeled from the cellulose backing pad using stainless steel tweezers, and placed into 50 ml beakers which were sufficiently large to accommodate the filters unfolded. To each filter was added 3% nitric acid (1 ml). This was subject to ultrasonic vibrations for 45 min at 60°C, to give an available fraction. The environmental significance of this will be discussed in section 2.3.2.1. The acid was decanted off, and the filter was washed twice with aliquots of distilled water (less than 0.5 ml), each with 5 min of ultrasonic vibration which were added to the leachate. The leachate was then diluted to 2 ml. Any particulate matter remaining in the leachate was

allowed to settle out before 1 ml of the sample was carefully drawn from the top for direct determination of arsenic and antimony. The remainder of the sample was diluted to 25 ml for the determination of sodium and magnesium. Recovery of additions of 50 ng arsenic and antimony to blank filters was at least 95%, within the analytical precision of the determination by GFAAS, showing no losses due to volatilisation or precipitation.

2.2.3.2 Standardisation

The extraction efficiency of the leachate method from an aerosol matrix was determined on samples of standard urban particulate matter (U.S. Department of Commerce, National Bureau of Standards, Standard Reference Material 1648), containing $115 \mu\text{g g}^{-1}$ arsenic and $45 \mu\text{g g}^{-1}$ antimony. The standard Reference Material (SRM) was prepared from urban dust collected in St. Louis, Missouri, over a period in excess of twelve months, so is typical of the aerosol that would be sampled in an industrialised urban area. Prior to digestion, the dust was dried at 105°C for 8 hrs, in accordance with the drying instructions supplied with the sample. The extraction of the trace constituents arsenic and antimony was determined in quadruplicate. Four aliquots of the dried dust were weighed onto four separate filters, and the leaching procedure performed on each up to the dilution of the leachate to 2 ml. After allowing the insoluble particulates to settle, 1 ml was withdrawn from the top of the leachate, and diluted to 10 ml. This was then analysed for arsenic and antimony by GFAAS. The results for the extraction are summarised in table 2.1 :

Table 2.1 Extraction Efficiency for Arsenic and Antimony

Weight of Sample (mg)	Extraction efficiency for arsenic (%)	Extraction efficiency for antimony (%)
3.2	59.8	38.8
1.7	61.4	41.8
1.4	62.1	38.1
2.5	59.1	44.4
Mean	60.6	40.8
S.D.	1.4	2.9

Thus, the available fraction from the SRM contains about 60% of the total arsenic and 40% of the total antimony.

The extraction efficiency for sodium and magnesium was standardised in duplicate. Two aliquots of the dried SRM, containing 0.425% sodium and 0.8% magnesium, were weighed onto two separate filters and treated by the leachate method. Dilutions were carried out as for the trace element standardisation.

Sodium was determined by flame photometry and magnesium by flame AAS. The extraction efficiencies for these elements are summarised in Table 2.2 :

Table 2.2 Extraction Efficiency for Sodium and Magnesium

Sample weight (mg)	Extraction efficiency for sodium (%)	Extraction efficiency for magnesium (%)
14.0	47.1	62.9
14.0	53.8	60.9
Mean	50.5	61.9
S.D.	4.7	1.4

The extraction efficiency for sodium is about 50%, and that for magnesium about 60%, similar to that for arsenic. In the leachates, the sodium concentrations were lower than those for magnesium, to give an apparent oceanic enrichment factor for magnesium of 20, so magnesium was used as a reference element for an urban end member. For those samples with a very high enrichment factor for magnesium an urban source is likely, whereas an enrichment factor near unity indicates the presence of a marine component (Duce et al, 1976 ; this work). Apparent oceanic enrichment factors for magnesium in a background continental aerosol are about 5 (Adams et al, 1977). As the matrix of marine aerosol samples

differs from that of continental aerosol samples (see for example : Harrison and Pio, 1983a and 1983b), the extraction efficiencies determined for the standard dust were considered inapplicable to the samples collected during the ship-board exercises.

2.2.3.3 Seawater leaching

Arsenic and antimony are both very toxic and mobile in the environment (Wood, 1974). As both probably enter the biosphere in the dissolved phase (Andreae, 1981; McBride and Wolfe, 1971), the solubility of anthropogenic arsenic and antimony in natural waters will influence the effect of these toxic elements on biota. A significant source of dissolved arsenic and antimony to coastal waters has been identified in riverine outflow (Martin and Meybeck, 1979). The contribution from aerosol deposition to the dissolved material in coastal waters is still unknown. If it is significant, it may play an important role in biological uptake of these elements in coastal waters, where the standing crop of primary biota may be an order of magnitude higher than in open ocean (Riley and Chester, 1971). Therefore, the solubility of arsenic and antimony in seawater was determined from the urban particulate SRM. The experiment was carried out in duplicate.

A small aliquot (about 10 mg) of the dried SRM was added to an aliquot (25 ml) of standard seawater (IAPSO standard, 31/10/1981, chlorinity 19.373‰). This was stirred for 2 hrs at 25°C, using a magnetic stirrer. After stirring, the remaining particulate material was filtered off, using an acetate filter of nominal pore size 0.45 µm, and the leachate retained. The particulate material was washed with distilled water, and dried for 8 hrs at 105°C. An aliquot of this was treated by the acid leach method used for the preparation of aerosol samples, except that the final leachate (1 ml) was diluted to 10 ml prior to analysis.

Two methods were employed for the determination of arsenic and antimony. The acid leach was analysed by GFAAS. Seawater solutions are notoriously difficult to analyse by this method, because of sodium emissions (Brooks, et al, 1981), so the seawater leachate was analysed for arsenic and antimony by AAS with a hydride generation system, and a heated quartz cell. A separate aliquot (25 ml) of standard seawater was stirred and filtered through an acetate filter to provide a procedural blank for the hydride analysis.

2.2.4 Chemical Analysis

Arsenic and antimony were determined in aerosol samples by GFAAS. As both elements are volatile, losses have been observed during the temperature programme prior to atomisation, even at low ashing temperatures (Walsh et al, 1976a). To overcome this problem, nickel is usually added in excess of the volatile elements to form nickel arsenides and nickel stibnides during the ashing stage of the temperature program. These are less volatile than most compounds of arsenic or antimony, so are not lost from the cuvette prior to atomisation (Bernard and Pinta, 1982; Iverson et al, 1979; Walsh et al, 1976b). Additions of nickel nitrate were made to each sample, such that the concentration of added nickel was $1 \mu\text{g ml}^{-1}$. The method was calibrated by standard addition to overcome spectral interferences from the matrix (Brooks et al, 1981). Additions of 10, 20 and 30 ng of arsenic or antimony were made to each sample using solutions of 250 ng ml^{-1} arsenic and 250 ng ml^{-1} antimony, prepared from stock solutions containing 1 mg ml^{-1} arsenic and 1 mg ml^{-1} antimony in 6 molar hydrochloric acid. Examples of the resultant calibration graphs are shown in figure 2.4. Antimony was generally less prone to signal suppression than was arsenic. All samples, except those collected on the R.V. "Frederick Russell" were analysed in duplicate (or triplicate if necessary) in an IL 555 electrothermal atomiser, coupled to an IL 151

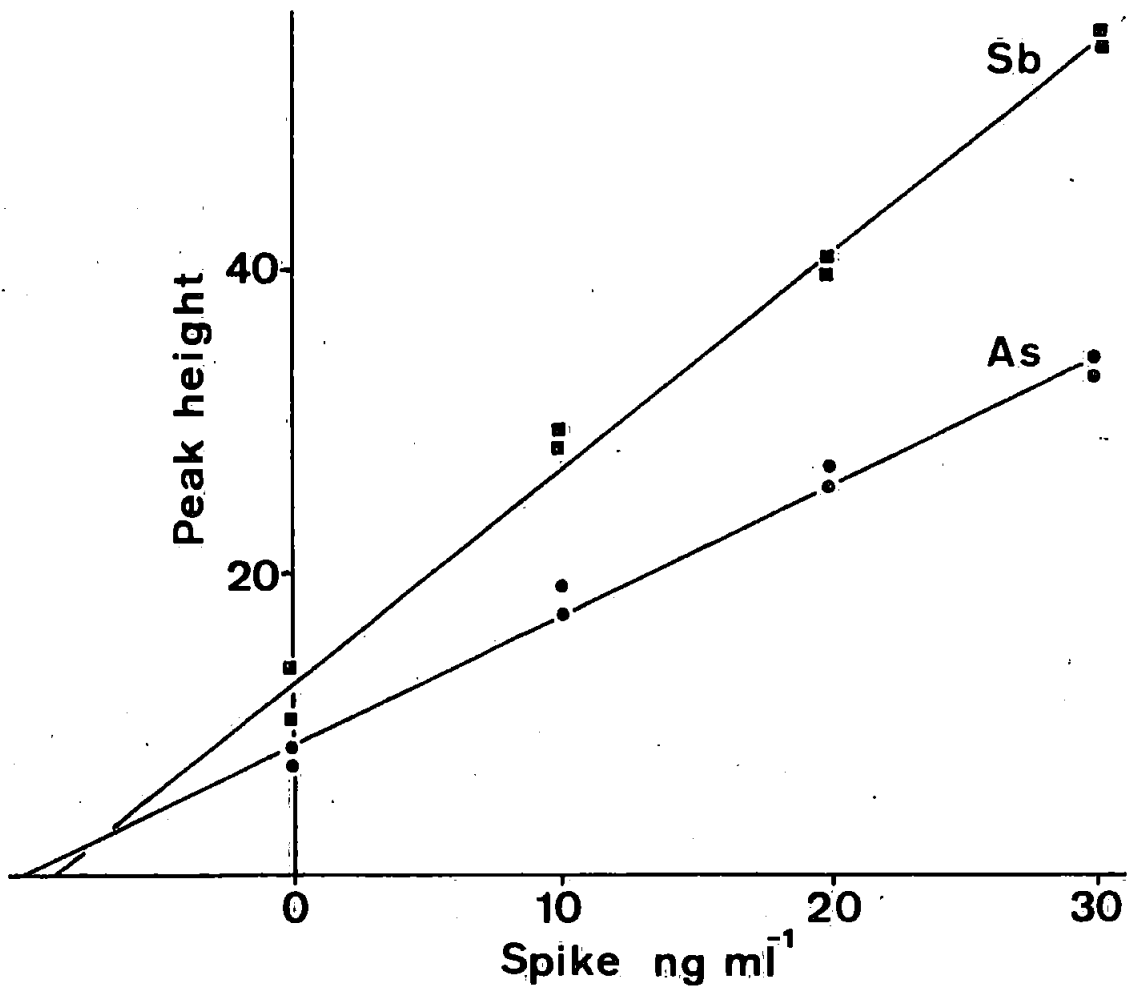


Figure 2.4 Examples of calibration curves for arsenic and antimony, from standard additions to a sample exposed on the Channel Lightvessel

atomic absorption spectrophotometer. Output was via a Lineeis chart recorder. The instrumental parameter for arsenic are shown in table 2.3(a). The detection limit for arsenic, 30 pg, was determined as a signal to background noise ratio of two (Harris, 1982). The method was shown to have a linear response to 1.2 ng. The coefficient of variation on five injections (20 μ l) of a 10 ng ml⁻¹ standard was 8.0%. The instrumental parameters for antimony on the IL GFAAS system are shown in table 2.3(b). The detection limit was assessed as 20 pg, with a working linear range up to 1 ng. The coefficient of variation on five injections (20 μ l) of a 10 ng ml⁻¹ standard was 6.5%.

The samples collected on board R.V. "Frederick Russell" were analysed on a Pye Unicam SP9 spectrophotometer, fitted with a Pye Unicam SP9 furnace. Output was via a Philips chart recorder. The instrumental parameters for arsenic are shown in table 2.4(a). The detection limit was 10 pg, with a linear range up to 1 ng. The coefficient of variation determined on three injections (20 μ l) of a standard of 10 ng ml⁻¹ was 4.6%.

Instrumental parameters for antimony on the Pye Unicam system are shown in table 2.4(b). The detection limit was 20 pg with a linear range to 1 ng. The coefficient of variation on three injections (20 μ l) of a 10 ng ml⁻¹ standard was 7.4%. All injections on both the IL system and Pye Unicam system were carried out manually using an adjustable Gilson micropipette. Operational detection limits were taken as twice the procedural blank value if this registered above the background noise.

The formation of gaseous hydrides from dissolved arsenic and antimony requires these elements to be in reduced form in solution (Castillo et al, 1982; Chu et al, 1972; Fernandez and Manning, 1971). Acidifying the

Table 2.3 Instrumental Parameters on the IL GFAAS System

a) Arsenic

<u>IL 151</u>	Lamp currents : As hollow cathode	8 mA		
		Deuterium background	12 mA	
	Photomultiplier voltage, HV	: 800		
	Spectral Line	: 193.7 nm		
	Bandpass	: 1 nm		
<u>IL 555</u>	Sample injection size	: 20 µl		
	Nitrogen purge rate	: 0.5 SCMH (standard cubic metres per hour)		
	Temperature programme	: 75 ⁰ C for 25 s	Drying	
		: 125 ⁰ C for 25 s		
		: 750 ⁰ C for 20 s	Ashing	
		: 1000 ⁰ C for 20 s		
	: 2000 ⁰ C for 10 s	Atomisation		

b) Antimony

<u>IL 151</u>	Lamp currents : As hollow cathode	5 mA		
		Deuterium background	12 mA	
	Photomultiplier voltage, HV	: 800		
	Spectral Line	: 217.6 nm		
	Bandpass	: 0.5 nm		
<u>IL 555</u>	Sample injection size	: 20 µl		
	Nitrogen purge rate	: 0.5 SCMH		
	Temperature programme	: 75 ⁰ C for 25 s	Drying	
		: 125 ⁰ C for 25 s		
		: 325 ⁰ C for 15 s	Ashing	
		: 400 ⁰ C for 15 s		
	: 2250 ⁰ C for 5 s	Atomisation		

Table 2.4 Instrumental Parameters on the Pye Unicam SP9

a) Arsenic

Spectrophotometer Lamp current : As hollow cathode 7 mA
Background : High
Spectral Line : 193.7 nm
Bandpass : 0.5 nm

Furnace Sample injection size : 20 µl
Temperature programme :
Dry : Ramp-6, 100^oC for 30 s
Ash : Ramp-8, 400^oC for 25 s
Atomisation : 2400^oC for 20 s

b) Antimony

Spectrophotometer Lamp current : Sb hollow cathode 10 mA
Background : High
Spectral line : 217.6 nm
Bandpass : 0.5 nm

Furnace Sample injection size : 20 µl
Temperature programme :
Dry : Ramp-6, 100^oC for 30 s
Ash : Ramp-7, 450^oC for 20 s
Atomisation : 2800^oC for 20 s

solution with 6 M hydrochloric acid is sufficient to carry out the reduction from the pentavalent to the trivalent state (Castillo *et al*, 1982; Marsh, 1983). Sodium borohydride may then be added to generate the gaseous hydrides (Knudsen and Christien, 1974; Thompson and Thomerson, 1974). A continuous flow method was used to analyse the seawater leachates for arsenic and antimony by hydride generation, taken from Marsh (1983), in which the elements were reduced to their gaseous hydrides, and swept into a heated quartz cell in the light beam of a Pye Unicam SP9 spectrophotometer. The operating conditions of the spectrophotometer were as described in table 2.4. Samples were drawn into the hydride generator using a peristaltic pump of flow rate 8.2 ml min^{-1} . Two Y-joints connected in tandem entrained 6 M hydrochloric acid and 4% sodium borohydride dissolved in an aqueous solution of 0.1 sodium hydroxide, which were drawn into the apparatus by a dual channel peristaltic pump of flow rate 1.6 ml min^{-1} . The mixture passed through a ten loop mixing coil, and then into a gas - liquid separator. The hydrides were swept into a heated quartz cell, based on the design of Thompson and Thomerson (1974), by an auxiliary nitrogen supply. The cell was heated by an air-acetylene flame. Output was via a Perkin-Elmer chart recorder. Standards of 50 ng ml^{-1} and 100 ng ml^{-1} arsenic and antimony were prepared from stock solutions of 1 mg ml^{-1} arsenic and antimony in 6M hydrochloric acid. The detection limit of the method for arsenic was 3 ng ml^{-1} , and for antimony was 4 ng ml^{-1} . Coefficients of variation determined on three injections of a standard of $100 \text{ } \mu\text{g L}^{-1}$ were 1% for arsenic and 2.9% for antimony.

Analyses for sodium in the acid leaches were carried out by flame photometry on a Corning 400 flame photometer. The working linear range was up to $5 \text{ } \mu\text{g ml}^{-1}$. Standards of $1 \text{ } \mu\text{g ml}^{-1}$, $3 \text{ } \mu\text{g ml}^{-1}$ and $5 \text{ } \mu\text{g ml}^{-1}$ were

prepared from a stock solution of sodium chloride containing $100 \mu\text{g ml}^{-1}$ sodium.

Magnesium was determined on an IL 151 atomic absorption spectrophotometer, using an oxidising air-acetylene flame. Standards were prepared from a stock solution of magnesium nitrate containing 1 mg ml^{-1} magnesium. The linear working range was up to $0.4 \mu\text{g ml}^{-1}$. Samples were aspirated directly into the flame. Instrumental parameters are shown in table 2.5.

Table 2.5 Instrumental Parameters for the Analysis of Magnesium

Lamp current : Mg-Ca hollow cathode 3 mA
Spectral line : 285.2 nm
Bandpass : 1 nm
No background correction

Unexposed filters were treated by the acid leach method to establish the procedural blank. The analyses from ten blank filters, determined during the course of the aerosol analyses, are summarised in table 2.6.

Table 2.6 Summary of Blank Analyses

Element	Average content per filter	Standard deviation
As	1.4 ng	1.7 ng
Sb	2.3 ng	2.2 ng
Na	17.0 μg	10.6 μg
Mg	1.5 μg	1.3 μg

Attempts to determine iron, calcium, potassium and chloride were abandoned because of high blank values.

2.3 ANALYTICAL RESULTS

2.3.1 Electron Microscopy

The combustion particle shown in plate 2.1 has a morphology which is typical of combustion particles from fossil fuels (Griffin, 1980), but may also be generated by natural processes such as forest fires (Griffin and Goldberg, 1975). Such particles, often termed "cokey spherules", are often about 10 μm or more in diameter, the spherule in plate 2.1 being 20 μm in diameter. The interstices in the spherule all have jagged, sharp edges, which suggests the particle was formed shortly before collection. Particles that have spent some time in the atmosphere usually have a well-rounded weathered appearance (see for example, Griffin, 1980). The chemistry of these particles is dominated by carbon, with traces of refractory lithogenous elements, such as silicon or aluminium. The microprobe analysis for this particle is shown in figure 2.5. Elements below carbon are not shown, but a small broad peak around aluminium and silicon is observable. The two large peaks are artefacts, emissions from the gold coating on the particle. Such artefacts are present in the other microprobe analyses shown in this section.

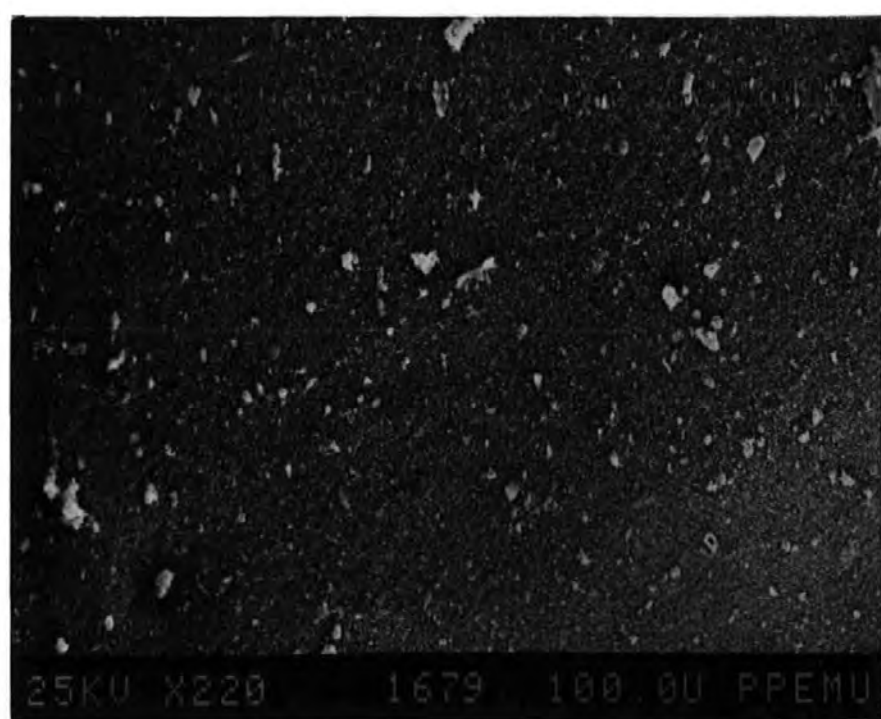
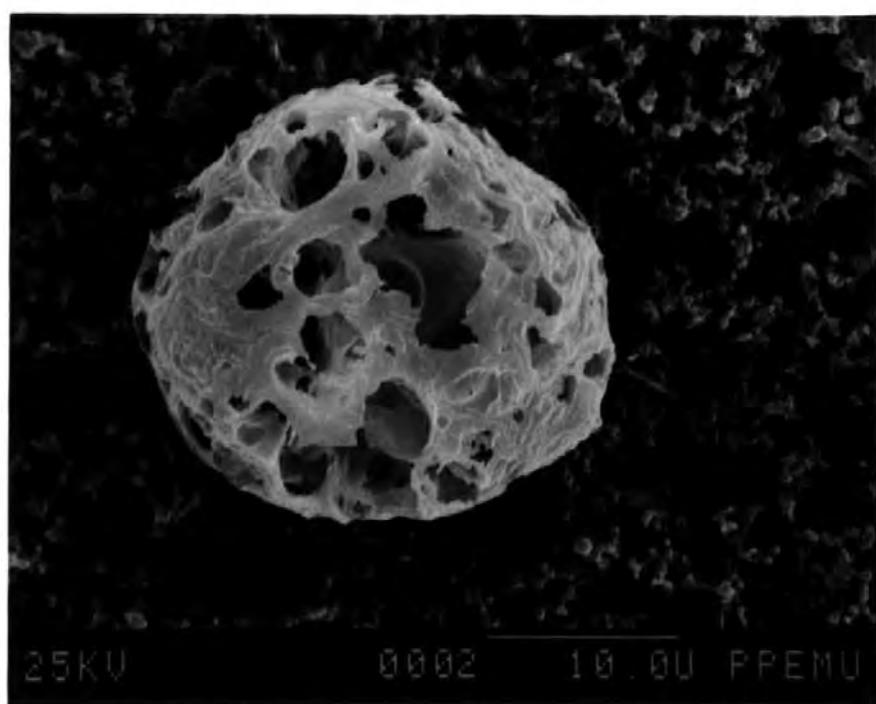
Many of the particles in an urban environment are of the cokey spherule type. Several such particles are visible in plate 2.2, which shows a section from a filter exposed overnight during a temperature inversion over Plymouth. This shows the highest particle density observed on any of the filters, 50 to 100 particles per 10 000 μm^2 . Although much unblemished filter surface was visible under the electron microscope, a particle coverage of this density was sufficient to turn the filter from white to black.

Plate 2.1

Electron micrograph of a combustion particle

Plate 2.2

Field of view shows a high particle density on a filter exposed during a temperature inversion over Plymouth. A number of possible combustion particles are present.



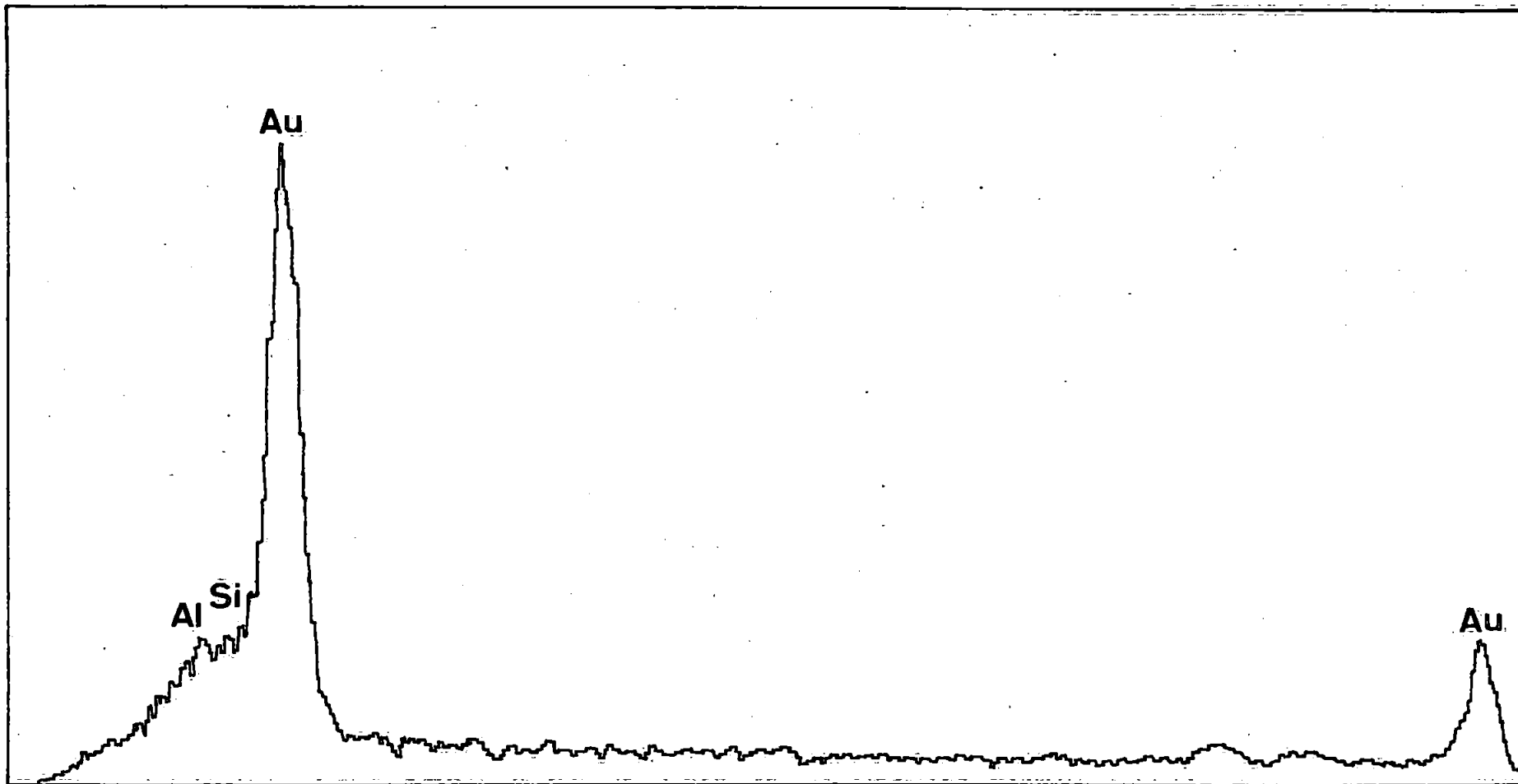


Figure 2.5 Microprobe analysis of the coke spherule.
Gold peaks are artefacts of the preparative technique.

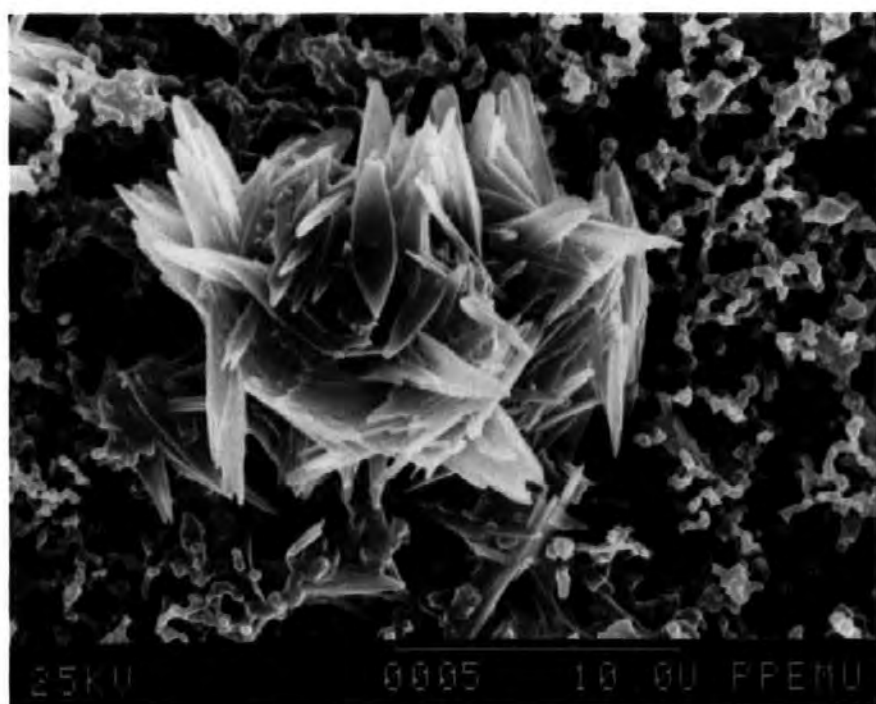
Sulphate particles are very common in the urban aerosol. Frank and coworkers (1972) observed droplets of sulphuric acid and ammonium sulphate crystals in the atmosphere. Two types of sulphate particle were observed in the air over Plymouth, particles of calcium sulphate (plate 2.3) and particles of potassium sulphate (plate 2.4). A microprobe analysis of the calcium sulphate particle is shown in figure 2.6. Microprobe analyses of potassium sulphate particles are similar, except the relative heights of the potassium and calcium peaks are reversed. Calcium sulphate particles are usually about 10 μm in diameter, and exhibit a platey morphology. In contrast, potassium sulphate particles are larger, up to 50 μm in diameter, and show a more rounded morphology. Sulphate particles were frequently observed in the marine atmosphere. However, these were of the calcium sulphate type, and no particles of the potassium sulphate type were observed.

Sodium chloride crystals are often seen in the marine aerosol (Frank et al, 1972; Griffin, 1980). However, the form that sodium chloride takes in the marine atmosphere is variable. It can be found in seawater droplets, concentrated brine droplets, or as sodium chloride crystals, depending on the ambient relative humidity and the initial drop size (Blanchard, 1983). Thus, although sodium chloride is always present in the marine atmosphere, crystals need not be present. In this work, crystals of sodium chloride were rarely found, but traces of sodium chloride were often observed in microprobe analyses. A poorly formed crystal, about 10 μm across, is shown in plate 2.5, and the corresponding microprobe analysis is shown in figure 2.7. The crystal shows the typical cubic habit of sodium chloride, but the crystal edges are well rounded, as if the crystal had been subject to a humid environment.

Aeolian transport is a most important mechanism for the input of terrestrial

Plate 2.3 Electron micrograph of a calcium sulphate particle.

Plate 2.4 Electron micrograph of a potassium sulphate particle.



material to the deep sea sediments in open ocean regions. Fine grained material, from the Sahara desert, can be transported across the Atlantic by the Trade winds (Riley and Chester, 1971). Particles involved in long range transport often have a near spherical morphology, produced by the sand-blasting action of aeolian erosion. Such particles are termed "millet-seed" sand (Read and Watson, 1968). A typical "millet seed" sand particle, about 10 μm in diameter was collected over the English Channel (plate 2.6). The aluminosilicate chemistry of the particle is clearly shown in figure 2.8.

Micro-organisms are usually enriched in the sea surface microlayer over bulk seawater (Gallagher, 1975; Hardy, 1973), so may be introduced into the aerosol by bursting bubbles (Blanchard, 1983). Certain marine micro-organisms may even be used as tracers for the marine aerosol (Sieburth, 1983). A siliceous test, possibly a radiolarian, was sampled above the waters of the North Atlantic at Ocean Station Lima (plate 2.7).

2.3.2 Chemical Analysis

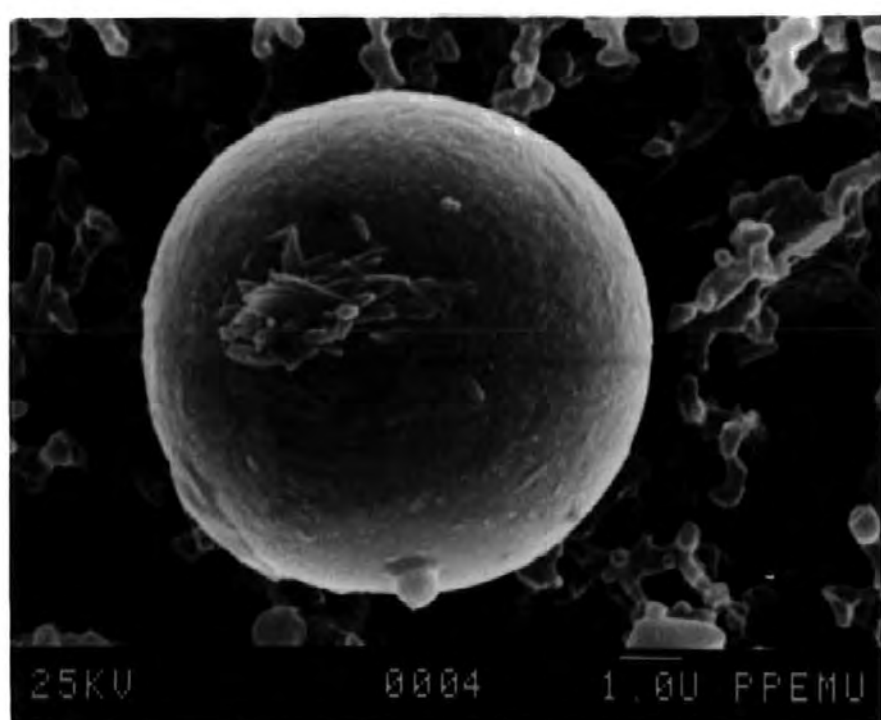
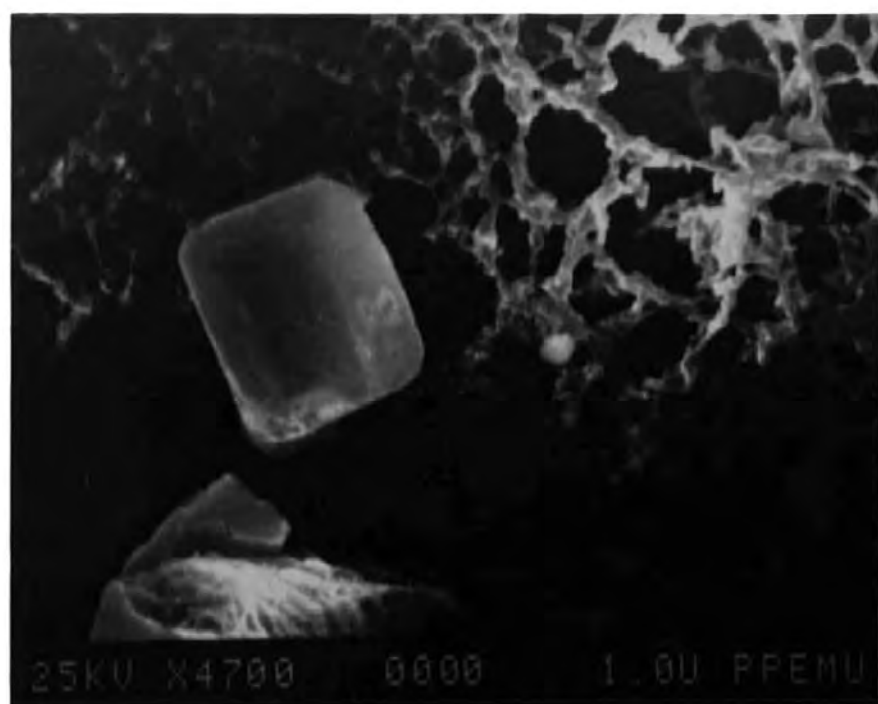
2.3.2.1 Environmental analysis

One cannot simply define a bioavailable fraction, because of the wide range of pH encountered in the guts of different organisms, the parameter usually determining bioavailability (Moore et al, 1984). The gastric fluid of crustacea has a pH between 4.7 and 7.6 (Vonk, 1960); that of zooplankton is similar, pH 4.5 - 6.0 (Mayzaud and Conover, 1976), whereas mammalian digestive systems operate at much lower pH, pH 1 - 2 (Morton, 1979). Therefore, a general bioavailability was considered in this work by using the dilute acid leach to represent the maximum possible bioavailable fraction.

Results for the analyses of the Plymouth aerosol are shown in table 2.7.

Plate 2.5 Electron micrograph of a sodium chloride crystal,
sampled over Ocean Station Lima.

Plate 2.6 Electron micrograph of a particle of "millet-seed"
morphology, sampled in the marine atmosphere
over the English Channel



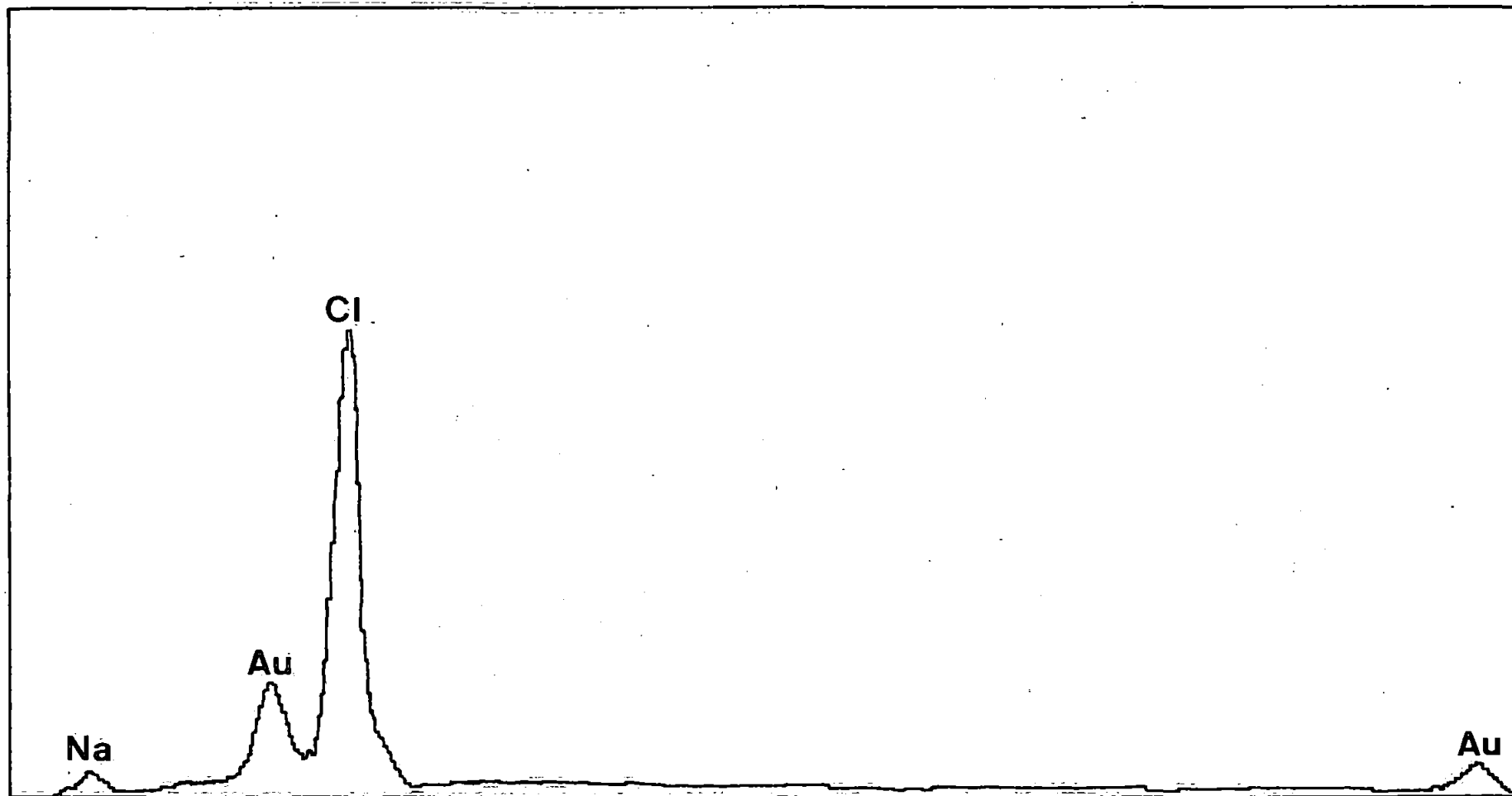


Figure 2.7 Microprobe analyses of the sodium chloride crystal in plate 2.5.
Gold peaks are artefacts of the preparative technique.

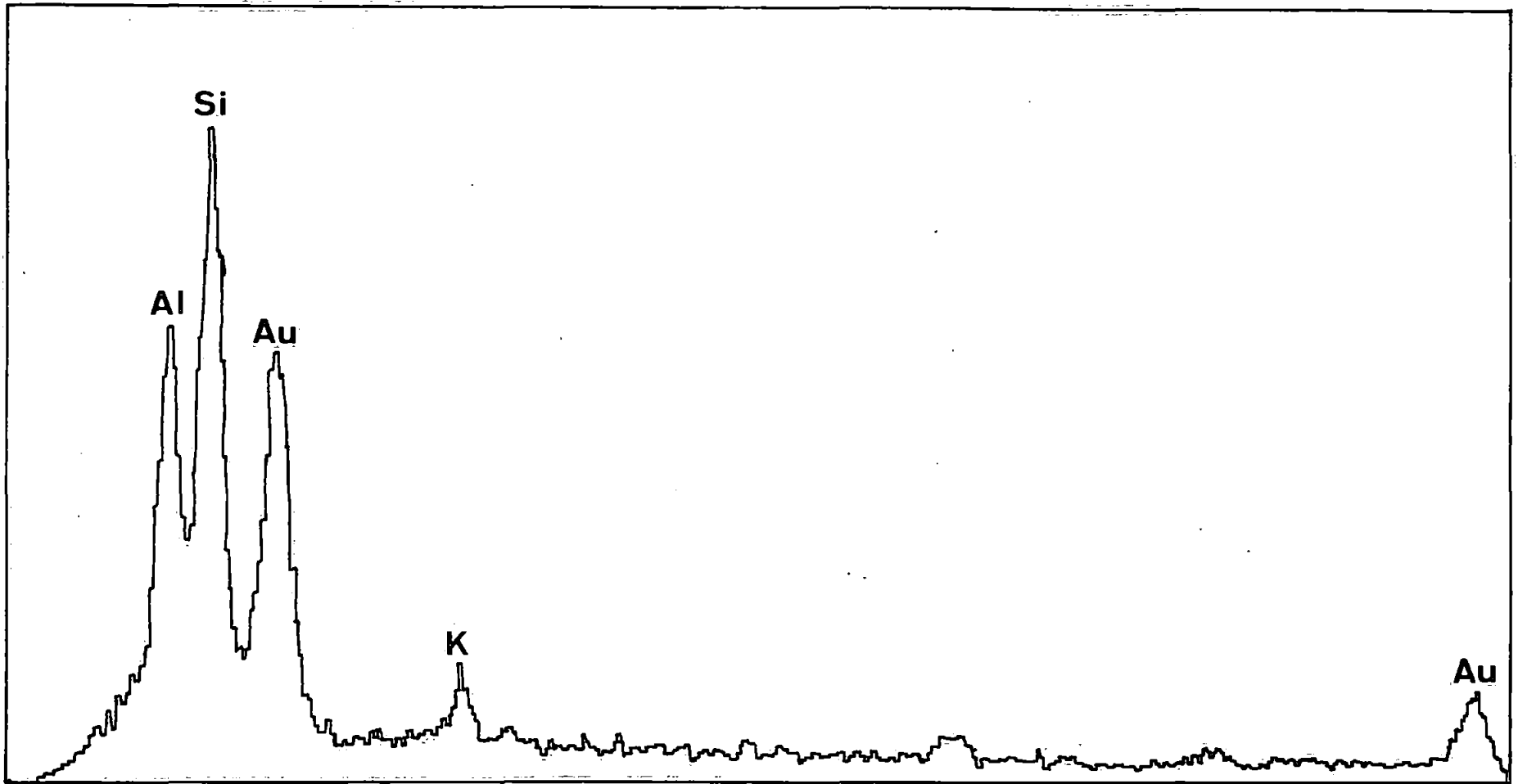


Figure 2.8 Microprobe analysis of the sand particle of "millet-seed" morphology, shown in plate 2.6. Gold peaks are artefacts of the preparative technique.

Plate 2.7 A siliceous test sampled from the aerosol 10 m
above the sea surface.

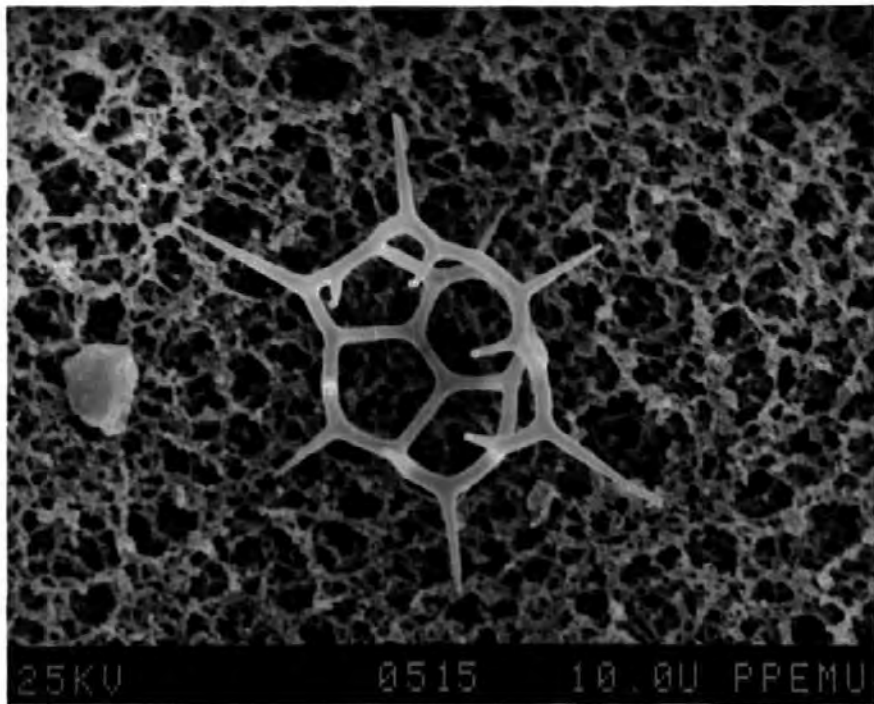


Table 2.7 Analyses of the Plymouth Aerosol

Date	Meter reading m ³	Volume SCM	Air Temp °C	Barometric Pressure mbar	Wind Direction	Windspeed ms ⁻¹	Trace element conc ⁿ ng (SCM) ⁻¹				C.F. (ocean)		
							As	Sb	Na	Mg	As	Sb	Mg
11.11.81	19.96	10.17	11.1	1014	280-300	4	4.7	-	-	-	-	-	-
13.11.81	21.62	11.21	6.0	1022	260-270	2.5	4.8	-	-	-	-	-	-
18.11.81	20.54	10.50	10.0	1044	110-130	12	1.3	-	-	-	-	-	-
19.11.81	21.07	10.85	8.0	1013	100-120	1.5	2.1	-	-	-	-	-	-
23.11.81	18.55	9.48	10.0	1008	190-330	12.5	2.4	-	-	-	-	-	-
14.1.82	16.31	8.44	6.5	1017	100-120	2.5	7.5	-	-	-	-	-	-
15.1.82	16.07	8.23	10.0	1008	100-120	5	4.1	-	-	-	-	-	-
18.1.82	18.00	9.14	12.0	1011	130-140	7.5	< 0.3	-	-	-	-	-	-
19.1.82	20.17	10.24	12.0	1011	115-160	4	1.9	-	-	-	-	-	-
23.3.82	23.54	11.99	11.0	1032	190-210	0.5	< 0.2	-	890	-	1.7 × 10 ³	-	-
23.3.82 - 24.3.82(a)	45.04	22.95	10.9	1033	190-210	1	4.5	-	660	-	5.1 × 10 ⁴	-	-
24.3.82	21.57	11.04	9.6	1033	190-200	1.5	2.5	-	1200	-	1.5 × 10 ⁴	-	-
30.11.82- 1.12.82 (a)	74.33	38.41	7.0	1023	010-030	2.5	1.0	1.0	340	100	2.3 × 10 ⁴	1.7 × 10 ⁵	2.5
1.12.82 - 2.12.82(a)	72.01	37.22	6.9	1017	-	0	1.2	1.0	500	160	1.8 × 10 ⁴	1.1 × 10 ⁵	2.7
8.12.82	19.76	10.08	10.7	993	230-250	7.5	< 0.3	0.59	2800	590	7.9 × 10 ²	1.1 × 10 ⁴	1.7
9.12.82	37.45	19.03	11.8	992	200-220	6	< 0.2	0.07	3400	710	4.3 × 10 ²	1.1 × 10 ³	1.8

(a) Sampled overnight

Table 2.7 continued, Analyses of the Plymouth Aerosol

Date	Meter Reading m ³	Volume SCM	Air Temperature °C	Barometric Pressure mbar	Wind Direction	Windspeed m s ⁻¹	Trace element conc ⁿ ng (SCM) ⁻¹				E.F. (ocean)		
							As	Sb	Na	Mg	As	Sb	Mg
4.7.83	109.92	54.60	18.3	1015	300-360	2.5	<0.05	0.05	590	42	6.2 × 10 ²	5.2 × 10 ³	0.6
5.7.83	33.57	16.50	21.3	1014	150-300	3	0.67	0.79	2300	500	2.2 × 10 ³	1.9 × 10 ⁴	1.8
8.7.83	26.19	12.80	23.1	1011	140-230	3.5	1.4	0.63	<490	550	2.1 × 10 ⁴	7.1 × 10 ⁴	9.5
11.7.83	29.20	14.26	23.2	1015	270-180	3	1.8	0.14	<440	250	3.1 × 10 ⁴	1.8 × 10 ⁴	4.7
12.7.83	30.40	14.72	25.8	1018	060-180	5	0.54	0.07	<430	160	9.3 × 10 ³	8.8 × 10 ³	3.1
18.7.83	30.38	14.90	22	1012	180-270	5	0.27	<0.3	<870	<130	2.2 × 10 ³	2.9 × 10 ⁴	1.4
3.8.83	108.56	54.46	15.4	1022	270-330	1	0.13	0.59	930	160	1.0 × 10 ³	3.5 × 10 ⁴	1.4
8.8.83	106.27	52.30	21.0	1017	330-080	2.5	0.86	0.38	290	110	2.2 × 10 ⁴	7.2 × 10 ⁴	3.1
9.8.83	33.22	16.23	23.2	1016	330-160	5	0.92	0.80	1200	<140	5.6 × 10 ³	3.7 × 10 ⁴	0.9
10.8.83	31.96	15.55	24.3	1014	100-200	5	0.51	2.5	<840	<140	4.5 × 10 ³	1.6 × 10 ⁵	1.4
11.8.83	21.27	10.49	20.5	1013	140-210	3.5	0.57	0.57	<1200	-	3.5 × 10 ³	2.6 × 10 ⁴	-
12.8.83	26.35	12.99	20.4	1012	290-030	5	<0.2	1.2	<1000	-	1.5 × 10 ³	6.6 × 10 ⁴	-
16.8.83	34.21	16.88	20.2	1009	210-280	9.5	0.47	0.71	<770	-	4.5 × 10 ³	5.1 × 10 ⁴	-
17.8.83	30.66	15.13	20.3	1012	160-210	3.5	0.40	0.33	2500	-	1.2 × 10 ³	7.1 × 10 ³	-
18.8.83	33.53	16.41	22.7	1010	080-170	7.5	0.55	1.2	<790	-	5.1 × 10 ³	8.4 × 10 ⁴	-
Geometric mean							0.83	0.45	880	200	6.9 × 10 ³	2.8 × 10 ⁴	1.9
Geometric s.d.							1.9	0.60	865	220			
Arithmetic mean							1.6	0.68	1100	270			

Air temperature was used in conjunction with the pressure correction factor determined in section 2.1.1 to correct the results to s.t.p. Thus, results are given in units of ng (SCM)^{-1} . The concentrations of atmospheric trace substances are usually log normal distributed, so it is appropriate to report the geometric mean and standard deviation of a group of samples. However, if the fluxes of a substance to the land and sea surface are proportional to its atmospheric concentration, then these fluxes should be calculated using the arithmetic mean (NAS, 1978). Therefore, geometric means and standard deviations are reported in this work, although arithmetic means are also quoted for the purpose of flux calculations. The correlation matrix for the Plymouth aerosol is shown in table 2.8. Levels of significance are taken from Murdoch and Barnes (1974). In tables 2.7 and 2.8 the means, enrichment factors have been calculated using "less than" values as actual values (Duce, et al, 1976), therefore the means should be regarded as upper limits to the true mean. For the oceanic enrichment factors, a dissolved arsenic concentration of $1.5 \mu\text{g L}^{-1}$ (Andreae, 1978), and a dissolved antimony concentration of $0.24 \mu\text{g L}^{-1}$ (Bowen, 1979) in seawater were used.

The geometric mean for arsenic in the Plymouth aerosol is $0.83 \text{ ng (SCM)}^{-1}$, the mean for antimony is $0.45 \text{ ng (SCM)}^{-1}$, and the means for sodium and magnesium are $880 \text{ ng (SCM)}^{-1}$ and $200 \text{ ng (SCM)}^{-1}$ respectively. The oceanic enrichment factor for the mean magnesium concentration is 1.9, slightly higher than the oceanic enrichment factor for magnesium in the Bermuda aerosol, 1.2, calculated from the data of Duce and coworkers (1976). The sea may, therefore be a major source of the bulk aerosol material over Plymouth, with smaller contributions from continental and urban sources. The maximum enrichment factor for magnesium over Plymouth is 9.5, indicative of an urban input to the aerosol (see section 2.2.3.2). Using the acid extraction efficiencies determined

Table 2.8 Correlation matrix for the Plymouth aerosol

	Sb	Na	Mg	Air Temperature	Barometric Pressure	Wind Speed
As	0.04	-0.38	-0.08	-0.58 ^a	0.24	-0.18
Sb		-0.02	-0.19	0.03	0.16	0.10
Na			0.80 ^a	0.03	-0.60 ^b	0.53 ^c
Mg				-0.17	-0.82 ^a	0.49

a Significant at the 0.1% level

b Significant at the 1% level

c Significant at the 2% level

from the SRM, an upper limit was assigned to the range of concentrations in the Plymouth aerosol, assuming all the particles were from an urban source (Table 2.9)

Table 2.9 Concentration ranges for elements in the Plymouth aerosol

Element	Extraction efficiency %	Observed concentration range ng (SCM) ⁻¹	Max. concentration range ng (SCM) ⁻¹
As	60	0.05 - 7.5	0.08 - 12.5
Sb	40	0.05 - 2.5	0.13 - 6.3
Na	50	340 - 3400	680 - 6800
Mg	60	42 - 710	70 - 1200

There are only sufficient data for arsenic to examine seasonal differences in atmospheric concentration. The mean for winter months is 1.5 ng (SCM)⁻¹, the mean for summer months 0.5 ng (SCM)⁻¹. This implies that there may be some input of arsenic from local fossil fuel burning during the colder months, in agreement with the observations of Salmon and coworkers (1978). However, the samples collected from the 30th November to the 2nd December 1982, when Plymouth was covered by an inversion layer, do not yield particularly high results, about 1 ng (SCM)⁻¹. In contrast, the results for antimony for the same period, again 1 ng (SCM)⁻¹ are amongst the highest observed for this element, suggesting that Plymouth may contain a significant atmospheric source of this element. The oceanic enrichment factors for arsenic and antimony, 6.9×10^3 and 2.8×10^4 respectively, also show these elements have a source other than the sea, as these enrichment factors are about twenty times higher than those determined for the aerosol over Bermuda (Duce et al, 1976). In contrast, enrichment shows much of the magnesium and sodium in the aerosol to be derived from the sea.

Windroses for each element (figure 2.9) give further evidence for the marine source of sodium and magnesium. Each segment of the windrose

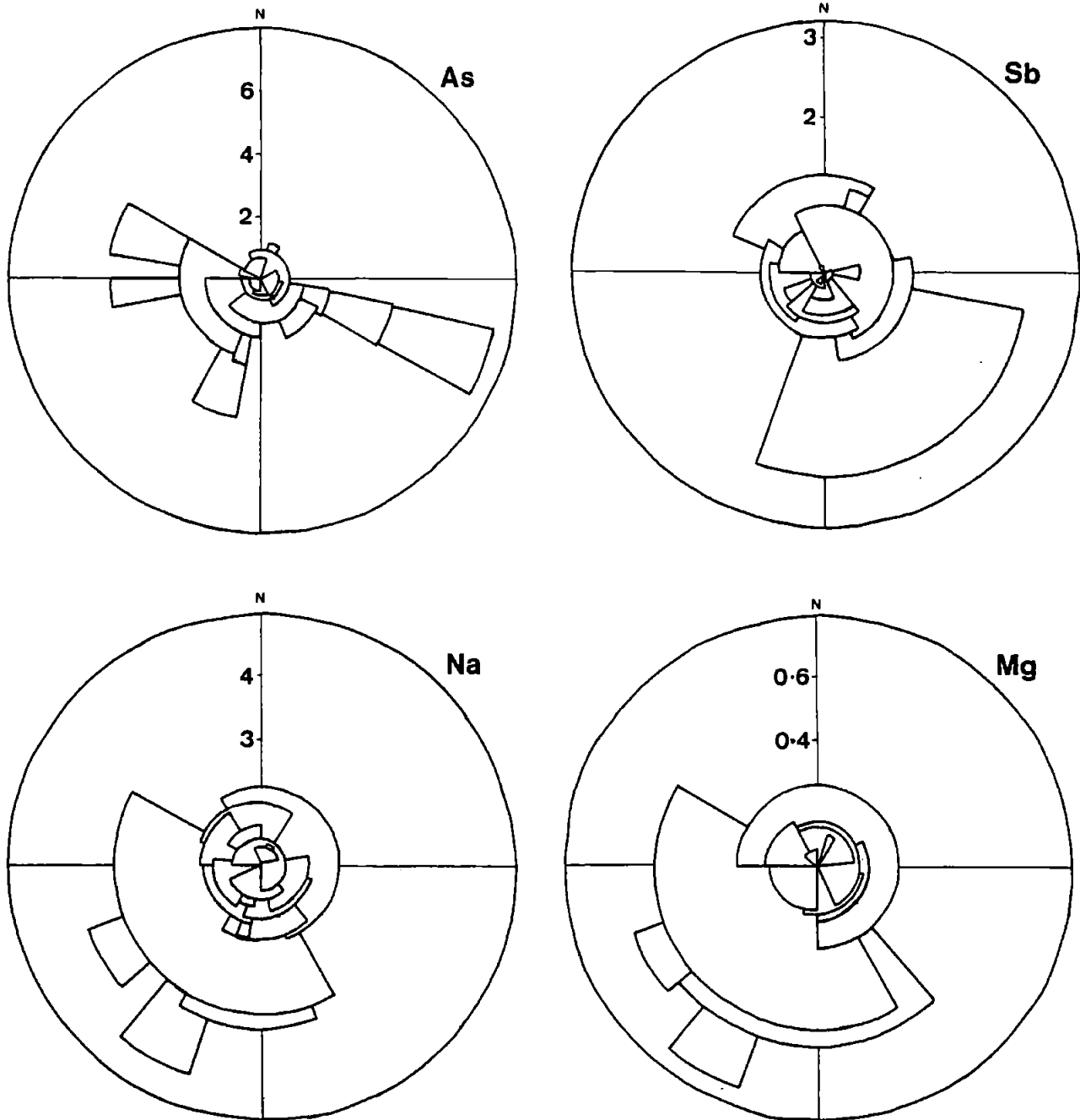


Figure 2.9 Windroses for the Plymouth aerosol. Element concentration is proportional to the radius of the segment arc. Arsenic and antimony are in units of ng (SCM)^{-1} , sodium and magnesium in $\mu\text{g (SCM)}^{-1}$

represents a single sample, with the sampling point at the centre of the rose. Concentration is given by distance from the centre, and the arc of each segment represents the variation in wind direction during sampling. The majority of airmasses over Plymouth with high sodium or magnesium concentrations were associated with south westerly breezes from over the English Channel. Sodium and magnesium are highly correlated (table 2.8), significant at the 0.1% level, and sodium exhibits a weak correlation with windspeed, evidence of aerosol production at the sea surface. Arsenic in the Plymouth aerosol, exhibits two possible sources, one to the west and one to the south east. From the relevant synoptic charts, it appears that the westerly airmasses were derived from over the Atlantic, passing over Cornwall, and the easterly airmasses were derived from the Channel Islands region. The highest concentration of antimony was observed in an airmass that may have come from over the Channel Islands, but the source direction is very imprecise, which complicates the formation of an accurate airmass trajectory. This is probably because the dispersion of aerosol material in maritime sites is often masked by the local sea breeze system (Shair et al, 1982).

The analytical results for the aerosol sampled on the Channel Lightvessel are summarised in table 2.10, and the corresponding correlation coefficients in table 2.11. The geometric mean for arsenic is $1.7 \text{ ng (SCM)}^{-1}$, which is higher than the corresponding results for Plymouth as three samples exceeded the maximum concentration of $7.5 \text{ ng (SCM)}^{-1}$ observed for arsenic in the Plymouth aerosol. Similarly the geometric mean for antimony, $0.8 \text{ ng (SCM)}^{-1}$ exceeds that for antimony in the Plymouth aerosol, although only one sample from the Lightvessel exercise exceeded the maximum antimony concentration over Plymouth, $2.5 \text{ ng (SCM)}^{-1}$. The means for sodium and magnesium, $1100 \text{ ng (SCM)}^{-1}$ and $225 \text{ ng (SCM)}^{-1}$ respectively,

Table 2.10 Analyses of the Aerosol Sampled from the Channel Lightvessel

Date	Meter reading m ³	Volume SCM	Air Temperature °C	Barometric Pressure mbar	Wind Direction	Wind speed m s ⁻¹	Trace element concentration ng (SCM) ⁻¹				E.F. (ocean)		
							Aa	Sb	Na	Mg	Aa	Sb	Mg
2.4.82	23.65	12.07	10.4	1016	220-330	6	< 0.2	1.2	580	120	2.4 × 10 ³	1.2 × 10 ⁵	1.8
3.4.82	37.01	18.90	10.4	1015	160-170	6	< 0.15	0.90	1300	260	3.4 × 10 ²	3.6 × 10 ⁴	1.7
4.4.82	36.70	18.73	10.5	1011	100-120	7	1.4	2.1	590	190	1.7 × 10 ⁴	1.9 × 10 ⁵	2.6
5.4.82	22.13	11.28	10.8	1009	020-150	4	1.6	2.7	760	140	1.5 × 10 ⁴	3.3 × 10 ⁵	1.5
6.4.82	24.00	12.26	10.3	1010	180-190	8.5	4.2	0.73	640	64	4.8 × 10 ⁴	6.5 × 10 ⁴	0.8
8.4.82	37.33	19.07	10.3	1016	310-340	6.5	10.0	0.73	2300	380	3.2 × 10 ⁴	1.7 × 10 ⁴	1.4
10.4.82	34.34	17.59	9.5	1020	320-330	7	6.3	0.91	2100	350	2.1 × 10 ⁴	2.4 × 10 ⁴	1.4
11.4.82	40.79	20.81	10.6	1020	320-010	4.5	9.1	0.23	1500	270	4.5 × 10 ⁴	8.6 × 10 ³	1.5
12.4.82	40.87	20.97	9.0	1020	360-035	6	< 0.1	< 0.2	790	350	1.3 × 10 ³	1.3 × 10 ⁴	3.6
13.4.82	33.10	17.04	8.0	1023	010-030	3.5	11.0	0.79	2500	500	3.2 × 10 ⁴	1.7 × 10 ⁴	1.7
Geometric mean							1.7	0.80	1100	225	1.1 × 10 ⁴	4.0 × 10 ⁴	1.7
Geometric s.d.							4.9	0.79	745	130			
Arithmetic mean							4.4	1.0	1300	260			

Table 2.11 Correlation matrix for the Channel Lightvessel aerosol

	Sb	Na	Mg	Air Temperature	Barometric Pressure	Windspeed
As	-0.72 ^b	0.87 ^a	0.80 ^a	-0.57	0.87 ^a	-0.27
Sb		-0.44	-0.38	0.34	-0.65	-0.27
Na			0.85 ^a	-0.52	0.68	-0.29
Mg				0.75 ^b	0.82 ^a	-0.41

a - significant at the 1% level

b - significant at the 2% level

both exceed those for the Plymouth aerosol, although the oceanic enrichment factor for magnesium, 1.7, is higher than would be expected for an uncontaminated marine aerosol. However, it is slightly lower than the oceanic enrichment for magnesium in the Plymouth aerosol. The enrichment factors for arsenic and antimony, 1.1×10^4 and 4.0×10^4 respectively, are both much higher than was observed in an open ocean environment (Duce, et al, 1976), so a continental or pollutant component is probable. However, the high correlation coefficients exhibited by arsenic between sodium and magnesium are indicative of a marine origin. This relationship is most striking in the windroses in figure 2.10. Arsenic, sodium and magnesium all show a northerly source. In contrast, the source for antimony is to the east. Analysis of the relevant synoptic charts shows the northerly airmasses to have transported material from south and south west England, and the easterly airmasses to have transported material from Europe. The high negative correlation coefficient between arsenic and antimony, -0.72, is surprising as they are geochemically very similar (Onishi, 1969a and 1969b), and often fall into the same group if subject to factor analysis to determine aerosol source (Li, 1981b), so this is probably due to different local sources for each. As no marine sample had an oceanic enrichment factor for magnesium greater than that of the crustal aerosol, the correction for urban source was not applied. Of the thirteen samples analysed from Ocean Station Lima (table 2.12), only five showed detectable levels of arsenic, and only one showed a detectable level of antimony. Therefore, the geometric means of $0.075 \text{ ng As (SCM)}^{-1}$ and $0.086 \text{ ng Sb (SCM)}^{-1}$ should be considered as upper limits to the true mean. Oceanic enrichment factors are of the same order of magnitude as those determined for the aerosol over Bermuda, 3.5×10^2 for arsenic and 1.1×10^3 for antimony (Duce et al, 1976). The oceanic enrichment factor for magnesium, 1.3, and the very high

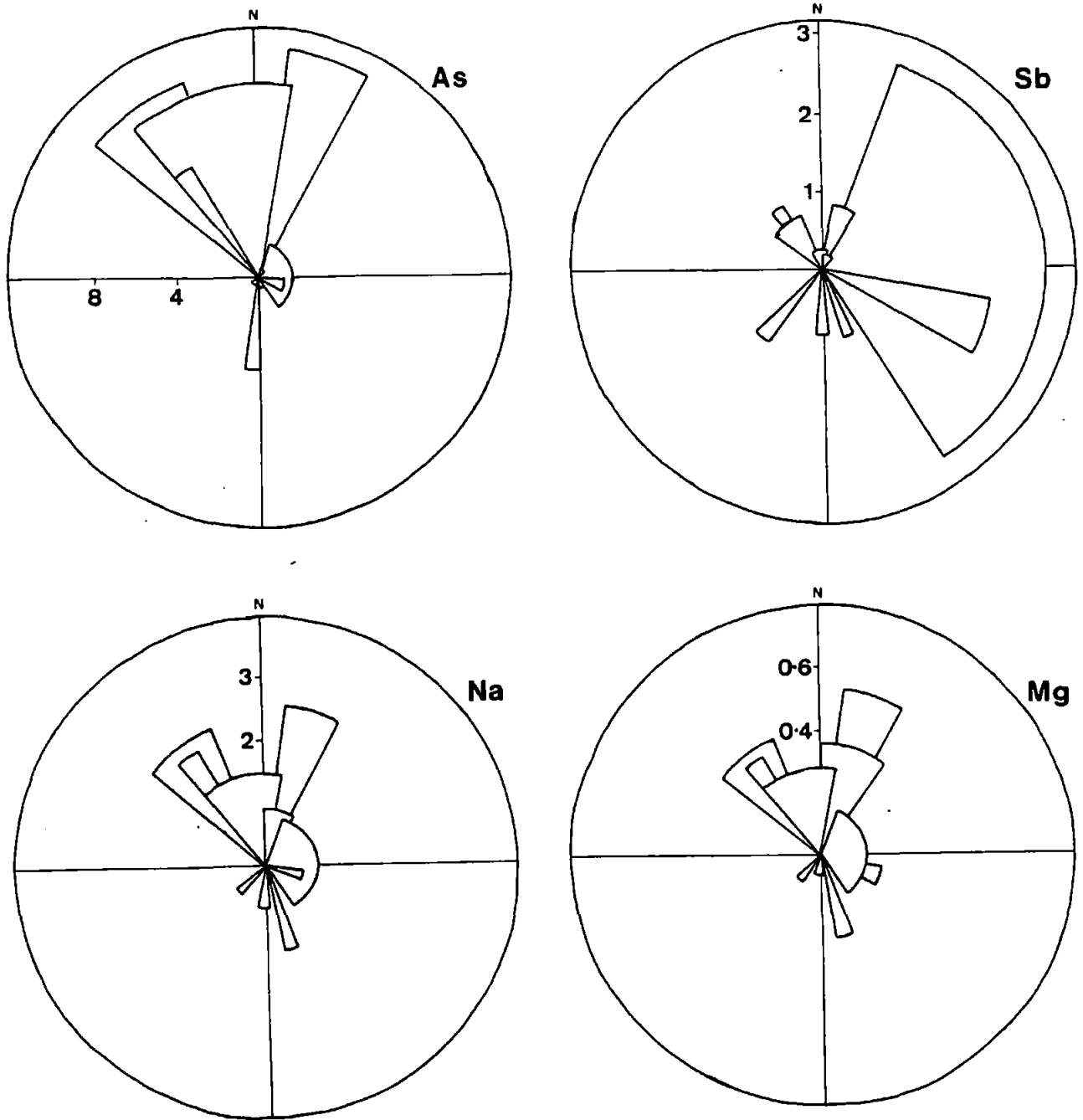


Figure 2.10 Windroses for the aerosol sampled over the Channel Lightvessel. Arsenic and antimony are in units of ng (SCM)^{-1} , sodium and magnesium in units of $\mu\text{g (SCM)}^{-1}$

Table 2.12 Analyses of the Aerosol Sampled at Ocean Station Lima

Date	Meter reading m ³	Volume SCM	Air Temperature °C	Barometric Pressure mbar	Wind Direction	Wind Speed m s ⁻¹	Trace element concentration ng (SCM) ⁻¹				E.F. (ocean)		
							As	Sb	Na	Mg	As	Sb	Mg
8.3.83	27.26	13.96	9.5	1008	170-220	10.2	0.29	<0.4	4400	720	4.8 × 10 ²	5.3 × 10 ³	1.4
9.3.83	52.14	26.69	9.7	1013	180-210	8.3	0.17	<0.2	3600	570	3.4 × 10 ²	3.2 × 10 ³	1.3
12.3.83- 13.3.83	101.67	52.28	8.4	995	160-320	7.4	0.04	<0.1	860	210	3.8 × 10 ²	6.8 × 10 ³	2.0
13.3.83- 14.3.83	103.77	53.78	6.2	997	270-320	11.8	<0.04	<0.1	2250	320	1.2 × 10 ²	2.6 × 10 ³	1.2
14.3.83- 15.3.83	104.07	53.70	7.4	1007	180-330	8.3	<0.04	<0.1	860	130	3.3 × 10 ²	6.9 × 10 ³	1.3
15.3.83- 16.3.83	104.30	53.50	9.1	999	200-240	9.7	0.36	<0.07	1150	150	2.3 × 10 ³	3.4 × 10 ³	1.1
17.3.83- 18.3.83	93.21	48.30	6.2	1012	250-300	8.9	0.06	<0.08	2400	360	2.1 × 10 ²	1.8 × 10 ³	1.3
18.3.83- 19.3.83	83.21	43.12	6.2	1011	130-320	8.8	<0.05	<0.09	3200	580	1.1 × 10 ²	1.5 × 10 ³	1.5
22.3.83- 23.3.83	116.50	60.50	5.6	1000	110-020	12.0	<0.03	<0.06	2800	490	8.8 × 10 ¹	1.2 × 10 ³	1.4
23.3.83	67.51	35.06	5.6	1013	320-350	15.3	<0.06	0.11	4000	480	1.1 × 10 ²	1.4 × 10 ³	1.0
25.3.83- 26.3.83	103.43	53.30	7.8	1014	190-280	12.2	<0.04	<0.02	2500	290	1.1 × 10 ²	3.0 × 10 ²	1.0
28.3.83	40.10	20.56	9.2	1011	240-250	10.4	<0.1	<0.05	1500	230	4.7 × 10 ²	1.3 × 10 ³	1.3
31.3.83	42.45	21.87	7.9	1022	300-360	7.3	<0.09	<0.05	2900	390	2.3 × 10 ²	6.6 × 10 ²	1.1
Geometric mean							0.075	0.086	2200	340	2.5 × 10 ²	2.2 × 10 ³	1.3
Geometric s.d.							0.11	0.10	1150	180			
Arithmetic mean							0.11	0.11	2500	380			

correlation between sodium and magnesium, 0.93, shown in table 2.13, show that the aerosol in this area is predominantly of marine origin. Mean concentrations for sodium and magnesium are $2200 \text{ ng (SCM)}^{-1}$ and $340 \text{ ng (SCM)}^{-1}$ respectively. As the correlations for arsenic and antimony are extensively based on "less than" values, they hold little real significance. Wind roses (figure 2.11) show those airmasses with high concentrations of the two atmophiles to be associated with westerly or southwesterly winds, transporting material from the North American continent. There is no strong dependancy on direction for either sodium or magnesium.

Analyses for the samples collected on board R.V. "Frederick Russell" are summarised in table 2.14. The transect numbers refer to the transects enumerated in figure 2.3. Geometric means for arsenic and antimony are $0.24 \text{ ng (SCM)}^{-1}$ and $0.12 \text{ ng (SCM)}^{-1}$ respectively, both lower than the Plymouth and Channel Lightvessel means. However, the means for sodium and magnesium, $4100 \text{ ng (SCM)}^{-1}$ and $585 \text{ ng (SCM)}^{-1}$ respectively, are higher than those for any of the previous sampling exercises. The lowest concentrations for arsenic were observed from transects 7, 8 and 9, in open ocean outside the English Channel. This reflects the strong dependancy of the atmospheric arsenic concentration on the proximity of a continental source, illustrated in figure 2.12 which shows the Frederick Russell data with the mean data for Plymouth, the Channel Lightvessel and Ocean Station Lima. Although the highest results for antimony are both very close to shore, the above relationship is not as obvious as that for arsenic, as there are more low antimony concentrations close to shore. This may reflect a shorter atmospheric residence time for antimony than for arsenic, with less of the former element reaching the atmosphere of the English Channel from the surrounding landmass. The oceanic enrichment factors for arsenic and antimony are the lowest

Table 2.13 Correlation matrix for the O.S. Lima samples

	Sb	Na	Mg	Air Temperature	Barometric Pressure	Windspeed
As	0.51	0.11	0.13	0.66 ^b	-0.1	-0.14
Sb		0.53	0.64 ^b	0.41	-0.09	-0.07
Na			0.93 ^a	-0.13	0.46	0.38
Mg				-0.07	0.30	0.17

a - significant at the 0.1% level

b - significant at the 2% level

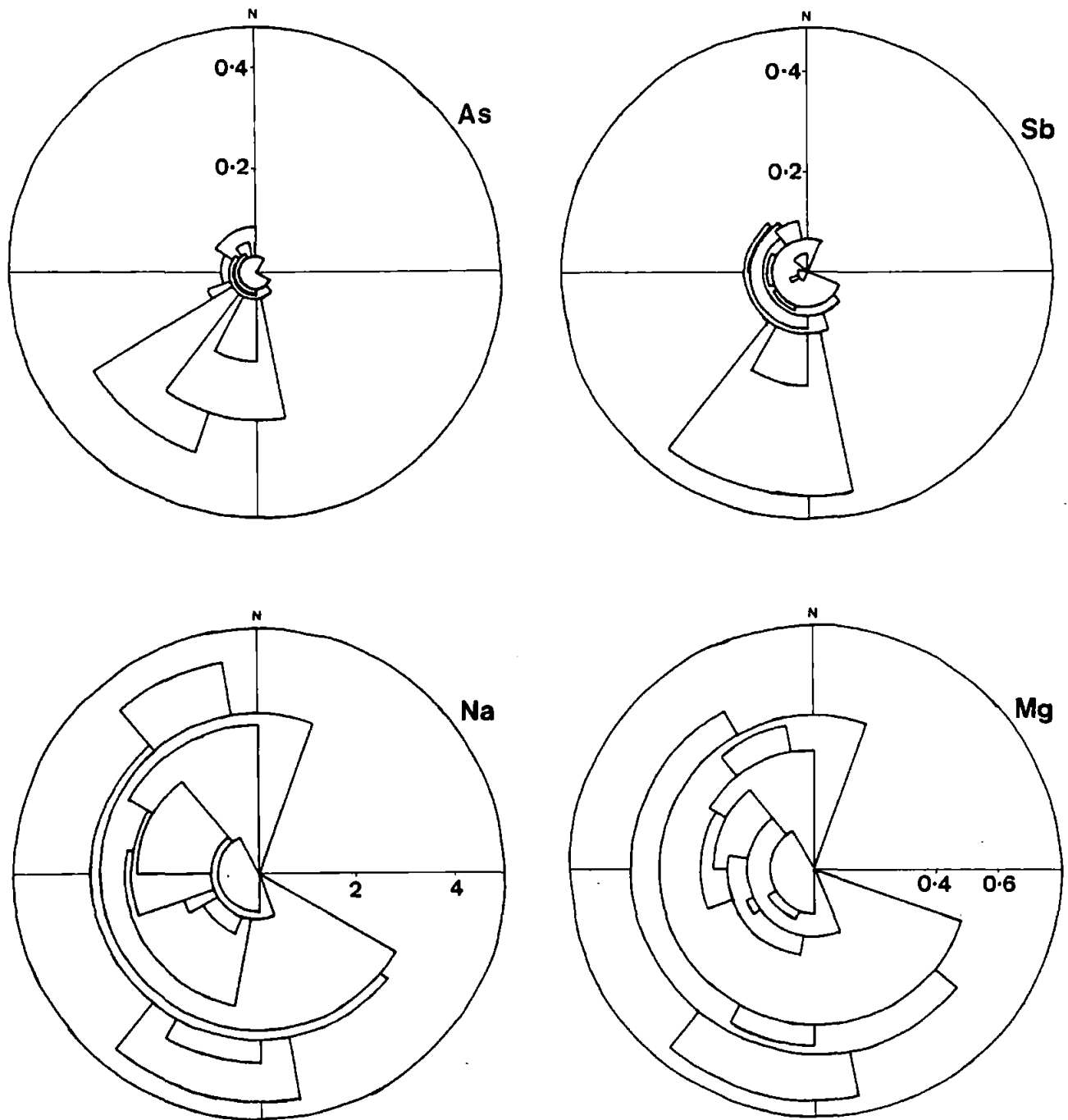


Figure 2.11 Windroses for the aerosol sampled at Ocean Station Lima. Arsenic and antimony are in units of ng (SCM)^{-1} , sodium and magnesium in units of $\mu\text{g (SCM)}^{-1}$

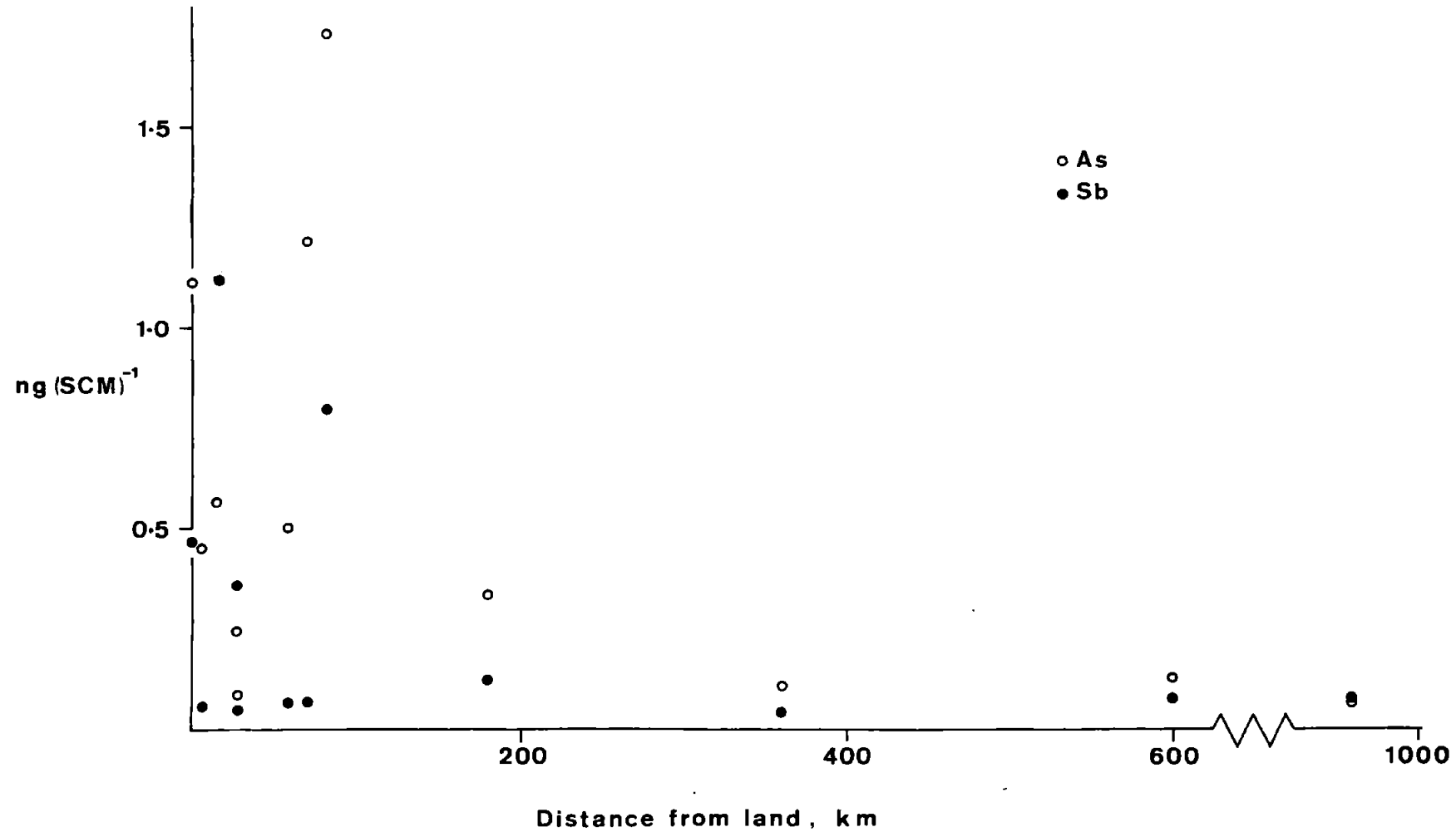


Figure 2.12 Depression of aerosol arsenic and antimony with distance from land. Data include samples taken on board R.V. "Frederick Russell", and mean data for Plymouth, the Channel Lightvessel and Ocean Station Lima

observed in this work, 4.3×10^2 and 1.6×10^3 respectively, and are comparable to those calculated for the Bermuda aerosol (Duce, et al, 1976). Similar sources may be operative at both locations.

The only significant correlation to emerge from these data is the very high correlation, 0.91, between sodium and magnesium (table 2.15). This indicates a probable marine origin for the bulk of the aerosol. The magnesium enrichment factor, 1.2, is the same as that derived from the data of Duce and coworkers (1976), which were also for a marine region. As the samples were not collected from a sampling station, but from a series of transects extending over 1000 km, it was deemed inappropriate to consider source directions by use of wind roses, as the use of such diagrams should be restricted to single point stations, or very small sampling areas.

The results from the Channel Lightvessel and Frederick Russell were combined to assess the overall concentrations in the English Channel atmosphere. The overall geometric means for arsenic and antimony are $0.67 \text{ ng (SCM)}^{-1}$ and $0.32 \text{ ng (SCM)}^{-1}$ respectively; arithmetic means are $2.5 \text{ ng (SCM)}^{-1}$ and $0.66 \text{ ng (SCM)}^{-1}$ respectively. Again, the most significant correlation is that between sodium and magnesium, at 0.93 (table 2.16). There is a significant correlation between sodium and windspeed, probably due to the mechanism of aerosol generation at sea. The significant negative correlation between arsenic and air temperature will be discussed later.

2.3.2.2 Seawater leaching

The analyses of the seawater leachates are summarised in table 2.17. The levels of antimony were too low for detection by the hydride generation

Table 2.15 Correlation matrix for the samples from the "Frederick Russell" voyage

	Sb	Na	Mg	Air Temperature	Pressure	Windspeed
As	0.14	0.63	0.36	-0.65	-0.27	0.66
Sb		-0.23	-0.20	0.28	0.38	0.39
Na			0.91 ^a	-0.57	0.01	0.43
Mg				-0.052	0.16	0.39

a - significant at the 0.1% level

Table 2.16 Correlation matrix for the English Channel aerosol

Combined data from the Channel Lightvessel and "Frederick Russell" voyages

	Sb	Na	Mg	Air Temperature	Pressure	Windspeed
As	0.09	-0.18	-0.16	0.60 ^b	0.48	-0.44
Sb		-0.41	-0.36	-0.48	0.19	-0.37
Na			0.93 ^a	0.41	-0.28	0.61 ^b
Mg				0.32	-0.11	0.53

a - significant at the 0.1% level

b - significant at the 1% level

Table 2.17 Analyses of seawater leachate by hydride generation

Weight of SRM sample (mg)	Concentration of element in seawater leachate (ng ml ⁻¹) ^a		Total of element in 25 ml seawater (ng)	Total in SRM sample (ng)	Percentage extraction
	As	Sb	As	As	As
7.3	9	BDL ^b	225	840	27
8.9	9	BDL	225	1024	22
				Mean	25

a) Seawater blanks were below detection limit

b) below detection limit

Detection limits for technique As : 2 ng ml⁻¹

Sb : 4.5 ng ml⁻¹

method. However, about 25% of the total arsenic in the SRM is seawater soluble. Crecelius (1980) found 23% of arsenic from a sample of industrial flyash to be soluble in seawater. The composition of such flyash is probably similar to that of the SRM. Twenty percent of the SRM consists of sulphate, nitrate and ammonia, so a large fraction of the SRM may be soluble in seawater. Therefore, direct comparison of the acid digests of the leachate residue with those on the untreated SRM is meaningless. As 60% of the total arsenic in the SRM is acid soluble, and 25% was lost to the seawater, 35% remains in an acid soluble form after the seawater leach. Using the analyses of the residual SRM from the seawater leach it is possible, therefore, to estimate the percentage loss of antimony to the seawater, summarised in table 2.18. About 13% of the total antimony in the SRM remains in an acid extractable form after the seawater leach. However, only 40% of the total antimony in the SRM is acid soluble, so the difference, about 27%, must be lost to the seawater. This compares favourably to the solubility of 24% determined for antimony from flyash (Creelius, 1980). These solubilities may be used to determine atmospheric fluxes to the dissolved phase in seawater. As 60% of the total arsenic and 40% of the total antimony in the urban dust was acid soluble, dissolved to particulate ratios of 25 : 35 for arsenic and 27 : 13 for antimony were used to calculate the deposition fluxes to the English Channel. Thus, about 40% of the available arsenic and 67% of the available antimony are regarded as seawater soluble, assuming the aerosol material to come from an urban source.

Table 2.18 Estimation of Antimony in the Residual SRM as an Acid-soluble Fraction

Weight of residual SRM after seawater leaching (mg) (a)	As acid-leached from the SRM residue (ng)	Total As in SRM (ng) (b)	Total Sb in SRM (ng) (c)	Sb, acid-leached from SRM residue (ng)	Fraction of total Sb in acid leach, %
1.0	200	571	223	30	13.5
1.2	230	657	257	30	12.0

a) Partial recovery of residue only

b) Assuming As in acid leach represents 35% of total As in the SRM (see text)

c) As : Sb (total) = 115:45

2.4 DISCUSSION

2.4.1 The Atmospheric Aerosol

Although the major source of sodium and magnesium in the Plymouth aerosol is most probably the sea, the sources of arsenic and antimony are less well defined. There appear to be two major sources of arsenic, one approximately south east of the city, the other to the west. To the east there is an active cement manufacturing plant and an old power station. The latter fell into disuse prior to the onset of this work, leaving the cement plant as the major local industrial source to the east. To the west lie the naval dockyards, which could be a source of emissions, through the burning of fuel oils. However, Walsh and coworkers (1979b) list the mining of mineral ores as a more significant source of arsenic emissions than the burning of fuel oils. To the west, in Cornwall, there are still several active mining concerns, mostly extracting tin. Arsenopyrite occurs with cassiterite, the major ore for tin, in the hypothermal zones of the mineralisation in south west England, whereas stibnite is found in the cooler epithermal zones (Edmonds et al, 1975). Therefore, the Cornish tin mines could be a major local source of atmospheric arsenic, but not necessarily antimony.

The highest concentration of antimony was observed in an airmass with a southeasterly source. This could be due to emissions from the cement plant, or may be from a more distant source across the Channel. Apart from this one sample, antimony does not exhibit a strong dependency on wind direction in Plymouth. Samples taken during an inversion over the city showed antimony concentrations well above the mean for the Plymouth aerosol. The city itself is the major local source of atmospheric antimony, probably through fossil fuel combustion, which would give a source well diffused throughout the city.

Fossil fuel combustion is also the most probable source of the combustion

particles and some of the sulphate particles viewed under the electron microscope. However, the calcium sulphate particles are probably of marine origin, as they are common in the marine aerosol, even in areas remote from anthropogenic influence, such as Ocean Station Lima. Calcium and sulphate are both plentiful in solution in the sea, although calcium sulphate itself is not very soluble, solubility about 3 mg ml^{-1} (Weast, 1980), so would readily crystallise from evaporating seawater droplets. Sodium chloride is far more soluble, so would require far less humid conditions before crystallisation. The evidence of this work supports the data of Duce and coworkers (1976), in which magnesium showed an enrichment over sodium in the marine aerosol, in contrast to the findings of Barker and Zeitlin (1972) and Chesselet and coworkers (1972), who reported depletion of magnesium in this environment.

Samples collected on board the "Frederick Russell" show diminution of atmospheric arsenic and antimony with increasing distance from land, so even in the marine aerosol over the remote open ocean, both may be derived from continental sources, rather than the sea.

Thus, the low concentrations at Ocean Station Lima may simply be a consequence of the remoteness of this site from any landmass. However, lithophile elements are more abundant over the Atlantic in low latitudes than in high latitudes, due to the influence of the Trade winds (Chester, 1982), so the low levels at Ocean Station Lima may be partly due to the lower levels of crustal material associated with the Westerly winds. Despite this, crustal enrichment factors for atmophile elements are higher in high latitudes than in low latitudes over open ocean (Lantzy and Mackenzie, 1979), probably because of dilution of the background aerosol by crustal aerosols at lower latitudes (Chester et al, 1983). This is because atmophile elements are enriched in the background aerosol (Maenhaut et al, 1979; Zoller et al, 1974), although their absolute

concentrations are very low.

The high levels observed at the Channel Lightvessel site are associated with maritime (i.e. mixed marine and continental) rather than true marine airmasses. Those airmasses high in arsenic were derived from over south and southwest England, so again Cornish tin mining may be a potential source. The high correlation between arsenic and sodium is of interest, as this would be expected if arsenic was derived from the sea, which contradicts the other results. It may, however, be an effect of partitioning between aerosol phase and vapour phase arsenic. Player and Wouterlood (1982) have shown that only 10% of an arsenic smelter emission could be removed as particulate phase within the stack; the remainder rapidly condensed onto available aerosol material after emission. As sodium chloride dominates the aerosol in marine and possibly maritime regions, such arsenic emissions would condense onto a sodium rich particulate phase, thereby forming an association between the two elements. In the correlations for the Plymouth aerosol, and the total Channel aerosol samples, arsenic was significantly negatively correlated against temperature, and showed a significant positive correlation against barometric pressure over the Channel Lightvessel. Both parameters may control a vapour-particulate partition, an increase in temperature favouring the vapour phase, an increase in pressure favouring the particulate phase, which are relationships supported by the observed correlations. The positive correlation between arsenic and temperature over Ocean Station Lima is unreliable, because of the imprecision in the data for the atmophile elements.

Although antimony is volatilised by high temperature processes (Creelius, 1975; Lantzy and Mackenzie, 1979), it is less volatile than arsenic; Sb_2O_3 sublimes at $1550^{\circ}C$, As_2O_3 at $193^{\circ}C$ (Weast, 1980). Thus,

antimony may already be in particulate form on emission, and not form associations with sodium. Antimony shows no relationship with air temperature and barometric pressure, so it is probable that there is little interaction between vapour phase and aerosol phase, in the manner proposed for arsenic. The source for antimony over the Channel Light-vessel is to the east, possibly the Channel Islands or Europe. This could be the same as for the south easterly, antimony - rich air mass over Plymouth. Therefore, although aerosol arsenic and antimony over marine regions are both probably of continental origin, they may be of different local source in the English Channel area.

2.4.2 Flux Calculations

The data from section 2.3.2 may be used to estimate fluxes from the atmosphere to the land and sea surfaces, and fluxes between different airmasses. As such fluxes are proportional to the atmospheric concentration, it is appropriate to use arithmetic means for these calculations (NAS, 1978).

2.4.2.1 Deposition from the atmosphere

Two methods may be used to calculate the downflux of material to the oceans and land surface. The first is to use a particle settling velocity, averaged between wet and dry deposition, of 1 cm sec^{-1} (Buat-Menard and Chesselet, 1979; Chester, 1982; Millward and Griffin, 1980). The settling velocity of 1 cm sec^{-1} is used for particles of submicron size. If larger particles are considered, such as continental particles often associated with aluminium, then a higher settling velocity of 1.5 cm sec^{-1} should be used (Chester, 1982). Arsenic and antimony are generally concentrated in submicron particles (Duce *et al*, 1976; Maenhaut *et al*, 1979), so the lower settling velocity was preferred. The downward flux (F_d) then becomes the product of the concentration near the sea or land surface (C_0) and the averaged aerosol settling velocity (V_a), shown in equation 2.1.

$$F_d = C_o \times V_a \quad (2.1)$$

In the second method, it is assumed that the atmosphere is washed clean forty times a year, from the average residence time of water vapour in the atmosphere, from a scale height of 5000 m (Bruiland et al, 1974; Chester, 1982; Goldberg, 1975; Millward and Griffin, 1980). Thus, the flux (F_w) is the product of the concentration over the land or sea surface (C_o), the scale height (S) and the washout rate, shown in equation 2.2.

$$F_w = C_o \times S \times 40 \text{ yr}^{-1} \quad (2.2)$$

Where localised fluxes are considered, estimates of local washout rates may provide a better estimate for the local flux. For the global averaged rainfall, 4.5×10^{20} g rainwater falls each year (Garrels et al, 1973) over the Earth's surface, $510.1 \times 10^6 \text{ km}^2$ (Turekian, 1976), to give an average annual rainfall of 880 mm. The average rainfall, over 1982 and 1983, for Plymouth was 883 mm. Therefore, the globally averaged washout rate provides a good approximation to local fluxes in this area. If fluxes into coastal waters, such as the English Channel are considered, then the seawater solubility of arsenic and antimony from urban dust may be used to estimate the contribution of the depositional fluxes to the dissolved and particulate phases in seawater, assuming all the aerosol material to come from an urban source.

Average concentrations for arsenic and antimony over Plymouth, the English Channel and Ocean Station Lima have been used to calculate the fluxes of each at those locations. For the English Channel, the seawater solubility of 40% of available arsenic and 67% of available antimony were used to assess the contribution of each to the dissolved phase. The resultant fluxes are summarised in table 2.19. Considering the crude assumptions involved in the two methods, there is reasonable agreement between them. The averaged wet and dry deposition method (equation 2.1,

Table 2.19 Depositional Fluxes from the Atmosphere

Location	Average Concentration ng (SCM) ⁻¹	Fluxes. $\mu\text{g m}^{-2} \text{yr}^{-1}$ Method I			Fluxes $\mu\text{g m}^{-2} \text{yr}^{-1}$ Method 2		
		Available	Dissolved ^a	Particulate ^a	Available	Dissolved ^a	Particulate ^a
<u>Arsenic</u>							
Plymouth	1.6	505	-	-	320	-	-
English Channel	2.5	790	329	461	500	208	292
O.S. Lima	0.11	35	-	-	22	-	-
<u>Antimony</u>							
Plymouth	0.68	215	-	-	136	-	-
English Channel	0.66	208	140	68	132	89	43
O.S. Lima	0.11	35	-	-	22	-	-

a) Dissolved and particulate fluxes only valid for coastal waters

method 1 on table 2.19) yields results a factor of 1.6 higher than those obtained using the washout equation (equation 2.2, method 2 on table 2.19). So about $400 \mu\text{g As m}^{-2} \text{ yr}^{-1}$ fall onto Plymouth, and about $200 \mu\text{g Sb m}^{-2} \text{ yr}^{-1}$. The flux into the English Channel is about $650 \mu\text{g As m}^{-2} \text{ yr}^{-1}$ and about $150 \mu\text{g Sb m}^{-2} \text{ yr}^{-1}$. Arsenic fluxes are summarised in figure 2.13, and antimony fluxes in figure 2.14. These fluxes into the English Channel may be compared to riverine fluxes from the Tamar. The English Channel covers an area of about $5 \times 10^{10} \text{ m}^2$. Thus, about 30 t of arsenic falls into the Channel each year, of which 40% is soluble in seawater. Therefore, the atmospheric flux of arsenic to the dissolved phase in the English Channel is 12 t yr^{-1} . The average discharge rate of the Tamar into the English Channel is about $30 \text{ m}^3 \text{ s}^{-1}$ (Ackroyd, 1983). The Tamar has a comparatively high dissolved arsenic load, with about $3 \mu\text{g L}^{-1}$ in the saline water flowing into Plymouth Sound (Marsh, 1983). Thus, the Tamar delivers about 3 t As yr^{-1} in the dissolved phase to the English Channel, so the atmospheric contribution to dissolved arsenic in the English Channel is quadruple that of a major arsenic-bearing river.

About 7.5 t Sb yr^{-1} is lost to the English Channel from the atmosphere, of which 67% is soluble. Thus, the atmospheric flux of antimony to the dissolved burden in the English Channel is 5 t yr^{-1} . Again, this may be compared to the flux from the Tamar. Dissolved antimony concentrations in the Tamar are about an order of magnitude lower than dissolved arsenic concentrations (Russell, 1984), so the annual flux is about 0.3 t yr^{-1} . Atmospheric deposition, therefore, is over fifteen times more important as a source for dissolved antimony in the English Channel, than is the outflow of a major river. Dissolved arsenic and antimony fluxes from many major rivers flowing into the English Channel, such as the Seine, are unquantified, so it is not yet possible to attempt a realistic budget

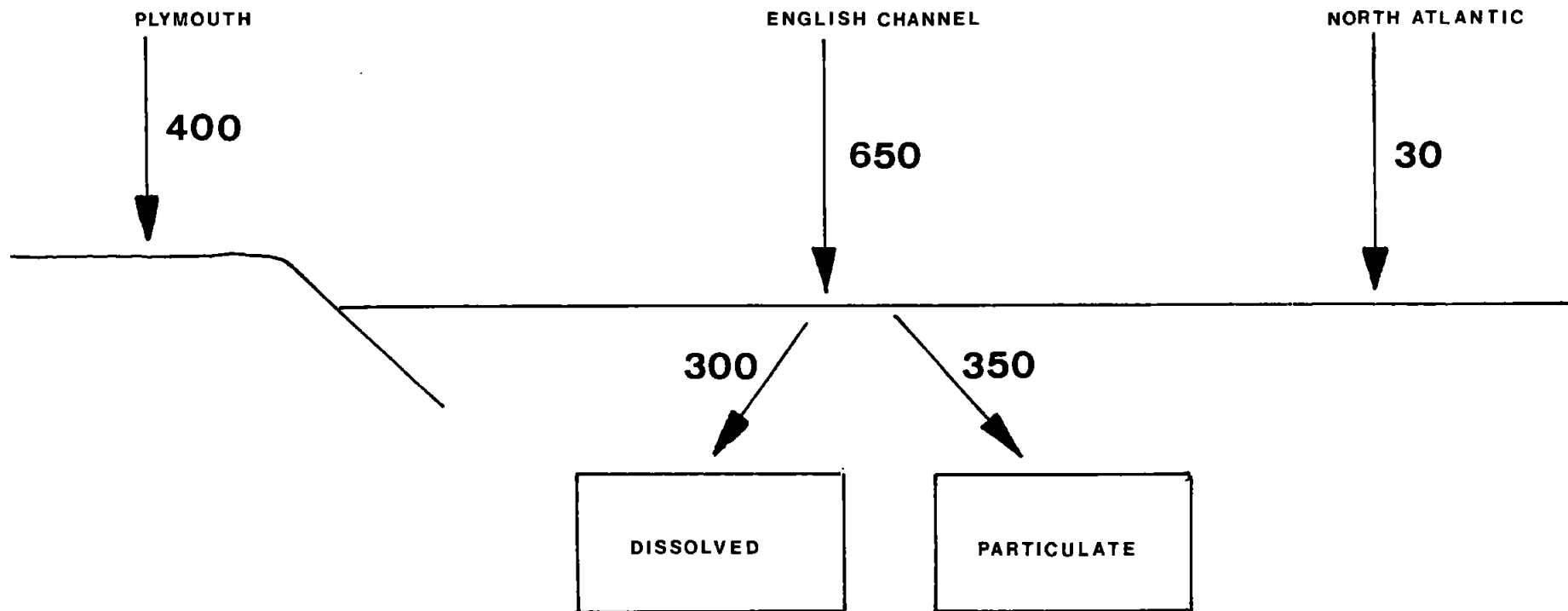


Figure 2.13 Average depositional fluxes of arsenic in $\mu\text{g m}^{-2} \text{yr}^{-1}$

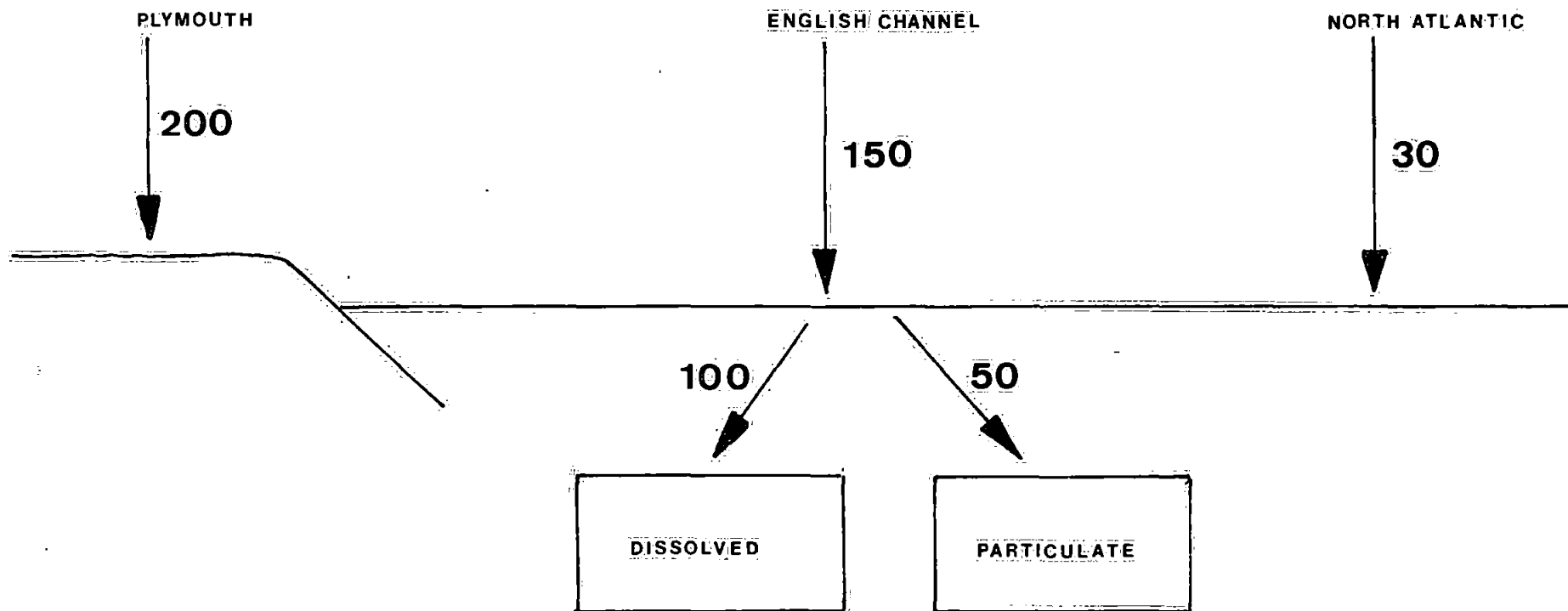


Figure 2.14 Average depositional fluxes of antimony in $\mu\text{g m}^{-2} \text{yr}^{-1}$

for arsenic and antimony in the English Channel. However, it would seem that atmospheric transport of arsenic and antimony is less important than it is for mercury, as Windom and Taylor (1979) found atmospheric transport of mercury to be eight times higher than the total river transport to the South Atlantic Bight.

Fluxes at Ocean Station Lima are about $30 \mu\text{g m}^{-2} \text{yr}^{-1}$ for both arsenic and antimony. The North Atlantic has an area of about $46 \times 10^{12} \text{m}^2$, so fluxes to the North Atlantic are about 1.4kt yr^{-1} for both arsenic and antimony. This is about twice the flux of mercury to the North Atlantic determined by Millward and Griffin (1980). Walsh and coworkers (1979b) calculated an arsenic flux of 2.2kt yr^{-1} to the oceans in the northern hemisphere. The concentrations for arsenic and antimony in this work yield a flux of 3.7kt yr^{-1} for each to the northern oceans, which is in reasonable agreement with the previous estimate for arsenic. Lantzy and Mackenzie (1979) estimated an atmospheric flux of 200kt yr^{-1} for arsenic to the world's oceans. The flux calculated for the North Atlantic yields a global arsenic flux to the oceans of 11kt yr^{-1} , much lower than the Lantzy and Mackenzie (v.s.) estimate. The figure of 11kt yr^{-1} probably represents an over estimate, as arsenic concentrations are much lower over the southern oceans than over the North Atlantic (Walsh et al, 1979b). Duce (1982) calculated a deposition flux of $0.24 \text{ng cm}^{-2} \text{yr}^{-1}$ for antimony at Enewetak Atoll in the North Pacific, about an order of magnitude lower than the flux determined for the North Atlantic. This may be due to the remoteness of Enewetak Atoll from any land source, compared to Ocean Station Lima, and may also be a consequence of the possible over estimation of the North Atlantic fluxes.

2.4.2.2. Trans-coastal fluxes

The atmospheric deposition of arsenic and antimony has been shown to be a very important transport mechanism for these elements to coastal waters. It also seems that these elements in marine air are probably of continental origin. Therefore, it is of interest to determine the quantities transported across the coast from continental to marine air-masses. Fluxes across the coast at Plymouth have been calculated using onshore and offshore windfields. The south coastline of England runs approximately 080° to 260° , so offshore winds have been defined as those with an average wind source north of this line, and onshore winds as those blowing from the south. The average offshore or onshore component, was calculated for each sample, corrected to 350° and 170° respectively. Therefore, the average offshore wind velocity was 1.9 ms^{-1} at 350° , and the average onshore wind velocity was 3.1 ms^{-1} at 170° . Arithmetic means were calculated for arsenic and antimony in the offshore and onshore winds. For offshore winds the averages are $1.8 \text{ ng As (SCM)}^{-1}$, and $0.6 \text{ ng Sb (SCM)}^{-1}$, for onshore winds they are $1.5 \text{ ng As (SCM)}^{-1}$ and $0.7 \text{ ng Sb (SCM)}^{-1}$. Thus offshore fluxes are $54 \text{ mg As m}^{-2} \text{ yr}^{-1}$, and $18 \text{ mg Sb m}^{-2} \text{ yr}^{-1}$, assuming an offshore wind is operating for half the year. Similarly, onshore fluxes are $73 \text{ mg As m}^{-2} \text{ yr}^{-1}$ and $34 \text{ mg Sb m}^{-2} \text{ yr}^{-1}$. The similarity between the offshore and onshore fluxes shows the well mixed nature of the air at a coastal environment, probably an effect of the coastal sea breeze system. The south coast of England is about $5 \times 10^5 \text{ m}$ long. Adopting the scale height of 5000 m used in the washout flux calculations, there is a total offshore transport of 135 t As yr^{-1} and 45 t Sb yr^{-1} . Onshore transport is 180 t As yr^{-1} , and 85 t Sb yr^{-1} . Much of this material is probably recycled back across the coastline by the local sea-breeze systems (Shair et al, 1982).

2.4.2.3 Inter-hemisphere fluxes

About 90% of the world's heavy industry is located in the northern hemisphere (Duce et al, 1975), so it is of interest to determine the exchange rate of air between the hemispheres, and thus evaluate the rate at which pollutant material may be passed down to the southern hemisphere. Newell and coworkers (1974) determined a mass transfer rate of about 1.9×10^{21} g yr⁻¹ from the north to the south hemisphere in the lower troposphere, with a return transfer rate of 2.7×10^{21} g yr⁻¹. The balance is achieved by transfer in the upper troposphere. The density of air is about 1.3 kg m^{-3} (Goldberg, 1975), so these transfer rates become $1.5 \times 10^{18} \text{ m}^3 \text{ yr}^{-1}$ and $2.1 \times 10^{18} \text{ m}^3 \text{ yr}^{-1}$ respectively. About 20% of the intertropical convergence zone (ITCZ) is underlain by land, so 20% of the air transferred in each direction will contain continental air mass concentrations of arsenic and antimony, the remainder will contain these elements at open ocean concentration.

For arsenic, the air crossing the ITCZ from the northern hemisphere has about $0.11 \text{ ng (SCM)}^{-1}$ (arithmetic mean) over open ocean and about $4.3 \text{ ng (SCM)}^{-1}$ (arithmetic mean calculated from Salmon et al, 1978) over land. Thus, the transfer rate becomes :

$$\begin{aligned} & 1.5 \times 10^{18} \text{ m}^3 \text{ yr}^{-1} (0.2 \times 4.3 \text{ ng m}^{-3} + 0.8 \times 0.11 \text{ ng m}^{-3}) \\ & = 1.4 \text{ kt yr}^{-1} \end{aligned} \quad (2.3)$$

About 90% of this material is transported over land. For the reverse flux, southern hemisphere marine air contains $0.018 \text{ ng As m}^{-3}$ (Walsh et al, 1979b), and continental air contains 1.5 ng As m^{-3} (Adams et al, 1977). Thus the flux from the south to the north hemisphere is :

$$2.1 \times 10^{18} \text{ m}^3 \text{ yr}^{-1} (0.2 \times 1.5 \text{ ng As m}^{-3} + 0.8 \times 0.018 \text{ ng As m}^{-3})$$

$$= 0.7 \text{ kt As yr}^{-1} \quad (2.4)$$

Over 95% of this material is transported over land. Thus, there is a residual flux of $0.7 \text{ kt As yr}^{-1}$ from the north to the south hemisphere in the lower troposphere.

Marine air in the northern hemisphere contains $0.11 \text{ ng Sb (SCM)}^{-1}$, continental air about $2.2 \text{ ng Sb (SCM)}^{-1}$ (Salmon et al, 1978). Thus, the transfer rate for antimony from north to south hemisphere is :

$$1.5 \times 10^{18} \text{ m}^3 \text{ yr}^{-1} (0.2 \times 2.2 \text{ ng Sb m}^{-3} + 0.8 \times 0.11 \text{ ng Sb m}^{-3})$$

$$= 0.8 \text{ kt Sb yr}^{-1} \quad (2.5)$$

Over 80% of the antimony is transported from the northern hemisphere over land. In the southern hemisphere marine air contains $5 \text{ pg Sb (SCM)}^{-1}$ (Duce, 1982), and continental air contains $0.7 \text{ ng Sb (SCM)}^{-1}$ (Adams et al, 1980b). Thus, the transfer rate from south to north is :

$$2.1 \times 10^{18} \text{ m}^3 \text{ yr}^{-1} (0.2 \times 0.7 \text{ ng Sb m}^{-3} + 0.8 \times 0.005 \text{ ng Sb m}^{-3})$$

$$= 0.3 \text{ kt Sb yr}^{-1} \quad (2.6)$$

Over 90% of this material is transported over land. There is a residual flux from the north to south hemisphere of $0.5 \text{ kt Sb yr}^{-1}$, in the lower troposphere.

Fluxes across even a short length of coastline in the northern hemisphere ($5 \times 10^5 \text{ m}$) are only an order of magnitude lower than the complete

transfer rate across the ITCZ. The total flux across the world's coastlines is likely to be many times larger than the interhemisphere fluxes. For this reason, transfer across the world's coastlines are considered as an important refinement to the box models of arsenic and antimony, which are described in subsequent chapters.

CHAPTER THREE
MODELLING TECHNIQUES

3.1 STEADY STATE MODELLING

3.1.1 Concepts for the Basic Model

The basic concepts of steady state modelling were introduced in Section 1.4.1. A five reservoir model for mercury is shown in Figure 3.1 (Millward, 1982). The five reservoirs comprise the atmosphere, land mass, sediments, and two oceanic reservoirs, a surface mixed layer and a deep water reservoir. All box models of this type include many simplifications, however the five box model contains several simplifications which may require further refinement for kinetic analysis. A major natural source of trace elements to the atmosphere is volcanism (Buat-Menard and Arnold, 1978; Hammer, 1977; Siègel et al 1973a; Walsh et al, 1979b; Zoller et al, 1974), which is not represented in the mercury model. As the land is defined as the ice-free continental soil cover (Mackenzie et al, 1979), it is inappropriate to assign the land mass as a source for a volcanic flux. Instead, a separate reservoir of magmatic material is required. A second, and perhaps more serious, shortcoming lies in the treatment of the oceans. Only the dissolved species are represented, whereas material is removed to the sediments in the particulate phase. Although the particulate mass in the oceans is insignificant compared to the dissolved mass, the particulates must be included to assess the role of what could be a major transport mechanism. Therefore, initial models in this work were developed from a seven reservoir scenario, illustrated in figure 3.2. Many of the important transport mechanisms are shown, although this does not represent an exhaustive list. In each case, the overall mass or volume of the reservoir is calculated, then the mass of arsenic or antimony in each is determined with the appropriate concentration value. The seven reservoirs in the basic model are the atmosphere, the ocean mixed layer, the ocean deep waters, the oceanic particulates, the landmass, the sediments and the

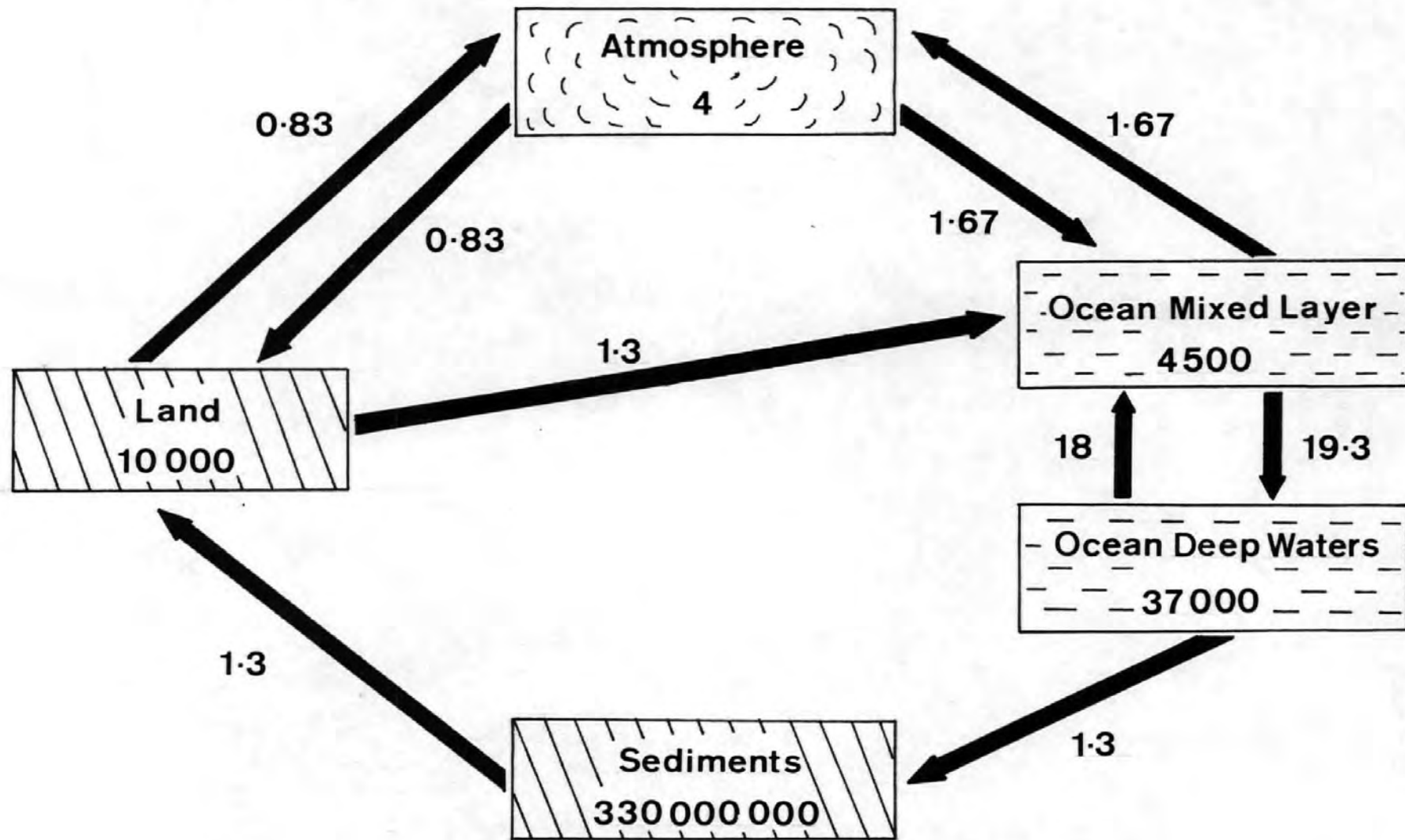


Figure 3.1 A five-box model for the global mercury cycle. Reservoirs in kt Hg, fluxes in kt Hg yr⁻¹. After Millward (1982)

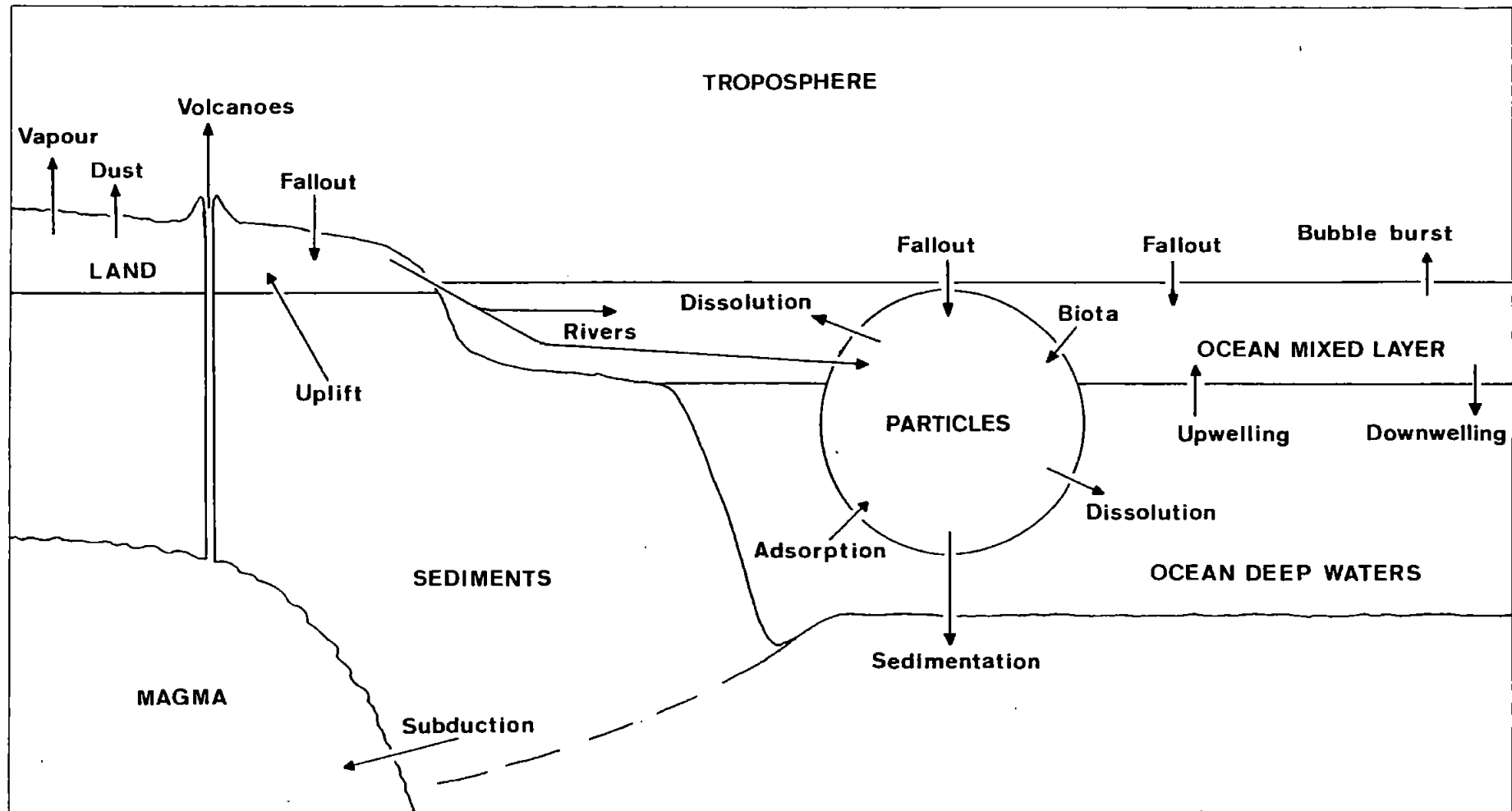


Figure 3.2 A general scenario for a seven-reservoir geochemical cycling model

magma, the volume or mass of each being defined as follows.

X The atmosphere consists of the tropospheric layer, about 10 km high (Mason, 1966) covering the Earth's surface, $510.1 \times 10^6 \text{ km}^2$ (Turekian, 1969). Thus, the overall volume becomes :-

$$5.101 \times 10^{14} \text{ m}^2 \times 10^4 \text{ m} = 5.101 \times 10^{18} \text{ m}^3 \quad (3.1)$$

The area covered by the world's oceans is $3.6 \times 10^{18} \text{ cm}^2$ (Turekian, 1969). Any box model with one surface and one deep water box must subdivide the intermediate water of the main thermocline between the two boxes. Thus, an arbitrary choice of depth for the surface layer must be made in the range of 75 m to 800 m (Bacastow and Björkström, 1981). Although a surface layer of 200 to 300 m is often used (see for example, Garrels et al, 1973), the thermocline has been observed at depths of about 650 m (Leetmaa, 1977), with an absolute depth limit of 1000 m (Broecker and Peng, 1982). Therefore, a mixed layer of 500 m depth was chosen in this work. Thus, the volume of the ocean mixed layer is :-

$$3.6 \times 10^{14} \text{ m}^2 \times 500 \text{ m} = 1.8 \times 10^{17} \text{ m}^3 \quad (3.2)$$

The deep water extends from 500 m to about 3700 m, the average depth of the oceans (Turekian, 1976), to give a water column height of 3200 m. As the continental shelf only extends to about 200 m depth, and covers about 10% of the ocean floor (Riley and Chester, 1971), the deep waters overlie 90% of the ocean floor. Thus, the volume of the deep water is :

$$3.6 \times 10^{14} \text{ m}^2 \times 0.9 \times 3200 \text{ m} = 1.04 \times 10^{18} \text{ m}^3 \quad (3.3)$$

The total particulate concentration of seawater is about $10 \mu\text{g L}^{-1}$ in surface water, and $5 \mu\text{g L}^{-1}$ in deep water (Brewer et al, 1980), giving a total of :-

$$1.8 \times 10^{20} \text{ L} \times 10 \times 10^{-6} \text{ g L}^{-1} + 1.04 \times 10^{21} \text{ L} \times 5 \times 10^{-6} \text{ g L}^{-1} \\ = 7 \times 10^{15} \text{ g} \quad (3.4)$$

This gives reasonable agreement with the total of 10^{16} g determined by Lal (1977).

The landmass is defined as a 60 cm soil cover, of average density 2.5 g cm^{-3} , extending over the ice-free surface of the Earth, $133 \times 10^{16} \text{ cm}^2$ (Mackenzie et al., 1979). Thus, the mass of the soil is :

$$133 \times 10^{16} \text{ cm}^2 \times 60 \text{ cm} \times 2.5 \text{ g cm}^{-3} = 2 \times 10^{20} \text{ g} \quad (3.5)$$

The global mass of sediments, about 2.5×10^{24} g, can be subdivided into shales (75%), carbonates (14%) and sandstones (11%) (Garrels and Mackenzie, 1971). Thus, the mass of each is 1.88×10^{24} g, 3.5×10^{23} g and 2.75×10^{23} g respectively.

Estimates for the size of the magmatic reservoir are unavoidably imprecise. However, the reservoir is so large, compared with the fluxes to and from the magma that the precision on the reservoir mass has no effect on the kinetic models, because the trace element content of the reservoir is not significantly changed by anthropogenic perturbations. The crust-forming magma is thought to be derived from the asthenosphere, a layer between 70 km and 260 km below the surface of the Earth. Seismic data have shown this layer to have an average density of 4.5 g cm^{-3} , and to be partially molten between 1 and 10% of the total volume (Press and Sæver, 1974). If the average radius of the Earth is 6370 km (Turekian, 1976) then the mass of the asthenosphere becomes:

$$\left(\frac{4}{3} \pi (6300 \text{ km})^3 - \frac{4}{3} \pi (6110 \text{ km})^3 \right) \times 4.5 \times 10^{15} \text{ g km}^{-3} = 4.14 \times 10^{26} \text{ g} \quad (3.6)$$

The molten fraction, which forms the magma, is the largest source of imprecision, between 1 and 10%, so 5% has been used for these calculations, to give a molten magmatic mass of about 2×10^{25} g. Although data for the trace element content of molten magma are absent from published literature, the trace element content of igneous rock is a reasonable substitute, as magma crystallises to form igneous rock.

Inter-reservoir fluxes may be estimated from direct measurement, such as volcanic fluxes to the atmosphere and riverine fluxes from the land to the oceans. Riverine transport is regarded as a flux, rather than considering rivers as a separate reservoir, because comparison of river water - rock and seawater - rock partition coefficients for trace elements shows that river water may be considered as a weathering intermediate between rock and seawater (Whitfield and Turner, 1979). Where reliable direct measurements are unavailable, indirect methods may be used. For the seven reservoir model in this work, three such estimates were used. Exchange between the mixed layer and deep waters was estimated from global upwelling rates (Broecker, 1974), with the appropriate trace element concentration for seawater. Dissolved-particulate interactions were derived from global oceanic productivity rates, and removal from the atmosphere was determined using an average aerosol settling velocity. All other fluxes were estimated by considering mass balance requirements for each reservoir.

3.1.2 Refinements to the Basic Model

The basic model may be considered inadequate in a number of respects, as several heterogeneous reservoirs are treated as if well mixed. Therefore, several refinements to the basic model have been considered.

Although the dissolved oceanic phase has been separated into two

reservoirs by the thermocline, the ocean particulates have been considered only as a single reservoir. The particulates were further divided into a surface and deep water mass, using a total particulate concentration of $10 \mu\text{g L}^{-1}$ for surface waters and $5 \mu\text{g L}^{-1}$ for deep waters (Brewer et al, 1980), to yield a mixed layer particulate reservoir of 1.8×10^{15} g, and a deep water particulate mass of 5.2×10^{15} g. As the ocean deep waters do not extend over the continental shelf, there is a direct input of particulate material to the shelf sediments from the mixed layer particulate reservoir. It was assumed, therefore, that the particulate riverine input to the oceans, plus 10% of material sinking from the mixed layer particulate reservoir is lost directly to the sediments without passing through the deep water particulate reservoir.

As many trace aerosol constituents exhibit markedly higher concentrations in continental air than in marine air (contrast, for example, Duce et al 1976 with Salmon et al, 1978), it is inappropriate to treat the atmosphere as a single well mixed reservoir. Therefore, the atmosphere was subdivided into two reservoirs, marine and continental airmasses. As the oceans underlie about 70% of the global atmosphere, the volumes of the marine and continental airmasses are $3.57 \times 10^{18} \text{ m}^3$ and $1.53 \times 10^{18} \text{ m}^3$ respectively. Exchange between the two airmasses was determined by considering the average windspeeds of the major airflows around the globe (Table 3.1). As these are all easterly or westerly winds, the exchange rate was calculated across the north-south component

Table 3.1 Major Global Air Movements

Wind	Latitude	Velocity
Trade Winds	$0^{\circ} - 30^{\circ}$	5 ms^{-1} E
Westerlies	$30^{\circ} - 65^{\circ}$	10 ms^{-1} W
High Latitudes	$65^{\circ} - 90^{\circ}$	5 ms^{-1} E

of the world's ice-free coastline (ice covered land does not significantly contribute to the burden of trace substances in the continental air mass) multiplied by the atmospheric height and appropriate windspeed (Table 3.2). Thus, $7.35 \times 10^{18} \text{ m}^3$ of continental air are lost to the marine atmosphere annually, and the same amount is transferred in the reverse direction.

The excess input from the continental to marine air is assumed to be removed to the ocean by the usual deposition processes. Volcanic input to the atmosphere was subdivided, with 17% entering the marine atmosphere, as 17% of active volcanoes lie within the ocean basins (Macdonald, 1972).

Finally, marine and terrestrial primary biospheres were introduced into the model. The dry weight of the terrestrial biomass is about $2.4 \times 10^9 \text{ kt}$, with a dry weight productivity of $1.73 \times 10^8 \text{ kt yr}^{-1}$ (Rodin et al, 1978). The standing crop of biomass in the ocean was calculated from measurements of adenosine triphosphate (ATP) by Holm-Hansen (1969) (Table 3.3).

Table 3.3 Variation in Living Carbon with Depth

Depth (m)	$\mu\text{g C L}^{-1}$
0	24
50	22
100	5.6
200	1.9
600	0.5

After Holm-Hansen (1969)

From the above, the world oceans contain $9.7 \times 10^{14} \text{ g}$ living Carbon.

Table 3.2 Air Transfer across Global Ice-free Coast

Landmass	Latitude	N-S Coastline component(km) *	Wind Speed m s ⁻¹	Transfer rate 10 ⁹ m ³ s ⁻¹
America 70°N - 55°S	70° - 65°N	556	5	2.8
	65° - 30°N	3890	10	38.9
	30° - 0°N	3340	5	16.7
	0° - 30°S	3340	5	16.7
	30° - 55°S	2780	10	27.8
Euro-China and Africa 75°N - 35°S	75° - 65°N	1110	5	5.6
	65° - 30°N	3890	10	38.9
	30° - 0°N	3340	5	16.7
	0° - 30°S	3340	5	16.7
	30° - 35°S	556	10	5.6
India	25° - 5°N	2220	5	11.1
Korea and Borneo 20°N - 5°S	20° - 0°N	2220	5	11.1
	0° - 5°S	556	5	2.8
Australia 10° - 40°S	10° - 30°S	2220	5	11.1
	30° - 40°S	1110	10	11.1
Total:				2.3 x 10 ¹¹ m ³ s ⁻¹
				7.3 x 10 ¹⁸ m ³ yr ⁻¹

* 1° of arc (latitude) = 111.18 km

The ratio of living carbon to dry biomass is 0.4 : 1 (Redfield et al, 1963; Steele, 1974), so the total biomass in the ocean is 2.42×10^{15} g (dry weight). The primary productivity of the oceans is 20×10^6 kt C yr⁻¹ (Menzel, 1974) of which 90% is recycled in the mixed layer, and about 3% reaches the ocean floor (Lorenzen et al, 1983; Menzel, 1974).

Applying the carbon to biomass ratio of 0.4, the total annual productivity is about 50×10^6 kt, with 45×10^6 kt recycled in the mixed layer.

Quantitative solutions to the models for arsenic and antimony, using the criteria established above, are considered in subsequent chapters.

3.2 CHOICE OF PARAMETERS FOR MODELLING

The biogeochemistries of arsenic and antimony were extensively reviewed in the introductory chapter. From the data presented there, a suitable choice must be made of the concentrations to be used in the models, preferably data determined by the most sensitive and reliable techniques available. For this reason, the most recent data were usually adopted. It is important to take the best estimate for an unpolluted environmental background, to construct pre-man steady state models, but the present day environment has already received a significant pollutant input. As both arsenic and antimony are atmophile elements, atmospheric concentrations are most seriously effected by pollutant emissions. Although ice-core data have been used to assess pre-industrial atmospheric levels of mercury (Millward, 1982), no reliable ice-core data exist for arsenic or antimony. However, as about 90% of heavy industry is located in the northern hemisphere (Duce et al, 1975), measurements taken in the southern hemisphere may be used to estimate a pre-man environment. Copper smelting is a major source of pollutant emissions of arsenic and antimony (Crececius, 1975; Larson et al, 1975), and there are major smelting operations in the southern hemisphere, notably in S. Africa and Australia. Therefore, the quantitative steady state models presented for arsenic and antimony can only be considered as approximations to pre-man models, the atmospheric burdens representing upper limits to the pre-man state. Data used to construct the basic steady state models for arsenic and antimony are tabulated in tables 3.4 and 3.5 respectively. Fluxes derived indirectly will be discussed when considering the relevant quantitative steady state models.

Despite careful consideration of the available data, the resultant basic models are not the only possible solutions to the steady state. Salmon

Table 3.4 Parameters for Arsenic Models

Reservoir	Parameter	Source
Atmosphere:		
Continental aerosol	1.5 ng m ⁻³	Adams <u>et al</u> , 1977 and 1980b
Marine Aerosol	0.018 ng m ⁻³	Walsh <u>et al</u> , 1979b
Vapour	7% of total	Walsh <u>et al</u> , 1979a
Ocean:		
Dissolved	1.5 µg L ⁻¹	Andreae, 1978
Particulate	10 ppm	Buat-Menard, pers. comm. 1982
Soil	7 ppm	Bennett, 1981 Kronberg <u>et al</u> , 1979
Sediments:		
Shale	13 ppm	(Bowen, 1966)
Sandstone	1 ppm	(Mason, 1966)
Limestone	1 ppm	(Onishi, 1969a)
Magma:		
Igneous rock	1.8 ppm	Bowen, 1966
Biota (dry weight)		
Marine Phytoplankton	10 ppm	Onishi, 1969a Sanders and Windom, 1980 Trefry and Presley, 1976
Terrestrial flora	0.2 ppm	Bowen, 1966
Flux	Parameter	Source
Riverine:		
Dissolved	1.7 µg L ⁻¹	Martin and Meybeck, 1979
Particulate	5 ppm	Martin and Meybeck, 1979
Volcanic	7 kt yr ⁻¹	Walsh <u>et al</u> , 1979b

All the other fluxes derived indirectly

Table 3.5 Parameters for Antimony Models

Reservoir	Parameter	Source
Atmosphere:		
Continental aerosol	0.7 ng m ⁻³	Adams <i>et al</i> , 1980b
Marine aerosol	5 pg m ⁻³	Duce, 1982
Ocean:		
Dissolved	0.24 µg L ⁻¹	Bowen, 1979
Surface particulates	7 ppm	Buat-Menard and Chesselet, 1979
Deep particulates	10 ppm	Buat-Menard and Chesselet, 1979 Martin and Meybeck, 1979
Soil	1 ppm	Bowen, 1979
Sediments:		
Shale	1.5 ppm	Onishi 1969b
Sandstone	0.05 ppm	Bowen, 1979 Onishi, 1969b
Limestone	0.3 ppm	Onishi, 1969b
Magma:		
Igneous rock	0.2 ppm	Bowen, 1966, Onishi, 1969b
Biota (dry weight):		
Marine plankton	0.15 ppm	Buat-Menard and Chesselet, 1979
Terrestrial flora	0.06 ppm	Bowen, 1966
Flux	Parameter	Source
Riverine :		
Dissolved	1 µg L ⁻¹	Martin and Meybeck, 1979 Turekian, 1969
Particulate	2.5 ppm	Martin and Meybeck, 1979

All other fluxes derived indirectly

and coworkers (1978) showed that trace element concentrations in the atmosphere are subject to temporal fluctuations of different frequencies. A seasonal fluctuation was observed for a wide range of elements, as was observed for arsenic in this work. There was also a longer frequency fluctuation, of about 4 yr wavelength, of about 2.5 ng As m^{-3} and 1.5 ng Sb m^{-3} . This has yet to be explained fully, but may be of meteorological origin. Thus, although the data chosen for the models may be reliable in terms of the accuracy and precision of the measurements, they may not necessarily reflect the true mean in the observed environment. In seawater, the difference between the concentration of $1.5 \text{ } \mu\text{g As L}^{-1}$ (Andreae, 1978) and $2.6 \text{ } \mu\text{g As L}^{-1}$ (Turekian, 1969) is probably due to improvements in analytical techniques, but may reflect an unrecognised temporal fluctuation. Similarly, the spatial variability of trace elements has not been fully examined, especially for the oceans. Again, reported data may not necessarily reflect the true mean, if such spatial variations have not been properly considered. Such variations and fluctuations may be of considerable importance if the element under study is significantly involved in the biological cycle. Variations may then follow spatial variations in primary productivity, and may also be effected by the seasonal and diel variability of productivity. It is possible to construct a number of quantitative steady state models to show the range of possible variations of this nature, but it is only possible to examine the significance of these variations by subjecting the steady state models to kinetic analysis.

3.3 KINETIC MODELLING

Geochemical fluxes are thought to obey first order kinetics, the magnitude of a flux being proportional to the mass of its source reservoir. Thus:

$$\frac{dA}{dt} = k.A \quad (3.7)$$

where dA/dt = flux rate ; k = first order rate constant; A = source reservoir mass.

Rate constants can be determined by rearrangement of the above equation, once the steady state model has been quantified, to give units of inverse time, usually yr^{-1} for geochemical cycles. The quantitative cycle can then be described in terms of its component rate equations. Once introduced into the environment, anthropogenic material is dispersed according to these same rate equations, with an eventual increment of the material in each reservoir, irrespective of where the pollutants enter the cycle.

3.3.1 The Environmental Pollutant Record

It has been shown that the temporal changes in the atmospheric burden of trace elements may be determined from concentration changes in ice cores taken from sites such as Greenland. Weiss and coworkers (1975 and 1978) presented data to show such changes for arsenic and antimony. Li (1981b) subjected this data to factor analysis, which showed that recent increases in the atmospheric concentrations were largely due to pollution, as had already been suggested for mercury (Weiss et al, 1971) and for lead (Patterson et al, 1976). Pollutant aerosols have now been confirmed in the Arctic atmosphere (Heintzenberg et al, 1981; Kerr, 1981) However, the possibility of analytical contamination has brought much ice core data into dispute (Dickson, 1972; Ng and Patterson, 1981;

Patterson, 1976), and the data for arsenic and antimony are thus considered to be unreliable.

Millward (1982) used the ice core data of Appelquist and coworkers (1978), considered to be amongst the most reliable, to establish the atmospheric pollutant trend for mercury. However, mercury has a longer residence time in the atmosphere, 1.5 yr. (Millward, 1982), than arsenic, 0.04 yr., or antimony, 0.03 yr. (this work), because the atmospheric burden of mercury is dominated by the vapour phase. Arsenic and antimony are removed from the atmosphere in areas more local to the pollutant source, within 300 km (Arafat and Glooschenko, 1982), than is mercury. Therefore, even if available, reliable ice core data for arsenic and antimony would probably yield underestimates for the temporal increase in the atmospheric arsenic and antimony burdens. To assess temporal variations in the atmospheric burdens of these elements, time-based analysis of air is required in areas less remote from pollutant sources than Greenland or the Antarctic, as has been carried out in Oxfordshire (Salmon et al., 1978). These data show a possible increase in arsenic and antimony burdens since 1965, although the trends are masked by the periodicity of the trace element concentrations. Cores taken from peat bogs have also been used to assess trends in atmospheric trace element concentrations (Madsen, 1981), but such data are unavailable for arsenic or antimony.

3.3.2 Modelling Pollutant Influences

3.3.2.1 High temperature processes

Arsenic and antimony are concentrated in metalliferous ores, especially in copper ores (Onishi, 1969a and 1969b), so are released to the environment during metal production (Brimblecombe, 1979; Brooks et al., 1982).

Copper smelting is the largest source of pollutant arsenic (Brimblecombe, 1979; N.A.S., 1977; Walsh et al., 1979b), and produces major emissions of

antimony (Crececius, 1975; Larson et al, 1975). In comparison, fossil fuel mobilisation is a minor source (Bertine and Goldberg, 1971). Table 3.6 lists the sources of global arsenic emissions in order of magnitude, with copper smelting contributing over 50% of the total. The copper industry also provides a large proportion of the pollutant arsenic in landfill. Data for the U.S.A. land and water pollutant burdens are listed in Table 3.7. Although copper smelting does not significantly contribute to water-borne pollution, the pollutant transport of arsenic by rivers is very small compared to pollutant fluxes to the land and atmosphere, so the growth of copper production may be used to estimate the growth of arsenic and antimony pollutant transport.

The copper industry is a fortunate choice on which to model pollutant transport, as the growth of global copper production is well documented (see, for example: Bain, 1978; Chadwick, 1958; Govett, 1976; Webster-Smith, 1967), and copper is an economically sensitive metal, which shows a more constant economic growth rate than other metals such as iron or gold (Bain, 1978). According to this latter worker, the annual growth of metal production can be divided into four stages: a youthful stage with growth in excess of 10%, a mature stage with growth rates between 8 and 2.5%, a gerontic stage with growth less than 1%, and a slow decline stage. For copper, the youthful stage of production is not recorded, as copper was one of the first metals to be produced by man. However, since 1800 AD global copper production has grown at a steady 3.6%, indicative of the mature stage. About one third of the total resources are removed by the end of the mature stage, one third during the gerontic stage, and the remainder during the decline (Bain, 1978). Current copper reserves are estimated at about 5×10^5 kt (Skinner, 1976), with a further 1.5×10^5 kt produced between 1800 and 1975 AD, derived from

Table 3.6 Anthropogenic Arsenic Emissions

Source	Emission (kt As yr ⁻¹)	Percentage of total
Copper production	13	55.1
Iron and steel production	4.2	17.8
Lead and zinc production	2.2	9.3
Agriculture	1.9	8.1
Wood fuel	0.6	2.5
Agricultural burning	0.56	2.4
Coal	0.55	2.3
Waste incineration	0.43	1.8
Chemicals	0.2	0.8
Cotton ginning	0.023	0.1
Mining	0.013	0.1
Residual fuels	0.0041	< 0.1
Light fuels	0.000 07	< 0.1
Total	23.6	

After Walsh and coworkers (1979b)

Table 3.7 Pollutant Arsenic Transport in the USA

Source	Emission (kt As yr ⁻¹)	Percentage of total:
<u>Transport to the air</u>		
Copper smelting	5.29	54.2
Pesticides	2.54	26.0
Coal	0.72	7.4
Others	1.21	12.4
	Total	
	9.76	
<u>Transport to the land</u>		
Steel production	39.7	48
Copper production	24.0	29
Pesticides	11.6	14
Coal	2.0	2
Others	5.4	7
	Total	
	82.7	
<u>Transport to rivers</u>		
Phosphates	0.12	75
Others	0.04	25
	Total	
	0.16	

After N.A.S. (1977)

integration of the curve in figure 3.3. Thus, the initial reserve is about 6.5×10^5 kt. Only the mature growth rate is known, although the gerontic growth rate and decline rate will probably be less than 1% (Bain, 1978), so 0.5% was chosen for both rates in the kinetic models in this study, to yield the growth curve in figure 3.3. These growth rates may now be applied to the growth of arsenic and antimony pollutant emissions from high temperature sources.

3.3.2.2 Low temperature processes

In addition to the mobilisation of arsenic and antimony by high temperature processes, such as metal production or fossil fuel combustion, these atmophile elements may be mobilised from the landmass due to low temperature anthropogenic processes. Ajax and Lee (1976) reported increases in dust emissions from arable land, due to breakup of the soil by ploughing. Such emissions varied between 13% and 290% of the natural dust flux, depending on climate and soil type. Thus, the rate constant for the flux of particulate material from arable land to the atmosphere is approximately double that from the natural undisturbed land surface. The total potential area of arable land is 4230×10^6 ha (Revelle, 1976), and the depth of disturbance due to ploughing does not exceed 30 cm (P.J. Hobbs, pers. comm., 1983). If the landmass is taken as a soil layer, 60 cm thick, over the ice-free area of the land, $13,300 \times 10^6$ ha (Mackenzie et al, 1979), then about one sixth of the landmass material is available for mobilisation by agricultural processes. The growth of arable land can be determined from global agricultural statistics (F.A.O., 1948-1957 and 1958-1982). Prior to 1948 AD there are no statistics available for global agricultural processes, but as agricultural growth is mainly driven by world population growth, the growth in population can be used as a guide to the growth of agriculture. The

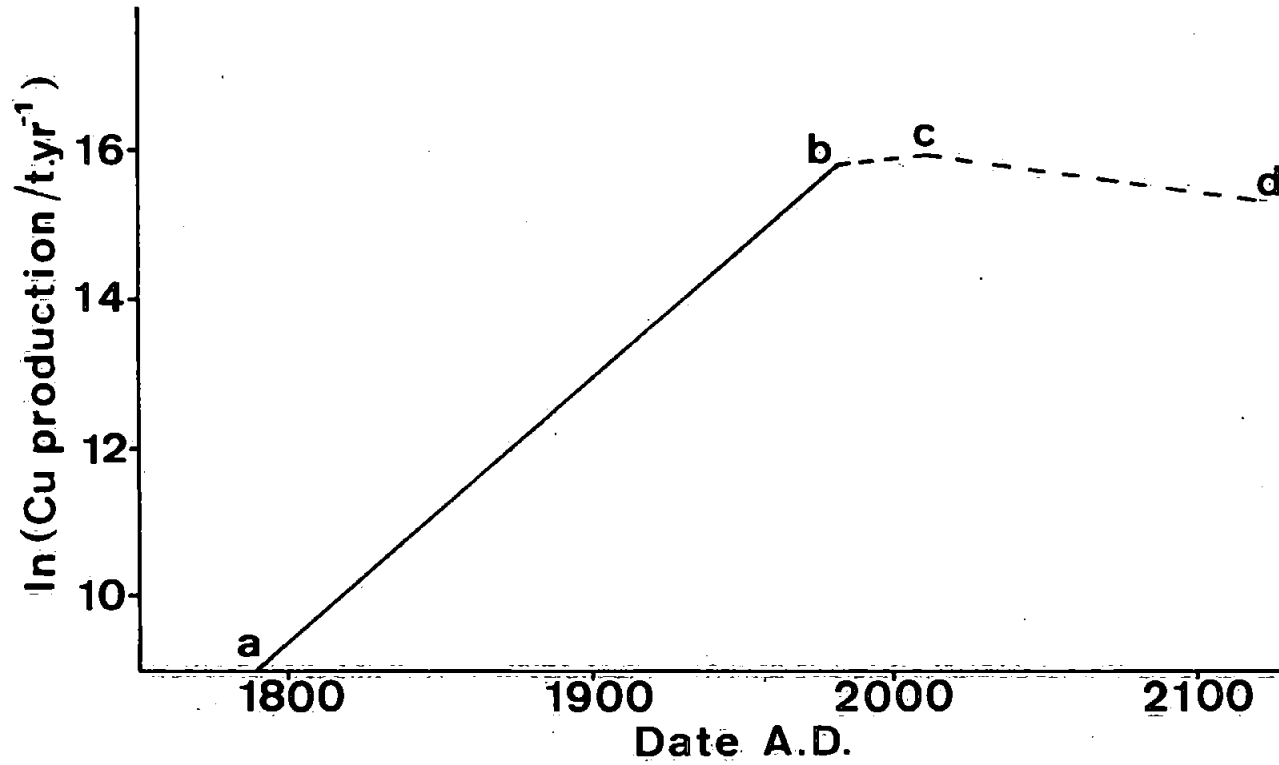


Figure 3.3 Growth of global copper production. The broken line indicates predicted growth. a-b, mature stage; b-c, gerontic stage; c-d, decline stage. After Bain (1978)

growth curve shown for arable land in figure 3.4 is a composite diagram from the F.A.O. statistics (v.s.) and population statistics for global population growth from 1340 to 1973 A.D. (Grigg, 1980).

Volatilisation from the land surface, by physical processes (Goldberg, 1976) or biological processes (Braman, 1975) may also be enhanced by man's increasing exposure of unweathered crustal material (Weiss et al, 1971). Plants also contribute to the transport of trace elements from land to atmosphere (Beauford et al, 1975 and 1977; Schnell and Vali, 1972 and 1973). Changes of land use in developed and developing countries may have caused the thickening of forests in the last 30 yr (Bolin, 1977), which would also enhance the biological transport of trace elements from the landsurface to the atmosphere. Such processes were considered by Griffin (1980) and Millward (1982), modelling the non-steady state mercury cycle using increased fluxes from land to atmosphere.

3.3.3 Computational Techniques

Matrix algebra has become a popular tool for the mathematical treatment of geochemical cycles, particularly for the treatment of non-linear coupled systems, such as the simultaneous treatment of the carbon and oxygen cycles (Lasaga, 1980). In this work, however, differential equations were derived from the flux rates in the cycle to describe the rate of change of mass for each reservoir. These differential equations were simultaneously integrated with respect to time, using a modified Runge-Kutta formula (Trenor, 1966). This integration is of a discrete nature, rather than continuous, so the time interval for the integration must be based on the most rapid process. At each time step, the rates operative on each reservoir, which are derived as the product of the appropriate rate constant and instantaneous source reservoir mass, are

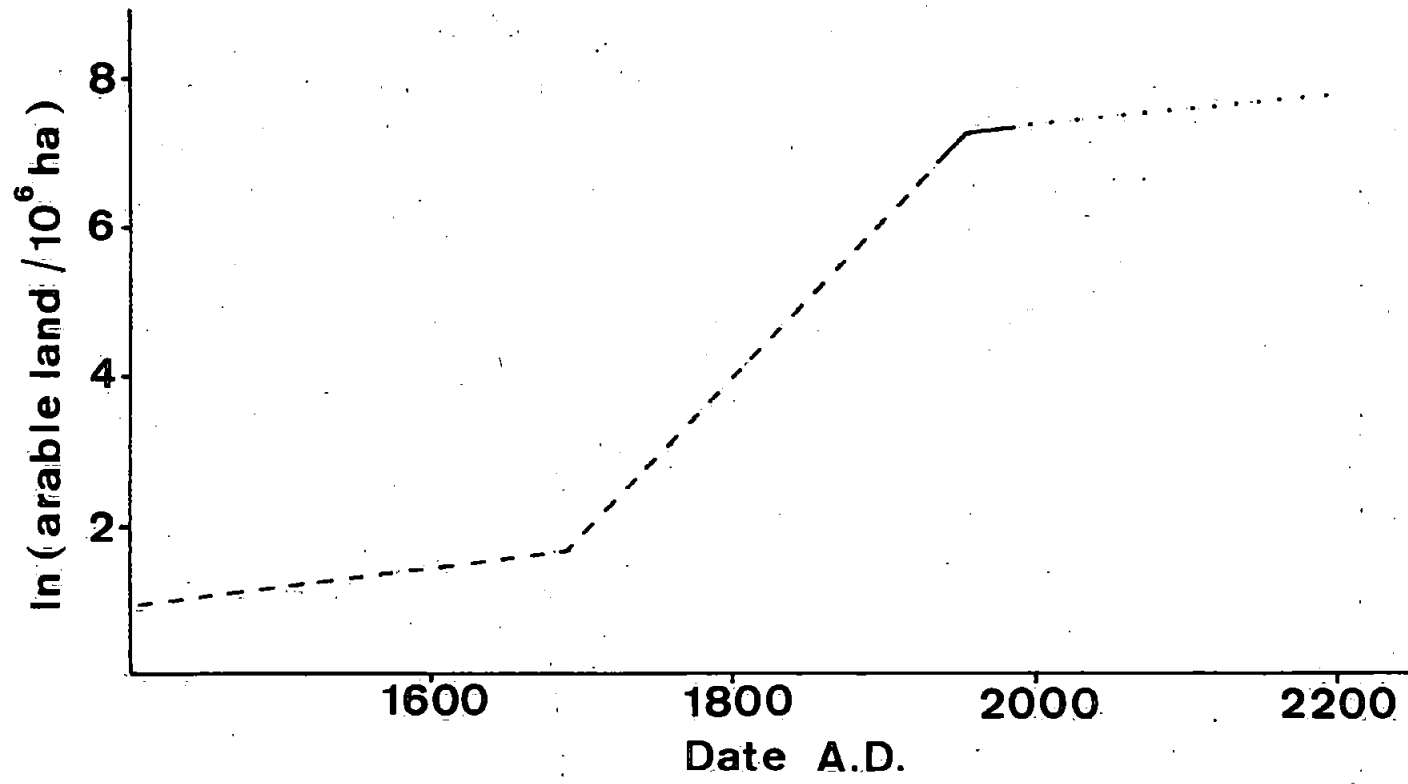


Figure 3.4 Growth of arable land. Broken line - inferred from Grigg (1980); solid line - observed (FAO, 1948-1957 and 1958-1982); dotted line - predicted growth from observed trend.

summed to yield the overall mass change of each reservoir over the time interval. The Runge-Kutta approximation is based on a fourth order Taylor's expansion, which may be imprecise for expansions involving large high order derivatives. The modification provides a better approximation for such expansions. The mathematics from Treanor (v.s.) is summarised in Appendix I. This mathematical method was incorporated into a FORTRAN 77 computer programme, included in Appendix II, to evaluate the temporal change in the reservoir masses. The time interval used was allowed to increase during the programme run, providing this did not result in instability oscillations, which are artefacts of too large a time interval. To achieve this, a section of code was incorporated into the programme, which reduced the time step if the change between successive passes of the integration loop was too large. However, this was only adequate to eliminate short frequency oscillations. Where longer frequency instability oscillations occurred, the models were re-run, using a smaller maximum for the time interval. Results were output in tabular and graphic form, for ease of interpretation. The programme was executed on a PRIME computer system, with a CALCOMP 1039 drum plotter for graphic output. The amount of c.p.u. time used in the computation varied from about 15 mins. to 300 mins, depending on the time duration, and the complexity of the steady state from which the kinetic model was derived.

CHAPTER FOUR
MODELS OF THE GEOCHEMICAL
ARSENIC CYCLE

4.1 STEADY STATE MODELS

4.1.1 The Basic Model

The basic model for the arsenic cycle consists of the seven reservoirs defined in Chapter 3. Further refinements to this model are considered separately, and their effects on sensitivity examined by kinetic analysis.

4.1.1.1 The reservoirs

The atmosphere is represented by the troposphere, with a volume of $5.101 \times 10^{18} \text{ m}^3$. Of the total, 70% is underlain by the oceans, so has an aerosol arsenic concentration of 0.018 ng m^{-3} (Walsh et al., 1979b) the remainder is continental, with an aerosol arsenic concentration of 1.5 ng m^{-3} (Adams et al., 1977). Thus total aerosol arsenic in the troposphere is :

$$5.101 \times 10^{18} \text{ m}^3 (0.7 \times 0.018 \times 10^{-18} \text{ kt As m}^{-3} + 0.3 \times 1.5 \times 10^{-18} \text{ kt As m}^{-3}) = 2.36 \text{ kt As} \quad (4.1)$$

However, 7% of the arsenic burden is in the vapour phase (Walsh et al., 1979a), so the total arsenic burden in the troposphere is 2.5 kt. The ocean mixed layer has a volume of $1.8 \times 10^{17} \text{ m}^3$, with an arsenic concentration of $1.5 \text{ } \mu\text{g L}^{-1}$ (Andreae, 1978). Thus the ocean mixed layer reservoir is :

$$1.8 \times 10^{17} \text{ m}^3 \times 1.5 \times 10^{-12} \text{ kt As m}^{-3} = 2.7 \times 10^5 \text{ kt As} \quad (4.2)$$

The deep waters have a volume of $1.04 \times 10^{18} \text{ m}^3$ with no significant change in arsenic concentration, thus :

$$1.04 \times 10^{18} \text{ m}^3 \times 1.5 \times 10^{-12} \text{ kt As m}^{-3} = 1.56 \times 10^6 \text{ kt As} \quad (4.3)$$

Particulates in the world's oceans have a total mass of $7 \times 10^{15} \text{ g}$, with an arsenic concentration of 10 ppm (Buat-Menard, pers. comm., 1982).

Thus, the ocean particulate reservoir becomes :

$$7 \times 10^6 \text{ kt} \times 10 \times 10^{-6} \text{ kt As kt}^{-1} = 70 \text{ kt As} \quad (4.4)$$

The reservoir mass is about 100 kt As, a reasonable approximation as the concentration of arsenic in ocean particulate matter is not well established.

The landmass is defined as the global mass of soil on the ice-free land surface, 2×10^{20} g. The concentration of arsenic in soil is 7 ppm (Bennett, 1981; Kronberg et al, 1979), so the landmass reservoir is :

$$2 \times 10^{11} \text{ kt} \times 7 \times 10^{-6} \text{ kt As kt}^{-1} = 1.4 \times 10^6 \text{ kt As} \quad (4.5)$$

The global mass of shale is about 1.88×10^{24} g (Garrels and Mackenzie, 1971), with an arsenic content of 13 ppm (Bowen, 1966; Mason, 1966; Onishi, 1969a), to give an arsenic mass of :

$$1.88 \times 10^{15} \text{ kt} \times 13 \times 10^{-6} \text{ kt As kt}^{-1} = 2.44 \times 10^{10} \text{ kt As} \quad (4.6)$$

Similarly, the global mass of arsenic in limestone can be computed from the global mass of limestone, 3.5×10^{23} g (Garrels and Mackenzie, 1971), and the average concentration of arsenic in limestone, 1 ppm (Bowen, 1966; Mason, 1966; Onishi, 1969a).

$$3.5 \times 10^{14} \text{ kt} \times 1 \times 10^{-6} \text{ kt As kt}^{-1} = 3.5 \times 10^8 \text{ kt As} \quad (4.7)$$

The average arsenic concentration in sandstones is also 1 ppm (Bowen, 1966; Mason, 1966; Onishi, 1969a). In the global mass of sandstone, 2.75×10^{23} g (Garrels and Mackenzie, 1971), this gives an arsenic mass of :

$$2.75 \times 10^{14} \text{ kt} \times 1 \times 10^{-6} \text{ kt As kt}^{-1} = 2.75 \times 10^8 \text{ kt As} \quad (4.8)$$

The sedimentary arsenic reservoir is then the sum of the masses calculated in equations 4.6, 4.7 and 4.8, 2.5×10^{10} kt As.

The global mass of magma is about 2×10^{25} g. If the concentration of arsenic in igneous rocks, 1.8 ppm (Bowen, 1966), is typical of arsenic concentrations in magma, then the magmatic reservoir of arsenic is :

$$2 \times 10^{16} \text{ kt} \times 1.8 \times 10^{-6} \text{ kt As kt}^{-1} = 3.6 \times 10^{10} \text{ kt As} \quad (4.9)$$

However, as the molten fraction of the asthenosphere is poorly known, between 1% and 10%, the above figure can only be interpreted as a mass of arsenic between 10^{10} kt and 10^{11} kt, a reservoir mass of about 5×10^{10} kt.

4.1.1.2 The fluxes

Aerosol deposition is the major mechanism of arsenic removal from the troposphere. Using the average aerosol settling velocity of 1 cm s^{-1} (Buat-Menard and Chesselet, 1979; Chester, 1982; Millward and Griffin, 1980), the aerosol content of a troposphere 10 km high could be deposited on the Earth's surface 31.5 times a year. For the basic model, the troposphere is regarded as well-mixed, so the portion of the aerosol falling onto land is given by the fraction of the Earth's surface not covered by oceans, about 30% (Garrels et al, 1973). Thus, the flux from troposphere to land is given by the product of the deposition rate of aerosol material and the mass of aerosol arsenic over the land :

$$31.5 \text{ yr}^{-1} \times 2.36 \text{ kt As} \times 0.3 = 22 \text{ kt As yr}^{-1} \quad (4.10)$$

About 49% of the arsenic in the marine aerosol is soluble in seawater (Creelius, 1980). Thus, the tropospheric flux of arsenic to the ocean mixed layer is :

$$31.5 \text{ yr}^{-1} \times 2.36 \text{ kt As} \times 0.7 \times 0.49 = 25 \text{ kt As yr}^{-1} \quad (4.11)$$

The insoluble portion forms a flux from the troposphere to the ocean particulates reservoir:

$$31.5 \text{ yr}^{-1} \times 2.36 \text{ kt As} \times 0.7 \times 0.51 = 26 \text{ kt As yr}^{-1} \quad (4.12)$$

Broecker (1974) estimated that upwelling was equivalent to an annual upwards transfer of a layer of water 1 m thick, extending across the interface between the mixed layer and deep waters. This overlies about 90% of the world's ocean floor, with the remainder occupied by continental shelf (Riley and Chester, 1971). Thus, the upwelling flux of arsenic can be determined from the upwelling volume of water and its arsenic concentration, $1.5 \mu\text{g L}^{-1}$ (Andreae, 1978) :

$$\begin{aligned} 1 \text{ m yr}^{-1} \times 3.6 \times 10^{14} \text{ m}^2 \times 0.9 \times 1.5 \times 10^{-12} \text{ kt As m}^{-3} \\ = 486 \text{ kt As yr}^{-1} \end{aligned} \quad (4.13)$$

As there is no difference in total dissolved arsenic concentration between surface and deep waters (Andreae, 1978 and 1979), the downwelling flux from the ocean mixed layer to the deep waters is also $486 \text{ kt As yr}^{-1}$.

The flux from the ocean mixed layer to the ocean particulate reservoir is controlled by two major transport mechanisms, biological uptake and inorganic adsorption. The first may be calculated from the annual productivity of $50 \times 10^6 \text{ kt}$ and the average arsenic concentration in plankton, 10 ppm (Onishi, 1969a; Sanders and Windom, 1980; Trefry and Presley, 1976) :

$$50 \times 10^6 \text{ kt yr}^{-1} \times 10 \times 10^{-6} \text{ kt As kt}^{-1} = 500 \text{ kt As yr}^{-1} \quad (4.14).$$

Inorganic adsorption must be quantified indirectly, and this will be discussed later. The return flux, from the particulates to the ocean mixed layer, may be represented as that fraction of the productivity, 90%, recycled in the mixed layer (Menzel, 1974). Thus, the particulates to ocean mixed layer flux is $450 \text{ kt As yr}^{-1}$. As 3% of the annual productivity reaches the sediments (Menzel, 1974), 7% must be lost to deep water. Therefore, 35 kt As yr^{-1} is lost from the particulates to the deep water reservoir. To balance the steady state for the deep water, an adsorption flux of 35 kt As yr^{-1} is required. The ocean deep waters contain $1.56 \times 10^6 \text{ kt As}$, so the adsorption rate constant is :

$$35 \text{ kt As yr}^{-1} / 1.56 \times 10^6 \text{ kt As} = 2.2436 \times 10^{-5} \text{ yr}^{-1} \quad (4.15)$$

Applying this rate constant to the ocean mixed layer reservoir of $2.7 \times 10^5 \text{ kt As}$ yields an adsorption flux of 6 kt As yr^{-1} from the ocean mixed layer to the particulates. Thus, the total flux from the ocean mixed layer to the particulate reservoir is $506 \text{ kt As yr}^{-1}$.

Transport of material from the landmass to the oceans can be separated into two fluxes: dissolved matter to the ocean mixed layer, and particulate matter to the particulate reservoir. The total stream discharge to the ocean is $3.6 \times 10^{16} \text{ L yr}^{-1}$ (Turekian, 1969), with a dissolved arsenic concentration of $1.7 \mu\text{g L}^{-1}$ (Martin and Meybeck, 1979). Thus, the dissolved flux is :

$$3.6 \times 10^{16} \text{ L yr}^{-1} \times 1.7 \times 10^{-15} \text{ kt As L}^{-1} = 61 \text{ kt As yr}^{-1} \quad (4.16)$$

The average suspended discharge from the oceans is 400 mg L^{-1} (Turekian, 1969), with an average arsenic concentration of 5 ppm (Martin and Meybeck, 1979), to give a particulate flux of :

$$3.6 \times 10^{16} \text{ L yr}^{-1} \times 4 \times 10^{-10} \text{ kt L}^{-1} \times 5 \times 10^{-6} \text{ kt As kt}^{-1}$$

$$= 72 \text{ kt As yr}^{-1} \quad (4.17)$$

The volcanic flux from the magma to the troposphere is 7 kt As yr^{-1} (Walsh et al, 1979b). The remaining unquantified fluxes must be solved by considering the steady state mass balance for each reservoir. As the smallest flux, the volcanic flux, lies between 10 and 1 kt As yr^{-1} , all fluxes have been calculated to the nearest whole number to facilitate the solution of the unknown fluxes by this mass balance approach.

The flux from the ocean mixed layer to troposphere may be quantified by considering the mass balance for the ocean mixed layer. The total input is $1022 \text{ kt As yr}^{-1}$, and the sum of the known fluxes from the ocean mixed layer is $992 \text{ kt As yr}^{-1}$. The remaining flux is the difference between the two, 30 kt As yr^{-1} . The efflux rate of arsenic from the land may now be solved by mass balance considerations for the troposphere. The total output is 73 kt As yr^{-1} , and the known input is 37 kt As yr^{-1} , so the land to troposphere flux is 36 kt As yr^{-1} .

Sedimentation rates are very difficult to establish for the global ocean, as there is a wide variety of estimates for such rates in the literature, based on sediment trap data or settling velocity measurements (see for example : Schwarzer, 1975; Shanks and Trent, 1980; Takahashi and Honjo, 1983; Wiebe et al, 1976). However, the settling rate of fine particulate matter is well established at about 1 m d^{-1} (Krishnaswami et al, 1976, Minagawa and Tsunogai, 1980). Particle sizes in the ocean cover a wide spectrum (O'Connors et al, 1976; Sheldon and Parsons, 1967), and the size distribution of arsenic is still unknown, so it is impossible to assign a suitable settling velocity for this element. However, it is

possible to consider a lower limit, if all arsenic is associated with the fine particulate matter, with a settling velocity of 1 m d^{-1} . Over the area of the global oceans, $3.6 \times 10^{14} \text{ m}^2$ (Turekian, 1969), the fine particulates settle through $1.3 \times 10^{17} \text{ m}^3$ of seawater annually. This is about 10% of the global ocean volume, so about 10% of the ocean particulate reservoir would be lost from the ocean annually, about 10 kt As yr^{-1} . The mass balance solution to the particulate reservoir is calculated from the difference between the total input, $639 \text{ kt As yr}^{-1}$, and the known output, $485 \text{ kt As yr}^{-1}$, to yield a sedimentation flux of $154 \text{ kt As yr}^{-1}$. This is much higher than the estimate for fine grained material alone, which suggests there is a significant sedimentation input from marine snow, either as a biogenic flux or by shear coagulation of arsenical fine particles by the more rapidly settling biotic particles (McCave, 1984). It is unlikely that arsenic is confined exclusively to large biotic particles, as the concentrations of particulate trace elements at depth cannot be explained by the sinking of organic detritus alone (Kharkar et al, 1976), so some small fraction is probably associated with fine particles. The flux from the ocean mixed layer to the particulate reservoir provides further evidence for this, as only 1% was associated with inorganic adsorption, a process controlled by fine particulate matter (Krishnaswami, et al, 1976).

Loss from the sediments to the magma by subduction is 7 kt As yr^{-1} , which balances the magmatic output of volcanic arsenic, and leaves $147 \text{ kt As yr}^{-1}$ as the flux from sediments to landmass by uplift and weathering. This completes the basic steady state model for arsenic, which is defined in terms of seven reservoirs with seventeen associated fluxes (figure 4.1).

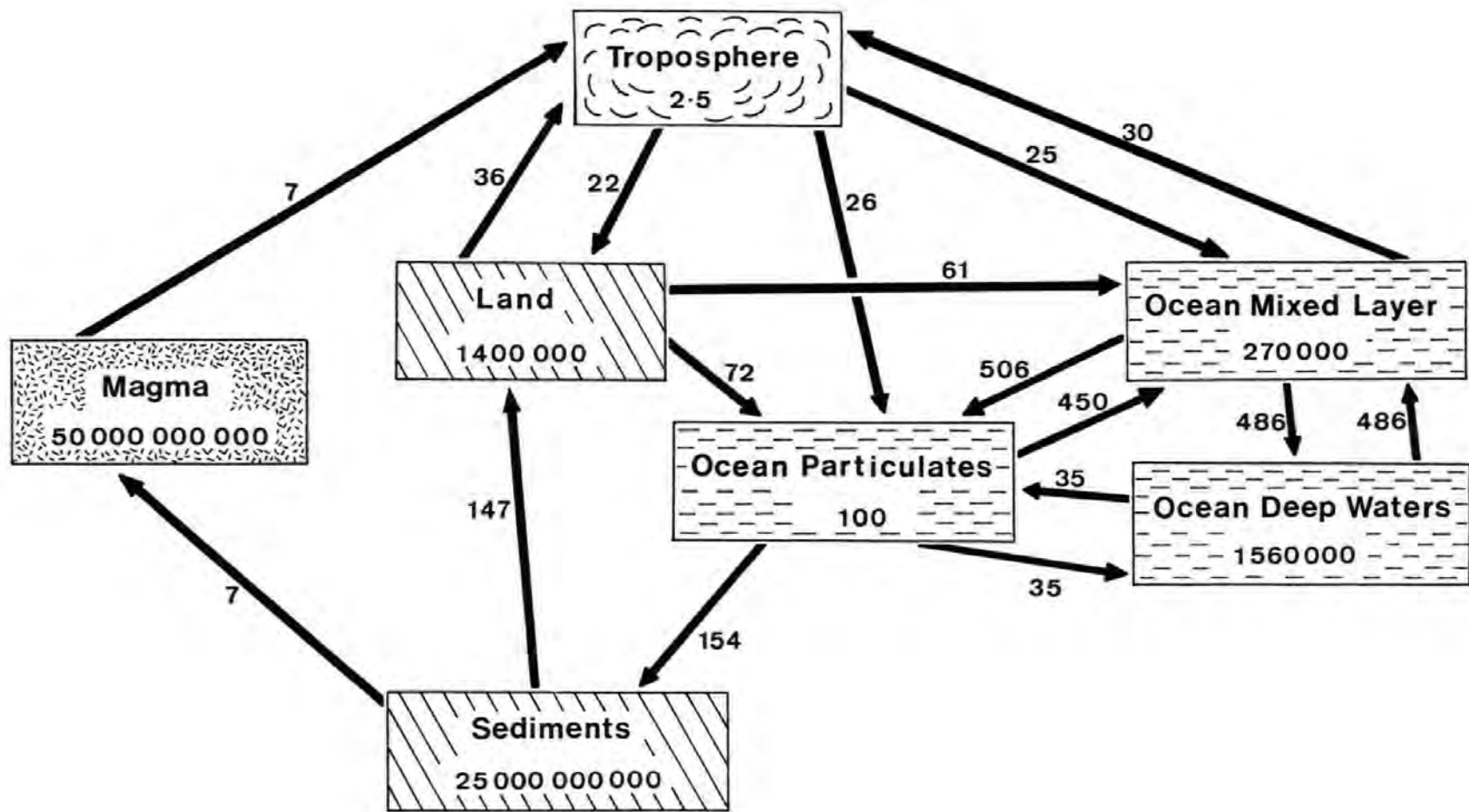


Figure 4.1 Basic steady state for the global arsenic cycle. Reservoirs in kt As, fluxes in kt As yr⁻¹

4.1.2 Subdivision of the Ocean Particulates

The oceanic reservoirs are treated inconsistently in the basic model. Although the dissolved phase is separated into two reservoirs, dependent on depth, the particulate phase is treated as a single well-mixed reservoir. Therefore, a second steady state was developed, in which the oceanic particulates were also subdivided into a mixed layer reservoir and a deep ocean reservoir. The particulate mass in the mixed layer is 1.8×10^{15} g, and in the deep waters 5.2×10^{15} g, with an arsenic concentration of 10 ppm (Buat-Menard, pers. comm., 1982). Thus, the arsenic mass of the mixed layer particulate reservoir is :

$$1.8 \times 10^6 \text{ kt} \times 10 \times 10^{-6} \text{ kt As kt}^{-1} = 18 \text{ kt As} \quad (4.18)$$

As the concentration of arsenic in particulates is not well established, a reservoir mass of 20 kt may be considered as a first order approximation. Similarly, the deep water particulate reservoir becomes :

$$5.2 \times 10^6 \text{ kt} \times 10 \times 10^{-6} \text{ kt As kt}^{-1} = 52 \text{ kt As} \quad (4.19)$$

Thus, the reservoir is about 50 kt As.

Most of the fluxes involving these reservoirs remain unchanged from the basic steady state. However, four new fluxes must be considered : exchange between the two reservoirs, and their individual input to the sediments. The upwelling particulate flux can be determined from the upwelling rate of $3.2 \times 10^{14} \text{ m}^3 \text{ yr}^{-1}$, derived from Broecker (1974) and Turekian (1969), the deep water particulate content, $5 \mu\text{g L}^{-1}$ (Brewer et al, 1980), and the arsenic concentration in oceanic particulates, 10 ppm :

$$\begin{aligned} & 3.2 \times 10^{14} \text{ m}^3 \text{ yr}^{-1} \times 5 \times 10^{-12} \text{ kt m}^{-3} \times 10 \times 10^{-6} \text{ kt As kt}^{-1} \\ & = 0.016 \text{ kt As yr}^{-1} \end{aligned} \quad (4.20)$$

This is very much smaller than any other flux in the cycle, and may be disregarded as insignificant.

As about 10% of the oceans are underlain by continental shelf, 10% of the mixed layer particulate reservoir settles directly onto the shelf sediments, and does not pass through the deep water reservoir. However, the fate of the riverine particulate matter should also be considered. This forms a flux from the land to the mixed layer particulates, but does not influence open ocean waters, and is lost predominantly to estuarine and coastal sediments (Wasilenchuk, 1978). The flux from the mixed layer particulates to the sediments is comprised of this riverine particulate flux and 10% of the remaining flux from the mixed layer particulate reservoir. Total input to this reservoir is $604 \text{ kt As yr}^{-1}$, and the known output, including the riverine particulates, is $522 \text{ kt As yr}^{-1}$, a difference of 82 kt As yr^{-1} . So about 8 kt As yr^{-1} are lost to the shelf sediments, giving a total flux from the mixed layer particulates to the sediments of 80 kt As yr^{-1} , and leaving 74 kt As yr^{-1} as the flux to the deep water particulates. The sedimentation flux from the deep water particulate reservoir is also 74 kt As yr^{-1} , completing the mass balance for the model. The total sedimentation flux is still $154 \text{ kt As yr}^{-1}$, as determined for the basic model. This refinement is shown in figure 4.2. Only the oceanic reservoirs are shown, all other reservoirs and fluxes are unchanged from the basic model. The kinetic models analysed in section 4.2 proved to be insensitive to this refinement, so in further refinements both a homogeneous particulate reservoir and the subdivision of the reservoir are considered, where appropriate. Although the subdivided particulate reservoir represents a more rigorous treatment of the geochemical cycle, kinetic analyses are considered using a homogeneous particulate reservoir to ease the inflexibility of the computer models.

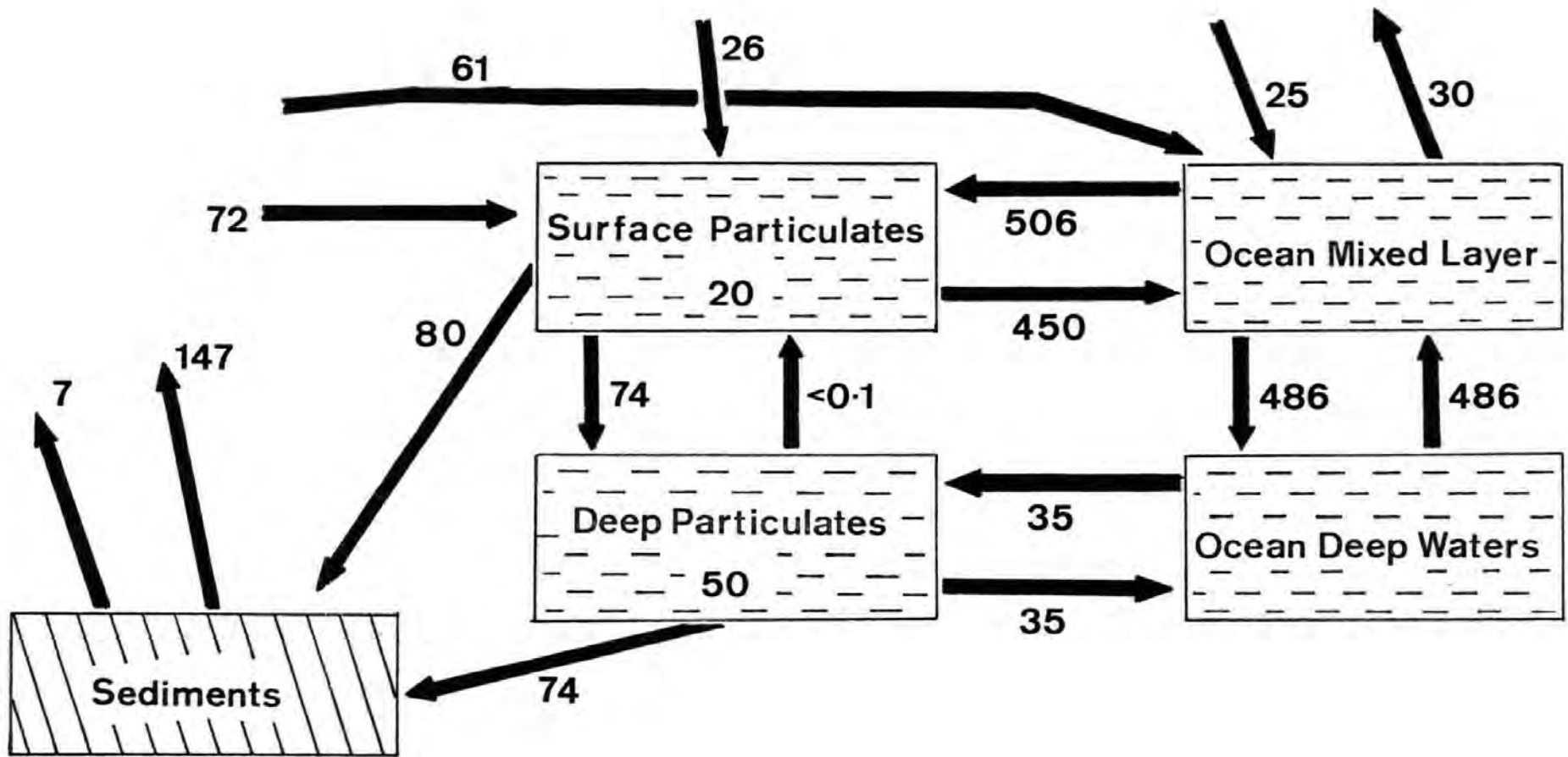


Figure 4.2 Refinement to basic steady state to include two particulate reservoirs. Reservoirs in kt As, fluxes in kt As yr⁻¹

4.1.3 A Heterogeneous Troposphere

4.1.3.1 A model with a homogeneous particulate reservoir

Although the atmosphere in the basic model is treated as a well-mixed troposphere, the large discrepancy between arsenic concentrations in marine air and continental air shows this to be an over-simplification. The troposphere was, therefore, subdivided into marine and continental airmasses, and exchange between them defined as in section 3.1.2.

The continental airmasses overly 30% of the global area, and have an aerosol arsenic concentration of 1.5 ng m^{-3} (Adams et al, 1977), so the aerosol reservoir is :

$$1.53 \times 10^{18} \text{ m}^3 \times 1.5 \times 10^{-18} \text{ kt As m}^{-3} = 2.3 \text{ kt As} \quad (4.21)$$

As 7% of atmospheric arsenic is in the vapour phase, the total reservoir is 2.5 kt As. The marine atmosphere covers a much larger portion of the globe, 70%, but has a much smaller aerosol arsenic concentration, 0.018 ng m^{-3} (Walsh et al, 1979b), so the marine aerosol reservoir is :

$$3.57 \times 10^{18} \text{ m}^3 \times 0.018 \times 10^{-18} \text{ kt As m}^{-3} = 0.064 \text{ kt As} \quad (4.22)$$

With the 7% vapour content, the total reservoir is 0.069 kt As. All other reservoirs are as in the basic model.

The major winds of the globe transfer $7.35 \times 10^{18} \text{ m}^3 \text{ yr}^{-1}$ of air from the marine to the continental troposphere, with an equal flux in the reverse direction, carrying material passively, irrespective of whether it is vapour or aerosol. Therefore, the fluxes of arsenic are proportional to the total concentrations in the marine and continental troposphere. The flux from the marine troposphere across the coast is :

$$7.35 \times 10^{18} \text{ m}^3 \text{ yr}^{-1} \times 0.018 \times 10^{-18} \text{ kt As m}^{-3} \times 100/93$$

$$= 0.14 \text{ kt As yr}^{-1} \quad (4.23)$$

Fluxes for the basic steady state were calculated to the nearest whole number. However, this flux is considerably less than 1 kt yr^{-1} , but not by more than an order of magnitude, so an approximation of $0.1 \text{ kt As yr}^{-1}$ will be used. All other fluxes will also be calculated to one decimal place. This does not imply that the fluxes are known to such precision, but is merely an artefact of calculating unknown fluxes by a mass balance approach. Therefore, the flux from the continental to marine troposphere is :

$$7.35 \times 10^{18} \text{ m}^3 \text{ yr}^{-1} \times 1.5 \times 10^{-18} \text{ kt As m}^{-3} \times 100/93$$

$$= 11.9 \text{ kt As yr}^{-1} \quad (4.24)$$

Removal to the land and sea surface is by aerosol deposition, so the vapour phase is unimportant for these calculations. It has been shown (this work) that elevated levels of arsenic persist over the ocean for about 300 km from the land, due to exchange with continental airmasses, resulting in elevated depositional fluxes to coastal waters compared with open ocean. Therefore, depositional fluxes must account for the difference in aerosol material exchanged between the marine and continental airmasses :

$$(11.9 \text{ kt As yr}^{-1} - 0.1 \text{ kt As yr}^{-1}) \times 0.93 = 11 \text{ kt As yr}^{-1} \quad (4.25)$$

Therefore, the depositional flux to the land surface is :

$$2.3 \text{ kt As} \times 31.5 \text{ yr}^{-1} - 11.0 \text{ kt As yr}^{-1} = 61.5 \text{ kt As yr}^{-1} \quad (4.26)$$

As 49% of aerosol arsenic falling into the oceans is soluble (Crececius, 1980), the depositional flux to the mixed layer is :

$$\begin{aligned}
 & (0.064 \text{ kt As} \times 31.5 \text{ yr}^{-1} + 11.0 \text{ kt As yr}^{-1}) \times 0.49 \\
 & = 6.4 \text{ kt As yr}^{-1} \qquad \qquad \qquad (4.27)
 \end{aligned}$$

Similarly, the atmospheric flux to the ocean particulates reservoir is :

$$\begin{aligned}
 & (0.064 \text{ kt As} \times 31.5 \text{ yr}^{-1} + 11.0 \text{ kt As yr}^{-1}) \times 0.51 \\
 & = 6.7 \text{ kt As yr}^{-1} \qquad \qquad \qquad (4.28)
 \end{aligned}$$

About 17% of volcanoes erupt in marine basins (Macdonald, 1972), so the volcanic flux to the marine troposphere is :

$$7.0 \text{ kt As yr}^{-1} \times 0.17 = 1.2 \text{ kt As yr}^{-1} \qquad \qquad \qquad (4.29)$$

The volcanic flux to the continental troposphere then becomes 5.8 kt As yr⁻¹.

Backfluxes to the atmosphere from land and sea can now be determined by calculating the mass balance for the marine and continental airmasses. The marine troposphere has a total output of 13.2 kt As yr⁻¹, and a known input of 13.1 kt As yr⁻¹, so the ocean to atmosphere flux is 0.1 kt As yr⁻¹. This is much lower than earlier estimates of about 200 kt yr⁻¹ (Lantzy and Mackenzie, 1979; Mackenzie *et al*, 1979), but is very similar to the estimate of 0.14 kt yr⁻¹ by Walsh and coworkers (1979b). As this latter figure was determined from atmospheric arsenic concentrations over the sea surface, it is more reliable than the larger estimate, which was determined from early data for arsenic in rain, and assumed a well-mixed troposphere. The land efflux rate can be determined by considering the mass balance for the continental troposphere. The total output is 73.4 kt As yr⁻¹, whereas known input is 5.9 kt As yr⁻¹, to give an efflux rate of 67.5 kt As yr⁻¹.

Upwelling and downwelling fluxes were determined using the same assumptions as in the basic model, but calculated to one decimal place, to give $486.0 \text{ kt As yr}^{-1}$ for both fluxes. Similarly, dissolution from the ocean particulates, and riverine fluxes from the land were calculated from the equations in the basic model, but to a higher precision. Thus, the particulate flux to the ocean mixed layer is $450.0 \text{ kt As yr}^{-1}$, and to the deep waters is $35.0 \text{ kt As yr}^{-1}$. The dissolved flux from the land is $61.2 \text{ kt As yr}^{-1}$, and the riverine particulate flux $72.0 \text{ kt As yr}^{-1}$. The flux from the ocean mixed layer to the ocean particulates must be recalculated to satisfy the steady state mass balance for the ocean mixed layer. The total input is $1003.6 \text{ kt As yr}^{-1}$, and the known output is $486.1 \text{ kt As yr}^{-1}$, so the remaining flux is $517.5 \text{ kt As yr}^{-1}$. As the component from biological uptake is $500.0 \text{ kt As yr}^{-1}$, the flux for inorganic adsorption is now increased to $17.5 \text{ kt As yr}^{-1}$, with a rate constant of $6.4815 \times 10^{-5} \text{ yr}^{-1}$. Therefore, the adsorption flux from the deep water reservoir, $1.56 \times 10^6 \text{ kt}$, is $101.1 \text{ kt As yr}^{-1}$, which leaves the ocean deep waters with an output of $587.1 \text{ kt As yr}^{-1}$, but an input of only $521.0 \text{ kt As yr}^{-1}$. To redress the balance, an additional flux was introduced, pore waters diffusing from the sediments to the deep waters, of $66.1 \text{ kt As yr}^{-1}$. Arsenic has been observed to diffuse from estuarine sediments (Carpenter et al, 1978), although no observations were made for marine sediments. However, arsenic may behave as a phosphate analogue (for example, compare Froelich et al, 1977 with Neal et al, 1979), and phosphate is known to diffuse from marine sediments (Fairbridge, 1972). Andreae (1979) reported slight elevations of dissolved arsenic in bottom waters, which he ascribed to the diffusion of pore waters from the sediments. Therefore, the extra flux in the model probably represents a real mechanism of arsenic transport in the oceans. A major source of this remobilised material is probably the

uppermost 6 cm of the sediments, with some remobilisation to a depth of 20 cm., below which the sediments become stable with no mixing (Aller and DeMaster, 1984). Some of the arsenic diffusing from deepwater sediments may be of hydrothermal origin, from sources such as the mid-Atlantic Ridge (Neal et al., 1979). The source of hydrothermal arsenic should be regarded as the magma reservoir rather than the sediments, but as the proportion of hydrothermal to remobilised arsenic is unknown, the sediments have been treated as the sole source of this flux.

Particulate sedimentation may now be determined by calculating the mass balance for the particulate reservoir. The total input is 697.3 kt As yr⁻¹, and the known output is 485.0 kt As yr⁻¹, to yield a sedimentation flux of 212.3 kt As yr⁻¹ by difference. This is equivalent to an arsenic accumulation rate in the sediments (sedimentary input minus pore water outflow) of about 40 µg As cm⁻² (10³ yr)⁻¹, about seven times higher than the accumulation rate measured by Neal and coworkers (1979) for the North Atlantic sediments. The same authors also calculated a residence time of 1 - 2 x 10⁵ yr for arsenic in the North Atlantic Ocean. The residence time in this model is much shorter, about 10⁴ yr. The subduction flux of arsenic from the sediments to the magma is 7.0 kt yr⁻¹, calculated as a mass balance for the magma reservoir, which leaves the flux from the sediments to the land to complete the steady state. The input to the sediments is 212.3 kt As yr⁻¹, known output is 73.1 kt As yr⁻¹, to leave an uplift flux of 139.2 kt As yr⁻¹. The resultant model, consisting of eight reservoirs and twenty one fluxes, is shown in figure 4.3.

4.1.3.2 Subdivision of the ocean particulates

The two particulate reservoirs are unchanged from Section 4.1.2, to give a mixed layer particulate reservoir of 20 kt As and a deep water

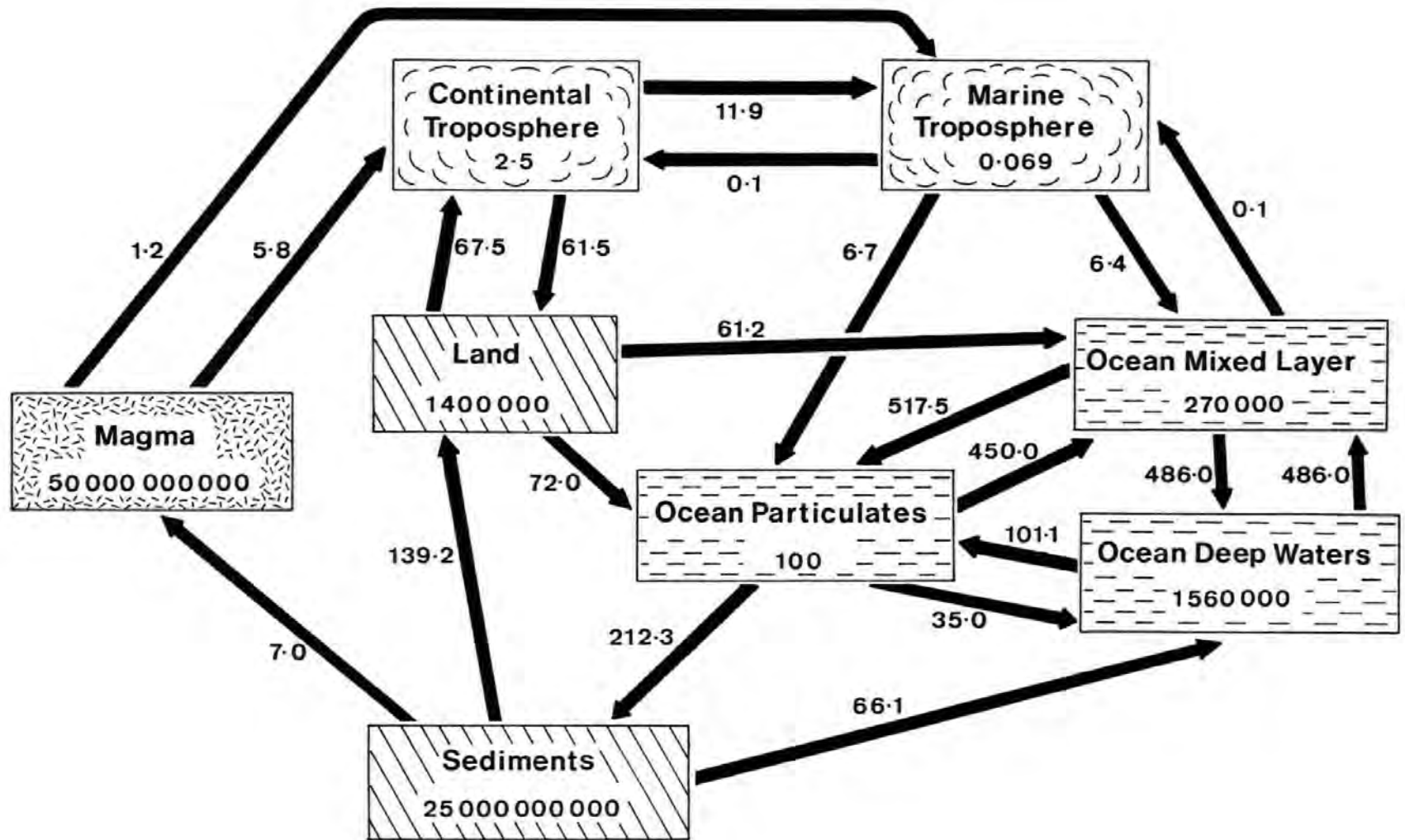


Figure 4.3 A steady state model with a heterogeneous troposphere. Reservoirs in kt As, fluxes in kt As yr⁻¹

particulate reservoir of 50 kt As. Again, the new fluxes to be considered are : exchange between the two reservoirs and sedimentation from each. The upwelling flux is still insignificant at less than $0.02 \text{ kt As yr}^{-1}$. Sedimentation from the mixed layer consists of the riverine particulate input with 10% of the remaining downflux from the mixed layer particulate reservoirs. Input to the mixed layer particulates is $596.2 \text{ kt As yr}^{-1}$, known removal, including the riverine flux, is $522.0 \text{ kt As yr}^{-1}$, a difference of $74.2 \text{ kt As yr}^{-1}$. Thus, the sedimentation flux from the mixed layer is :

$$72.0 \text{ kt As yr}^{-1} + 74.2 \text{ kt As yr}^{-1} \times 0.1 = 79.4 \text{ kt As yr}^{-1} \quad (4.30)$$

The flux from the mixed layer to deep water particulates then becomes $66.8 \text{ kt As yr}^{-1}$, and the sedimentation flux from the deep water particulates is $132.9 \text{ kt As yr}^{-1}$, completing the mass balance for the model (Figure 4.4).

The deep water particulate flux gives an arsenic accumulation rate in the deep ocean sediments of about $20 \mu\text{g As cm}^{-2} (10^3 \text{ yr})^{-1}$, about three times the accumulation rate measured by Neal and coworkers (1979). This is a better approximation to the measured rate than was provided by the homogeneous particulates model, but still rather high. Primary productivity in the coastal ocean is about twice that in open ocean (Manzel, 1974), and aerosol deposition into coastal waters is also higher than in the open ocean (this work), but apart from the riverine input, the mixed layer particulate reservoir was regarded as well mixed in the model. As the increased productivity and aerosol input probably lead to high removal rates to coastal sediments, the sedimentation to the continental shelf was probably underestimated, leaving an overestimate for the deep sea sedimentation and deep sea arsenic accumulation rates.

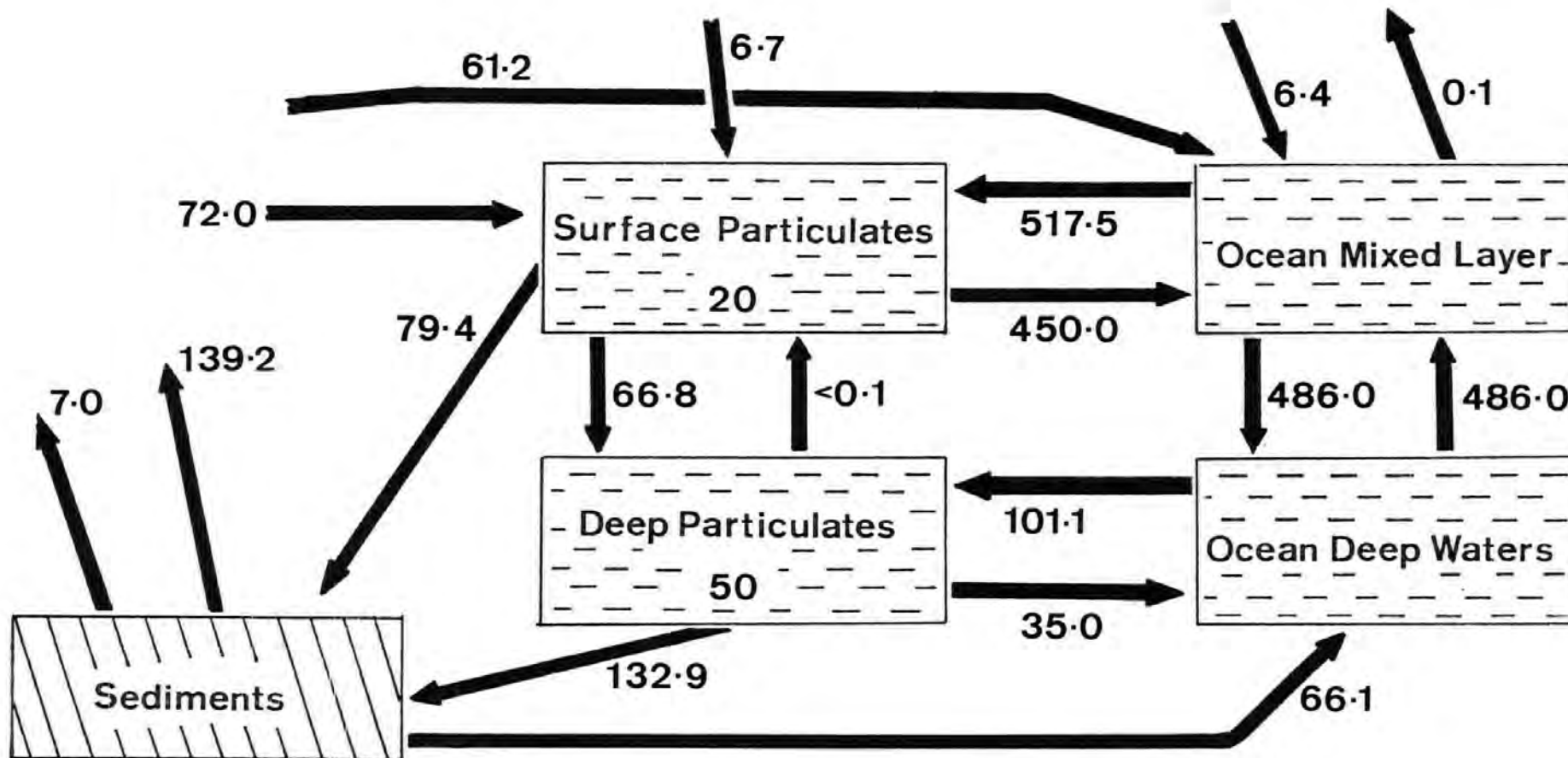


Figure 4.4 Refinement to the heterogeneous troposphere model to include two particulate reservoirs. Reservoirs in kt As, fluxes in kt As yr⁻¹

4.1.4 The Biosphere

4.1.4.1 The marine biosphere

In the previous models the marine biosphere was represented by transport mechanisms between the dissolved and particulate phase. However, it is important to assess the interaction between the biosphere and its environment, and the extent to which the biosphere is effected by anthropogenic activity. Therefore, a separate reservoir for the marine biosphere was devised, using the heterogeneous troposphere model as a basis.

The primary marine biomass is 2.42×10^{15} g, with an arsenic content of 10 ppm (Onishi, 1969a; Sanders and Windom, 1980; Trefry and Presley, 1976), so the marine biomass reservoir is :

$$2.42 \times 10^6 \text{ kt} \times 10 \times 10^{-6} \text{ kt As kt}^{-1} = 24 \text{ kt As} \quad (4.31)$$

Plankton growth is limited to a narrow zone near the surface (Fairbanks et al., 1982), and the biomass decreases exponentially with depth to become negligible in deep waters (Wishner, 1980), so only biological uptake from the surface ocean need be considered. As uptake from the ocean mixed layer was calculated to be $500.0 \text{ kt As yr}^{-1}$, the flux from the ocean mixed layer to the particulate is $17.5 \text{ kt As yr}^{-1}$. The organic material recycled in the mixed layer is partially released from living plankton, and partially from decaying dead matter. Sanders (1980) considered the release of dissolved arsenic from the biomass by three mechanisms : the release of methyl arsenic by phytoplankton, the release of arsenite by phytoplankton, and the excretion of arsenic by zooplankton. These represented a total of 61.5% of the arsenic taken up by the biosphere in the Georgia Bight, so the flux from the biomass to the ocean mixed layer is :

$$500.0 \text{ kt As yr}^{-1} \times 0.615 = 307.5 \text{ kt As yr}^{-1} \quad (4.32)$$

which leaves a flux of $192.5 \text{ kt As yr}^{-1}$ from the biomass to the particulates to complete the steady state for the biomass. This latter flux represents the death of organisms and the release of fecal pellets. The mass balance for the ocean mixed layer and particulate reservoirs may now be completed by the flux from the particulates to the ocean mixed layer, representing the dissolution of organic detritus. A flux of $142.5 \text{ kt As yr}^{-1}$ satisfied these mass balance requirements. The amendment to the heterogeneous troposphere model (figure 4.5) applies to a model with a homogeneous particulate reservoir or a model with a subdivided particulate reservoir.

4.1.4.2 The terrestrial biosphere

In addition to the marine biota, it is important to assess the effect of man's activities on the terrestrial biosphere. The primary terrestrial biomass has a dry weight of $2.4 \times 10^9 \text{ kt}$, with an annual productivity of $1.73 \times 10^8 \text{ kt}$ (Rodin et al, 1978). The arsenic content of terrestrial flora is about 0.2 ppm (Bowen, 1966), somewhat lower than the marine biota. Thus, the terrestrial biomass reservoir is 480 kt As, with an uptake of $34.6 \text{ kt As yr}^{-1}$ from the land. Arsenic in terrestrial biota may either be lost to the atmosphere or returned to the landmass as detritus. Losses to the atmosphere may either be in the form of direct emission (Beauford et al, 1975 and 1977; Schnell and Vali, 1972 and 1973), or by forest and grassland fires (Bolin et al, 1983). Walsh and coworkers (1979b) estimated that these processes mobilise $0.16 \text{ kt As yr}^{-1}$ and $0.26 \text{ kt As yr}^{-1}$ respectively, to yield a flux of about $0.4 \text{ kt As yr}^{-1}$ from the biomass to the atmosphere. The mass balance requirements of the terrestrial biomass are satisfied by a flux of $34.2 \text{ kt As yr}^{-1}$ from the biomass to the land. The efflux of arsenic from the land must now be

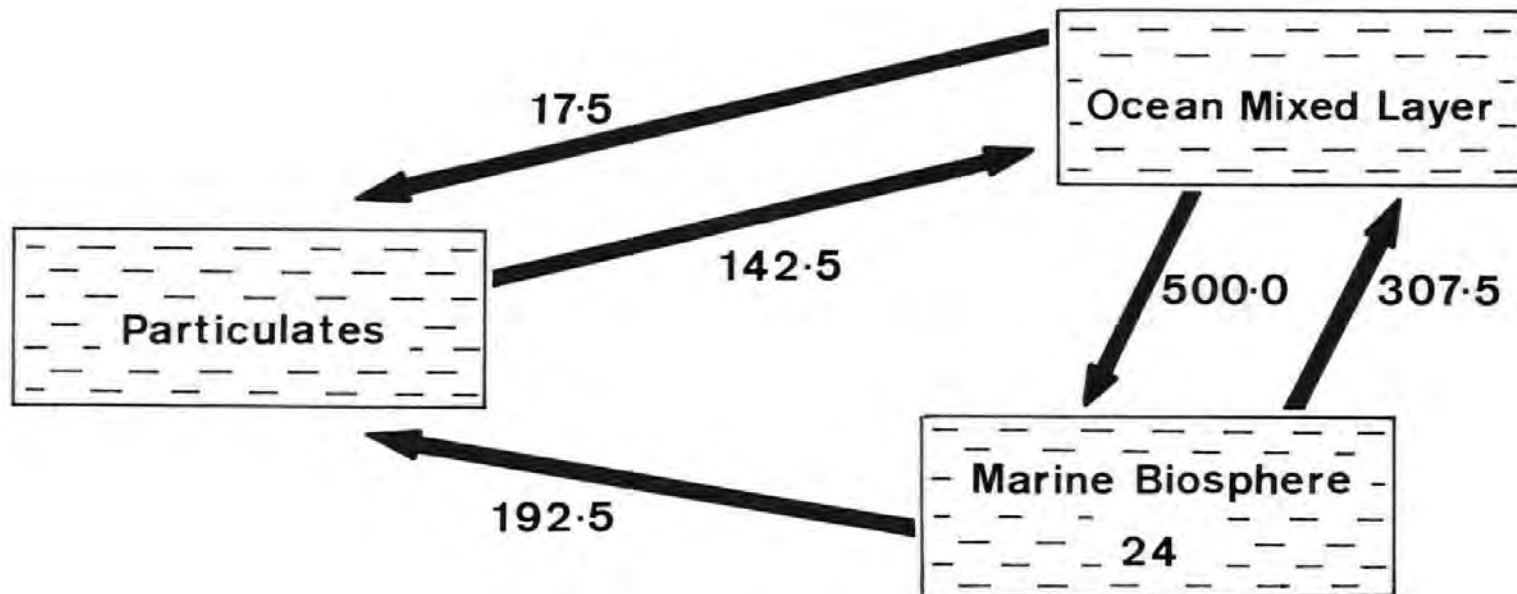


Figure 4.5 Addition of a marine biosphere to the heterogeneous troposphere model.
Reservoir in kt As, fluxes in kt As yr⁻¹

amended to satisfy the mass balance requirements for the land and the continental troposphere, which are restored by reducing the flux from $67.5 \text{ kt As yr}^{-1}$ to $67.1 \text{ kt As yr}^{-1}$ (figure 4.6).

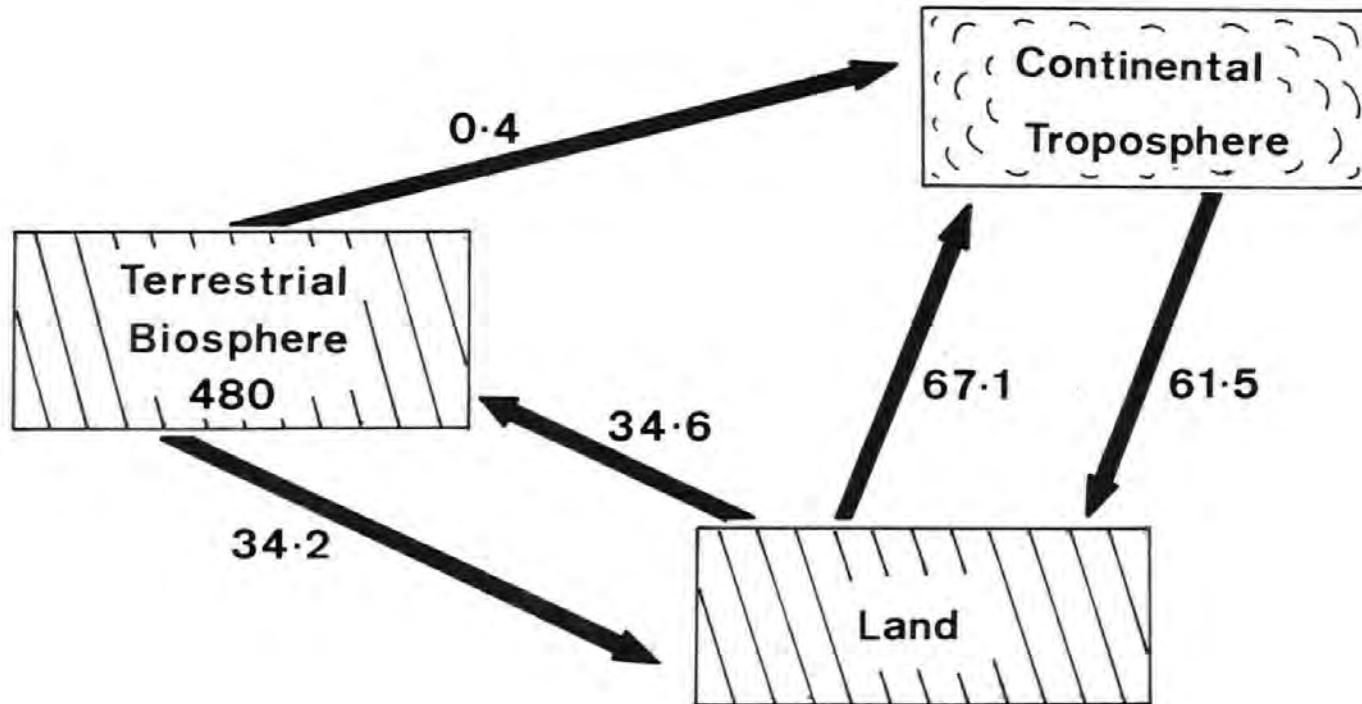


Figure 4.6 Addition of a terrestrial biosphere to the heterogeneous troposphere model. Reservoir in kt As, fluxes in kt As yr⁻¹

4.2 KINETIC MODELLING

4.2.1 The Basic Model

The basic steady state model in section 4.1.1 may be described in terms of the overall residence-time of arsenic in each reservoir, with the first order rate constants for each process, summarised in tables 4.1 and 4.2 respectively.

Table 4.1 Residence Times for Arsenic in the Basic Model

Reservoir	Mass (kt)	Residence time (yr)
Troposphere	2.5	3.4×10^{-2}
Ocean mixed layer	2.7×10^5	2.6×10^2
Ocean deep waters	1.56×10^6	3.0×10^3
Ocean particulates	100	1.6×10^{-1}
Land	1.4×10^6	8.3×10^3
Sediments	2.5×10^{10}	1.6×10^8
Magma	5×10^{10}	7.1×10^9

Arsenic is cycled very rapidly through the troposphere, with a residence time of about 12 d, and rapidly through the particulates, with a residence time of about 2 months, but very slowly through the sediments and magma. Pollutant arsenic may be introduced into the environment directly to the troposphere, oceans or landmass, and then cycled through this system according to the rate constants listed in table 4.2.

Initially, it was assumed that arsenic pollution is released solely from high temperature processes.

4.2.1.1 High temperature processes

The present day pollutant arsenic flux to the atmosphere is 23.6 kt yr^{-1} (Walsh et al, 1979b). Global data for pollutant arsenic fluxes to the land and oceans are unavailable, but are available for the U.S.A.

Table 4.2 Fluxes and Rate Constants for the Basic Model

Flux	Magnitude (kt yr ⁻¹)	Rate constant (yr ⁻¹)
Troposphere to ocean mixed layer	25	1.0000 × 10 ¹
to ocean particulates	26	1.0400 × 10 ¹
to land	22	8.8000
Ocean mixed layer		
to troposphere	30	1.1111 × 10 ⁻⁴
to ocean deep waters	486	1.8000 × 10 ⁻³
to ocean particulates	506	1.8741 × 10 ⁻³
Ocean deep waters		
to ocean mixed layer	486	3.1154 × 10 ⁻⁴
to ocean particulates	35	2.2536 × 10 ⁻⁴
Ocean particulates		
to ocean mixed layer	450	4.5000
to ocean deep waters	35	3.5000 × 10 ⁻¹
to sediments	154	1.5400
Land		
to troposphere	36	2.5714 × 10 ⁻⁵
to ocean mixed layer	61	4.3571 × 10 ⁻⁵
to ocean particulates	72	5.1429 × 10 ⁻⁵
Sediments		
to land	147	5.8800 × 10 ⁻⁹
to magma	7	2.8000 × 10 ⁻¹⁰
Magma		
to troposphere	7	1.4000 × 10 ⁻¹⁰

(NAS, 1977), with 82.7 kt yr^{-1} to the land and $0.16 \text{ kt As yr}^{-1}$ to the oceans. By comparing global atmospheric transport of pollutant arsenic with atmospheric transport from the U.S.A., $9.76 \text{ kt As yr}^{-1}$ (NAS, 1977), an estimate can be made of the percentage of global emissions emanating from the U.S.A., about 41%. If this figure applies to all pollutant arsenic transport, the global transport to the land becomes about $200 \text{ kt As yr}^{-1}$, and to the oceans $0.4 \text{ kt As yr}^{-1}$. Assuming that aqueous pollutant arsenic has the same solubility as natural riverine arsenic, then $0.2 \text{ kt As yr}^{-1}$ is the riverine pollutant flux in both dissolved and particulate forms. The mass of the pollutant arsenic reservoir, and the growth of arsenic pollution may be estimated from the size of the global copper reserves and the growth of copper production (section 3.3.2.1). Present day copper reserves are estimated to be $5 \times 10^5 \text{ kt}$, with a current production of 6044 kt yr^{-1} (Skinner, 1976). This present day production is equivalent to a total pollutant arsenic transport of 224 kt yr^{-1} , so that the reserves are equivalent to a pollutant reservoir of about $2 \times 10^4 \text{ kt As}$. The present day scenario for pollutant arsenic transport is shown in figure 4.7. However, pollutant transport has been significant since about 1750 AD, which has been shown from the data for mercury concentrations in ice cores from Greenland (Appelquist et al, 1978; Millward, 1982), so to model the pollutant influence from the steady state, a pre-industrial pollutant reservoir must be estimated. Copper reserves for the year 1800 AD were estimated at $6.5 \times 10^5 \text{ kt}$ (section 3.3.2.1), which are equivalent to a pollutant reservoir of $2.4 \times 10^4 \text{ kt As}$, and gives a pre-industrial reservoir of about $2.5 \times 10^4 \text{ kt As}$.

Growth of the pollutant fluxes were estimated from the growth curve of copper production (section 3.3.2.1), with a growth rate of 3.6% until the exhaustion of the first third of the reserves, then at 0.5% until two

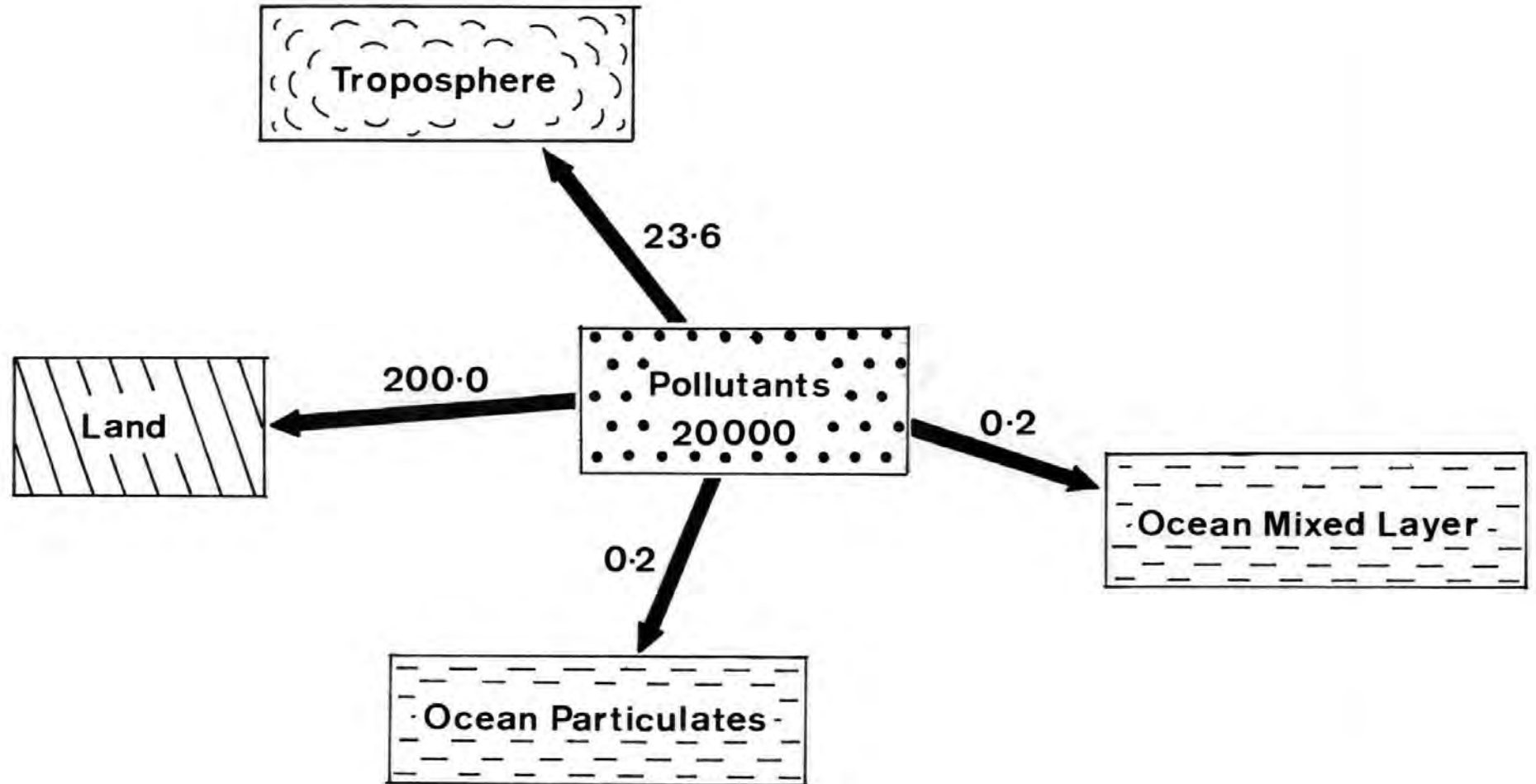


Figure 4.7 Present day scenario for pollutant transport of arsenic from high temperature processes

thirds of the reserves have been exhausted, and finally a decline rate of 0.5% (Bain, 1978). The pollutant rate constants were determined for the present day scenario, and the equations established to describe the change of rate constant with time (table 4.3). The term "rate constant" is a misnomer in these circumstances, but is more familiar than expressions such as "first order rate variable".

Using the equations from table 4.3 to define pollutant arsenic transport, a non-steady state time-dependant model was simulated by computer (figure 4.8). The changes in arsenic burden of the troposphere, ocean mixed layer and landmass are shown as a function of time. The maximum arsenic burden in the troposphere was achieved by the year 2000 AD, with an increase of 30% over the steady state. This relaxed to a new steady state value by about 2400 AD, 2.55 kt As, slightly higher than the original burden. In contrast, the ocean and landmass were hardly effected, with maxima representing increases of less than 3% over the steady state. Ferguson and Gavis (1972) also showed that anthropogenic distribution of arsenic over the land would have a negligible effect on the oceans, causing only localised pollution in rivers and lakes. Pollutant arsenic reserves fell to a constant level of 700 kt by the year 3000 AD, in a sigmoidal curve, with a half life of 600 yr (figure 4.9). This differs from earlier economic models (see for example, Meadows et al, 1974) in which pollutant reserves were exponentially depleted to zero using a single growth rate.

The results from this simulation suggest that the present day burden of arsenic in the troposphere is about 3.2 kt. The actual present day burden may be determined from observations of the atmospheric arsenic concentration. Concentrations of aerosol arsenic in the southern hemisphere

Table 4.3 Equations to Determine Instantaneous Rate Constants for
Pollutant Arsenic Fluxes

Atmospheric transport

Mature stage :

$$\ln (k) = 0.036 \times \text{date} - 77.98$$

Gerontic stage :

$$\ln (k) = 0.005 \times \text{date} - 16.54$$

Decline stage :

$$\ln (k) = (-0.005) \times \text{date} + 3.54$$

Riverine transport

(dissolved or particulate)

Mature stage :

$$\ln (k) = 0.036 \times \text{date} - 82.75$$

Gerontic stage :

$$\ln (k) = 0.005 \times \text{date} - 21.31$$

Decline stage :

$$\ln (k) = (-0.005) \times \text{date} - 1.23$$

Land transport

Mature stage :

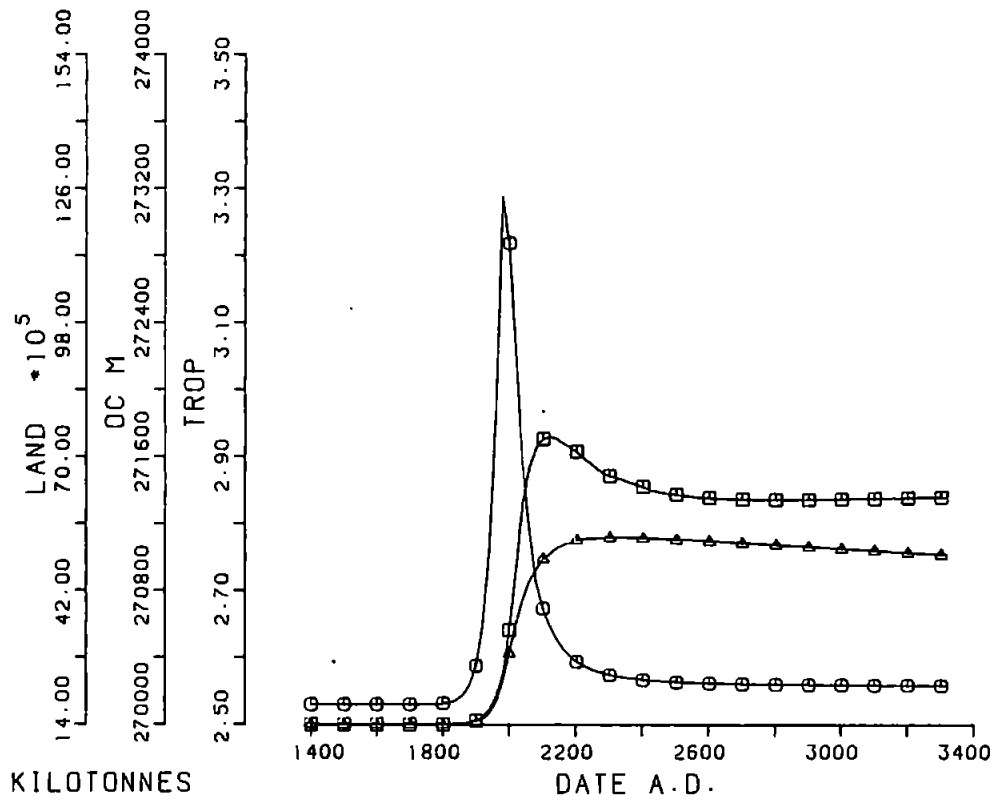
$$\ln (k) = 0.036 \times \text{date} - 75.85$$

Gerontic stage :

$$\ln (k) = 0.005 \times \text{date} - 14.41$$

Decline stage :

$$\ln (k) = (-0.005) \times \text{date} + 5.67$$



KEY
 ○ TROPOSPHERE
 □ OCEAN MIXED LAYER
 ▲ LAND

Figure 4.8 The effect of the pollutant input from high temperature processes on the arsenic burden in the environment

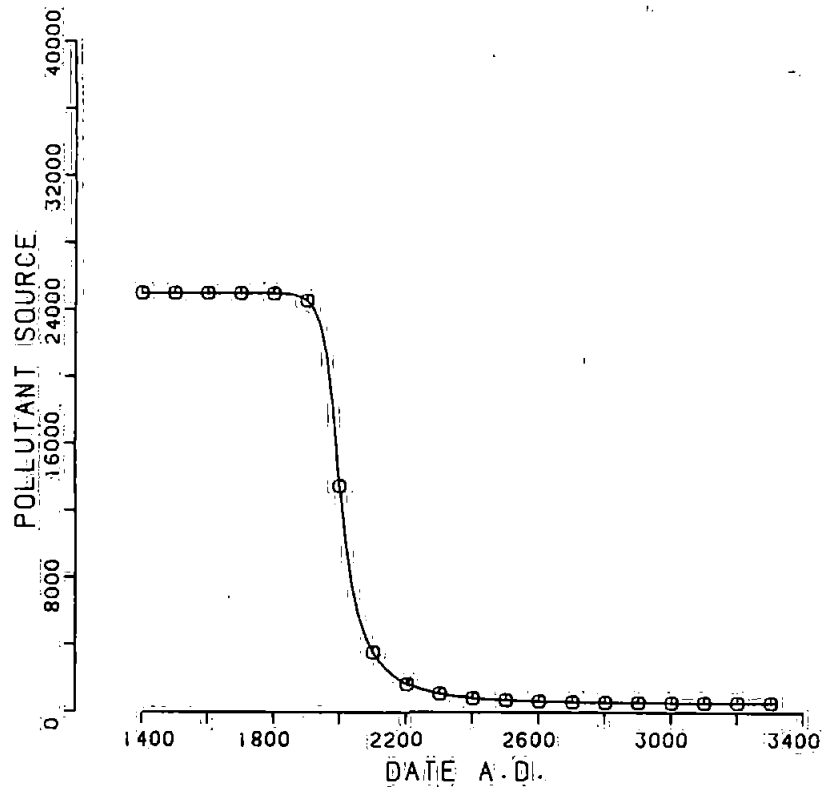


Figure 4.9: The depletion of pollutant arsenic sources, in kt As.

are the same as those used to establish the steady state, 1.5 ng m^{-3} for the continental atmosphere (Adams et al, 1977) and 0.018 ng m^{-3} for the marine atmosphere (Walsh et al, 1979b). The mean concentration of arsenic over the North Atlantic, $0.075 \text{ ng (SCM)}^{-1}$ (this work), represents the concentration of arsenic over the northern oceans. However, the arsenic concentration of air over Plymouth, $0.83 \text{ ng (SCM)}^{-1}$ (this work), is lower than that for continental air in the southern hemisphere because Plymouth is influenced by marine airmasses. A better approximation to the concentration of aerosol arsenic over the northern continents is provided from the data of Salmon and coworkers (1978) for rural air over Oxfordshire, to give a geometric mean of 4.2 ng m^{-3} . As 80% of the southern hemisphere and 60% of the northern hemisphere are covered by oceans, the total observed aerosol arsenic burden is 5.2 kt As, to give a total burden of 5.6 kt As, allowing for the vapour content of 7% (Walsh et al, 1979a). Therefore, there is a shortfall in the simulation of 2.4 kt As for the troposphere, if only high temperature sources are considered. The remainder must be due to mobilisation of arsenic by man's activities on the land, using low temperature mobilisation processes.

4.2.1.2 Low temperature processes

Agricultural processes increase the dust flux to the atmosphere about two-fold (Ajax and Lee, 1976), so could represent a major contribution to the mobilisation of arsenic by low temperature processes. To model this, the landmass was divided into a reservoir for arable land and a reservoir for non-arable land. About 4230×10^6 ha are potentially available for agriculture (Revelle, 1976), in which the soil cover is disturbed to a depth not exceeding 30 cm (Hobbs, pers. comm., 1983). If the average density of arable soil is 2.5 g cm^{-3} , and the average arsenic content is 7 ppm, the arable reservoir is :

$$4.23 \times 10^{17} \text{ cm}^2 \times 30 \text{ cm} \times 2.5 \text{ g cm}^{-3} \times 7 \times 10^{-15} \text{ kt As g}^{-1}$$

$$= 2.2 \times 10^5 \text{ kt As} \quad (4.33)$$

Therefore, the remaining soil reservoir is 1.18×10^6 kt As. The area of arable land is equivalent to 31.8% of the ice-free land surface, so 31.8% of the exchange with the troposphere, and landmass fluxes to the oceans, is associated with the arable reservoir. Thus, efflux from the arable land is 11 kt As yr^{-1} , and 25 kt As yr^{-1} from the remaining land. Return fluxes from the troposphere are 7 kt As yr^{-1} to the arable reservoir, and 15 kt As yr^{-1} to the undisturbed soil. Arable fluxes to the ocean mixed layer and ocean particulates are 19 kt As yr^{-1} and 23 kt As yr^{-1} respectively, leaving 42 kt As yr^{-1} and 49 kt As yr^{-1} to the ocean mixed layer and particulates from the non-arable reservoir. As the arable land only extends down to half the depth of the global soil cover, weathering of undisturbed soil to the arable land must be considered to satisfy the mass balance requirements for both reservoirs. A flux of 46 kt As yr^{-1} completes the steady state for this refinement to the basic model (figure 4.10).

The growth curve for the use of arable land, devised in section 3.3.2.2, may be applied to the doubling of the natural rate constant for the efflux of arsenic from the arable land surface (Ajax and Lee, 1976). If simulated in conjunction with the pollutant transport by high temperature processes (figure 4.11), the simulated present day arsenic burden in the troposphere is about 3.4 kt, again much less than the observed burden. Therefore, low temperature mobilisation of arsenic cannot be modelled only by the the increase of dust fluxes from arable land, but must be considered on a wider scale.

Weiss and coworkers (1971) suggested that rising trends in atmospheric

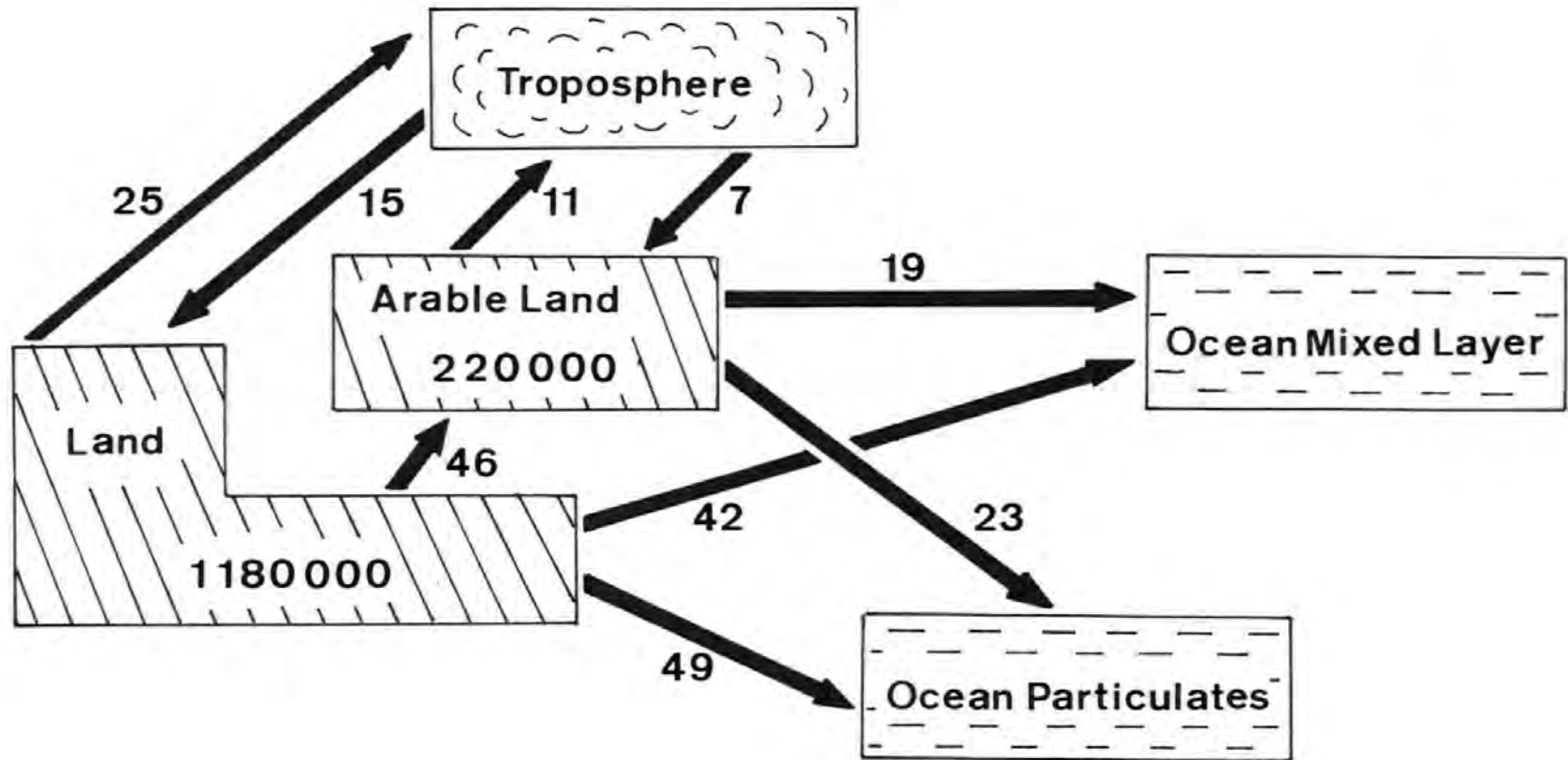
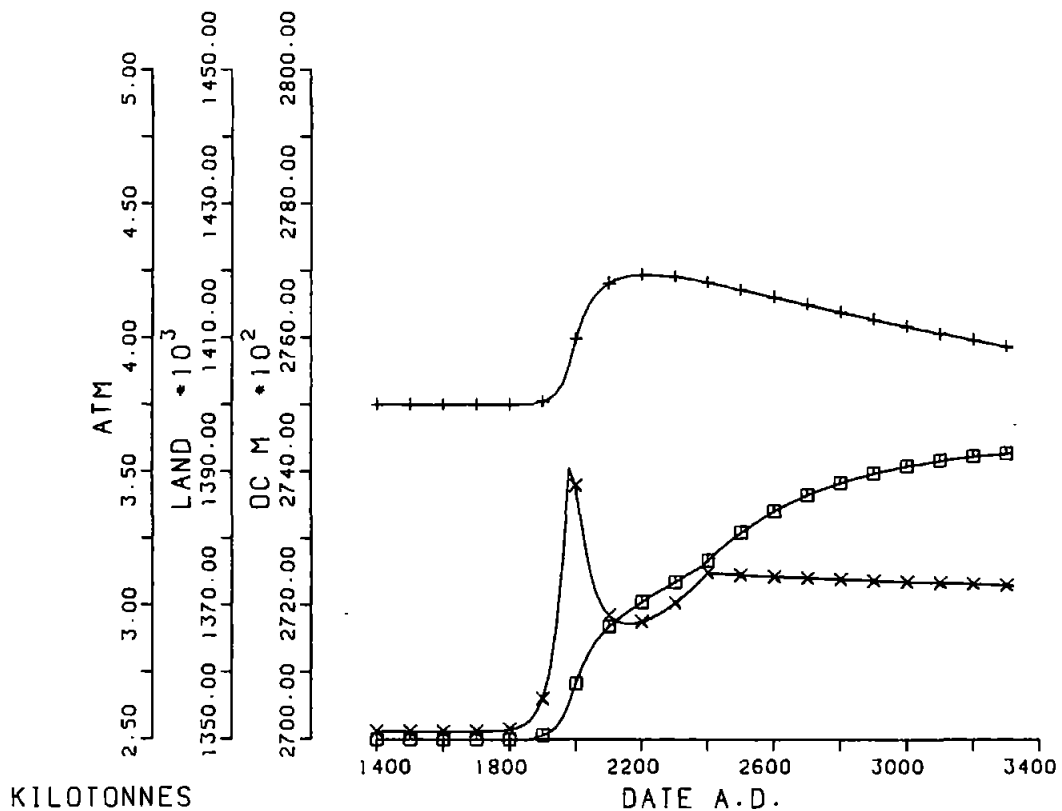


Figure 4.10 Refinement to the basic steady state to subdivide the landmass into arable and non-arable land. Reservoirs in kt As, fluxes in kt As yr⁻¹

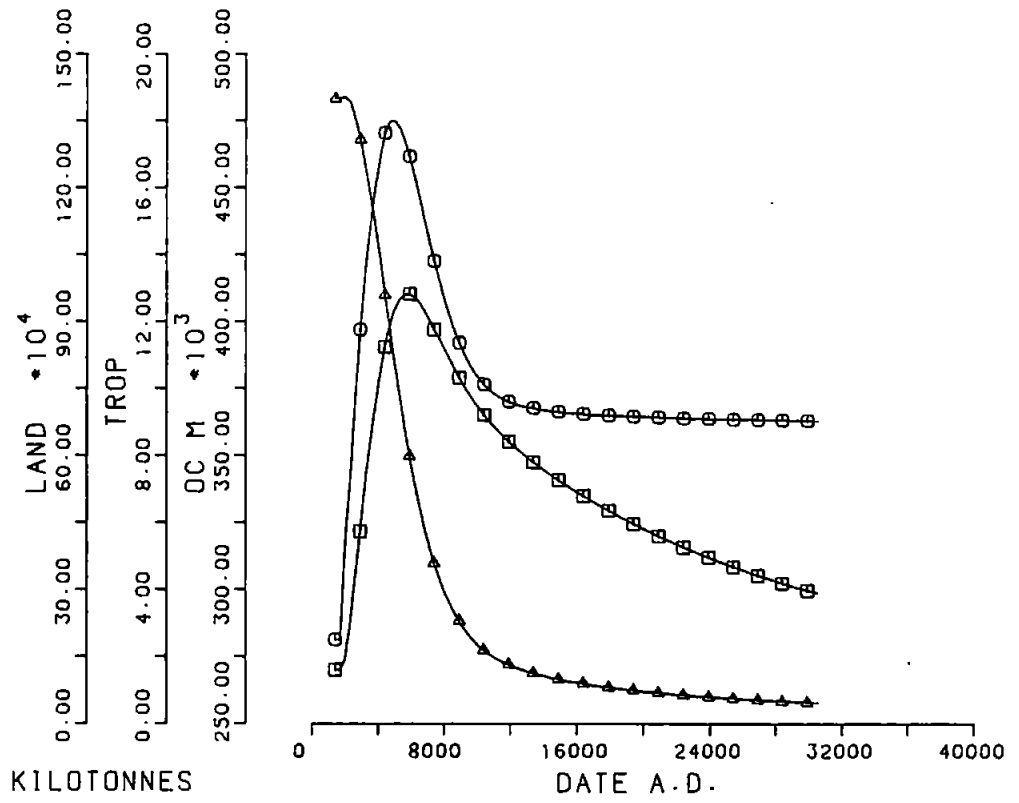


KEY
 □ OCEAN MIXED
 + LAND
 x TROPOSPHERE

Figure 4.11 Combination of high temperature pollutant input of arsenic to the environment with increased mobilisation of arsenic as dust from arable land

concentrations of atmophile elements were caused by man's increasing exposure of raw crustal material, including processes other than those associated with agriculture. This perturbation may be modelled by increasing the efflux rate from the land surface (Millward, 1982). The additional tropospheric arsenic burden of 2.4 kt, not provided by high temperature processes, was simulated by increasing the land efflux rate constant by $1.6 \times 10^{-7} \text{ yr}^{-2}$. This was applied from 1750 AD, on the evidence of mercury concentrations in ice cores from Greenland (Appelquist et al, 1978; Weiss et al, 1971). By applying the perturbation without constraint, the landmass was exhausted of arsenic with a half life of about 3550 yr (figure 4.12). At the same time as the landmass was half depleted, about 5300 AD, the tropospheric arsenic burden achieved a maximum of 18 kt, increasing by a factor of seven over the steady state. Although the time scale is vast, it was expressed as Date A.D. because the rate constants for high temperature emission, which were still operative in this simulation, were determined from the data (see table 4.3). Tropospheric arsenic is ultimately lost to the oceans, resulting in an increase of 50% in the mixed layer burden, about 700 yr after the tropospheric maximum. The troposphere relaxed to a new steady state in about 10 000 yr, but the ocean mixed layer did not achieve a new steady state before the end of the simulation, as the residence time of arsenic is much longer in the mixed layer than in the troposphere. The influence of high temperature sources was insignificant compared with the low temperature mobilisation.

The above simulation represents an extreme situation, where the landmass is totally depleted of arsenic. The effect of arable land on the low temperature mobilisation of particulate arsenic has already been discussed. However, up to 10% of arsenic in cultivated soil is labile, and may be volatilised by processes such as biogenic arsine generation,

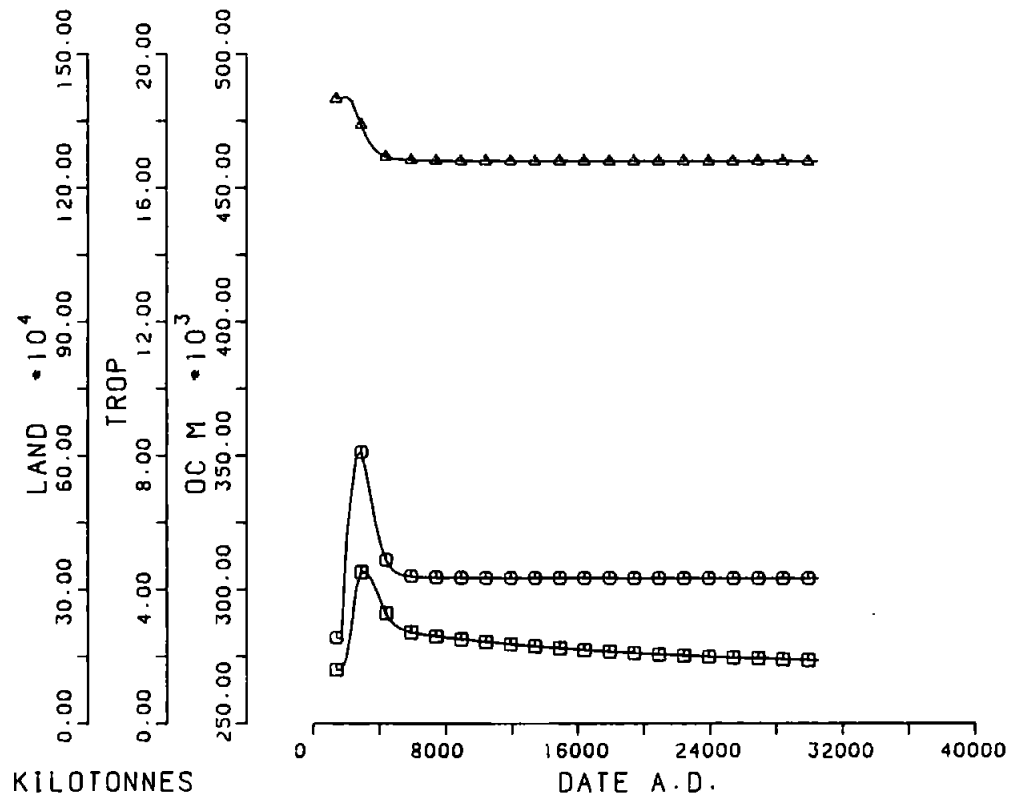


KEY
 □ OCEAN MIXED
 ○ TROPOSPHERE
 ▲ LAND

Figure 4.12 Basic simulation with complete anthropogenic mobilisation of landmass arsenic. The high temperature input has been reduced to a small shoulder on the main anthropogenic peak

whereas only about 1% of arsenic in virgin soil is similarly labile (NAS, 1977), so agriculture may enhance the evolution of volatile arsenic species more significantly than the enhancement of dust emissions. Therefore, a more restrained simulation was considered by restricting the source of the low temperature anthropogenic transport to the arable reservoir, defined earlier. The observed tropospheric arsenic burden was achieved in the model by applying a perturbation of $1.2 \times 10^{-6} \text{ yr}^{-2}$ to the rate constant for the efflux from arable land, again starting in 1750 AD, with far less dramatic results than by mobilising the complete land surface (figure 4.13). In this simulation, the landmass arsenic burden fell by 10% to a new steady state value of $1.26 \times 10^6 \text{ kt As}$ by 9000 AD, with an associated increase of 5.5 kt As in the troposphere to give a tropospheric maximum of 8 kt As in 2670 AD. This coincided with the half life of arsenic in the arable reservoir, about 920 yr after the start of the perturbation. In the same time period, the ocean mixed layer increased by 13% to a maximum of $3 \times 10^5 \text{ kt As}$. Although about 16% of the total landmass burden was available for mobilisation, it was only depleted by about 10%. As anthropogenic mobilisation did not effect the entire land surface, the undisturbed land was available as a sink for mobilised material, so arsenic was partly redistributed over the land surface, rather than completely transported to the oceans via the troposphere.

The marked difference between these two scenarios raises an important question as to the size of the potential reservoir for low temperature mobilisation. Even with a restricted source, the long term effects of low temperature mobilisation were far more significant than the high temperature pollution input. Without a better estimate for the low temperature source, it was not possible to construct reliable predictive models. Instead, the computer simulations were limited to the assessment



KEY
 □ OCEAN MIXED
 ○ TROPOSPHERE
 ▲ LAND

Figure 4.13 Low temperature volatilisation restricted to arable land

of sensitivity, which is important to identify those environmental parameters that most require further study. In the remaining arsenic simulations, low temperature mobilisation was modelled by the linear perturbations determined above. Attempts to implement exponential perturbations for low temperature mobilisation proved too expensive in computer processing time.

The model illustrated in figure 4.12 was resimulated using the basic steady state with the subdivided particulate reservoir. No difference was discernable between the result for the initial experiment and the more refined simulation, probably because the refinement only effects the particulate reservoir, and does not effect processes or reservoir external to the particulates. Therefore, all further simulations were derived from models with a single particulate reservoir to avoid unnecessary complexity in the programming.

4.2.2 The Heterogeneous Troposphere

The residence times of arsenic in each reservoir are given in table 4.4, and the rate constants for the fluxes in table 4.5. The residence time in the continental troposphere is slightly longer than the residence time in the single troposphere of the basic model, and the residence time of arsenic in the ocean mixed layer is also longer. In contrast, arsenic is cycled 10 - 15% faster through the deep waters, particulates, land and sediments. The residence time in the marine troposphere is very short, about 2 d, due to the high deposition fluxes to coastal waters.

As for the basic model, this model was perturbed by changing the land efflux rate constant by $1.6 \times 10^{-7} \text{ yr}^{-2}$ from 1750 AD, simultaneously allowing transport of pollutant arsenic from high temperature processes

Table 4.4 Residence Times for Arsenic in the Model with a Heterogeneous Troposphere

Reservoir	Mass (kt)	Residence time (yr)
Troposphere (continental)	2.5	4.1×10^{-2}
Troposphere (marine)	6.9×10^{-2}	5.2×10^{-3}
Ocean mixed layer	2.7×10^5	2.7×10^2
Ocean deep waters	1.56×10^6	2.7×10^3
Ocean particulates	100	1.4×10^{-1}
Land	1.4×10^6	7.0×10^3
Sediments	2.5×10^{10}	1.2×10^8
Magma	5×10^{10}	7.1×10^9

but with markedly different results (figure 4.14). Both continental and marine tropospheres (which are coincident on figure 4.14) increased by a factor of about 15, not the factor of 7 seen in the equivalent simulation for the basic model, and took twice as long to achieve these maxima, about 7150 yr. These were followed by only small relaxations, by about 25% of the maximum burden, over the next 11000 yr, compared with a 50% relaxation over 8000 yr for the basic model. The ocean mixed layer increased by only 44%, not 50% as before, again over a much longer timescale, 7150 yr. The half life of arsenic in the landmass was extended from 3550 yr to 8450 yr.

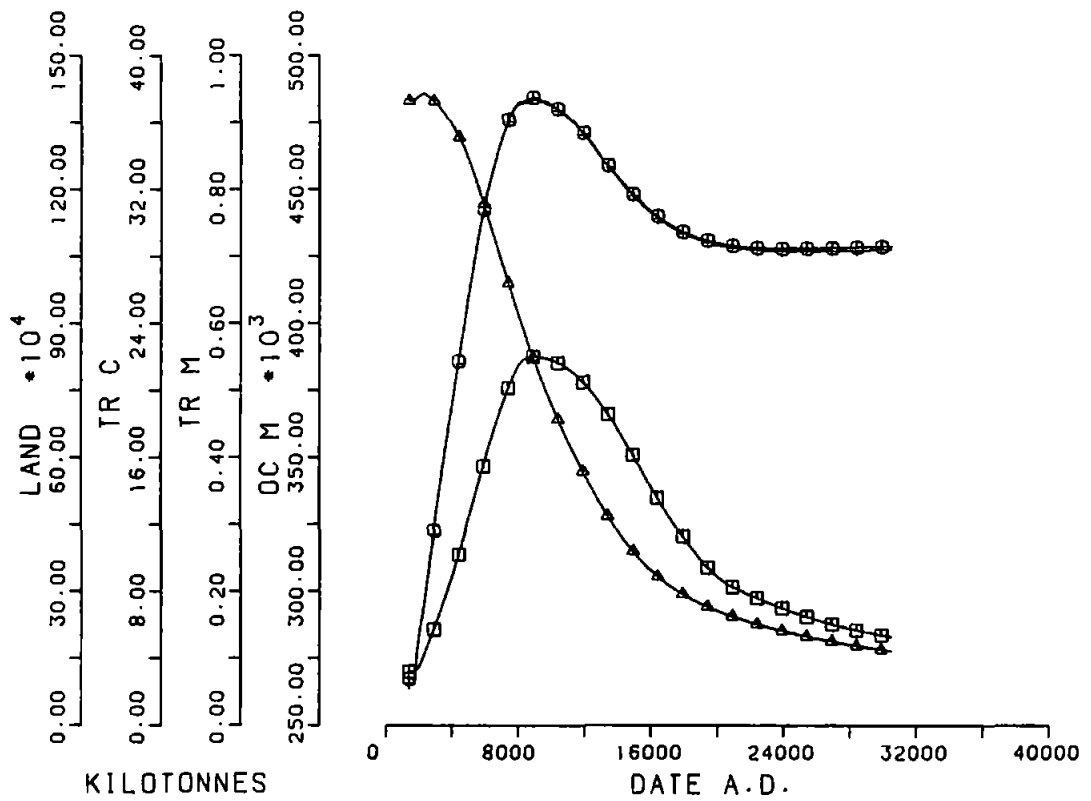
There are three major differences between the model with a heterogeneous troposphere and the basic model. The importance of the ocean as a source and sink for tropospheric arsenic has been greatly reduced, a mixing time has been introduced into the troposphere, and finally a pore water flux has been introduced from the sediments to the ocean deep waters. This latter process is unlikely to effect the simulations, as it is far removed from the land, troposphere and mixed layer. An experiment with

Table 4.5 Fluxes and Rate Constants for the Model with a Heterogeneous Troposphere

Flux	Magnitude kt yr ⁻¹	Rate constant yr ⁻¹
Troposphere (c) to troposphere (m)	11.9	4.7600
to land	61.5	2.4600 × 10 ¹
Troposphere (m) to troposphere (c)	0.1	1.4493
to ocean mixed layer	6.4	9.2754 × 10 ¹
to ocean particulates	6.7	9.7101 × 10 ¹
Ocean mixed layer to troposphere (m)	0.1	3.7037 × 10 ⁻⁷
to ocean deep waters	486.0	1.8000 × 10 ⁻³
to ocean particulates	517.5	1.9167 × 10 ⁻³
Ocean deep waters to ocean mixed layer	486.0	3.1154 × 10 ⁻⁴
to ocean particulates	101.1	6.4808 × 10 ⁻⁵
Ocean particulates to ocean mixed layer	450.0	4.5000
to ocean deep waters	35.0	3.5000 × 10 ⁻¹
to sediments	212.3	2.1230
Land to troposphere (c)	67.5	4.8214 × 10 ⁻⁵
to ocean mixed layer	61.2	4.3714 × 10 ⁻⁵
to ocean particulates	72.0	5.1492 × 10 ⁻⁵
Sediments to ocean deep waters	66.1	2.6440 × 10 ⁻⁹
to land	139.2	5.5680 × 10 ⁻⁹
to magma	7.0	2.8000 × 10 ⁻¹⁰
Magma to troposphere (c)	5.8	1.1600 × 10 ⁻¹⁰
to troposphere (m)	1.2	2.4000 × 10 ⁻¹¹

Troposphere (c) = continental troposphere

Troposphere (m) = marine troposphere

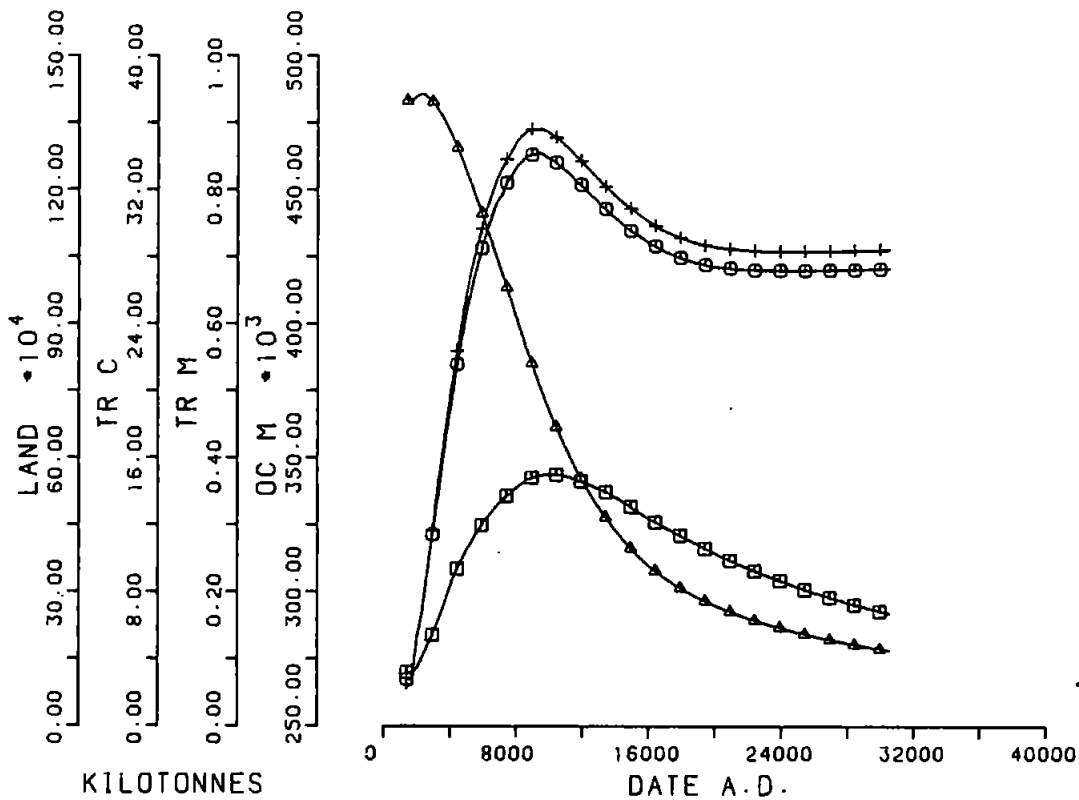


KEY
 □ OCEAN MIXED
 ○ TROPOSPHERE (M)
 + TROPOSPHERE (C)
 △ LAND

Figure 4.14 Basic simulation for the model with a heterogeneous troposphere. The curves for the continental and marine airmasses are coincident

a similar flux added to the basic model did not effect the simulation, so the differences between the simulations are due to the tropospheric changes, which were investigated further.

Simply increasing the mixing rate between the continental and marine airmasses resulted in depression of the continental troposphere and enhancement of the marine troposphere by less than 2% of their maxima, not very different from the simulation in figure 4.14. A more significant difference was achieved by increasing the interaction with the ocean. Instead of allowing just aerosol material exchanged across the coastline to effect the air-sea and land-air exchanges, the vapour phase from the trans-coast exchange was also taken into account. Tropospheric input to the ocean mixed layer and particulates was increased to $6.8 \text{ kt As yr}^{-1}$ and $7.0 \text{ kt As yr}^{-1}$ respectively, with an increase in the backflux from the ocean mixed layer to $0.8 \text{ kt As yr}^{-1}$. Aerosol deposition on the land was reduced to $60.7 \text{ kt As yr}^{-1}$, and the land efflux was also reduced to $66.7 \text{ kt As yr}^{-1}$. The result of the simulation was unexpected (figure 4.15), as the maximum for the ocean mixed layer was further reduced to about $3.4 \times 10^5 \text{ kt}$, an increase of 27% over the steady state burden. This was probably due to the eight fold increase in the flux from the ocean to the troposphere. Tropospheric maxima were reduced, however, to a factor of 13 for the continental troposphere and a factor of 11 for the marine troposphere over their respective steady state values. When both the sea-air exchange rate and the tropospheric mixing rate were further increased, the ocean mixed layer was once again enhanced. The exchange rate between the airmasses were increased to $23.8 \text{ kt As yr}^{-1}$ from the continental troposphere and $12.0 \text{ kt As yr}^{-1}$ from the marine troposphere; exchange rates between the ocean and atmosphere were increased to $7.6 \text{ kt As yr}^{-1}$ from the mixed layer and $13.6 \text{ kt As yr}^{-1}$



KEY

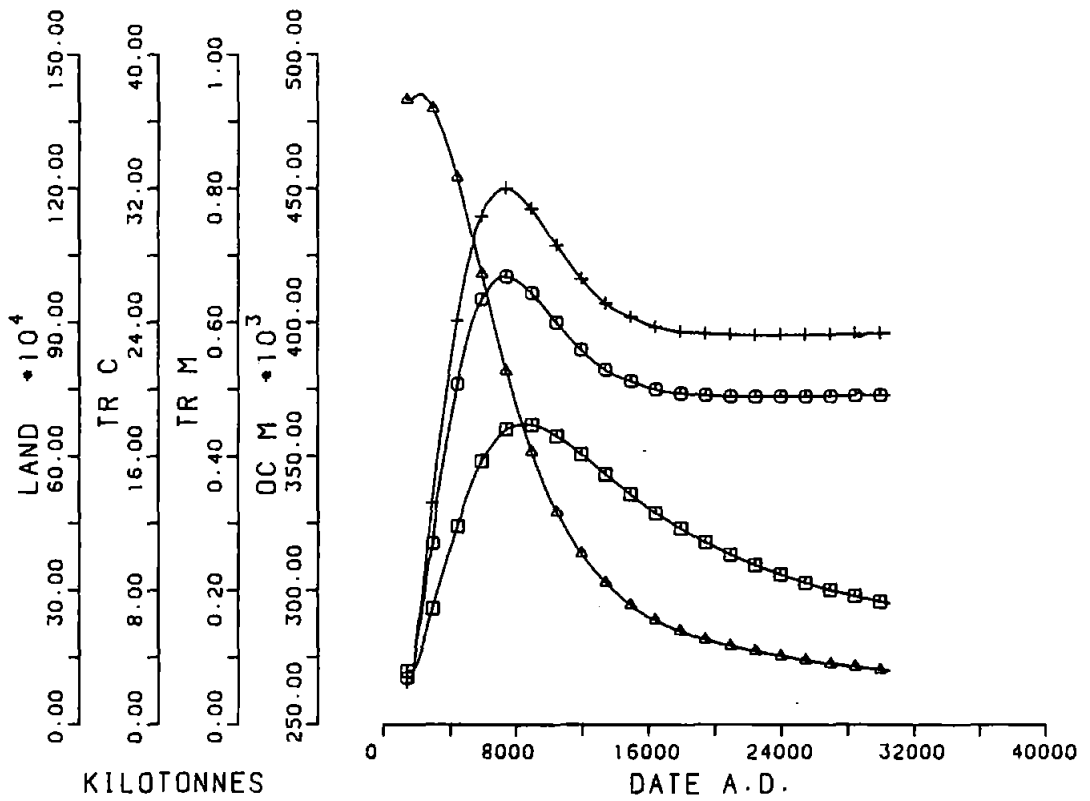
- OCEAN MIXED
- TROPOSPHERE (M)
- + TROPOSPHERE (C)
- △ LAND

Figure 4.15 Deposition of both aerosol and vapour phase arsenic transported across the coast

from the marine troposphere. In the resultant simulation, the ocean mixed layer increased by 34% of its steady state burden (figure 4.16), and the maxima for the continental and marine tropospheres were further suppressed to factors of 12 and 9 over their respective steady state. The half life of arsenic in the landmass was reduced to 6455 yr. Thus, the model is most sensitive to changes in both sea-air exchange and tropospheric mixing, rather than to changes in just one of the parameters.

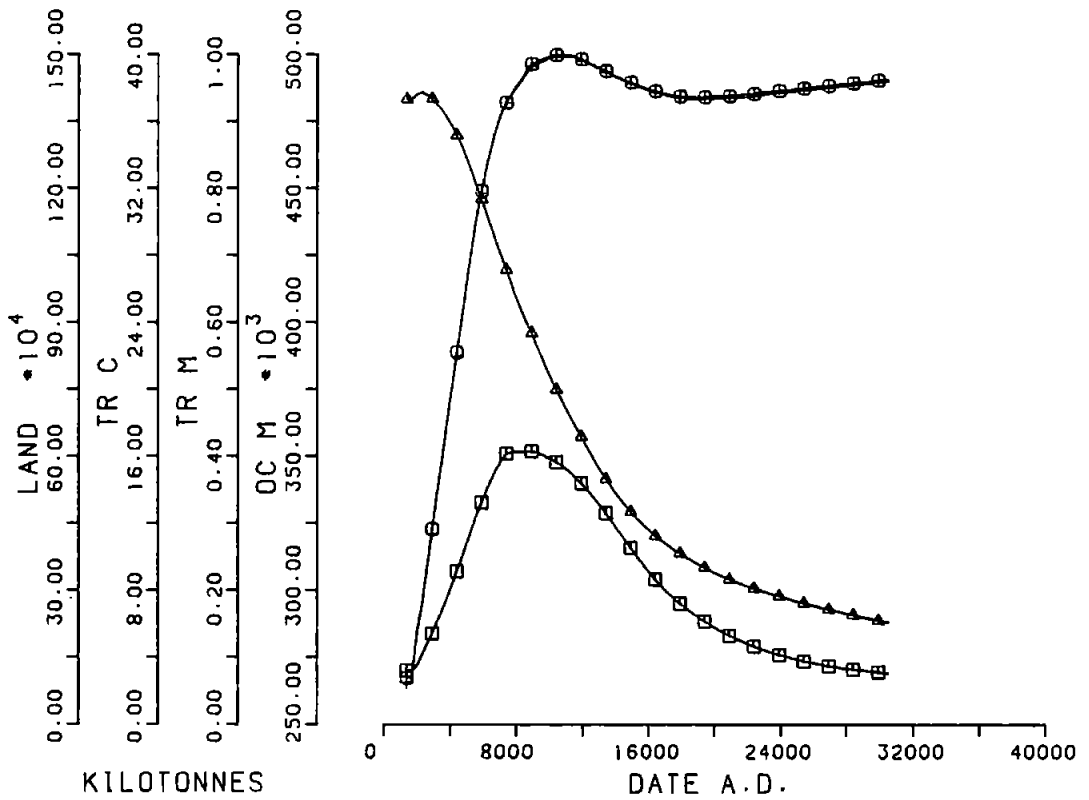
The effect of river flow was investigated by doubling the dissolved riverine flux, as Martin and Meybeck (1979) listed dissolved riverine transport as the major transport mechanism from land to sea. The steady state was restored by increasing the fluxes through the particulates and sediments to the landmass. In the resulting simulation (figure 4.17), the two tropospheres show enhanced maxima, by about 7%, with a delay of about 1800 yr, whilst ocean mixed layer maximum was depressed by 10%, occurring about 360 yr earlier than before. This was probably influenced by the enhanced flux from the sediments to the land, extending the half life of arsenic in the landmass by 900 yr. The source of mobilised arsenic to the troposphere was thereby augmented, whilst the increased dissolved flux to the oceans necessitated a more rapid removal to the sediments, reducing the residence time of arsenic in the surface waters.

In an additional sensitivity test, the steady state masses of the dissolved ocean reservoirs were recalculated using the concentration of $2.6 \mu\text{g As L}^{-1}$ (Turekian, 1969), to yield a mass of 4.7×10^5 kt As for the mixed layer, and 2.7×10^6 kt As for the deep waters. The tropospheric reservoirs were not significantly effected, with both maxima suppressed by about 1%. The ocean mixed layer maximum occurred about 1000 yr later than before, but only showed an increase of 35% over the steady state.



KEY
 □ OCEAN MIXED
 ○ TROPOSPHERE (M)
 + TROPOSPHERE (C)
 ▲ LAND

Figure 4.16 Arsenic simulation with an increased tropospheric exchange rate and an increased sea-air exchange rate



KEY
 □ OCEAN MIXED
 ⊙ TROPOSPHERE (M)
 + TROPOSPHERE (C)
 ▲ LAND

Figure 4.17 Simulation with the dissolved riverine flux of arsenic doubled. Curves for continental and marine troposphere are coincident

The half life of arsenic in the landmass was unaffected. Increasing the particulates reservoir to a particulate load of 1 mg L^{-1} (Parsons, 1975) similarly had little effect on the simulation.

Finally, the effect of limiting the perturbation was considered by restricting the low temperature source to arable land (figure 4.18). The arable land efflux rate constant was perturbed by $1.2 \times 10^{-6} \text{ yr}^{-2}$, starting in 1750 AD, which resulted in quite small changes in the tropospheric and mixed layer reservoirs, as most mobilised arsenic was redistributed over the undisturbed landmass (figure 4.19). The continental troposphere increased by a factor of 2.5, the marine troposphere only doubled, while the ocean mixed layer exhibited a maximum only 4% higher than the steady state. The half life of arsenic in the arable reservoir was extended to 1320 yr. The simulation in figure 4.19 also illustrates the limitations on the computation. After about 7000 AD the landmass shows a baseline drift caused by arithmetic imprecision. Rate constants were input to 5 significant figures for this simulation; when the maximum precision available on the PRIME system was used (13 significant figures), the baseline drift was still apparent, but did not become obvious before 16000 AD. Therefore, simulations of this type may only be used to compare gross differences between scenarios, as minor differences may be due to arithmetic artefacts.

4.2.3 The Biosphere

4.2.3.1 First order kinetics

Arsenic has a very short residence time in marine biota, 0.048 yr (about 20 d), but a much longer residence time in terrestrial biota, 14 yr. About 90% of the arsenic ingested annually by the marine biota is recycled to the dissolved surface ocean reservoir, either directly or via the

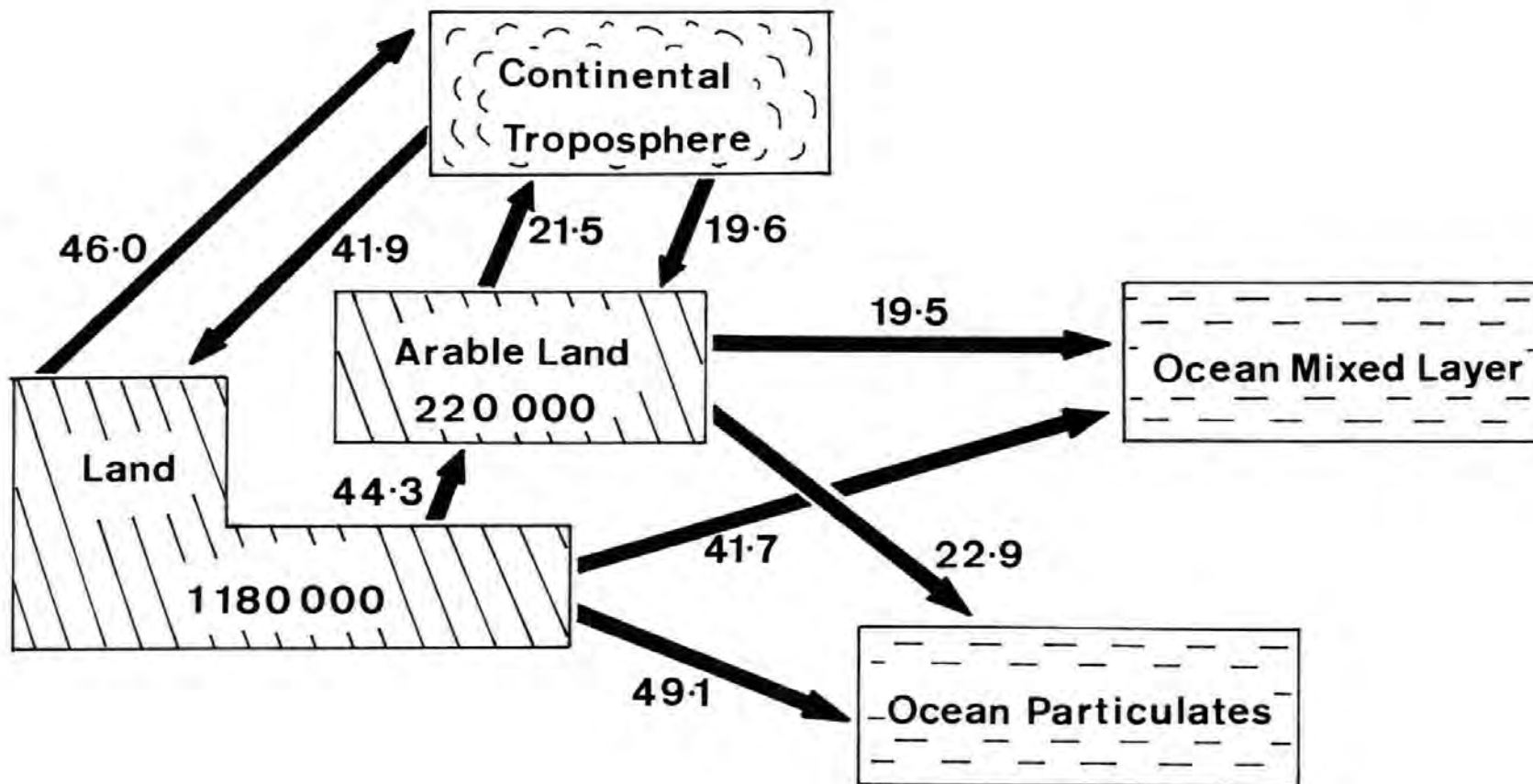
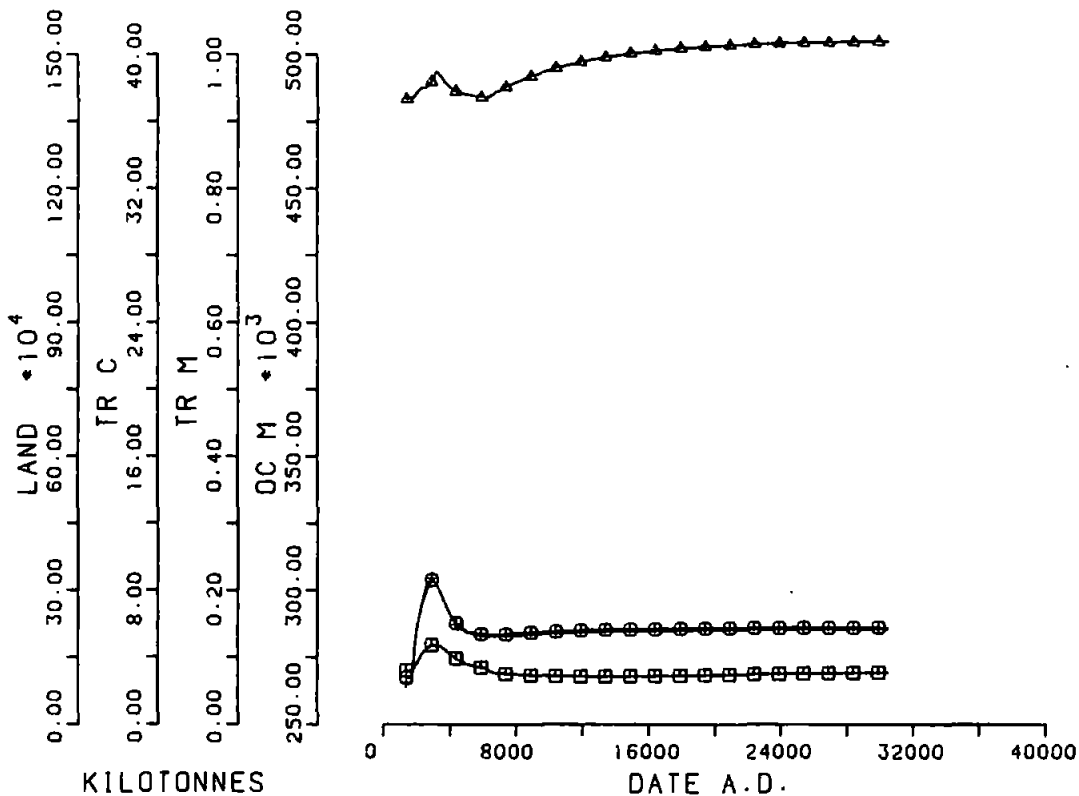


Figure 4.18 Refinement to the heterogeneous troposphere model to subdivide the landmass into arable and non-arable land. Reservoirs in kt As, fluxes in kt As yr⁻¹



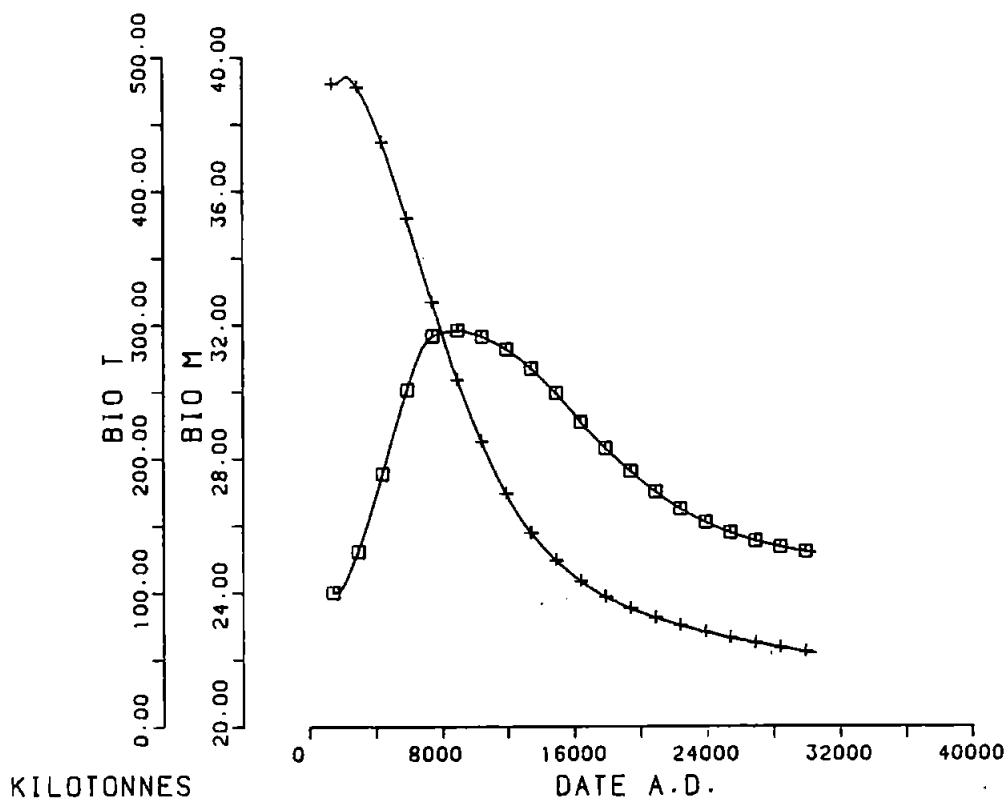
KEY
 □ OCEAN MIXED
 ○ TROPOSPHERE (M)
 + TROPOSPHERE (C)
 ▲ LAND

Figure 4.19 Mobilisation of arsenic in arable land for the heterogeneous troposphere model. The curves for the continental and marine tropospheres are coincident

particulate phase. On land the recycled portion is higher, about 99%. However, the major difference between the two reservoirs in the simulations is controlled by external factors.

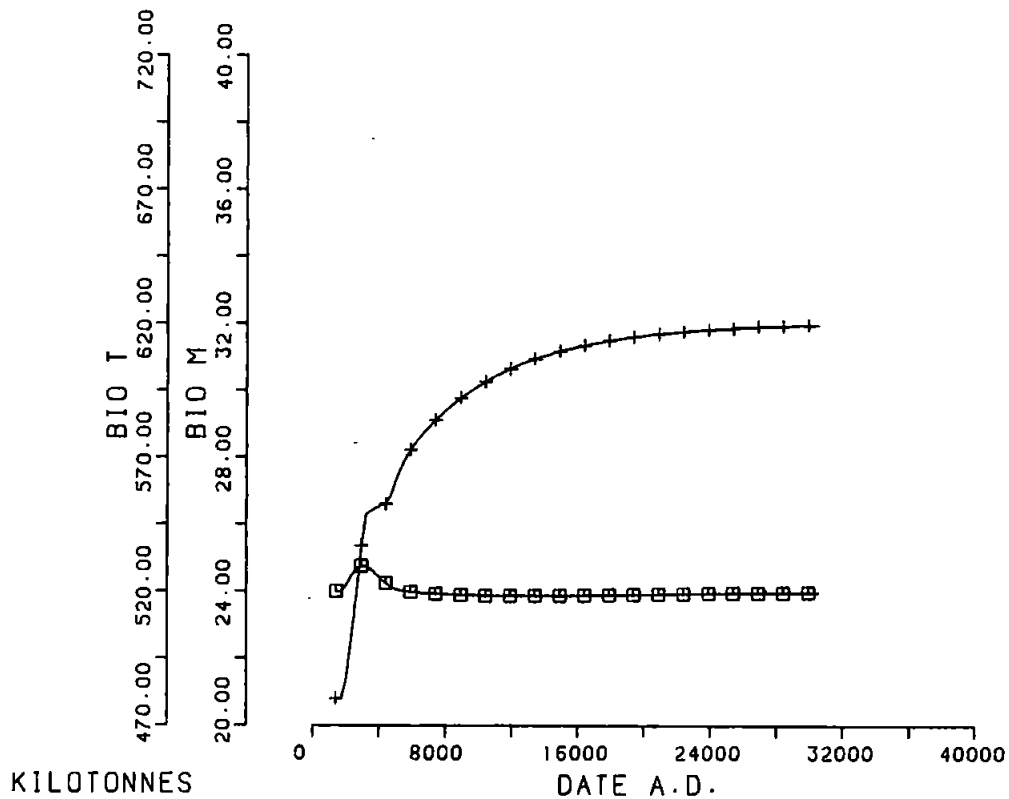
Uptake for the two biomasses was modelled by first order kinetics, using rate constants for the marine and terrestrial biota of $1.8519 \times 10^{-3} \text{ yr}^{-1}$ and $2.4714 \times 10^{-5} \text{ yr}^{-1}$, dependant on the concentration of arsenic in the ocean mixed layer and landmass respectively. When the perturbation was applied to the land efflux without constraint, the terrestrial biosphere was depleted of arsenic with a half life of about 8500 yr, similar to the landmass (figure 4.20). The marine biosphere increased by 33% over a period of 7000 yr after the perturbation was applied. By limiting the perturbation to arable land there was a considerable difference in behaviour. The marine biota exhibited an increase of only 3%, whereas the terrestrial biota increased by 30% by the end of the simulation (figure 4.21). In the latter simulation, the arsenic source for the terrestrial biota was modelled as the non-arable land; any vegetation on the arable land is regularly cropped, so has less opportunity to reach equilibrium with its environment. The increase in arsenic content of the terrestrial biota reflects the redistribution of the landmass arsenic, so restricting the source of mobilised arsenic has a more serious consequence for land based vegetation, although it has far less dramatic consequences for the troposphere and oceanic reservoirs.

Sensitivity tests were applied to the "worst case" scenarios for each of the biosphere reservoirs, which are complete landmass depletion for the marine biosphere, and arable land depletion for the terrestrial biosphere. Doubling the uptake rates for both marine and terrestrial biota had little effect on the simulations. Although the rate at which arsenic is



KEY
 □ MARINE BIOTA
 + TERRESTRIAL BIOTA

Figure 4.20 Biosphere response to the mobilisation of landmass arsenic



KEY
 □ MARINE BIOTA
 + TERRESTRIAL BIOTA

Figure 4.21 Biosphere response to mobilisation of arsenic in arable land

volatilised from leaf surfaces is poorly known, the effect has been observed for other elements (Beauford et al, 1975 and 1977; Schnell and Vali, 1972 and 1973), so the effect of increasing their transpiration rate was examined. Instead of 1% loss to the atmosphere, the simulation was run with 50% loss of the terrestrial biotic uptake to the atmosphere. This had no significant effect on the simulation, maxima for both terrestrial biosphere and continental troposphere showed suppression of less than 1%. The effect of arsenic transfer through the food web has not been examined, as the mechanisms of uptake for higher organisms are varied, even if uptake through the gut alone is considered; Abrahams (1983) showed that cattle swallowed up to 70% of ingested arsenic as soil particles adhering to herbage, rather than as arsenic in the herbage itself.

4.2.3.2 The effect of phosphorus

All of the non-steady state simulations in the previous sections have involved only first order kinetics. However, the kinetics of biological uptake may be more complex (see for example, Dugdale, 1977), so the application of first order kinetics to biological uptake may be inappropriate. Arsenate and phosphate have been shown to inhibit competitively in uptake by single celled organisms, because they may share the same transport mechanism across the cell membrane (Blum, 1966; Button et al, 1973; Pilson, 1974; Sanders and Windom, 1980). Increased levels of phosphate may inhibit the biotic methylation of arsenic (Cox and Alexander, 1973b), a detoxification process which may reduce the uptake of arsenic by lipids onto important phosphorus binding sites (Wrench and Addison, 1981). Therefore, the biological uptake of arsenic was modelled as a phosphorus analogue, rather than by simple first order kinetics. However, like phosphorus, arsenic may follow

Michaelis - Menten kinetics of nutrient uptake for some organisms, so the appropriate kinetic equations may be very complex (Rothstein, 1963). Furthermore, other organisms may have the ability to discriminate between phosphorus and arsenic (Morris et al, 1984), so modelling arsenic as a simple phosphorus analogue can only be regarded as an elaborate sensitivity test.

The first order rate constants for biological uptake were redefined by expressing the initial arsenic concentration as a fraction of the total arsenic and phosphorus concentration in the source reservoir :

$$k_i = \text{Rate}_i / \frac{[\text{As}]}{[\text{As}]_i + [\text{P}]_i} \quad (4.34)$$

This "rate constant" now has the same units as the rate. The rate of arsenic uptake at time t was then expressed as :

$$\text{Rate}_t = k_i \times \frac{[\text{As}]_t}{[\text{As}]_t + [\text{P}]_t} \quad (4.35)$$

Equations 4.34 and 4.35 were used to assess the influence of the phosphorus concentration on the uptake of arsenic by marine and terrestrial biota, again simulating the "worst case" scenario for each. In both cases, the effect of a constant phosphorus concentration was negligible. To assess the effect of a varying phosphorus concentration required the simultaneous simulation of a non-steady state arsenic cycle and a non-steady state phosphorus cycle.

The phosphorus cycle described by Lerman and coworkers (1975) has a perturbation from a mineable source, but no atmospheric transport. Atmospheric phosphorus is dominated by the aerosol phase (Nicholls and

Cox, 1978), so a model was constructed combining the model of Lerman and coworkers (1975) with that described by Graham and Duce (1979), which includes atmospheric transport (figure 4.22). The production of phosphorus doubles every 10 yr (Lerman et al, 1975), so the growth rate is 6.9% indicative of a mature growth stage (Bain, 1978). Mined phosphorous is lost either to the troposphere, at a present rate of 300 kt yr^{-1} (Graham and Duce, 1979) or to arable land as fertilizer at a present rate of 1.2 Mt yr^{-1} (Lerman et al, 1975). The rate equations for the transport of mineable phosphorus (table 4.6) were determined assuming a growth rate of 0.5% for the gerontic stage and a decline of 0.5%, as for pollutant arsenic transport from high temperature processes. In addition, the present day efflux of phosphorus from arable land has risen to 1.2 Mt P yr^{-1} from the steady state value of 1.0 Mt P yr^{-1} (Graham and Duce, 1979), which was modelled by perturbing the rate constant for the efflux from arable land by $2.9 \times 10^{-8} \text{ yr}^{-2}$, from 1750 AD onwards.

For the marine biota, with no constraint on the depletion of landmass arsenic, the increasing phosphorus in the ocean mixed layer suppressed the maximum arsenic burden to 28 kt, so the increase was only half that observed for first order uptake (figure 4.23). By the end of the simulation, arsenic uptake was so severely suppressed that the marine biotic reservoir had fallen below its steady state value by 15%.

A similar result was obtained for terrestrial biota when simulating arsenic mobilisation from arable land (figure 4.24). The biotic burden reached a maximum of 560 kt As, then relaxed to 520 kt As by the end of the simulation, 16% lower than was observed at the end of the first order simulation. The initial enhancement of arsenic uptake by terrestrial biota may have been due to the more rapid perturbation of arsenic from the arable reservoir, compared with the perturbation of phosphorus. In these

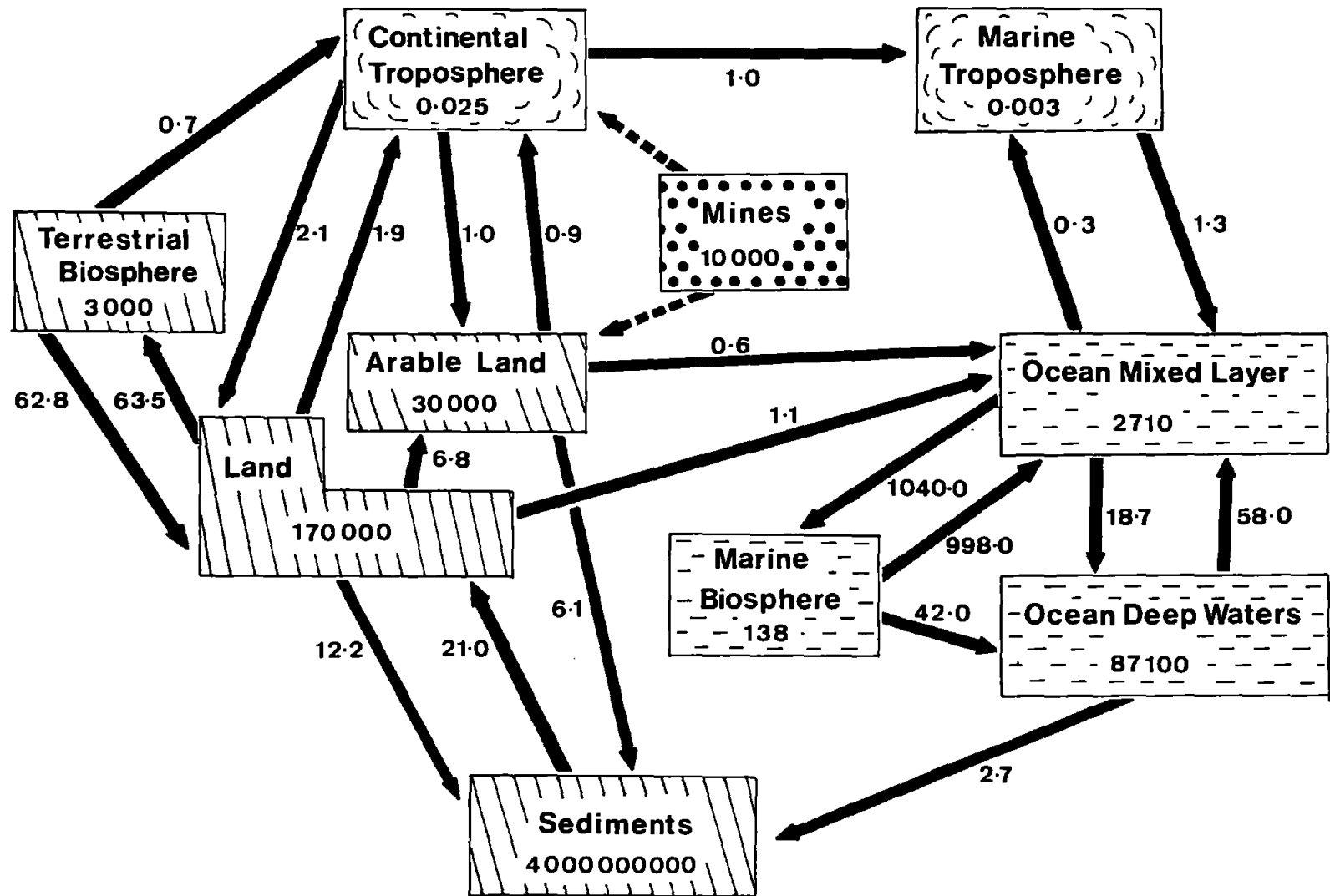


Figure 4.22 Steady state model for phosphorus. Reservoirs in Mt P, fluxes in Mt P yr⁻¹.
 After Graham and Duce (1979) and Lerman *et al.*, (1975)

Table 4.6 Equations to Determine the Instantaneous Rate Constants
for Mineable Phosphorus Fluxes

Atmospheric transport

Mature stage :

$$\ln (k) = 0.069 \times \text{date} - 147$$

Gerontic stage :

$$\ln (k) = 0.005 \times \text{date} - 15.8$$

Decline stage :

$$\ln (k) = -0.005 \times \text{date} + 4.9$$

Transport to Arable land

Mature stage :

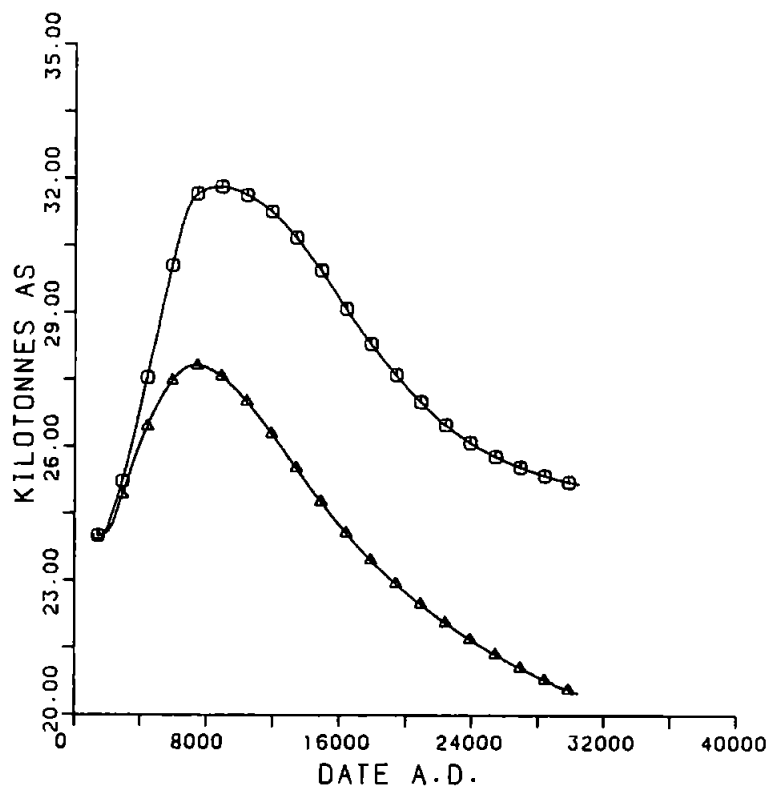
$$\ln (k) = 0.069 \times \text{date} - 145$$

Gerontic stage :

$$\ln (k) = 0.005 \times \text{date} - 13.8$$

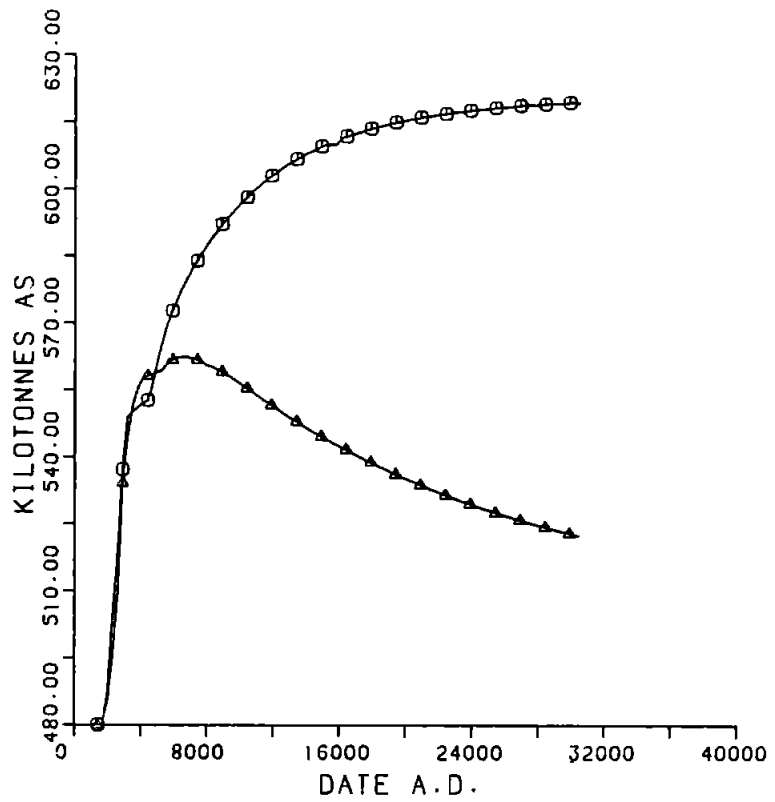
Decline stage :

$$\ln (k) = -0.005 \times \text{date} + 6.9$$



○ FIRST ORDER UPTAKE
 ▲ UPTAKE AS PHOSPHORUS ANALOGUE

Figure 4.23 Comparison of first order uptake of arsenic with uptake of arsenic as a phosphorus analogue for the marine biosphere



○ FIRST ORDER UPTAKE
 ▲ UPTAKE AS PHOSPHORUS ANALOGUE

Figure 4.24 Comparison of first order uptake of arsenic with uptake of arsenic as a phosphorus analogue for the terrestrial biosphere

simulations, phosphorus only effected the biological uptake of arsenic. In reality, the increased nutrient levels for the biosphere would cause an increase in the biomass, resulting in a further increase in biomass arsenic (Andree and Klumpp, 1979), an effect which has not been considered in this work.

In summary, the models presented are most sensitive to changes which effect the anthropogenic mobilisation of arsenic from the landmass. Reducing the removal of arsenic from the atmosphere to the ocean prolongs the elevation of atmospheric arsenic in the simulations, and increases the half life of arsenic in the land. The models are insensitive to changes in the reservoir masses, and to changes in fluxes acting in closely associated couples. Increasing a series of fluxes, involving a multiple reservoir loop, has a greater effect. The biospheres are also very sensitive to departure from first order kinetics, when competitive uptake with the other elements are considered, but are largely insensitive to other sensitivity experiments.

CHAPTER FIVE
MODELS OF THE GEOCHEMICAL
ANTIMONY CYCLE

5.1 STEADY STATE MODELS

The models presented in this section are highly tentative, because data for antimony in the environment are sparse, so many of the fluxes cannot be regarded as reliable. It was unreasonable, therefore, to attempt anything other than cursory kinetic analyses of the antimony models; the unreliability in the antimony data base does not allow for the detailed analyses that were applied to the arsenic cycle. However, although the models described in this chapter are tentative, they represent the first attempt to quantify the global antimony cycle, and may provide a basis for future attempts to study the geochemical cycle of this element.

5.1.1 The Basic Model

An attempt to create a basic pre-man steady state with a well mixed troposphere, comparable to that for arsenic, failed because it was impossible to balance the fluxes using the criteria developed for the homogeneous troposphere; there was a net gain to the troposphere and a net loss from the land. Therefore, the basic steady state for antimony was based on the heterogeneous troposphere model, with separate continental and marine airmasses.

5.1.1.1 The reservoirs

There are no data available for the global distribution of vapour phase antimony in the troposphere, so the reservoirs for both continental and marine airmasses contain aerosol antimony only. The continental troposphere has a volume of $1.53 \times 10^{18} \text{ m}^3$, with an aerosol antimony concentration of 0.7 ng m^{-3} (Adams et al, 1980b), to give a reservoir mass of :

$$1.53 \times 10^{18} \text{ m}^3 \times 0.7 \times 10^{-18} \text{ kt Sb m}^{-3} = 1.1 \text{ kt Sb} \quad (5.1)$$

As there are no data available for aerosol antimony over the oceans in

the southern hemisphere, the concentration of 5 pg m^{-3} (Duce, 1982) for antimony over Enewetak Atoll, a remote atoll in the tropical North Pacific, was used to represent the steady state concentration of antimony in the marine atmosphere. The marine troposphere has a volume of $3.57 \times 10^{18} \text{ m}^3$, so:

$$3.57 \times 10^{18} \text{ m}^3 \times 5 \times 10^{-21} \text{ kt Sb m}^{-3} = 1.8 \times 10^{-2} \text{ kt Sb} \quad (5.2)$$

The ocean mixed layer has a volume of $1.8 \times 10^{17} \text{ m}^3$, with an antimony concentration of $0.24 \text{ } \mu\text{g L}^{-1}$ (Bowen, 1979). The dissolved antimony reservoir in the mixed layer is, therefore :

$$1.8 \times 10^{17} \text{ m}^3 \times 0.24 \times 10^{-12} \text{ kt Sb m}^{-3} = 4.3 \times 10^4 \text{ kt Sb} \quad (5.3)$$

The deep waters have a volume of $1.04 \times 10^{18} \text{ m}^3$, with no reported change from the surface waters in antimony concentration, so the deep water reservoir is :

$$1.04 \times 10^{18} \text{ m}^3 \times 0.24 \times 10^{-12} \text{ kt Sb m}^{-3} = 2.5 \times 10^5 \text{ kt Sb} \quad (5.4)$$

The surface particulates, with a mass of $1.8 \times 10^{15} \text{ g}$, have an antimony concentration of 7 ppm (Buat-Menard and Chesselet, 1979), whereas the deep water particulates, $5.2 \times 10^{15} \text{ g}$, have a higher antimony concentration, 10 ppm (Buat-Menard and Chesselet, 1979), so the particulate reservoir is :

$$1.8 \times 10^6 \text{ kt} \times 7 \times 10^{-6} \text{ kt Sb kt}^{-1} + 5.2 \times 10^6 \text{ kt} \times 10 \times 10^{-6} \text{ kt Sb kt}^{-1} = 65 \text{ kt Sb} \quad (5.5)$$

The global mass of soil on the ice-free land surface is $2 \times 10^{20} \text{ g}$, with an antimony concentration of 1 ppm (Bowen, 1979), to give a reservoir mass of :

$$2 \times 10^{11} \text{ kt} \times 1 \times 10^{-6} \text{ kt Sb kt}^{-1} = 2 \times 10^5 \text{ kt Sb} \quad (5.6)$$

As before, the sediment reservoir was calculated from the global masses of shale, 1.88×10^{24} g, limestone, 3.5×10^{23} g and sandstone, 2.75×10^{23} g (Garrels and Mackenzie, 1971). Antimony concentrations in each are 1.5 ppm (Onishi, 1969b), 0.3 ppm (Onishi, 1969b) and 0.05 ppm (Bowen, 1979; Onishi, 1969b). Therefore, the mass of antimony in shales is :

$$1.88 \times 10^{15} \text{ kt} \times 1.5 \times 10^{-6} \text{ kt Sb kt}^{-1} = 2.82 \times 10^9 \text{ kt Sb} \quad (5.7),$$

the mass of antimony in limestone is :

$$3.5 \times 10^{14} \text{ kt} \times 0.3 \times 10^{-6} \text{ kt Sb kt}^{-1} = 1.05 \times 10^8 \text{ kt Sb} \quad (5.8),$$

and the mass of antimony in sandstone is :

$$2.75 \times 10^{14} \text{ kt} \times 0.05 \times 10^{-6} \text{ kt Sb kt}^{-1} = 1.38 \times 10^7 \text{ kt Sb} \quad (5.9).$$

The total sedimentary reservoir is then the sum of the three masses determined for the different rock types, 2.9×10^9 kt Sb. The concentration of antimony in igneous rocks, 0.2 ppm (Bowen, 1966; Onishi, 1969b), was used to represent the concentration of antimony in magma. The magmatic mass is about 2×10^{25} g, so the reservoir mass is :

$$2 \times 10^{16} \text{ kt} \times 0.2 \times 10^{-6} \text{ kt Sb kt}^{-1} = 4 \times 10^9 \text{ kt Sb} \quad (5.10)$$

As the magmatic mass is only an approximation, because of the imprecision in the molten fraction of the asthenosphere, the magmatic reservoir of antimony lies between 10^9 kt and 10^{10} kt, so is represented as 5×10^9 kt Sb.

5.1.1.2 The fluxes

About $7.35 \times 10^{18} \text{ m}^3$ of air is annually transferred from the marine to

the continental airmasses, with an antimony concentration of 5 pg m^{-3} (Duce, 1982). Therefore, the antimony flux is :

$$7.35 \times 10^{18} \text{ m}^3 \text{ yr}^{-1} \times 5 \times 10^{-21} \text{ kt Sb m}^{-3} = 0.04 \text{ kt Sb yr}^{-1} \quad (5.11)$$

Although fluxes of this low order were disregarded as insignificant in the arsenic models, the concentration of antimony in the environment is generally lower than that of arsenic, so all antimony fluxes were calculated to two decimal places. This was necessitated by the restrictions of the kinetic analyses, where the precision was required to stabilise the steady state in the computer simulations. The return flux from the continental troposphere, with an antimony concentration of 0.7 ng m^{-3} (Adams et al, 1980b), is :

$$7.35 \times 10^{18} \text{ m}^3 \text{ yr}^{-1} \times 0.7 \times 10^{-18} \text{ kt Sb m}^{-3} = 5.15 \text{ kt Sb yr}^{-1} \quad (5.12)$$

Like arsenic, elevated levels of aerosol antimony persist over the ocean for about 200 km from the coast (this work), so the difference in the exchange of antimony across the global coastline, $5.11 \text{ kt Sb yr}^{-1}$, was accounted for when determining removal to the ocean and land surface. The averaged aerosol deposition rate of 1 cm s^{-1} (Buat-Menard and Chesselet, 1979; Chester, 1982; Millward and Griffin, 1980) was used to yield a tropospheric removal rate of 31.5 times per year. Therefore, removal to the land surface is :

$$31.5 \text{ yr}^{-1} \times 1.1 \text{ kt Sb} - 5.11 \text{ kt Sb yr}^{-1} = 29.54 \text{ kt Sb yr}^{-1} \quad (5.13)$$

A lower fraction of antimony in the marine aerosol is seawater soluble than is arsenic, 37% (Creelius, 1980), so the tropospheric flux to the ocean mixed layer is :

$$\begin{aligned} & (31.5 \text{ yr}^{-1} \times 0.018 \text{ kt Sb} + 5.11 \text{ kt Sb yr}^{-1}) \times 0.37 \\ & = 2.10 \text{ kt Sb yr}^{-1} \end{aligned} \quad (5.14)$$

The remaining antimony falling into the oceans enters the particulate phase :

$$\begin{aligned} & (31.5 \text{ yr}^{-1} \times 0.018 \text{ kt Sb} + 5.11 \text{ kt Sb yr}^{-1}) \times 0.63 \\ & = 3.58 \text{ kt Sb yr}^{-1} \end{aligned} \quad (5.15)$$

The volcanic input of antimony to the atmosphere was estimated from the ratio of arsenic to antimony in a number of volcanic emissions (table 5.1), to give a mean arsenic to antimony ratio of about 8.

Table 5.1 Ratios of Arsenic to Antimony in Volcanic Emissions

Volcano	Ratio As:Sb	Reference
Etna	11	Buat-Menard and Arnold, 1978
Augustine	6.2	Lepel <u>et al</u> , 1978
Tolbachik (aerosol)	4.4	Mikhshenskiy <u>et al</u> , 1979
(condensate)	19.7	"
Kileauua	0.2	"

About 7 kt As yr⁻¹ enter the troposphere from volcanic emissions (Walsh et al, 1979b), so about 1 kt Sb yr⁻¹ enters the troposphere from the same source. As 17% of volcanic emissions enter marine airmasses (Macdonald, 1972), the volcanic flux to the marine troposphere is 0.17 kt Sb yr⁻¹, and to the continental troposphere 0.83 kt Sb yr⁻¹. Backfluxes to the atmosphere from the land and sea surface were determined by calculating the steady state for the two tropospheric reservoirs. Output from the marine troposphere is 5.72 kt Sb yr⁻¹, the known input is 5.32 kt Sb yr⁻¹, so the remaining input from the ocean mixed layer is 0.40 kt Sb yr⁻¹. The total output from the continental troposphere is 34.69 kt Sb yr⁻¹, known input is 0.87 kt Sb yr⁻¹, leaving a landmass efflux of 33.82 kt Sb yr⁻¹ by difference.

There are no observed differences between dissolved antimony concentrations in surface and deep waters, so the upwelling and downwelling fluxes are the same. These were calculated from the upwelling rate, 1 m yr^{-1} (Broecker, 1974), over the area of the mixed layer - deep water interface, about 90% of the global ocean area (Riley and Chester, 1971), with the seawater concentration of dissolved antimony, $0.24 \mu\text{g L}^{-1}$ (Bowen, 1979), to give:

$$\begin{aligned}
 & 1 \text{ m yr}^{-1} \times 3.6 \times 10^{14} \text{ m}^2 \times 0.9 \times 0.24 \times 10^{-12} \text{ kt Sb m}^{-3} \\
 & = 77.76 \text{ kt Sb yr}^{-1} \qquad \qquad \qquad (5.16)
 \end{aligned}$$

Dissolution fluxes from the particulates reservoir consist of 90% of the annual biological uptake to the ocean mixed layer, and 7% to the deep waters (Menzel, 1974). The annual productivity (dry weight) is $50 \times 10^6 \text{ kt}$, with an antimony concentration of 0.15 ppm (Buat-Menard and Chesselet, 1979), to yield a dissolution flux to the mixed layer of :

$$\begin{aligned}
 & 50 \times 10^6 \text{ kt yr}^{-1} \times 0.9 \times 0.15 \times 10^{-6} \text{ kt Sb kt}^{-1} \\
 & = 6.75 \text{ kt Sb yr}^{-1} \qquad \qquad \qquad (5.17)
 \end{aligned}$$

and to the deep waters :

$$\begin{aligned}
 & 50 \times 10^6 \text{ kt yr}^{-1} \times 0.07 \times 0.15 \times 10^{-6} \text{ kt Sb kt}^{-1} \\
 & = 0.53 \text{ kt Sb yr}^{-1} \qquad \qquad \qquad (5.18)
 \end{aligned}$$

The dissolved riverine flux from the land to the ocean mixed layer was calculated from the total annual stream discharge, $3.6 \times 10^{16} \text{ L}$ (Turekian, 1969), and the dissolved antimony concentration in river water, $1 \mu\text{g L}^{-1}$ (Martin and Meybeck, 1979; Turekian, 1969) :

$$\begin{aligned}
 & 3.6 \times 10^{16} \text{ L yr}^{-1} \times 1 \times 10^{-15} \text{ kt Sb L}^{-1} \\
 & = 36.00 \text{ kt Sb yr}^{-1} \qquad \qquad \qquad (5.19)
 \end{aligned}$$

The average suspended solids concentration in rivers, 400 mg L^{-1} (Turekian, 1969), and the antimony concentration in riverine particulates, 2.5 ppm (Martin and Meybeck, 1979) give the riverine flux to the ocean particulate reservoir :

$$\begin{aligned}
 & 3.6 \times 10^{16} \text{ L yr}^{-1} \times 4 \times 10^{-10} \text{ kt L}^{-1} \times 2.5 \times 10^{-6} \text{ kt Sb kt}^{-1} \\
 & = 36.00 \text{ kt Sb yr}^{-1} \qquad \qquad \qquad (5.20)
 \end{aligned}$$

Therefore, 50% of the fluvial antimony transport is in the dissolved phase.

The flux from the ocean mixed layer to the particulate phase was calculated as a mass balance for the ocean mixed layer. The total input is $122.61 \text{ kt Sb yr}^{-1}$, and the known output is $78.16 \text{ kt Sb yr}^{-1}$, to yield a flux of $44.45 \text{ kt Sb yr}^{-1}$ by difference. As the component of this flux from biological uptake is $7.50 \text{ kt Sb yr}^{-1}$, the component due to inorganic scavenging is $36.95 \text{ kt Sb yr}^{-1}$, to yield a scavenging rate constant of $8.5953 \times 10^{-4} \text{ yr}^{-1}$. Craig (1974) determined a scavenging rate constant of $3.125 \times 10^{-4} \text{ yr}^{-1}$ for antimony, which compares well with the rate constant determined in this work, especially as the latter calculation involved numerous assumptions. In this respect there is a contrast between arsenic and antimony in the oceans. Only about 3% of the arsenic flux from the mixed layer to the particulates was effected by inorganic scavenging, whereas this process is far more important for antimony, effecting 83% of the flux from mixed layer to particulates. Although it is thought that the ultimate removal mechanism from the oceans is inorganic adsorption for both elements, arsenic is removed on iron oxides (Li, 1981a; Marsh, 1983), but antimony is removed on manganese oxides (Li, 1981a), so the scavenging mechanism is not necessarily the same for both elements. The scavenging rate constant determined above was applied

to the deep ocean reservoir, 2.5×10^5 kt Sb, to yield a flux of $214.88 \text{ kt Sb yr}^{-1}$ from the ocean deep waters to the particulates. Although there is an outflow of $292.64 \text{ kt Sb yr}^{-1}$ from the deep waters, the known input is only $78.29 \text{ kt Sb yr}^{-1}$, which requires an input of $214.35 \text{ kt Sb yr}^{-1}$ from the sediments to complete the mass balance of this reservoir.

The sedimentation flux was calculated as the mass balance for the ocean particulate reservoir. The total input is $298.91 \text{ kt Sb yr}^{-1}$, with a known output of $7.28 \text{ kt Sb yr}^{-1}$, giving a sedimentation flux of $291.63 \text{ kt Sb yr}^{-1}$ by difference. This may be compared with the minimum sedimentation rate due to the settling of fine particles, with a settling velocity of 1 m d^{-1} (Krishnaswami et al, 1976; Minagawa and Tsunogai, 1980). The concentration of antimony in particulates settling on the continental shelf is 7 ppm, and in particles settling into deep sea sediments is 10 ppm (Buat-Menard and Chesselet, 1979). Therefore the minimum sedimentation flux is :

$$\begin{aligned}
 & 3.6 \times 10^{14} \text{ m}^2 \times 0.1 \times 365 \text{ m yr}^{-1} \times 10 \times 10^{-12} \text{ kt m}^{-3} \times 7 \\
 & \times 10^{-6} \text{ kt Sb kt}^{-1} + 3.6 \times 10^{14} \text{ m}^2 \times 0.9 \times 365 \text{ m yr}^{-1} \\
 & \times 5 \times 10^{-12} \text{ kt m}^{-3} \times 10 \times 10^{-6} \text{ kt Sb kt}^{-1} = 7.32 \text{ kt Sb yr}^{-1} \quad (5.21)
 \end{aligned}$$

If instead, the particulate antimony concentrations of 0.2 ng L^{-1} for the surface waters and 0.16 ng L^{-1} for deep waters are used (Buat-Menard and Chesselet, 1979), the minimum sedimentation flux is :

$$\begin{aligned}
 & 3.6 \times 10^{14} \text{ m}^2 \times 0.1 \times 365 \text{ m yr}^{-1} \times 0.2 \times 10^{-15} \text{ kt Sb m}^{-3} \\
 & + 3.6 \times 10^{14} \text{ m}^2 \times 0.9 \times 365 \text{ m yr}^{-1} \times 0.16 \times 10^{-15} \text{ kt Sb m}^{-3} \\
 & = 21.55 \text{ kt Sb yr}^{-1} \quad (5.22)
 \end{aligned}$$

Therefore, the concentrations of particulate matter observed by Bust-Menard and Chesselet (1979) were about three times the average total particulate matter concentrations (Brewer et al, 1980; Lal, 1977). Even allowing for the riverine particulate input to coastal sediments, both estimates from equations 5.21 and 5.22 are much lower than the model sedimentation flux. This is surprising, as removal of antimony from seawater to the sediments is largely controlled by inorganic scavenging usually associated with fine particulates, which provide a large surface area for adsorption (Krishnaswami et al, 1976). Either large particles are effective in scavenging, or the settling velocity of 1 m d^{-1} is inappropriate for fine particles, once they leave the surface ocean. Settling velocities for fine particles in deep waters may be enhanced by particle aggregation, effected by fecal pellets and other large particles collecting smaller particles by processes such as shear coagulation (McCave, 1984). If aggregation is an important process in deep waters, there would be a reduction in the surface area available for adsorption, so the model fluxes for deep water scavenging, sedimentation and pore water remobilisation may be overestimated. The scavenging rate constant of $3.125 \times 10^{-4} \text{ yr}^{-1}$ determined by Craig (1974) may provide a better estimate for deep water scavenging than the rate constant determined in this work, which would still remain suitable for surface waters.

The remaining two fluxes are from the sediments to the magma and to the landmass. A flux of $1.00 \text{ kt Sb yr}^{-1}$ satisfies the mass balance requirements for the magma. The sedimentation flux is $291.63 \text{ kt Sb yr}^{-1}$, with a known output from the sediments of $215.35 \text{ kt Sb yr}^{-1}$, which leaves a flux to the landmass of $76.28 \text{ kt Sb yr}^{-1}$. This satisfies the mass balance for both sediments and land, so completes the steady state for antimony (figure 5.1).

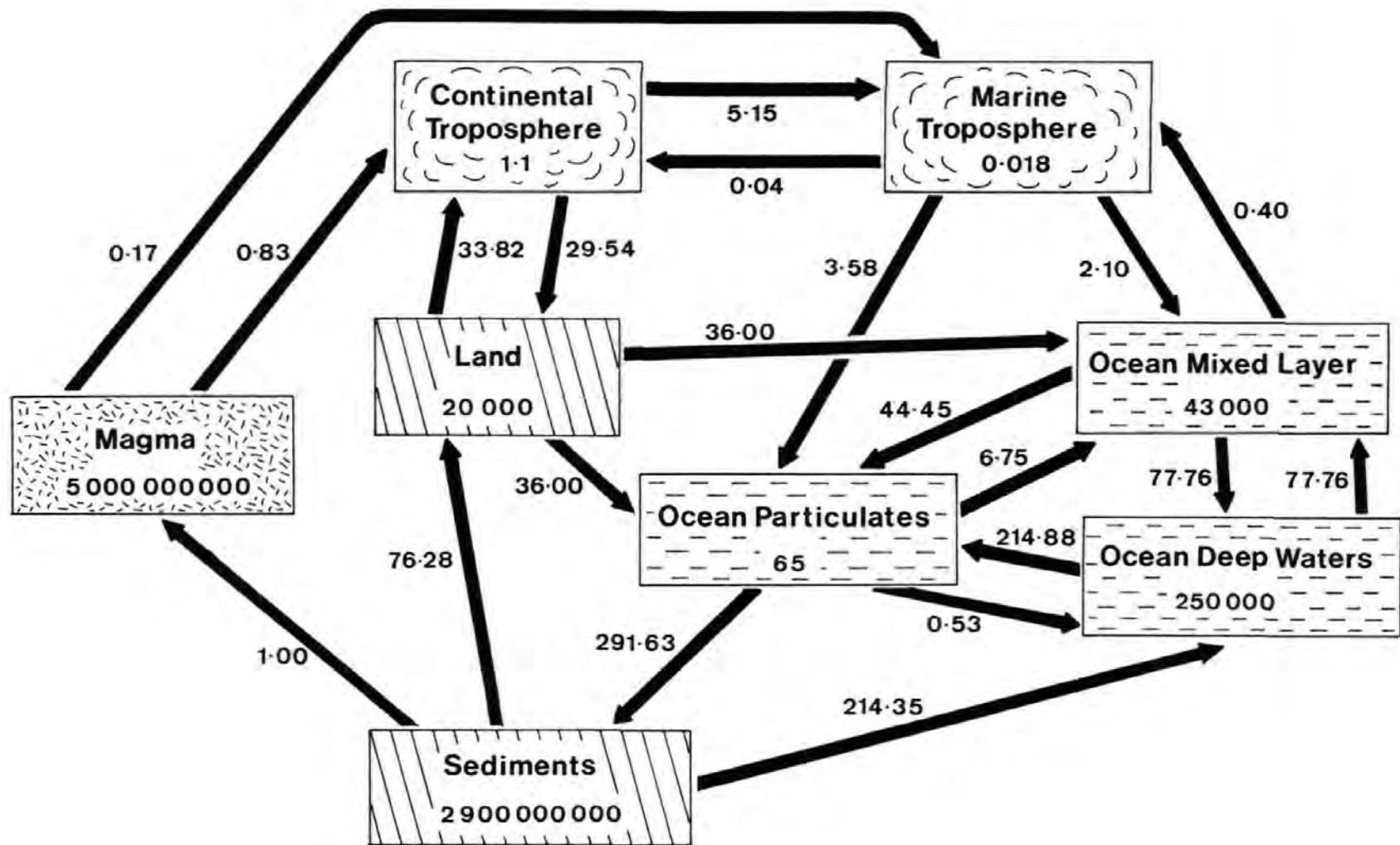


Figure 5.1 The basic steady state for antimony. Reservoirs in kt Sb, fluxes in kt Sb yr⁻¹

5.1.2 Subdivision of the Ocean Particulates

A more rigorous treatment of the antimony cycle was considered by subdividing the ocean particulates into surface and deep water reservoirs. The mixed layer particulate reservoir was calculated from the total particulate mass in the mixed layer, 1.8×10^{15} g, with an antimony concentration of 7 ppm (Buat-Menard and Chesselet, 1979) :

$$1.8 \times 10^6 \text{ kt} \times 7 \times 10^{-6} \text{ kt Sb kt}^{-1} = 13 \text{ kt Sb} \quad (5.23),$$

and the deep water particulate reservoir was calculated from the deep water particulate mass of 5.2×10^{15} g, with an antimony concentration of 10 ppm (Buat-Menard and Chesselet, 1979) :

$$5.2 \times 10^6 \text{ kt} \times 10 \times 10^{-6} \text{ kt Sb kt}^{-1} = 52 \text{ kt Sb} \quad (5.24)$$

The upwelling particulate flux was calculated from an upwelling rate of $3.2 \times 10^{14} \text{ m}^3 \text{ yr}^{-1}$, from Broecker (1974) and Turekian (1969), a total particulate concentration in deep waters of $5 \mu\text{g L}^{-1}$ (Brewer et al, 1980), with an antimony concentration of 10 ppm (Buat-Menard and Chesselet, 1979) :

$$\begin{aligned} & 3.2 \times 10^{14} \text{ m}^3 \text{ yr}^{-1} \times 5 \times 10^{-12} \text{ kt m}^{-3} \times 10 \times 10^{-6} \text{ kt Sb kt}^{-1} \\ & = 0.02 \text{ kt Sb yr}^{-1} \end{aligned} \quad (5.25)$$

The sedimentation flux from the mixed layer particulates, onto the continental shelf, consists of the riverine particulate flux with 10% of the remaining particulate downflux from the surface waters. The total input to the surface particulates is $84.05 \text{ kt Sb yr}^{-1}$. Known output, including the riverine particulates, is $42.75 \text{ kt Sb yr}^{-1}$, to the sedimentation flux from the surface particulates is :

$$\begin{aligned}
 & (84.05 \text{ kt Sb yr}^{-1} - 42.75 \text{ kt Sb yr}^{-1}) \times 0.1 + 36.00 \text{ kt Sb yr}^{-1} \\
 & = 40.13 \text{ kt Sb yr}^{-1} \qquad \qquad \qquad (5.26)
 \end{aligned}$$

This leaves $37.17 \text{ kt Sb yr}^{-1}$ as the particulate flux from the mixed layer to deep waters, completing the mass balance for the surface particulates. Sedimentation from the deep water particulates was calculated as the mass balance for the deep water particulate reservoir. Total input is $252.05 \text{ kt Sb yr}^{-1}$, known output is $0.55 \text{ kt Sb yr}^{-1}$, which yields a sedimentation flux of $251.50 \text{ kt Sb yr}^{-1}$ to complete the steady state (figure 5.2).

The accumulation rate for antimony in the deep water sediments, over an area of $3.24 \times 10^{14} \text{ m}^2$, is about $10 \mu\text{g Sb cm}^{-2} (10^3 \text{ yr})^{-1}$, half that determined for arsenic. Antimony is about 15 times less abundant than arsenic in deep sea clays (Martin and Meybeck, 1979; Onishi, 1969a and 1969b), so the deep sea antimony accumulation rate may have been over-estimated in this work, or antimony is associated with deep sea sediments other than clay.

5.1.3 The Biospheres

5.1.3.1 The marine biosphere

The marine biosphere has a mass of $2.42 \times 10^{15} \text{ g}$ (dry weight), with an antimony concentration of 0.15 ppm (Buat-Menard and Chesselet, 1979), to give a reservoir mass of :

$$2.42 \times 10^6 \text{ kt} \times 0.15 \times 10^{-6} \text{ kt Sb kt}^{-1} = 0.36 \text{ kt Sb} \qquad (5.27)$$

The annual dry weight productivity is $50 \times 10^6 \text{ kt}$ (Menzel, 1974), so the antimony uptake rate is :

$$\begin{aligned}
 & 50 \times 10^6 \text{ kt yr}^{-1} \times 0.15 \times 10^{-6} \text{ kt Sb kt}^{-1} \\
 & = 7.50 \text{ kt Sb yr}^{-1} \qquad \qquad \qquad (5.28)
 \end{aligned}$$

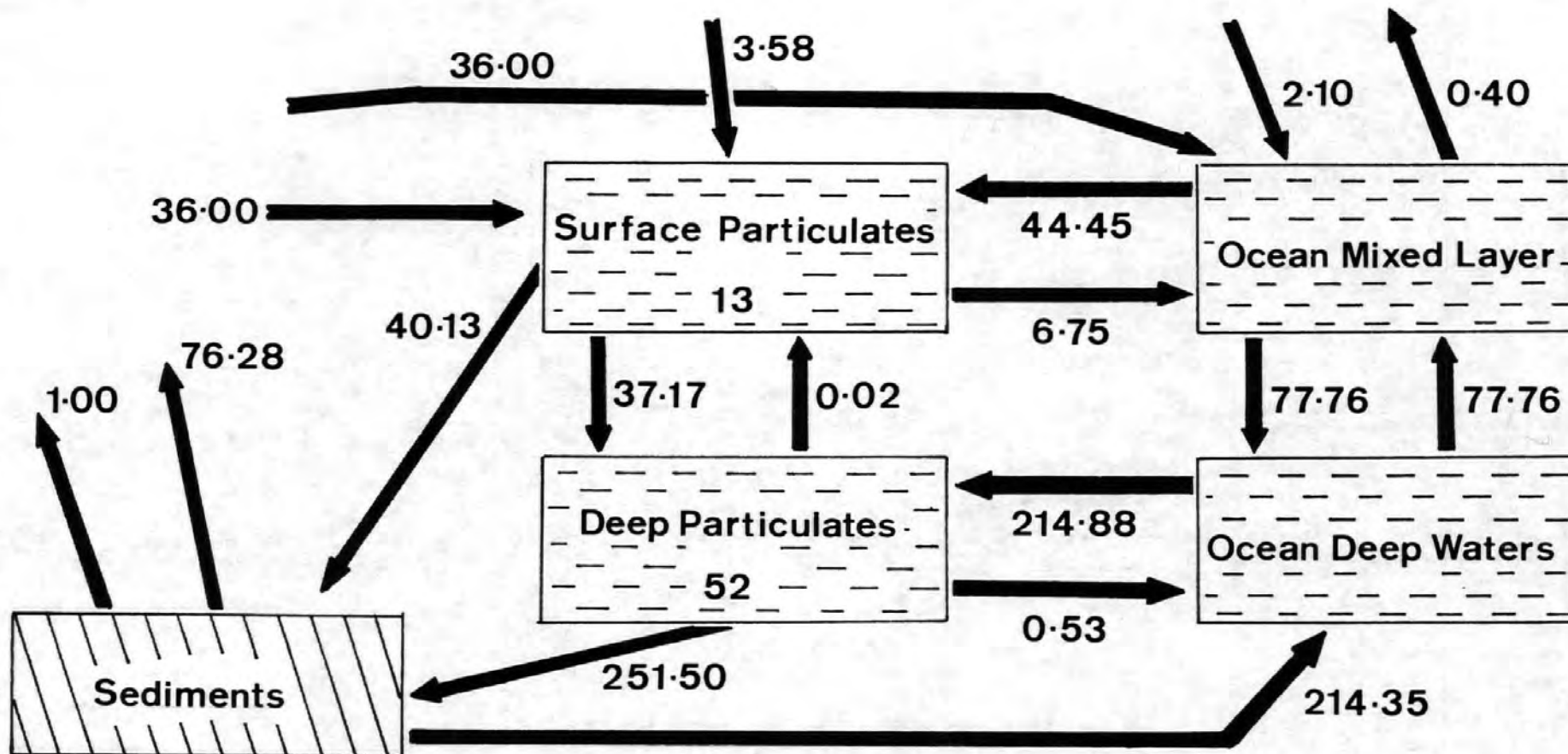


Figure 5.2 Refinement to the basic steady state to include two particulate reservoirs. Reservoirs in kt Sb , fluxes in kt Sb yr^{-1}

Data on the excretion rate of antimony are very scarce, so the excretion rate in this model was estimated from the excretion rate for arsenic. As both arsenic and antimony are biologically reduced by the same mechanism (Wood, 1974), it was assumed that they are reduced to the same extent, the only difference being the rate at which the reduced forms are excreted. All excreted arsenic is in the reduced form (Sanders, 1980), so the only mechanism by which As(V) is released to solution is by the dissolution of organic debris from the particulate reservoir. This is preceded by transport of As(V) from the biota to the particulates, either in fecal pellets or in dead organisms. Assuming that the proportion of arsenic as As(V) is the same in living and decaying biota, about 6% of the arsenic flux from the biota to the particulates is in the reduced form (Johnson and Braman, 1975b). Therefore, 181.0 kt As(V) yr⁻¹ are lost from the biosphere to the particulates, with a rate constant of 7.5417 yr⁻¹. The flux of Sb(V) from the biosphere to the particulates is, therefore, 2.72 kt yr⁻¹. However, about 1% of biological antimony is in a reduced form (Kentin, 1983), so the total flux to the particulate is 2.75 kt Sb yr⁻¹. The excretion flux to the mixed layer was calculated as the mass balance for the marine biosphere, to give a flux of 4.75 kt Sb yr⁻¹.

The inorganic scavenging flux from the ocean mixed layer to the particulates is 36.95 kt Sb yr⁻¹. To complete the model, the mass balance for the particulate reservoir was considered. Total input is 294.16 kt Sb yr⁻¹, the known output is 292.16 kt Sb yr⁻¹, so the dissolution flux to the mixed layer is 2.00 kt Sb yr⁻¹. The marine biosphere model is illustrated in figure 5.3(a).

5.1.3.2 The terrestrial biosphere

The terrestrial biosphere has a dry mass of 2.4×10^9 kt (Rodin et al, 1978)

with an antimony concentration of 0.06 ppm (Bowen, 1966), to give :

$$2.4 \times 10^9 \text{ kt} \times 0.06 \times 10^{-6} \text{ kt Sb kt}^{-1} = 140 \text{ kt Sb} \quad (5.29)$$

The annual terrestrial productivity is 1.73×10^8 kt (Rodin et al, 1978), so the uptake of antimony is :

$$1.73 \times 10^8 \text{ kt yr}^{-1} \times 0.06 \times 10^{-6} \text{ kt Sb kt} = 10.38 \text{ kt Sb yr}^{-1} \quad (5.30)$$

Like excretion from the marine biosphere, loss of antimony from the terrestrial biota to the atmosphere was estimated from the corresponding arsenic flux. Loss of antimony from the biomass to the atmosphere occurs by two mechanisms. The first is forest and grassland fire (Bolin et al, 1983), which volatilises $0.26 \text{ kt As yr}^{-1}$ from a biological reservoir of 480 kt As (Walsh et al, 1979b), to give a rate constant of $5.4167 \times 10^{-4} \text{ yr}^{-1}$. Therefore, $0.08 \text{ kt Sb yr}^{-1}$ are volatilised by the same process. The second process is direct emission from the plant surface (Beauford et al, 1975 and 1977; Schell and Vali, 1972 and 1973), which volatilises $0.16 \text{ kt As yr}^{-1}$ (Walsh et al, 1979b), to give a rate constant of $3.3333 \times 10^{-4} \text{ yr}^{-1}$. Antimony is more enriched in plants over soils than is arsenic. The average arsenic concentration in plants is 0.2 ppm (Bowen, 1966), and in soils is 7 ppm (Bennett, 1981; Kronberg et al, 1979), to give a biological enrichment of 0.03. The average concentration of antimony in plants is 0.06 ppm (Bowen, 1966), with 1 ppm in soils (Bowen, 1979), to give a biological enrichment of 0.06. Therefore, antimony is twice as enriched as arsenic in plants, so is twice as available for direct emission, to give a rate constant of $6.6666 \times 10^{-4} \text{ yr}^{-1}$. This yields an emission flux of $0.09 \text{ kt Sb yr}^{-1}$, so the total flux from the biosphere to the atmosphere is $0.17 \text{ kt Sb yr}^{-1}$. The flux from the biosphere to the landmass is $10.21 \text{ kt Sb yr}^{-1}$, completing the mass balance for the terrestrial biosphere. Finally, the

efflux from the landmass was reduced from $33.82 \text{ kt Sb yr}^{-1}$ to $33.65 \text{ kt Sb yr}^{-1}$ to restore the mass balance to the landmass and continental troposphere. The terrestrial biosphere model is shown in figure 5.3(b).

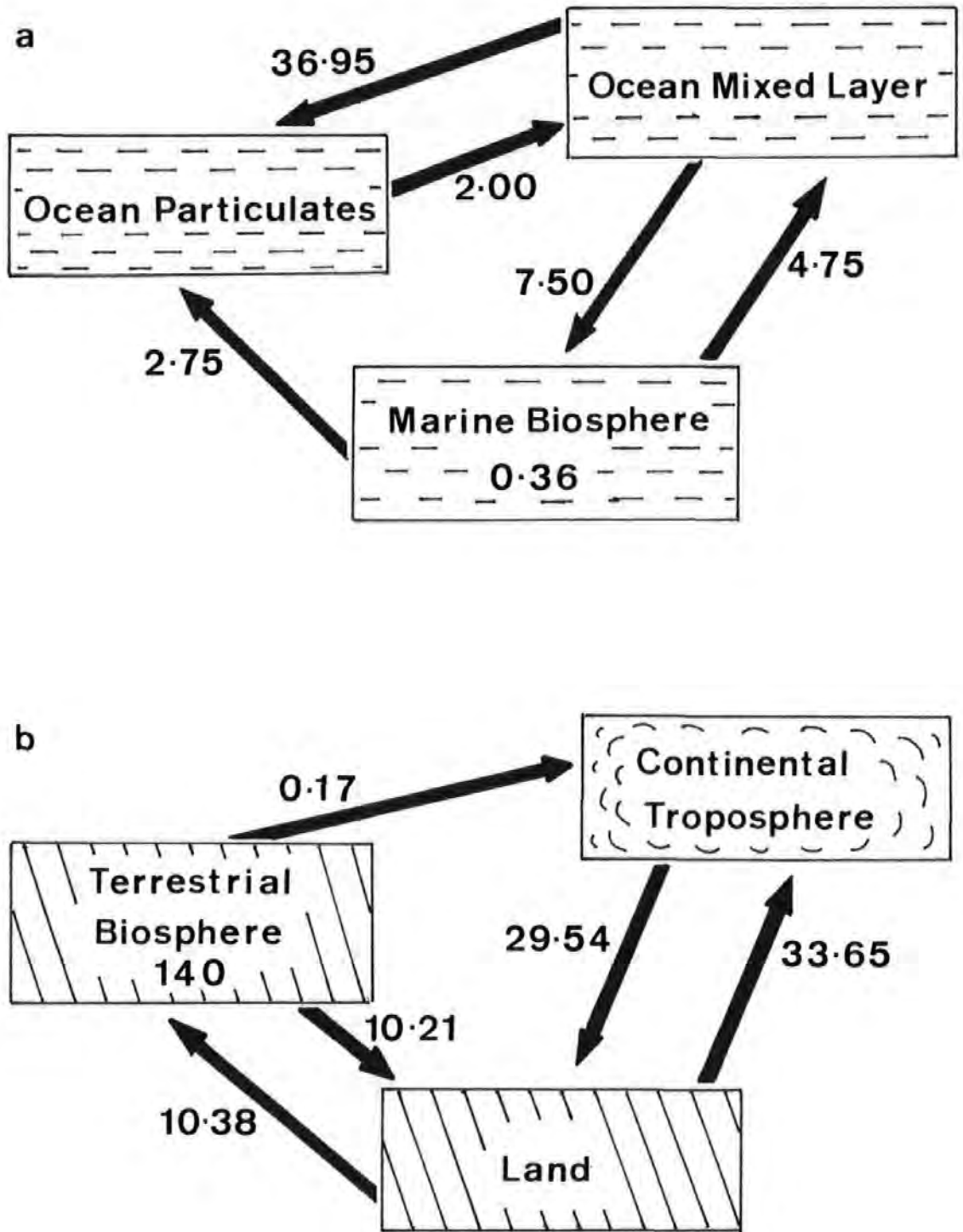


Figure 5.3 Addition of a) the marine biosphere, and b) the terrestrial biosphere to the basic steady state. Reservoirs in kt Sb, fluxes in kt Sb yr⁻¹

5.2 KINETIC MODELLING

5.2.1 The Basic Model

The residence times of antimony in each of the eight reservoirs in the basic model are listed in table 5.2. As in the equivalent arsenic model,

Table 5.2 Residence Times for Antimony in the Basic Model

Reservoir	Mass (kt)	Residence time (yr)
Troposphere (continental)	1.1	3.2×10^{-2}
Troposphere (marine)	1.8×10^{-2}	3.1×10^{-3}
Ocean mixed layer	4.3×10^4	3.5×10^2
Ocean deep water	2.5×10^5	8.5×10^2
Ocean particulates	65	2.2×10^{-1}
Landmass	2.0×10^5	1.9×10^3
Sediments	2.9×10^9	9.9×10^6
Magma	5.0×10^9	5.0×10^9

antimony is cycled most rapidly through the troposphere and ocean particulates, and most slowly through the sediments and magma. The very short residence time for antimony in the marine troposphere, about 1 d, is due to the high depositional fluxes to coastal waters, from continental aerosol material transported across the coast. The residence times are similar to those for arsenic, except the residence time for antimony in the sediments is about twelve times shorter than that for arsenic, because of the higher antimony sedimentation rate and pore water output. Rate constants for the basic antimony model are listed in table 5.3. The steady state was examined by kinetic analysis using high temperature and low temperature perturbations.

5.2.1.1 High temperature processes

Like arsenic, there is a major contribution to the pollutant transport of

Table 5.3 Fluxes and Rate Constants for the Basic Model

Flux	Magnitude kt yr ⁻¹	Rate Constant yr ⁻¹
Troposphere (c)		
to troposphere (m)	5.15	4.6818
to landmass	29.54	2.6855 x 10 ¹
Troposphere (m)		
to troposphere (c)	0.04	2.2222
to ocean mixed layer	2.10	1.1667 x 10 ²
to ocean particulates	3.58	1.9889 x 10 ²
Ocean mixed layer		
to troposphere (m)	0.40	9.3023 x 10 ⁻⁶
to ocean deep waters	77.76	1.8084 x 10 ⁻³
to ocean particulates	44.45	1.0337 x 10 ⁻³
Ocean deep waters		
to ocean mixed layer	77.76	3.1104 x 10 ⁻⁴
to ocean particulates	214.88	8.5952 x 10 ⁻⁴
Ocean particulates		
to ocean mixed layer	6.75	1.0385 x 10 ⁻¹
to ocean deep waters	0.53	8.1538 x 10 ⁻³
to sediments	291.63	4.4866
Land to troposphere (c)	33.82	1.6910 x 10 ⁻⁴
to ocean mixed layer	36.00	1.8000 x 10 ⁻⁴
to ocean particulates	36.00	1.8000 x 10 ⁻⁴
Sediments		
to ocean deep water	214.35	7.3914 x 10 ⁻⁸
to land	76.28	2.6303 x 10 ⁻⁸
to magma	1.00	3.4483 x 10 ⁻¹⁰
Magma		
to troposphere (c)	0.83	1.6600 x 10 ⁻¹⁰
to troposphere (m)	0.17	3.4000 x 10 ⁻¹¹

Troposphere (c) = continental troposphere

Troposphere (m) = marine troposphere

antimony from copper production (Crececius, 1975; Larson et al, 1975; Onishi, 1969b). It was shown in the simulation of high temperature pollutant transport of arsenic that only the pollutant input to the atmosphere had any significant effect on the environment. Therefore, the high temperature pollutant transport of antimony was modelled as a pollutant flux to the atmosphere alone. About 10% of high temperature pollutant arsenic transport was associated with atmospheric emissions, so the initial reserves for atmospheric transport were about 2.5×10^3 kt As. The ratio of antimony to arsenic in emissions from copper smelters is about 1 : 10 (Crececius et al, 1974; Larson et al, 1975), so the antimony reserves for high temperature atmospheric emissions are about 2.5×10^2 kt Sb. The antimony to arsenic ratio in chalcopyrite, a major copper ore, is about 1 : 60 (Onishi, 1969a and 1969b), so the volatile fraction of the total pollutant antimony reserves may be greater than 10%, and pollutant antimony transport to the land and ocean may be even less significant than that for arsenic.

The growth of antimony pollution was modelled on the growth of copper production, determined in section 3.3.2.1, with growth rates of 3.6% and 0.5% for the mature and gerontic growth stages, and a decline rate of 0.5% (Bain, 1978). The time dependant equations for the rate constant for pollutant antimony emissions are listed in table 5.4.

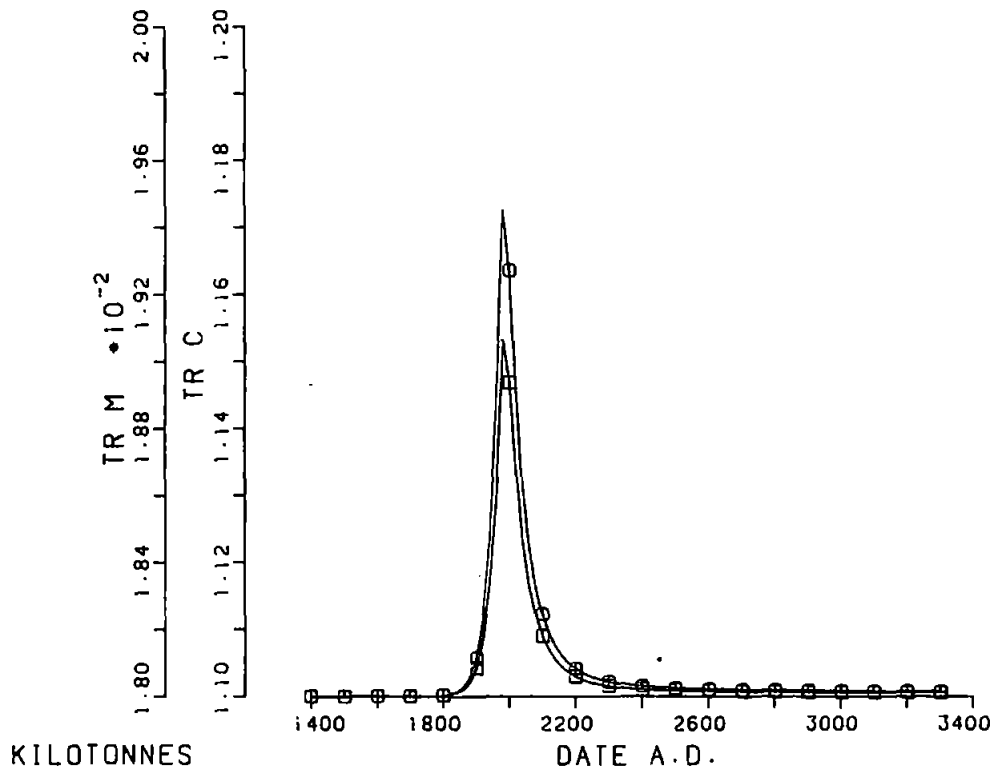
Table 5.4 Equations to Determine the Instantaneous Rate Constants for the Flux of Pollutant Antimony to the Continental Troposphere

Mature stage	:	$\ln(k) = 0.036 \times \text{date} - 75.62$
Gerontic stage	:	$\ln(k) = 0.005 \times \text{date} - 14.18$
Decline stage	:	$\ln(k) = -0.005 \times \text{date} + 5.90$

The release of pollutant antimony to the continental troposphere was simulated according to the rate equations in table 5.4 and the rate constants in table 5.3. The effect on the continental and marine troposphere is shown in figure 5.4. The continental troposphere reached a maximum of 1.17 kt Sb in 1980 A.D.; at the same time, the marine troposphere reached a peak of 0.019 kt Sb. Both represent increases over the tropospheric steady state by only about 6%, much less than was observed for arsenic. The pollutant reserves were depleted in a sigmoidal curve, with a half life of 600 yr after the start of the simulation, very similar to the behaviour of the arsenic reserves.

The simulated present day antimony burdens in the troposphere were about 1.17 kt for the continental troposphere, and 0.019 kt for the marine troposphere. The observed present day burden for the continental troposphere was calculated from the concentration of aerosol antimony over the southern continents, 0.7 ng m^{-3} (Adams et al, 1980b), and over the polluted northern continents, 2.1 ng m^{-3} (Salmon et al, 1978). As 40% of the northern hemisphere and 20% of the southern hemisphere are covered by land, these concentrations yield present day burdens of 2.14 kt Sb and 0.36 kt Sb over the northern and southern continents respectively, to yield a total burden of about 2.5 kt Sb. Therefore, there is a shortfall of 1.33 kt Sb for the continental troposphere in the simulation.

An upper limit to the present day antimony burden in the marine troposphere was calculated from the data of Duce (1982), 5 pg Sb m^{-3} , for the concentration of aerosol antimony in unpolluted marine air, and the mean value of $0.086 \text{ ng Sb m}^{-3}$ (this work) for the concentration of antimony in the northern polluted marine air. Although the data from Duce (1982) represent samples taken at Enewetak Atoll in the tropical North Pacific, the site is well removed from any anthropogenic influence, and may



KEY
 ○ TROPOSPHERE (CONT)
 □ TROPOSPHERE (MARINE)

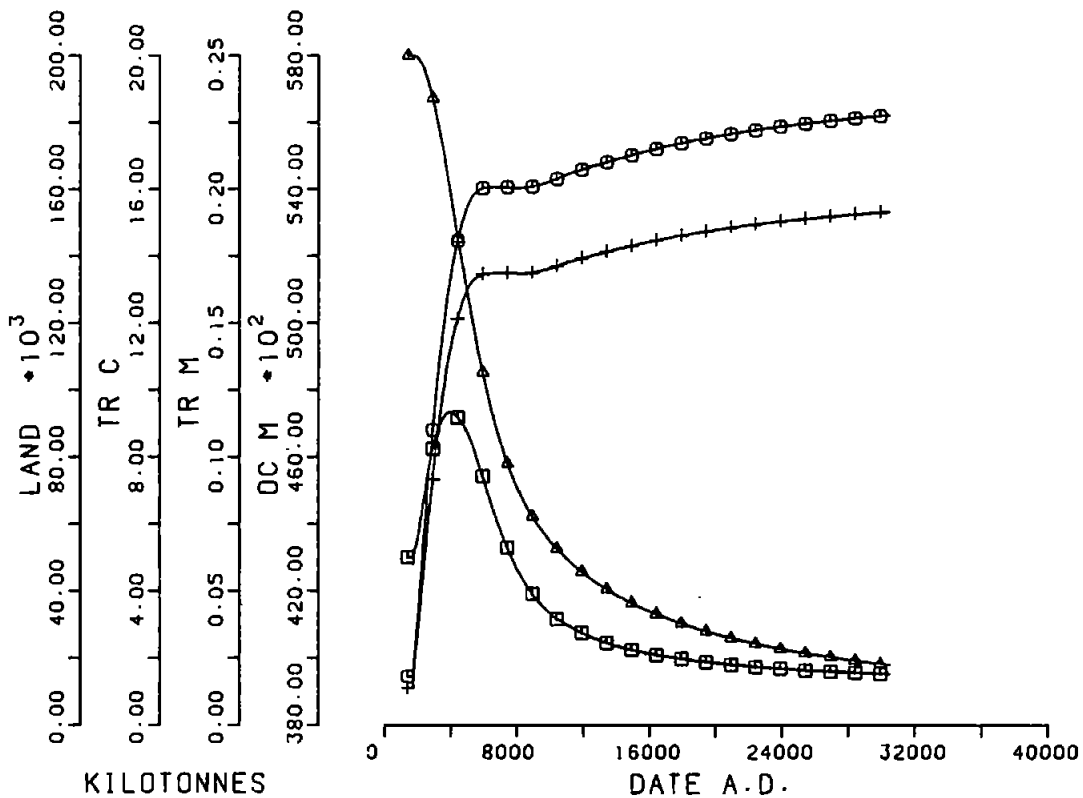
Figure 5.4 Response of the troposphere to the input of pollutant antimony from high temperature sources

therefore be used as an estimate for background marine conditions. As the mean value for aerosol antimony over the North Atlantic (this work) was calculated using 'less than' values, this can only be regarded as an upper limit to the true mean in this environment. The total burden over the southern oceans is 0.01 kt Sb, that over the northern oceans is 0.132 kt Sb, to give a total burden of about 0.14 kt Sb for the marine troposphere, much higher than the simulated present day burden of 0.019 kt Sb. Therefore, the input from low temperature process must be highly significant.

5.2.1.2 Low temperature processes

It was shown in the arsenic simulations (section 4.2.1.2) that the increased dust flux from arable land was not a significant pollutant input of atmosphere elements to the atmosphere. Low temperature mobilisation of arsenic accounted for 80% of the observed pollutant burden in the troposphere. The low temperature contribution to the pollutant antimony burden in the continental troposphere is even higher, about 95%. Therefore, the effect of increasing the arable dust flux for antimony was not considered, and the low temperature mobilisation was simulated by increasing the land efflux rate constant.

Although ice core data are available for antimony (Weiss et al, 1975 and 1978), like those for arsenic, they are not considered reliable, and should not be used to estimate perturbation rates. Therefore, the rate constant for the landmass efflux was perturbed by $9.2 \times 10^{-7} \text{ yr}^{-2}$, from 1750 AD onwards, to simulate the observed antimony burden in the continental troposphere. This perturbation was applied without constraint, exhausting the landmass of antimony with a half life of 4400 yr (figure 5.5). The continental troposphere reached an initial maximum of



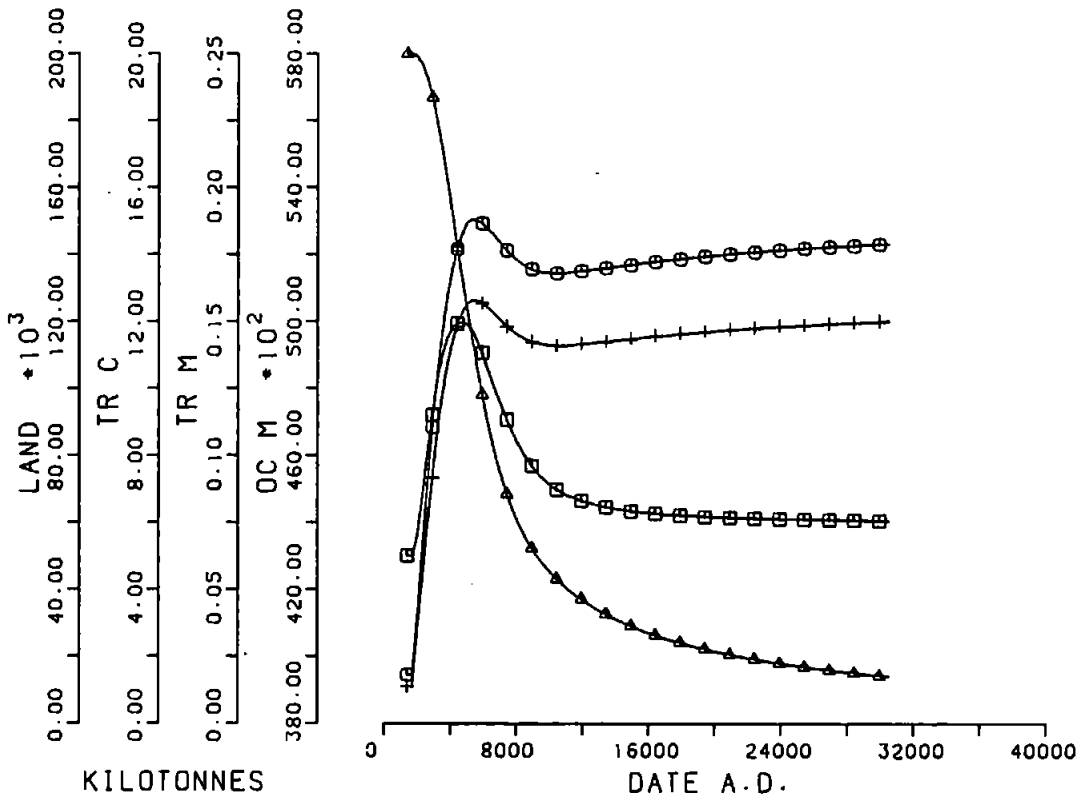
KEY
 □ OCEAN MIXED
 ⊙ TROPOSPHERE (M)
 + TROPOSPHERE (C)
 ▲ LAND

Figure 5.5 Basic simulation for the antimony cycle, with complete anthropogenic volatilisation of landmass antimony

13.5 kt Sb, 5050 yr after the application of the perturbation, increasing by a factor of twelve over the steady state. The marine troposphere achieved its maximum in a slightly shorter period, 4750 yr, increasing by a factor of eleven over the steady state. The simulated present day burden for the marine troposphere was about 0.04 kt Sb, much lower than the estimated upper limit from the observed concentrations. The ocean mixed layer achieved a maximum of about 4.73×10^4 kt Sb in 4100 AD, 2350 yr after the start of the perturbation. However, by the end of the simulation this had fallen to 3.95×10^4 kt Sb, a reduction of 8% from the steady state. Tests were applied to ensure that this was not an arithmetic artefact. Reduction of the maximum integration step had no effect, and resimulation with no low temperature perturbation resulted in no baseline drift, so another test was carried out to examine the cause of the suppression of the ocean mixed layer.

As the landmass reservoir falls to zero, so do the riverine fluxes to the ocean mixed layer and particulates reservoir. The dissolved riverine flux is a major source of antimony to the ocean mixed layer, accounting for about 30% of the total input to this reservoir. Although Martin and Meybeck (1979) determined an average dissolved antimony concentration of $1 \mu\text{g L}^{-1}$ in rivers, Russell (1984) showed that the concentration of dissolved antimony was usually less than $0.5 \mu\text{g L}^{-1}$ in the Tamar estuary, which drains a mineralised catchment area. Therefore, the steady state was recalculated with half the dissolved riverine flux of the basic model, $18.00 \text{ kt Sb yr}^{-1}$. To restore the steady state, the flux from the mixed layer to the particulates, the sedimentation flux and the uplift flux to the land were all reduced.

In a resulting simulation (figure 5.6), the ocean mixed layer achieved



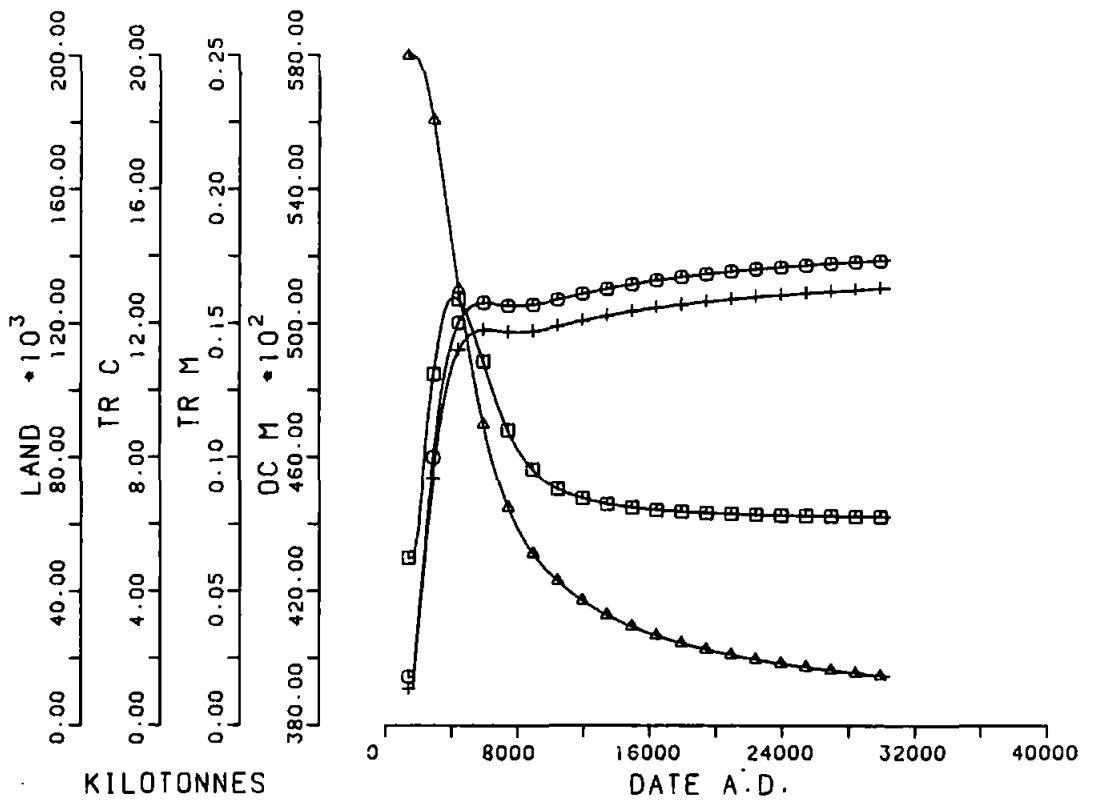
KEY
 □ OCEAN MIXED
 ○ TROPOSPHERE (M)
 + TROPOSPHERE (C)
 ▲ LAND

Figure 5.6 Simulation with half the dissolved riverine flux of antimony

a maximum of about 5×10^4 kt Sb, 6% higher and 600 yr later than in the basic model. This then relaxed to about 4.4×10^4 kt Sb, slightly higher than the steady state burden. The tropospheric maxima were slightly lower, but more clearly defined, than in the basic model, and the half life of antimony in the landmass was reduced to about 4100 yr. The reduction in the uplift flux from the sediments to the landmass caused an increase in the rate at which the landmass was depleted. Therefore, the tropospheric maxima were achieved more rapidly than in the basic simulation. The suppression of the ocean mixed layer was alleviated by the reduced river flow. This suppression was not apparent in the equivalent arsenic simulation, as dissolved riverine input is less significant in the arsenic cycle than in the antimony cycle.

The effect of increasing the tropospheric transfer of antimony from the land to the ocean mixed layer was investigated. Initially, the tropospheric mixing rate was increased by doubling the transfer rate from the continental airmasses to the marine airmasses. This had little effect, with a slight suppression of the continental troposphere, and a slight elevation of the marine troposphere. The model proved to be more sensitive to changes in the air-sea exchange rate, when aerosol deposition of antimony to the ocean mixed layer was doubled. The continental troposphere was not significantly effected, but the maximum for the marine troposphere was reduced to 0.15 kt Sb from 0.2 kt Sb in the basic simulation. The ocean mixed layer achieved a maximum of 5.06×10^4 kt Sb, then relaxed to 4.4×10^4 kt Sb, so even a slight reduction of the importance of riverine transport, by elevating other fluxes, was sufficient to alleviate the suppression of the mixed layer.

The greatest effects were achieved when both the tropospheric sensitivity tests were applied simultaneously (figure 5.7). The maximum for the



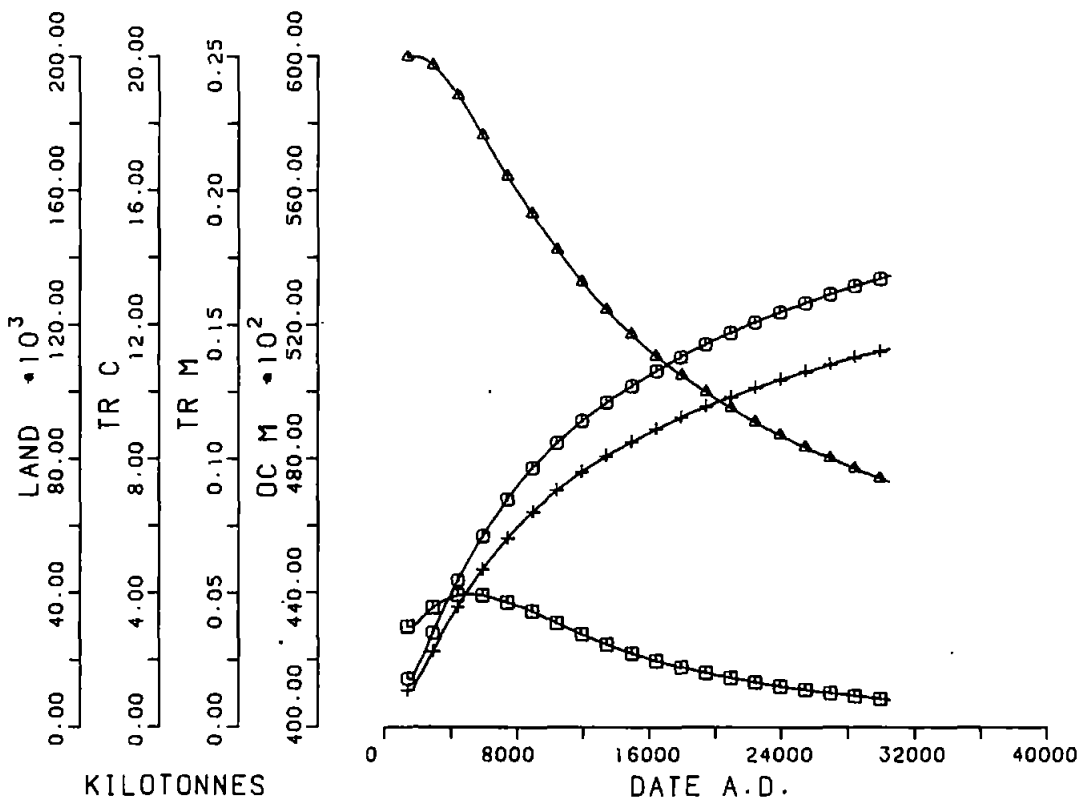
KEY
 □ OCEAN MIXED
 ○ TROPOSPHERE (M)
 + TROPOSPHERE (C)
 ▲ LAND

Figure 5.7 Antimony simulation with increased tropospheric exchange rate and increased sea-air exchange rates

continental troposphere was reduced to 11.8 kt Sb, that for the marine troposphere was reduced to 0.16 kt Sb, both maxima occurring about 300 yr earlier than in the basic simulation. The ocean mixed layer achieved a maximum of 5.08×10^4 kt Sb, then again relaxed to 4.4×10^4 kt Sb. The half life of antimony in the landmass was reduced by about 15% to 3700 yr. Therefore, the air-sea exchange rate is the most important factor affecting the sensitivity of the model to changes in tropospheric transport of antimony.

The sensitivity of the ocean deep waters to scavenging was examined by reducing the adsorption flux from the deep waters to $78.13 \text{ kt Sb yr}^{-1}$, using the scavenging rate constant of $3.125 \times 10^{-4} \text{ yr}^{-1}$ determined by Craig (1974). This also allowed for the possibility of a lower scavenging rate constant in deep waters because of the lower concentration of particulate material in deep waters than in the mixed layer (Brewer et al, 1980). The steady state was restored by reducing the sedimentation flux and pore water remobilisation. There was no significant effect on the ocean mixed layer, troposphere or landmass in the ensuing simulation. However, as the residence time of antimony in deep waters had been increased, the deep waters achieved a maximum of 2.60×10^5 kt Sb in 3850 yr, slightly higher than the maximum in the basic simulation, which was 2.57×10^5 kt Sb in 2950 yr.

The perturbation applied to the land efflux rate constant in the basic simulation was $9.2 \times 10^{-7} \text{ yr}^{-2}$. Instead, the perturbation for the basic arsenic simulation, $1.6 \times 10^{-7} \text{ yr}^{-2}$, was applied to the antimony steady state, again starting in 1750 AD. The tropospheric reservoir did not achieve maxima during the experiment (figure 5.8) but continued to rise until the end of the simulation. The terminal burden in the continental



- KEY
- OCEAN MIXED
 - TROPOSPHERE (M)
 - + TROPOSPHERE (C)
 - △ LAND

Figure 5.8 Antimony simulation using the landmass perturbation determined for arsenic

troposphere was 11.3 kt Sb, and for the marine troposphere was 0.17 kt Sb. By 6800 AD, the position of the maxima for the tropospheres in the basic simulation, both tropospheric reservoirs achieved burdens less than half their respective maxima in the basic simulation. The ocean mixed layer achieved a maximum of about 4.4×10^4 kt Sb, then relaxed to 4.1×10^4 kt Sb by the end of the simulation, 5% lower than the steady state burden. The half life of antimony in the landmass was extended to 17000 yr.

When the low temperature source was restricted to arable land, as in the arsenic simulations, the results were very similar to those observed for arsenic. The tropospheric maxima were almost three times their respective steady state burdens, and occurred rapidly, after 550 yr. The ocean mixed layer reached a maximum of 4.35×10^4 kt Sb, an increase of just over 1% over the steady state, also after 550 yr. The half life of antimony in the arable reservoir was 656 yr, with most of the mobilised material redistributed over the undisturbed land surface. Therefore, the nature of the low temperature perturbation is an important factor in assessing the potential anthropogenic influence on the global antimony cycle.

5.2.2 The Biospheres

The residence time of antimony in the marine biosphere is 4.8×10^{-2} yr, about 20 d, and in the terrestrial biosphere is 13 yr. The rate constants for the biosphere fluxes are shown in table 5.5.

When the model was perturbed according to the basic simulation, with no constraint on the low temperature perturbation, the marine biosphere exhibited similar behaviour to the ocean mixed layer, increasing by 10% over about 500 yr, then relaxing to 0.33 kt Sb by the end of the simulation, 8% lower than the original steady state. The terrestrial biosphere was

comparable to the arsenic scenario. Thus, the sensitivity of the terrestrial biosphere is effected by the rate of anthropogenic perturbation.

Competitive biological uptake between antimony and phosphorus was not considered, although both are dominated by the pentavalent state in seawater and freshwater (Andreae et al, 1981; Turner et al, 1981). Arsenic is speciated mainly as HAsO_4^{2-} in seawater and H_2AsO_4^- in freshwater (Turner et al, 1981), analogous to the phosphorus species HPO_4^{2-} and H_2PO_4^- which are also abundant in both environments. In contrast, the dominant species of antimony in natural waters is Sb(OH)_6^- (Riley and Chester, 1971; Turner et al, 1981), similar to the reduced forms of arsenic and antimony (Turner et al, 1981), but with no phosphorus analogue. Therefore, it was considered unlikely that antimony would share the same uptake mechanism as phosphorus. Once biologically absorbed, however, antimony may undergo methylation like arsenic, as the speciation is similar to that of As(III), which is formed in the first stage of the biological methylation process (Wood, 1974).

The sensitivity tests applied in this chapter have shown that the antimony cycle is most sensitive to changes in the air-sea exchange rate, and to changes in the dissolved river flow. The marine biosphere is controlled by the ocean mixed layer, and the terrestrial biosphere by the landmass. However, the terrestrial biosphere may exert some influence on the behaviour of the troposphere.

CHAPTER SIX

CONCLUSIONS

6.1 GENERAL DISCUSSION

6.1.1 The Atmospheric Aerosol

The aerosol material analysed in this work was sampled in marine or coastal environments. The concentrations of arsenic and antimony were about an order of magnitude lower in the marine atmosphere than in coastal air. Geometric means for Ocean Station Lima were $0.075 \text{ ng As (SCM)}^{-1}$ and $0.086 \text{ ng Sb (SCM)}^{-1}$, whereas the overall means for the coastal samples were $0.70 \text{ ng As (SCM)}^{-1}$ and $0.35 \text{ ng Sb (SCM)}^{-1}$. In contrast, the mean concentrations for sodium and magnesium in the marine aerosol, $2200 \text{ ng Na (SCM)}^{-1}$ and $340 \text{ ng Mg (SCM)}^{-1}$, were very similar to the overall means for the coastal environment, $1600 \text{ ng Na (SCM)}^{-1}$ and $310 \text{ ng Mg (SCM)}^{-1}$. The differences between the true marine environment and the coastal environment are best treated by discussing these environments separately.

6.1.1.1 Arsenic and antimony in the marine aerosol

The mean data for the samples from Ocean Station Lima are compared with other published data for the open ocean atmosphere in table 6.1. The mean arsenic concentration for O.S. Lima is in reasonable agreement with other measurements of arsenic over the northern oceans, as are the measurements of sodium and magnesium. The mean for antimony is about three times higher than that reported for Bermuda. Ocean Station Lima, at 57° N , is influenced strongly by the Westerly winds, whereas Bermuda, at about 32° N , is near the boundary between the Westerlies and the North East Trades, and may be influenced by either airstream. Although the crustal enrichment factors for atmophile elements are much higher over the oceans in high latitudes than in low latitudes, the absolute concentrations of several such elements, such as lead and mercury, are very similar in the Westerlies and North East Trades, because of the higher dust loadings in the latter wind system (Chester et al., 1974). As the mean antimony

Table 6.1 Trace Elements in the Marine Atmosphere

Location	Concentration ng (SCM) ⁻¹				Source
	As	Sb	Na	Mg	
Ocean Station Lima	0.075	0.086	2200	340	This work
Bermuda (1973)	0.072	0.03	1500	220	Duce <u>et al</u> , 1976
Bermuda (1974)	0.093	-	2200	270	Duce <u>et al</u> , 1976
Tropical North Atlantic	-	0.11	-	-	Buat-Menard and Chesselet, 1979
North Atlantic	0.16	-	-	-	Walsh <u>et al</u> , 1979b
North Pacific and Indian Ocean	0.072	-	-	-	Walsh <u>et al</u> , 1979b
Southern Oceans	0.018	-	-	-	Walsh <u>et al</u> , 1979b
Enewetak Atoll (Tropical North Pacific)	-	0.005	-	-	Duce, 1982

value in this work was calculated from 'less than' values, the disparity between the results for Ocean Station Lima and Bermuda may indicate the scale of the overestimation. In contrast, the mean antimony concentration at Ocean Station Lima is similar to that observed by Buat-Menard and Chesselet (1979), so the overestimation in this work is not necessarily very large. The enrichment factors reported in this work are oceanic enrichment factors, so do not follow the same relationship as crustal enrichment factors. Unfortunately, sodium is often not determined in samples of marine aerosol, so it is not possible to compare the oceanic enrichment factors in this work with those for many other data sets. An exception is the data set from Bermuda (Duce et al, 1976). The oceanic enrichment factor for arsenic at Ocean Station Lima was about 2.5×10^2 , and for Bermuda was 3.5×10^2 and 3.0×10^2 for the 1973 season and 1974 season respectively. These are all much lower than the oceanic enrichment factor determined for arsenic from the data of Maenhaut and coworkers (1979) for samples from Antarctica, about 5×10^4 . It is interesting to note that much of the recent ice-core and aerosol data from remote regions have shown that earlier samples were probably severely contaminated (Peel, 1984), and there is now a tendency to move towards lower enrichment factors for the atmosphere elements. This may also be apparent in this work, as the oceanic enrichment factor for arsenic at Ocean Station Lima is slightly lower than that at Bermuda. This may, however, also indicate a larger continental component from the Trade Winds at Bermuda, or possibly a greater influence from North America, the North American continent being the most likely source of aerosol arsenic and antimony at Ocean Station Lima. The oceanic enrichment factor for antimony at Ocean Station Lima, 1.8×10^3 , is about twice that determined from the data at Bermuda, 9.2×10^2 . Again, this may indicate the scale of the overestimate for the antimony concentration over Ocean Station Lima. The data from Chester and coworkers (1974) only refer to

soil-sized particles. Arsenic and antimony are concentrated on fine particles, so direct comparison of the latitudinal variability of arsenic and antimony with that of lead and mercury should only be made with caution.

Since the occurrence of Saharan dust was first observed over Barbados (Delany et al, 1967), the importance of atmospheric transport as a source of trace elements to the open ocean has been recognised, especially those that are predominantly of continental origin (Dyrssen et al, 1972). The total deposition fluxes determined for arsenic and antimony to the North Atlantic were about 1.4 kt yr^{-1} for each. This is very similar to the dissolved arsenic flux from the Mississippi, $1.7 \text{ kt As yr}^{-1}$ (Trefry and Presley, 1976), which is the important flux in terms of oceanic supply (Waslenchuk, 1979). The material flowing from a river is only of major importance to coastal waters, and may well have undergone considerable modification by adsorption biological uptake or complexation before any is swept to the open ocean. In contrast, aerosol material still represents a direct input to the open ocean environment, from which surface-bound elements may still be available for biological processing. Although only about 25% of the urban aerosol arsenic and antimony was shown to be seawater soluble, the occurrence of acid rain may increase the dissolved portion during washout, before any material has even reached the ocean. Acid rain now pervades almost all the North Atlantic atmosphere, and rain as acid as pH 4.3 has been collected at Bermuda (Jickells et al, 1982). Therefore, atmospheric deposition represents a major source of dissolved arsenic and antimony to the surface waters and biota of the North Atlantic, compared with riverine input. Atmospheric deposition of arsenic and antimony may be slightly less important than for mercury, as Trefry and Presley (1976) reported a dissolved flux of only $0.2 \text{ kt Hg yr}^{-1}$ from the Mississippi, compared with a deposition flux of about $0.5 \text{ kt Hg yr}^{-1}$ to

the North Atlantic (Millward and Griffin, 1980). Indeed, Windom and Taylor (1979) showed that atmospheric deposition of mercury was eight times the riverine input to the Georgia Bight, a coastal area where riverine input is usually thought to dominate over aerosol deposition.

6.1.1.2 Arsenic and antimony in the coastal environment

The data for arsenic and antimony from the coastal sampling exercises are within the range reported for this environment, although the mean for the channel and Biscay includes samples from the open ocean (Table 6.2). The upper limits for arsenic and antimony over Plymouth are very similar to other data for aerosol arsenic and antimony around the British coast (Peirson et al, 1974). As the latter samples were analysed by neutron activation, they represent total analyses, not an available fraction. However, the upper limits for the Plymouth aerosol do not exceed these total analyses of Peirson and coworkers (v.s.), which gives further evidence that the samples in this work were free from contamination. Such available fractions should not be treated as total determinations, and confusion can occur if available fractions are not labelled as such (Janssens and Dams, 1973; Vijan and Wood, 1974). As sodium and magnesium in the Plymouth aerosol appear to be of marine origin, all enrichment factors were calculated using the observed concentrations of these two elements, not the upper limits determined from the urban particulate extracts. Enrichment factors determined on the observed concentrations of arsenic and antimony over Plymouth are 6.9×10^3 and 2.4×10^4 respectively, whereas those for their upper limit concentrations are 1.2×10^4 and 5.8×10^4 , similar to the enrichment factors for the observed concentrations of arsenic and antimony over the Channel Lightvessel, 1.1×10^4 and 3.3×10^4 . Again, these fall into the range determined from the data of Peirson and coworkers (v.s.) for samples around the British coast, 5.2×10^3 to 4.5×10^4 for arsenic, and

Table 6.2 Trace Elements in the Coastal Atmosphere

Location	Concentration, ng (SCM) ⁻¹				Source
	As	Sb	Na	Mg	
Plymouth (a)	0.83	0.45	880	220	This work
Plymouth (b)	1.4	1.1	1760	370	This work
Channel Lightvessel	1.7	0.80	1100	225	This work
Channel and Biscay (c)	0.24	0.12	4100	585	This work
Collefirth, Shetland Is.	1.6	0.64	2200	-	Peirson <u>et al</u> , 1974
Lerwick, Shetland Is.	2.0	0.57	2300	-	Peirson <u>et al</u> , 1974
Arran, Bute	2.4	1.7	1800	-	Peirson <u>et al</u> , 1974
Leiston, Suffolk	6.6	3.7	1200	-	Peirson <u>et al</u> , 1974
Gas platform, North Sea	5.5	3.1	4300	-	Peirson <u>et al</u> , 1974
Petten, Holland	4.8	3.3	2000	-	Peirson <u>et al</u> , 1974
Washington coast	0.13	0.11	-	-	Crececius, 1980

(a) observed

(b) estimated from extraction efficiencies on urban dust

(c) Includes samples from the open ocean

1.1×10^4 to 1.6×10^5 for antimony. The arsenic enrichment factor for the Channel and Biscay exercise, 4.3×10^2 , falls inbetween the coastal and open ocean enrichment factors, whereas that for antimony, 1.3×10^3 , is the lowest reported for the sampling exercises in this work. The lowest observed for antimony from this exercise was 2.8×10^2 , and 1.6×10^2 for arsenic. Again, these show the tendency towards lower enrichment factors for atmophile elements in marine aerosols.

The trends observed in this work show aerosol arsenic and antimony over coastal waters to be derived from continental sources, with concentrations falling to the low level of the marine aerosol about 300 km from the coast. A similar relationship with distance from source was observed for aerosol deposition of arsenic emitted from a smelter stack (Arafat and Glooschenko, 1982), which suggests that the diminution observed over the open ocean is a function of aerosol deposition of the continental material, in addition to dilution by marine airmasses of low atmophile content (Chester et al, 1983). As a consequence of this deposition, the deposition fluxes may be very large to coastal waters. The contribution of deposition to the dissolved arsenic and antimony burdens of the English Channel was determined as 7.5 t As yr^{-1} and 2.3 t Sb yr^{-1} . These were compared with the dissolved fluxes from the River Tamar, 3 t As yr^{-1} and 0.3 t Sb yr^{-1} . The contribution of fallout was determined from the solubility of urban dust in seawater. As before, if acid rain was an important washout agent, the soluble portion could be effectively increased two fold. This shows that aerosol deposition may make a significant contribution to the trace element budget of coastal waters, despite the view that riverine input is most important in this environment (Dryssen et al, 1972; Trefry and Presley, 1976). As many atmophile elements are toxic (Wood, 1974), deposition processes of anthropogenic material could represent a major transport mechanism of unmodified toxic material to coastal waters, which are biologically very active.

Some particles of natural continental origin were observed in the aerosol over the English Channel : "millet-seed" sand produced by desert erosion. The nearest desert is the Sahara, to the south. Although long range transport of Saharan dust is usually associated with the Trade Winds, northwards transport over the Mediterranean has also been observed (Chester et al, 1984b), so such material may be transported over western Europe. This may be the source of the material rich in antimony, which was blown over the English Channel from an easterly direction. A possible source of aerosol arsenic over South West England and the English Channel is the active tin mining industry in Cornwall.

Arsenic may be emitted in the vapour phase (Braman, 1975; Johnson and Braman, 1975a), and then rapidly condense onto the background aerosol, which is rich in marine sodium over South West England. Thus, a secondary association between arsenic and sodium may be developed, like that observed over the English Channel, although the two elements are derived from different sources. If this is the case, then arsenic is concentrated on the surface of aerosol material which is highly soluble in seawater. A greater fraction of the aerosol arsenic over the Channel may, therefore, be soluble than was calculated from the solubility of the urban dust, and may be directly available for biological uptake. In this way, aerosol deposition may represent a major source of arsenic to the surface biota of the English Channel.

6.1.2 Models of Geochemical Cycles

6.1.2.1 The arsenic cycle

The aim of modelling the arsenic cycle was to summarise the large amount of data available in a steady state geochemical cycle, and study the response of this steady state to various perturbations. Although such an

approach may be criticised over inadequacies in the data base, from both natural variability and artefacts of collection and analysis, the intention was to assess those parts of the arsenic cycle which were most sensitive to perturbations, and thereby warrant further detailed study.

The simulations showed that anthropogenic activities may seriously effect the long term balance of the arsenic cycle. The effect on the troposphere was of extreme importance, with the long term elevation due to low temperature processes posing a more serious problem than emissions from high temperature industrial processes. There is a crucial weakness in the knowledge base of the environmental behaviour of arsenic. Although the nature of the high temperature industrial emissions of arsenic is well established, they only account for about 20% of the present day pollutant burden, and little is known of the low temperature sources, which appear to be of far greater consequence. Much further study is required on this problem before predictive models of the arsenic cycle can be attempted.

The division of the troposphere into marine and continental airmasses had the effect of reducing the magnitude of sea-air exchange, in agreement with the known distribution of arsenic in the troposphere. Although this reduced the effects of any perturbation on the oceans, and thus on the marine biota, the effect on the troposphere was to dramatically enhance the long term elevation of the arsenic burden, especially in continental air. As such atmophiles are preferentially concentrated on sub-micron particles (Linton et al, 1976; Natusch et al, 1974), they are easily taken into the alveoli of the lungs, where absorption across the lung membrane may be up to 80% efficient (Natusch et al, 1974). Therefore, the enhancement of the long term elevation of tropospheric arsenic may have serious consequences for air-breathing biota, including man.

Several other sensitivity tests were carried out. The cycle was insensitive to changes in the particulate burden in the oceans. The rate determining step for the removal of arsenic is adsorption from solution, not the sedimentation of the particulate phase. The cycle is slightly more sensitive to river flow, if this is dramatically increased, although this does not greatly effect the overall trends observed from the perturbation. The major control on the long term elevation is the magnitude of the air-sea interaction. As this was only estimated to meet mass balance requirements, further study is required to establish the magnitude of this exchange process.

Although the long term consequences of the perturbations were not very large for the marine biota, the effects were considerable for land-based biota on virgin soil, which was not disturbed by man's activities. When arsenic uptake was modelled as a phosphorus analogue, the long term biological uptake of arsenic was suppressed. Much further work is required to examine element interactions of this nature, before the effects of any perturbation on the biosphere can be quantitatively assessed. However, it is clear that the concentration of arsenic in the biosphere will increase with further anthropogenic mobilisation. This may be very serious on local scales, as the simulations presented in this work only describe the overall effect on the biosphere. In reality, with an uneven distribution, the biota in some areas would receive a far higher anthropogenic input than was suggested from these simulations.

6.1.2.2 The antimony cycle

Unlike arsenic, the environmental distribution of antimony is not well established, so rather than perform numerous sensitivity tests on the cycling model, the primary aim of this section of the study was to make

a first attempt at quantifying the geochemical cycle of an element for which no previous cycling models have been published. Obviously, such a model must be regarded as highly tentative, but it is hoped that this will provide a basic study, against which future models may be compared as the knowledge of the behaviour of antimony in the environment improves.

The basic model for antimony was comparable to the arsenic model with a subdivided troposphere; air-sea interactions were small, and the landmass was the major source of antimony to the atmosphere. The perturbation from high temperature industrial sources was almost insignificant in comparison with the perturbation by low temperature processes. However, as neither are clearly established, further work should be assigned to the determination of both. The long term perturbation of the landmass created a large elevation of the antimony burden in the continental troposphere, with the same effects on air-breathing biota as were outlined for arsenic. It should be noted, however, that the consequences for health may not be as severe as those for arsenic, as antimony is the less toxic of the two elements. Again, the magnitude of the air-sea exchange exerts a major influence in controlling the long term trend in the troposphere, although the antimony cycle was more sensitive to changes in the riverine flow than was the arsenic cycle. The biological reservoirs behave in accordance with their individual host reservoir, although interactions with other elements have not been considered at this stage. Many of the interactions in the steady state were estimated from the equivalent interactions in the arsenic cycle, so these will require more study before a reliable assessment of the antimony cycle may be made.

6.1.2.3 Comparison of arsenic with antimony

As it was not possible to construct an antimony steady state with a well mixed troposphere, comparison of arsenic with antimony will be limited to

the heterogeneous troposphere models, and the biosphere models. For both cycles, the main control of tropospheric transport of pollutant material to the oceans was the air-sea exchange rate. If this was small, then material mobilised from the land was trapped in the tropospheric reservoirs. Removal from the oceans was a function of uptake onto the particulate phase from solution, rather than sedimentation of the particulate phase.

There were several important differences between the cycling behaviour of the two elements. Inorganic scavenging from seawater is more important for antimony than for arsenic, possibly because arsenic is ultimately removed on goethite, whereas antimony is ultimately removed on manganese oxides (Li, 1981a). Rivers exert a larger influence on antimony cycling in the ocean mixed layer, than on arsenic cycling. Riverine input accounts for 30% of the total antimony input to the ocean mixed layer, but only 6% of the total arsenic input, with much greater inputs from the particulates and deep waters. Large variations in the particulate reservoir do not influence the behaviour of the ocean mixed layer, as arsenic and antimony have very short residence times in the particulates. However, arsenic has a much longer residence time than antimony in the deep waters, which undergo very little change during the perturbation. Therefore, upwelling may act to stabilise the response of the ocean mixed layer to changes in the riverine input of arsenic. Upwelling for arsenic is about eight times the dissolved riverine flux, whereas upwelling of antimony is only twice the dissolved riverine input, so would not be so effective in stabilising the ocean mixed layer from the decay of the riverine fluxes.

The biological uptake of arsenic may be influenced by changes in the ambient phosphorus concentration. Although antimony is also a group (V) element, its speciation in natural waters differs from that of arsenic and phosphorus, so it does not probably enter the biosphere as a phosphorus analogue.

The low temperature perturbation rate of antimony is over five times higher than that for arsenic. This is most surprising as antimony compounds are generally less volatile than their arsenic analogues. It is possible that the high temperature component for the antimony perturbations was overestimated, if the influence of fossil fuel combustion observed on the aerosol antimony concentration over Plymouth is applicable on a global scale. However, if the low temperature mobilisation is genuinely greater than that of arsenic, then it is unlikely that they are volatilised in analogous forms. Much of the arsenic volatilised from the land surface is emitted via soil microbes as methyl arsines. If stibine (SbH_3) is the dominant species of antimony to leave the land surface, then antimony may be effectively more volatile than arsenic. The rate at which antimony is methylated may also be important, if this is faster than for arsenic. However, there has been little work published on the microbial methylation of antimony. The mechanisms of low temperature mobilisation of both elements require much further study, as these play an important role in the anthropogenic influence on the geochemical cycles of arsenic and antimony.

6.1.3 Overall Conclusions

Arsenic and antimony in the marine aerosol are mainly derived from continental airmasses, even in open ocean environments; airmasses derived from over North America transported more arsenic and antimony to Ocean Station Lima than did airmasses from other directions. Thus, atmospheric transport is a major pathway of pollutant material to the open ocean. Even though atmospheric input of these elements to the oceans is only about 10% of the riverine input, atmospheric input may still be important in coastal areas which are not under the influence of a major world river. Such an area is the English Channel, to which the dissolved input from the

River Tamar is only about 40% of the dissolved input from aerosol deposition of arsenic, and about 13% of the dissolved input from aerosol deposition of antimony. Local anthropogenic emissions of toxic elements, such as arsenic from the tin mining in Cornwall, can be a major anthropogenic input to these coastal waters, especially if deposited by acid rain, thereby dissolving much of the surface-bound toxic material before it reaches the sea surface. In such situations, it is essential to impose strict controls on the emissions of such toxic elements, if localised pollution is to be avoided.

Although high temperature emissions may have a drastic effect on local biota, they are unimportant globally, when compared with mobilisation by low temperature processes, even with a restricted low temperature source. This poses a most serious problem, as few low temperature mobilisation processes have been identified, so the potential source of this pollutant material has not been assessed. Before any remedial action can be considered, the mechanisms of low temperature mobilisation must be identified and quantified. If physical land disturbance is a major mechanism, there is probably little that can be done to alleviate the problem, short of restricting those volatile elements involved to their least mobile forms, by the mass use of chemical additives, a solution which may be unacceptable in the light of environmental problems associated with the widespread use of artificial insecticides and herbicides. Man's influence on these mobilisation processes must also be thoroughly assessed, before any quantitative predictive modelling can be attempted. In addition, the kinetics of many of the environmental cycling processes should be thoroughly examined, possibly by laboratory experimentation. Thus perturbations may be applied to realistic steady state models, to yield predictions that are relevant to the environment. The areas which most require such scrutiny are listed in the final section on recommendations for future study.

6.2 RECOMMENDATIONS FOR FURTHER WORK

Possible areas for further study can be broadly divided into environmental studies, laboratory studies and mathematical modelling. Environmental parameters requiring further scrutiny are as follows :

1. To establish a true baseline for pollution studies, more data are required for the environmental concentrations of trace elements in areas remote from man's influence, preferably in the southern hemisphere.
2. Short and medium term temporal variations of element concentrations in the environment should be determined at polluted and pristine sites, to obtain meaningful averages for the assessment of long term trends.
3. Important processes, like oceanic scavenging in deep waters, require further investigation, as there are still few data for processes in remote environments.
4. The extent of man's influence should be established. The pollutant input from industrial processes is poorly known for many elements, whilst information on low temperature mobilisation is almost non-existent. Atmospheric concentrations of toxic substances should be monitored where activities such as agriculture, or building construction are in progress, to assess the effect of all man's activities on the mobilisation of toxic elements.
5. Long term monitoring of atmophile elements is required to elucidate any global trends in anthropogenic mobilisation.
Contributions to the understanding of environmental processes could also come from the following laboratory studies :
6. Most transport processes in the environment are assumed to obey first order kinetics, but this is not proven. Therefore, programmes to

investigate the kinetics of processes like aerosol generation, scavenging and biological uptake should be undertaken.

7. The effects of controlled perturbations could be studied on trace element mobilisation in controlled environments.

Once further information on the behaviour of trace elements in the environment has been established, the following refinements to the models are recommended :

8. The Earth should be divided into north and south hemispheres, and transport of atmophiles across the ITCZ simulated.
9. Low temperature pollutant sources should be quantified, and appropriate growth rates determined for the low temperature perturbation.
10. Where still unclear, the high temperature pollutant input of atmophile elements to the environment should be established.
11. Further refinement of the box models may include : the subdivision of the oceans into coastal and open ocean reservoirs, the subdivision of the continental troposphere into regions of rural, urban and industrial influence, and the vertical variation in aerosol concentrations could be modelled by vertical division of the atmosphere.
12. The modelling technique should be extended to other toxic elements, such as lead, cadmium and selenium.
13. Finally, the introduction of non-linear processes, including the competition between different elements in the environment, would be an important step away from considering element cycles in isolation, with the ultimate aim of providing a model of the environment in its totality.

- Abrahams P.W. (1983) Distribution, dispersion and agricultural significance of metals in soils of mining regions of South West England. Ph.D. thesis, Imperial College, London, 369 pp.
- Ackroyd D.R. (1983) The removal and remobilisation of heavy metals during estuarine mixing. Ph.D. thesis, Plymouth Polytechnic, 231 pp.
- Adams F., R. Dams, L. Guzman and J.W. Winchester (1977) Background aerosol composition, Chacaltaya Mountain, Bolivia. *Atmos. Environ.*, 11, 629 - 634
- Adams F.C., M.J. van Craen and P.J. van Espen (1980a) Enrichment of trace elements in remote aerosols. *Environ. Sci. Technol.*, 14, 1002 - 1005
- Adams F., M. van Craen, P. van Espen and D. Andreuzzi (1980b) The elemental composition of atmospheric aerosol particles at Chacaltaya, Bolivia. *Atmos. Environ.*, 14, 879 - 893
- Ajax R. and R.E. Lee (1976) Non-pesticidal air pollution from agricultural processes. In "Air Pollution from Pesticides and Agricultural Processes", Ed : R.E. Lee. CRC Press, Cleveland, Ohio, pp 227 - 253
- Aller R.C. and D.J. DeMaster (1984) Estimates of particle flux and reworking at the deep-sea floor using $^{234}\text{Th}/^{238}\text{U}$ disequilibrium. *Earth Plan. Sci. Lett.*, 67, 308 - 318
- Andreae M.O. (1978) Distribution and speciation of arsenic in natural waters and some marine algae. *Deep Sea Res.*, 25, 391 - 402
- Andreae M.O. (1979) Arsenic speciation in seawater and interstitial waters: The influence of biological-chemical interactions on the chemistry of a trace element. *Limnol. Oceanogr.*, 24, 440 - 452
- Andreae M.O. and D. Klumpp (1979) Biosynthesis and release of organoarsenic compounds by marine algae. *Environ. Sci. Technol.*, 13, 738 - 741
- Andreae M.O., J.F. Asmode, P. Foster and L. Van't dack (1981) Determination of antimony (III), antimony (V) and methylantimony species in natural waters by atomic absorption spectrometry with hydride generation. *Anal. Chem.*, 53, 1766 - 1771
- Andreae M.O., J.T. Byrd and P.N. Froelich Jr. (1983) Arsenic, antimony, germanium and tin in the Tejo Estuary, Portugal : modelling a polluted estuary. *Environ. Sci. Technol.*, 17, 731 - 737
- Appelquist H., K.O. Jensen, T. Sevel and C. Hammer (1978) Mercury in the Greenland ice sheet. *Nature*, 273, 657 - 659
- Arafat N.M. and W.A. Glooschenko (1982) The use of bog vegetation as an indicator of atmospheric deposition of arsenic in northern Ontario. *Environ. Poll. (Series B)*, 4, 85 - 90
- Bacastow R. and A. Björkström (1981) Composition of ocean models for the carbon cycle. In "Carbon Cycle Modelling", Ed: B. Bolin. SCOPE 16, J. Wiley and Sons, Chichester, pp 29 - 79

REFERENCES:

- Bain G.W. (1978) Production growth rate stages as an index for amount of total resources. In "Proceedings of the Eleventh Commonwealth Mining and Metallurgical Congress", Ed : M.J. Jones. Institution of Mining and Metallurgy, London, pp 13 - 24
- Baker M.D., W.E. Inniss, C.I. Mayfield, P.T.S. Wong and Y.K. Chau (1983a) Effect of pH on the methylation of mercury and arsenic by sediment micro organisms. Environ. Tech. Lett., 4, 89 - 100
- Baker M.D., P.T.S. Wong, Y.K. Chau, C.I. Mayfield and W.E. Inniss (1983b) Methylation of arsenic by freshwater green algae. Can. J. Fish. Aquat. Sci., 40, 1254 - 1257
- Barker D.R. and H. Zeitlin (1972) Metal-ion concentrations in sea-surface microlayer and size-separated atmospheric aerosol samples in Hawaii. J. Geophys. Res., 77, 5076 - 5086
- Baur W.H. (1978) Arsenic : crystal chemistry. In "Handbook of Geochemistry" Ed : K.H. Wedepohl. Vol. II(3), Springer-Verlag, Berlin, pp 33.A.1 - 33.A.8.
- Beauford W., J. Barber and A.R. Barringer (1975) Heavy metal release from plants into the atmosphere. Nature, 256, 35 - 37
- Beauford W., J. Barber and A.R. Barringer (1977) Release of particles containing metals from vegetation into the atmosphere. Science, 195, 571 - 573
- Bennett B.G. (1981) Exposure commitment assessment of environmental pollutants. Vol. I(1), MARC report 23, Chelsea College, London, 59 pp.
- Bernard H. and M. Pinta (1982) Determination of arsenic in atmospheric aerosols by atomic absorption with electrothermal atomization. At. Spectrosc., 3, 8 - 12
- Bertine K.K. and E.D. Goldberg (1971) Fossil fuel combustion and the major sedimentary cycle. Science, 173, 233 - 235
- Bigg E.K., Z. Kviz and W.J. Thompson (1972) An October influx of submicron particles into the lower stratosphere. J. Geophys. Res., 77, 3916 - 3923
- Blanchard D.C. (1983) The production, distribution and bacterial enrichment of the sea-salt aerosol. In "Air-Sea Exchange of Gases and Particles", Ed : P.S. Liss and W.G. Slinn. D. Riedel, Dordrecht, pp 407 - 454
- Bloch M.R. and W. Luecke (1972) Geochemistry of ocean water bubble spray. J. Geophys. Res., 77, 5100 - 5105
- Bloch M.R., D. Kaplan, V. Kertes and J. Schnerb (1966) Ion separation in bursting air bubbles : an explanation for the irregular ion ratios in atmospheric precipitations. Nature, 209, 802 - 803
- Blum J.J. (1966) Phosphate uptake by phosphate-starved Euglena. J. General Physiol., 49, 1125 - 1137

- Bolin B. (1977) Changes of land biota and their importance for the carbon cycle. *Science*, 196, 613 - 615
- Bolin B., A. Björkström, C.D. Keeling, R. Bacastow and U. Siegenthaler (1981) Carbon cycle modelling. In "Carbon Cycle Modelling", Ed : B. Bolin, SCOPE 16, J. Wiley and Sons, Chichester, pp 1 - 28
- Bolin B., P.J. Crutzen, P.M. Vitousek, R.G. Woodmansee, E.D. Goldberg and R.B. Cook (1983) Interactions of biogeochemical cycles. In "The Major Biogeochemical Cycles and their Interactions", Ed : B. Bolin and R.B. Cook. SCOPE 21, J. Wiley and Sons, Chichester, pp 1 - 39
- Bothner M.H., P.J. Aruscavage, W.M. Ferrebee and P.A. Baedecker (1980) Trace metal concentrations in sediment cores from the continental shelf off the South-eastern United States. *Estuar. Coastal Mar. Sci.*, 10, 523 - 541
- Bowen H.J.M. (1966) The biogeochemistry of the elements. In "Trace Elements in Biochemistry", Academic Press, London, pp 173 - 210
- Bowen H.J.M. (1979) Elements in the geosphere and biosphere. In "Environmental Chemistry of the Elements", Academic Press, London pp 237 - 273
- Braman R.S. (1975) Arsenic in the environment. In "Arsenical Pesticides", Ed : E.A. Woolson. ACS Symposium Series 7, Washington DC, pp 109 - 123
- Braman R.S. (1984) Efficiency of filter sampling for arsenic in the atmosphere. *Atmos. Environ.*, 18, 1043
- Braman R.S. and C.C. Foreback (1973) Methylated forms of arsenic in the environment. *Science*, 182, 1247 - 1249
- Breslin V.T. and I.W. Duedall (1983) The behaviour of flyash derived arsenic in seawater. *Mar. Chem.*, 13, 341 - 355
- Brewer P.G., Y. Nozaki, D.W. Spencer and A.P. Fleer (1980) Sediment trap experiments in the deep North Atlantic : isotopic and elemental fluxes. *J. Mar. Res.*, 38, 703 - 728
- Brimblecombe P. (1979) Atmospheric arsenic. *Nature*, 280, 104 - 105
- Brimblecombe P. and K.A. Hunter (1977) Rock volatility and aerosol composition. *Nature*, 265, 761 - 762
- Brinckman F.E., G.E. Parris, W.R. Blair, K.L. Jewett, W.P. Iverson and J.M. Bellama (1977) Questions concerning environmental mobility of arsenic : needs for a chemical data base and means for speciation of trace organoarsenicals. *Environ. Health Perspect.*, 19, 11 - 24
- Broecker W.S. (1971) A kinetic model for the composition of seawater. *Quaternary Res.*, 1, 188 - 207
- Broecker W.S. (1974) *Chemical Oceanography*. Harcourt Brace Jovanovich, New York, pp 59 - 87

- Broecker W.S. and T-H. Peng (1982) Tracers in the Sea. Lamont-Doherty Geological Observatory, Palisades, New York, pp 1 - 44
- Brooks R.R., J.E. Ferguson, J. Holzbecher, D.E. Ryan, H.F. Zhang, J.M. Dale and B. Freedman (1982) Pollution by arsenic in a gold-mining district in Nova Scotia. Environ. Poll. (Series B), 4, 109 - 117
- Brooks R.R., D.E. Ryan and H. Zhang (1981) Atomic absorption spectrometry and other instrumental methods for quantitative measurements of arsenic. Anal. Chim. Acta, 131, 1 - 16
- Bruland K.W., K. Bertine, M. Koide and E.D. Goldberg (1974) History of metal pollution in Southern California coastal zone. Environ. Sci. Technol., 8, 425 - 432
- Bryan G.W., W.J. Langston, L.G. Hummerstone, G.R. Burt and Y.B. Ho (1983) An assessment of the gastropod, Littorina littorea, as an indicator of heavy metal contamination in United Kingdom estuaries. J. Mar. Biol. Ass. UK, 63, 327 - 345
- Buat-Menard P. and M. Arnold (1978) The heavy metal chemistry of atmospheric particulate matter emitted by Mount Etna volcano. Geophys. Res. Lett., 5, 245 - 248
- Buat-Menard P. and R. Chesselet (1979) Variable influence of atmospheric flux on the trace metal chemistry of ocean suspended matter. Earth Plan. Sci. Lett., 42, 399 - 411
- Burkitt A., P. Lester and G. Nickless (1972) Distribution of heavy metals in the vicinity of an industrial complex. Nature, 238, 327 - 328
- Burton J.D. (1983) A comment on the behaviour of dissolved organic carbon during estuarine mixing. In "The Major Biogeochemical Cycles and their Interactions", Ed : B. Bolin and R.B. Cook. SCOPE 21, J. Wiley and Sons, Chichester, pp 408 - 410
- Button D.K., S.S. Dunker and M.L. Morse (1973) Continuous culture of Rhodotorula rubra : kinetics of phosphate - arsenate uptake, inhibition, and phosphate - limited growth. J. Bacteriol., 113, 599 - 611
- Byrne A.R. and M. Tusek-Znidaric (1983) Arsenic accumulation in the mushroom Laccaria amethystina. Chemosphere, 12, 1113 - 1117
- Calvert S.E. and N.B. Price (1977) Geochemical variation in ferromanganese nodules and associated sediments from the Pacific Ocean. Mar. Chem., 5, 43 - 74
- Carpenter R., M.L. Peterson and R.A. Jahnke (1978) Sources, sinks and cycling of arsenic in the Puget Sound region. In "Estuarine Interactions", Ed : M.L. Wiley. Academic Press, London, pp 459 - 480
- Castillo J.R., J. Lanaja, M.C. Martinez and J. Aznarez (1982) Flame atomic adsorption spectroscopic determination of antimony in atmospheric particulates by using direct atomisation of the covalent hydride. Analyst, 107, 1488 - 1492

- Chadwick R. (1958) New extraction processes for metals. In "A History of Technology", Ed : C. Singer, E.J. Holmyard, A.R. Hall and T.I. Williams. Vol. 5, Oxford Clarendon Press, pp 72 - 101
- Chesselet R., J. Morelli and P. Buat-Menard (1972) Variations in ionic ratios between reference seawater and marine aerosols. J. Geophys. Res., 77, 5116 - 5131
- Chester R. (1971) Geological, geochemical and environmental implications of the marine dust veil. In "The Changing Chemistry of the Oceans", Ed : D. Dyrssen and D. Jagner. J. Wiley and Sons, New York, pp 291 - 305
- Chester R. (1975) Arsenic and selenium. In "Background papers for a Workshop on the tropospheric Transport of Pollutants to the Ocean", National Research Council, Miami, Florida, pp 13 - 18
- Chester R. (1982) Particulate aluminium fluxes in the eastern Atlantic. Mar. Chem., 11, 1 - 16
- Chester R., S.R. Aston, J.H. Stoner and D. Bruty (1974) Trace metals in soil-sized particles from the lower troposphere over the world ocean. J. Rech. Atmos., 8, 777 - 789
- Chester R., E.J. Sharples, K. Murphy, A.C. Saydam and G.S. Saunders (1983) The atmospheric distribution of lead over a number of marine regions. Mar. Chem., 13, 57 - 72
- Chester R., E.J. Sharples, G. Sanders, F. Oldfield and A.C. Saydam (1984a) The distribution of natural and non-crustal ferrimagnetic minerals in soil-sized particles from the Mediterranean atmosphere. Water Air Soil Pollut., 23, 25 - 35
- Chester R., E.J. Sharples, G.S. Sanders and A.C. Saydam (1984b) Saharan dust incursion over the Tyrrhenian Sea. Atmos. Environ., 18, 929 - 935
- Chu R.C., G.P. Barron and P.A.W. Baumgarner (1972) Arsenic determination at sub-microgram levels by arsine evolution and flameless atomic absorption technique. Anal. Chem., 44, 1476 - 1479
- Cox D.P. (1975) Microbiological methylation of arsenic. In "Arsenical Pesticides", Ed : E.A. Woolson. ACS Symposium Series 7, Washington D.C, pp 81 - 96
- Cox D.P. and M. Alexander (1973a) Production of trimethylarsine gas from various arsenic compounds by three sewage fungi. Bull. Environ. Contam. Toxicol., 9, 84 - 88
- Cox D.P. and M. Alexander (1973b) Effect of phosphate and other anions on trimethylarsine formation by Candida humicola. Appl. Microbiol., 25, 408 - 413
- Craig H. (1974) A scavenging model for trace elements in the deep sea. Earth Plan. Sci. Lett., 23, 149 - 159
- Crevelius E.A. (1975) The geochemical cycle of arsenic in Lake Washington and its relation to other elements. Limnol. Oceanogr., 20, 441 - 451

- Creelius E.A. (1977) Changes in the chemical speciation of arsenic following ingestion by man. *Environ. Health Perspect.*, 19, 147-150
- Creelius E.A. (1980) The solubility of coal fly ash and marine aerosols in seawater. *Mar. Chem.*, 8, 245-250
- Creelius E.A., C.J. Johnson and G.C. Hofer (1974) Contamination of soils near a copper smelter by arsenic, antimony and lead. *Water Air Soil Pollut.*, 3, 337-342
- Crock J.G. and F.E. Lichte (1982) An improved method for the determination of trace levels of arsenic and antimony in geological materials by automated hydride generation - atomic absorption spectroscopy. *Anal. Chim. Acta*, 144, 223-233
- Dams R. and J. De Jonge (1976) Chemical composition of Swiss aerosols from the Jungfrauoch. *Atmos. Environ.*, 10, 1079-1084
- Dams R., K.A. Rahn and J.W. Winchester (1972) Evaluation of filter materials and impaction surfaces for nondestructive neutron activation analysis of aerosols. *Environ. Sci. Technol.*, 6, 441-448
- Delany A.C., A.C. Delany, D.W. Parkin, J.J. Griffin, E.D. Goldberg and B.E.F. Reimann (1967) Airborne dust collected at Barbados. *Geochim. Cosmochim. Acta*, 31, 885-909
- Dethier D.P. (1979) Atmospheric contributions to stream water chemistry in the North Cascade Range, Washington. *Water Resour. Res.*, 15, 787-794
- Dickson E.M. (1972) Mercury and lead in the Greenland ice sheet. A re-examination of the data. *Science*, 177, 536-538
- Dissanayake C.B., H.J. Tobschall, H. Palme, U. Rast and B. Spettel (1983) The abundance of some major and trace elements in highly polluted sediments from the Rhine River near Mainz, West Germany. *Sci. Tot. Environ.*, 29, 243-260
- Duce R.A. (1982) Sea salt and trace element transport across the sea-air interface. Paper presented at JDA, 2-13 August 1982, Halifax, Nova Scotia
- Duce R.A. and G.L. Hoffman (1976) Atmospheric vanadium transport to the ocean. *Atmos. Environ.*, 10, 989-996
- Duce R.A., G.L. Hoffman and W.L. Zoller (1975) Atmospheric trace metals at remote northern and southern hemisphere sites : Pollution or natural? *Science*, 187, 59-61
- Duce R.A., G.L. Hoffman, B.J. Ray, I.S. Fletcher, G.T. Wallace, J.L. Fasching, S.R. Piotrowicz, P.R. Walsh, E.J. Hoffman, J.M. Miller and J.L. Heffter (1976) Trace metals in the marine atmosphere : sources and fluxes. In "Marine Pollutant Transfer", Ed : H.L. Windom and R.A. Duce. Lexington Books, Massachusetts, pp 77-119
- Duce R.A., J.G. Quinn, C.E. Olney, S.R. Piotrowicz, B.J. Ray and T.L. Wade (1972) Enrichment of heavy metals and organic compounds in the surface microlayer of Narragansett Bay, Rhode Island. *Science*, 176, 161-163

- Dugdale R.C. (1977) Modelling. In "The Sea", Vol. 6, Ed : E.D. Goldberg, I.N. McCave, J.J. O'Brien and J.H. Steele. J. Wiley and Sons, New York, pp 789-806
- Dyrssen D., C. Patterson, J. Ui and G.F. Weichart (1972) Inorganic chemicals. In "A Guide to Marine Pollution", Ed : E.D. Goldberg. Gordon and Breach, New York, pp 41-58
- Edmonds E.A., M.C. McKeown and M. Williams (1975) British Regional Geology: South West England. 4th ed'n. H.M.S.O., London, pp 85-106
- Fairbanks R.G., M. Sverdrlove, R. Free, P.H. Wiebe and A.W.H. Be (1982) Vertical distribution and isotopic fractionation of living planktonic foraminifera from the Panama Basin. *Nature*, 298, 841-844
- Fairbridge R.W. (Ed.) (1972) The Encyclopedia of Geochemistry. Environmental Sciences IVA, Van Nostrand Reinhold, New York, pp 1072-1073
- Ferguson J.F. and J. Gavis (1972) A review of the arsenic cycle in natural waters. *Water Res.*, 6, 1259-1274
- Fernandez F.J. and D.C. Manning (1971) The determination of arsenic at sub-microgram levels by atomic absorption spectrophotometry. *At. Absorpt. Newslett.*, 10, 86-88
- Fisher G.L., D. Silberman, B.A. Prentice, R.E. Heft and J.M. Ondov (1979) Filtration studies with neutron-activated coal fly ash. *Environ. Sci. Technol.*, 13, 689-693
- Food and Agriculture Organisation (F.A.O.) (1948-1957) Yearbook of Food and Agricultural Statistics. Vols. 1-10, Washington D.C., until 1951, then Rome, Italy
- Food and Agriculture Organisation (F.A.O.) (1958-1982) Production Yearbook. Vols. 11-35, Rome, Italy
- Frank E.R., J.P. Lodge and A. Goetz (1972) Experimental sea salt profiles. *J. Geophys. Res.*, 77, 5147-5151
- Froelich P.N., M.L. Bender and G.R. Heath (1977) Phosphorus accumulation rates in metalliferous sediments on the East Pacific Rise. *Earth Plan. Sci. Lett.*, 34, 351-359
- Fuller C.W. (1977) Electrothermal Atomization for Atomic Absorption Spectrometry. The Chemical Society, London, pp 61-64
- Gallagher J.L. (1975) The significance of the surface film in salt marsh plankton metabolism. *Limnol. Oceanogr.*, 20, 120-123
- Garrels R.M. and F.T. Mackenzie (1971) Evolution of Sedimentary Rocks. W.W. Norton and Co., 397 pp
- Garrels R.M., F.T. Mackenzie and C. Hunt (1973) Chemical Cycles and the Global Environment. W. Kaufmann Inc., Los Altos, California, 206 pp
- Gibbs P.E., W.J. Langston, G.R. Burt and P.L. Pascoe (1983) Tharyx marioni (Polychaeta) : a remarkable accumulator of arsenic. *J. Mar. Biol. Ass. U.K.*, 63, 313-325

- Goldberg E.D. (1963) The oceans as a chemical system. In "The Sea", Vol. 2, Ed : M.N. Hill. J. Wiley and Sons, New York, pp 3-25
- Goldberg E.D. (1971) Man's role in the major sedimentary cycle. In "The Changing Chemistry of the Oceans", Ed : D. Dyrssen and D. Jagner. J. Wiley and Sons, New York, pp 267-288
- Goldberg E.D. (1975) Atmospheric transport of mercury from continents to the oceans. In "Background papers for a Workshop on the Tropospheric Transport of Pollutants to the Ocean", National Research Council, Miami, Florida, pp 40-43
- Goldberg E.D. (1976) Rock volatility and aerosol composition. *Nature*, 260, 128-129
- Govett M.H. (1976) Geographic concentration of world mineral supplies, production and consumption. In "World Mineral Supplies", Ed : G.J.S. Govett and M.H. Govett. Elsevier, Amsterdam, pp 99-146
- Graham W.F. and R.A. Duce (1979) Atmospheric pathways of the phosphorus cycle. *Geochim. Cosmochim. Acta*, 43, 1195-1208
- Griffin J.H. (1980) Atmospheric mercury and the global mercury cycle. M. Phil. Thesis, Plymouth Polytechnic, 106 pp
- Griffin J.J. and E.D. Goldberg (1975) The fluxes of elemental carbon in coastal marine sediments. *Limnol. Oceanogr.* 20, 456-463
- Grigg D.B. (1980) Population Growth and Agrarian Change. An Historical Perspective. Cambridge University Press, 340 pp
- Halter B. and E. Robinson (1977) Nuclei concentrations over the extreme Eastern Pacific Ocean. *J. Geophys. Res.*, 82, 991-994
- Hammer C.U. (1977) Past volcanism revealed by Greenland ice sheet impurities. *Nature*, 270, 482-486
- Hardy J.T. (1973) Phytoneuston ecology of a temperate marine lagoon. *Limnol. Oceanogr.*, 18, 525-533
- Harris D.C. (1982) Quantitative Chemical Analysis. W.H. Freeman, San Francisco, pp 523-524
- Harrison R.M. and C.A. Pio (1983a) Major ion composition and chemical associations of inorganic atmospheric aerosols. *Environ. Sci. Technol.*, 17, 169-174
- Harrison R.M. and C.A. Pio (1983b) Size-differentiated composition of inorganic aerosols of both marine and polluted continental origin. *Atmos. Environ.*, 17, 1733-1738
- Heintzenberg J., H.C. Hansson and H. Lannefors (1981) The chemical composition of Arctic haze at Ny-Ålesund, Spitsbergen. *Tellus*, 33, 162-171
- Hoffman G.L., R.A. Duce and E.J. Hoffman (1972) Trace metals in the Hawaiian marine atmosphere. *J. Geophys. Res.*, 77, 5322-5329

- Holm-Hansen O. (1969) Determination of microbial biomass in ocean profiles. *Limnol. Oceanogr.*, 14, 740-747
- Hood R.D. and W.P. Harrison (1982) Effects of prenatal arsenite exposure in hamster. *Bull. Environ. Contam. Toxicol.*, 29, 671-678
- Hood R.D., W.P. Harrison and G.C. Vedel (1982) Evaluation of arsenic metabolites for prenatal effects in the hamster. *Bull. Environ. Contam. Toxicol.*, 29, 679-687
- Horne, R.A. (1978) *The Chemistry of Our Environment*. J. Wiley and Sons, New York, pp 159-232
- Howard A.G. and M.H. Arbab-Zavar (1981) Determination of "inorganic" arsenic (III) and arsenic (V), "methylarsenic" and "Dimethylarsenic" species by selective hydride evolution atomic absorption spectroscopy. *Analyst*, 106, 213-220
- Howard A.G., M.H. Arbab-Zavar and S. Apte (1982) Seasonal variability of biological arsenic methylation in the estuary of the River Beaulieu. *Mar. Chem.*, 11, 493-498
- Iverson D.G., M.A. Anderson, T.R. Holm and R.R. Stanforth (1979) An evaluation of column chromatography and flameless atomic absorption spectrophotometry for arsenic speciation as applied to aquatic systems. *Environ. Sci. Technol.*, 13, 1491-1497
- Janssens M. and R. Dams (1973) Determination of lead in atmospheric particulates by flameless atomic absorption spectrometry with a graphite tube. *Anal. Chim. Acta*, 65, 41-47
- Jedwab J. (1975) Characterisation and identification of discrete pollutant particles. In "Background papers for a Workshop on the Tropospheric Transport of Pollutants to the Ocean", National Research Council, Miami, Florida, pp 33-39
- Jickells T., A. Knap, T. Church, J. Galloway and J. Miller (1982) Acid rain on Bermuda. *Nature*, 297, 55-57
- Johnson D.L. and R.S. Braman (1975a) Alkyl and inorganic arsenic in air samples. *Chemosphere*, 4, 333-338
- Johnson D.L. and R.S. Braman (1975b) The speciation of arsenic and the content of germanium and mercury in members of the pelagic Sargassum community. *Deep Sea Res.*, 22, 503-507
- Junge C.E. (1963) *Air Chemistry and Radioactivity*. Academic Press, New York, 328 pp
- Junge C.E. (1972) Our knowledge of the physico-chemistry of aerosols in the undisturbed marine environment. *J. Geophys. Res.*, 77, 5183-5200
- Junge C.E. (1974) Residence time and variability of tropospheric trace gases. *Tellus*, 26, 477-488
- Junge C. and R. Jaenicke (1971) New results in background aerosol studies from the Atlantic expedition of the R.V. Meteor, Spring 1969. *Aerosol Sci.*, 2, 305-314

- Kantin R. (1983) Chemical speciation of antimony in marine algae. *Limnol. Oceanogr.*, 28, 165-168
- Keeling C.D. and B. Bolin (1967) The simultaneous use of chemical tracers in oceanic studies. I General theory of reservoir models. *Tellus*, 19, 566-581
- Keeling C.D. and B. Bolin (1968) The simultaneous use of chemical tracers in oceanic studies. II A three-reservoir model of the North and South Pacific Oceans. *Tellus*, 20, 17-54
- Kerr R.A. (1981) Pollution of the Arctic atmosphere confirmed. *Science*, 212, 1013-1014
- Kharkar D.P., J. Thomson, K.K. Turekian and W.O. Forster (1976) Uranium and thorium decay series nuclides in plankton from the Caribbean. *Limnol. Oceanogr.*, 21, 294-299
- Kirkham M.B. (1979) Trace elements. In "The Encyclopedia of Soil Science", Part 1, Ed : R.W. Fairbridge and C.W. Finkl. Dowden Hutchinson and Ross, Pennsylvania, pp 571-575
- Knauss K. and T-L. Ku (1983) The elemental composition and decay-series radionuclide content of plankton from the East Pacific. *Chem. Geol.*, 39, 125-145
- Knudson E.J. and G.D. Christian (1974) A note on the determination of arsenic using sodium borohydride. *At. Absorpt. Newslett.*, 13, 74
- Kosta L., A.R. Byrne and M. Dermelj (1983) Trace elements in some human milk samples by radiochemical neutron activation analysis. *Sci. Tot. Environ.*, 29, 261-268
- Kowalczyk G.S., G.E. Gordon and S.W. Rheingrover (1982) Identification of atmospheric particle sources in Washington D.C. using chemical mass balances. *Environ. Sci. Technol.*, 16, 79-90
- Krishnaswami S., D. Lal, B.L.K. Somayajulu, R.F. Weiss and H. Craig (1976) Large-volume in-situ filtration of deep Pacific waters : mineralogical and radioisotope studies. *Earth Plan. Sci. Lett.*, 32, 420-429
- Kronberg B.I., W.S. Fyfe, O.H. Leonardos and A.M. Santos (1979) The chemistry of some Brazilian soils : Elemental mobility during intense weathering. *Chem. Geol.*, 24, 211-229
- Kupcik V. (1974) Antimony, crystal chemistry. In "Handbook of Geochemistry", Ed : K.H. Wedepohl. Vol. II(4), Springer-Verlag, Berlin, pp 51.A.1-51.A.11
- Lakso J.U. and S.A. Peoples (1975) Methylation of inorganic arsenic by mammals. *J. Agric. Food Chem.*, 23, 674-676
- Lal D. (1977) The oceanic microcosm of particles. *Science*, 198, 997-1009
- Langston W.J. (1980) Arsenic in UK estuarine sediments and its availability to benthic organisms. *J. Mar. Biol. Ass. UK*, 60, 869-881

- Lantzy R.J. and F.T. Mackenzie (1979) Atmospheric trace metals : global cycles and assessment of man's impact. *Geochim. Cosmochim. Acta*, 43, 511-525
- Larson T.V., R.A. Charlson, E.J. Knudson, G.D. Christian and H. Harrison (1975) The influence of a sulphur dioxide point source on the rain chemistry of a single storm in the Puget Sound region. *Water Air Soil Pollut.*, 4, 319-328
- Lasaga A.C. (1980) The kinetic treatment of geochemical cycles. *Geochim. Cosmochim. Acta*, 44, 815-828
- La Touche Y.D. and M.C. Mix (1982) Seasonal variations of arsenic and other trace elements in bay mussels (*Mytilus edulis*). *Bull. Environ. Contam. Toxicol.*, 29, 665-670
- Leatherland T.M., J.D. Burton, F. Culkin, M.J. McCartney and R.J. Morris (1973) Concentrations of some trace metals in pelagic organisms and of mercury in Northeast Atlantic Ocean water. *Deep Sea Res.*, 20, 679-685
- Leetmaa A. (1977) Effects of the winter of 1976-1977 on the north western Sargasso Sea. *Science*, 198, 188-189
- Lepel E.A., K.M. Stefansson and W.H. Zoller (1978) The enrichment of volatile elements in the atmosphere by volcanic activity : Augustine Volcano 1976. *J. Geophys. Res.*, 83, 6213-6220
- Lerman A., F.T. Mackenzie and R.M. Garrels (1975) Modelling of geochemical cycles : phosphorus as an example. *Geol. Soc. Amer. Mem.*, 142, 205-218
- Li Y-H (1981a) Ultimate removal mechanisms of elements from the ocean. *Geochim. Cosmochim. Acta*, 45, 1659-1664
- Li Y-H (1981b) Geochemical cycles of elements and human perturbation. *Geochim. Cosmochim. Acta*, 45, 2073-2084
- Linton R.W., A. Loh, D.F.S. Natusch, C.A. Evans and P. Williams (1976) Surface predominance of trace elements in airborne particles. *Science*, 191, 852-854
- Lion L.W., R.W. Harvey and J.O. Leckie (1982) Mechanisms for trace metal enrichment at the surface microlayer in an estuarine salt marsh. *Mar. Chem.*, 11, 235-244
- Liss P.S. (1975) Chemistry of the sea surface microlayer. In "Chemical Oceanography", Vol. 2, Ed : J.P. Riley and G. Skirrow. 2nd Ed'n., Academic Press, London, pp 193-244
- Lorenzen C.J., N.A. Welschmeyer and A.E. Copping (1983) Particulate organic flux in subarctic Pacific. *Deep Sea Res.*, 30, 639-643
- Luten J.B., G. Riekwel-Booy, J. van der Greef and M.C. t.N. de Brauw (1983) Identification of arsenobetaine in sole, lemon sole, flounder, dab, crab and shrimps by field desorption and fast atom bombardment mass spectrometry. *Chemosphere*, 12, 131-141
- Macdonald G.A. (1972) *Volcanoes*. Prentice Hall, New Jersey, pp 344-369

- MacIntyre F. (1974) Chemical fractionation and sea-surface microlayer processes. In "The Sea", Vol. 5, Ed : E.D. Goldberg. J. Wiley and Sons, New York, pp 245-299
- Mackenzie F.T. (1975) Sedimentary cycling and the evolution of seawater. In "Chemical Oceanography", Vol. 1, Ed : J.P. Riley and G. Skirrow. 2nd ed'n., Academic Press, London, pp 309-364
- Mackenzie F.T. and R. Wollast (1977) Sedimentary cycling models of global processes. In "The Sea", Vol. 6, Ed : E.D. Goldberg, I.N. McCave, J.J. O'Brien and J.H. Steele. J. Wiley and Sons, New York, pp 739-765
- Mackenzie F.T., R.J. Lantzy and V. Paterson (1979) Global trace metal cycles and predictions. *Math. Geol.*, 11, 99-142
- Madsen P.P. (1981) Peat bog records of atmospheric mercury deposition. *Nature*, 293, 127-130
- Maenhaut W., W.H. Zoller, R.A. Duce and G.L. Hoffman (1979) Concentration and size distribution of particulate trace elements in the South Polar atmosphere. *J. Geophys. Res.*, 84, 2421-2431
- Marsh J.G. (1983) The removal of arsenic from aquatic systems by iron oxyhydroxides. Ph.D. thesis, Plymouth Polytechnic, 258 pp
- Martin J.M. and M. Maybeck (1979) Elemental mass-balance of material carried by major world rivers. *Mar. Chem.*, 7, 173-206
- Mason B. (1966) Principles of Geochemistry. 3rd ed'n., J. Wiley and Sons, New York, 329 pp.
- Mayzaud P. and R.J. Conover (1976) Influence of potential food supply on the activity of digestive enzymes of neritic zooplankton. In "Proceedings of the 10th European Symposium on Marine Biology", Vol. 2, Ed : G. Persoone and E. Jaspers. Universa, Wetteren. pp 415-427
- Meadows D.H., D.L. Meadows, J. Randers and W.W. Behrens (1974) The Limits to Growth. Pan, London, 205 pp
- Menzel D.W. (1974) Primary productivity, dissolved and particulate organic matter, and the sites of oxidation of organic matter. In "The Sea", Vol. 5, Ed : E.D. Goldberg. J. Wiley and Sons, New York, 659-678
- Meszaros A. (1977) On the size distribution of atmospheric aerosol particles of different composition. *Atmos. Environ.*, 11, 1075-1081
- Mikhshenskiy A.Z., Uy, V. Yakovlev, I.A. Menyailov, L.P. Nikitira and B.V. Savelyev (1979) Geochemical significance of element transport with volatiles in active volcanism. *Geochem. International*, 16(6), 33-40
- Millward G.E. (1982) Nonsteady state simulations of the global mercury cycle. *J. Geophys. Res.*, 87, 8891-8897
- Millward G.E. and J.H. Griffin (1980) Concentrations of particulate mercury in the Atlantic marine atmosphere. *Sci. Tot. Environ.*, 16, 239-248
- Minagawa M. and S. Tsunogoi (1980) Removal of ²³⁴Th from a coastal sea: Funka Bay, Japan. *Earth Plan. Sci. Lett.*, 47, 51-64

- Moore R.M., J.E. Milley and A. Chatt (1984) The potential for biological mobilisation of trace-elements from aerolian dust in the ocean and its importance in the case of iron. *Oceanol. Acta*, 7, 221-228
- Morris K. (Ed.) (1977) *Methods of Air Sampling and Analysis*. 2nd ed'n., A.P.H.A., Washington D.C.
- Morris R.J., M.J. McCartney, A.G. Howard, M.H. Arbab-Zaver and J.S. Davis (1984) The ability of a field population of diatoms to discriminate between phosphate and arsenate. *Mar. Chem.*, 14, 259-265
- Morton J. (1979) *Guts*. 2nd ed'n., Edward Arnold, London. 59 pp
- Mroz E.J. and W.H. Zoller (1975) Composition of atmospheric particulate matter from the eruption of Heimaey, Iceland. *Science*, 190, 461-464
- Murdoch J. and J.A. Barnes (1974) *Statistical Tables for Science Engineering, Management and Business Studies*. 2nd Ed'n., Macmillan, London, p 20
- McBride B.C. and R.S. Wolfe (1971) Biosynthesis of dimethylarsine by methanobacterium. *Biochem.*, 10, 4312-4317
- McCave I.N. (1984) Size spectra and aggregation of suspended particles in the deep ocean. *Deep Sea Res.*, 31, 329-352
- National academy of Sciences (NAS) (1977) *Arsenic. Medical and Biological Effects of Environmental Pollutants Series*. NAS, Washington D.C., 332 pp
- National Academy of Sciences (NAS) (1978) *The Tropospheric Transport of Pollutants and Other Substances to the Oceans*. NAS, Washington D.C., pp 124-145
- Natusch D.F.S., J.R. Wallace and C.A. Evans (1974) Toxic trace elements : preferential concentration in respirable particles. *Science*, 183, 202-204
- Neal C., H. Elderfield and R. Chester (1979) Arsenic in the sediments of the North Atlantic Ocean and the Eastern Mediterranean Sea. *Mar. Chem.*, 7, 207-219
- Newell R.E., G.J. Boer and J.W. Kidston (1974) An estimate of the inter-hemispheric transfer of carbon monoxide from tropical general circulation data. *Tellus*, 26, 103-107
- Ng A and C. Patterson (1981) Natural concentrations of lead in ancient Arctic and Antarctic ice. *Geochim. Cosmochim. Acta*, 45, 2109-2121
- Nicholls K.H. and C.M. Cox (1978) Atmospheric nitrogen and phosphorus loading to Harp Lake, Ontario, Canada. *Water Reservoir. Res.*, 14, 589-592
- Norin H., R. Ryhage, A. Christakopoulos and M. Sandstrom (1983) New evidence for the presence of arsenocholine in shrimps (*Pandalus borealis*) by use of pyrolysis gas chromatography - atomic absorption spectrometry/mass spectrometry. *Chemosphere*, 12, 299-315
- Norris L.A., P.R. Canutt and J.F. Neumann (1983) Arsenic in the forest environment after thinning with MSMA and cacodylic acid. *Bull. Environ. Contam. Toxicol.*, 30, 309-316
- O'Connors H.B., L.R. Small and P.L. Donaghay (1976) Particle size modification by two classes of the estuarine copepod *Acartia clausi*. *Limnol. Oceanogr.*, 21, 300-308

- Olafsson J. (1975) Volcanic influence on seawater at Heimaey. *Nature*, 255, 138-141
- Onishi H. (1969a) Arsenic. In "Handbook of Geochemistry", Ed : K.H. Wedepohl. Vol. II(3), Springer-Verlag, Berlin, pp 33.B.1-33.O.1
- Onishi H. (1969b) Antimony. In "Handbook of Geochemistry", Ed : K.H. Wedepohl. Vol. II(4), Springer-Verlag, Berlin, pp 51.B.1-51.O.1
- Oscarson D.W., P.M. Huang, U.T. Hammer and W.K. Liaw (1983) Oxidation and sorption of arsenite by manganese dioxide as influenced by surface coatings of iron and aluminium oxides and calcium carbonate. *Water Air Soil Pollut.*, 20, 233-244
- Parkin D.W., D.R. Philips, R.A.L. Sullivan and L. Johnson (1970) Airborne dust collections over the North Atlantic. *J. Geophys. Res.*, 75, 1782-1793
- Parsons T.R. (1975) Particulate organic carbon in the sea. In "Chemical Oceanography", Vol. 2, Ed : J.P. Riley and G. Skirrow. 2nd ed'n, Academic Press, London, pp 365-383
- Patterson C.C. (1975) Glacial record of tropospheric aerosols. In "Background papers for a Workshop on the Tropospheric Transport of Pollutants to the Ocean", National Research Council, Miami, Florida, pp 52-63
- Patterson C., D. Settle, B. Schaule and M. Burnett (1976) Transport of pollutant lead to the oceans and within ocean ecosystems. In "Marine Pollutant Transfer", Ed : H.L. Windom and R.A. Duce. Lexington Books, Massachusetts, pp 23-36
- Peel D.A. (1984) Trace metals in Antarctic snow. Presented at CCRAC Workshop on Atmospheric Chemistry, July 1984, Oxford University
- Peirson D.H., P.A. Cawse, L. Salmon and R.S. Cambray (1973) Trace elements in the atmospheric environment. *Nature*, 241, 252-256
- Peirson D.H., P.A. Cawse and R.S. Cambray (1974) Chemical uniformity of airborne particulate material, and a maritime effect. *Nature*, 251, 675-679
- Perry A.E. (1982) Hot-wire Anemometry. Clarendon Press, Oxford, 184 pp
- Peterson M.L. and R. Carpenter (1983) Biogeochemical processes affecting total arsenic and arsenic species distributions in an intermittently anoxic fjord. *Mar. Chem.*, 12, 259-321
- Pilson M.E.Q. (1974) Arsenate uptake and reduction by Pocillopora verrucosa. *Limnol. Oceanogr.*, 19, 339-341
- Player R.L. and H.J. Wouterlood (1982) Removal and recovery of arsenious oxide from flue gases. A pilot study of the activated carbon process. *Environ. Sci. Technol.*, 16, 808-814
- Poet S.E., H.E. Moore and E.A. Martell (1972) Lead 210, bismuth 210 and polonium 210 in the atmosphere: Accurate ratio measurement and application to aerosol residence time determination. *J. Geophys. Res.*, 77, 6515-6527

- Press F. and R. Siever (1974) Earth. W.H. Freeman, San Francisco, pp 631-668
- Read H.H. and J. Watson (1968) Introduction to Geology : Volume 1, Principles. 2nd ed'n. Macmillan Press, London, pp 152-160
- Redfield A.C., B.H. Ketchum and F.A. Richards (1963) The influence of organisms on the composition of seawater. In "The Sea", Vol. 2, Ed : M.N. Hill. J. Wiley and Sons, New York, pp 26-77
- Revelle R. (1976) The resources available for agriculture. Sci. Amer., 235 (3), 164-178
- Riley J.P. and R. Chester (1971) Introduction to Marine Chemistry. Academic Press, London, 465 pp
- Robberecht H., H. Deelstra, D. Vanden Berghe and R. Van Grieken (1983) Metal pollution and selenium distributions in soil and grass near a non-ferrous plant. Sci. Tot. Environ., 29, 229-241
- Rodin L.E., N.I. Bazilevich and N.N. Rozov (1978) Productivity of the world's main ecosystems. In "Patterns of Primary Production in the Biosphere", Ed : H.F.H. Lieth. Dowden Hutchinson and Ross, Pennsylvania, pp 294-299
- Rothstein A. (1963) Interactions of arsenate with the phosphate-transporting system of yeast. J. General Physiol., 46, 1075-1085
- Russell D.A. (1984) Geochemical cycles of arsenic and antimony in estuarine systems. B.Sc.(hons) project report, Plymouth Polytechnic, 63 pp
- Sabbioni E., L. Goetz, A. Springer and R. Pietra (1983) Trace metals from coal-fired power plants : derivation of an average data base for assessment studies of the situation in the European Communities. Sci. Tot. Environ., 29, 213-227
- Sadiq M., T.H. Zaidi and A.A. Mian (1983) Environmental behaviour of arsenic in soils : theoretical. Water Air Soil Pollut., 20, 369-377
- Salmon L., D.H.F. Atkins, E.M.R. Fisher, C. Healy and D.V. Law (1978) Retrospective trend analysis of UK air particulate material. Sci. Tot. Environ., 9, 161-200
- Sanders J.G. (1980) Arsenic cycling in marine systems. Mar. Environ. Res., 3, 257-266
- Sanders J.G. and H.L. Windom (1980) The uptake and reduction of arsenic species by marine algae. Estuar. Coastal Mar. Sci., 10, 555-567
- Schnell R.C. and G. Vali (1972) Atmospheric ice nuclei from decomposing vegetation. Nature, 236, 163-165
- Schnell R.C. and G. Vali (1973) World-wide source of leaf-derived freezing nuclei. Nature, 246, 212-213
- Schwarzacher W. (1975) Sedimentation Models and Quantitative Stratigraphy. Elsevier, Amsterdam, p 26

- Shair F.H., E.J. Sasaki, D.E. Carlan, G.R. Cass, W.R. Goodin, J.G. Edinger and G.E. Schacher (1982) Transport and dispersion of airborne pollutants associated with the land breeze - sea breeze system. *Atmos. Environ.*, 16, 2043-2053
- Shanks A.L. and J.D. Trent (1980) Marine snow : sinking rates and potential role in vertical flux. *Deep Sea Res.*, 27, 137-143
- Sheldon R.W. and T.R. Parsons (1967) A continuous size spectrum for particulate matter in the sea. *J. Fish. Res. Board Canada*, 24, 909-915
- Sieburth J. McN. (1983) Microbiological and organic-chemical processes in the surface and mixed layers. In "Air-Sea Exchange of Gases and Particles", Ed : P.S. Liss and W.G. Slinn. D. Reidel, Dordrecht, pp 121-172
- Siegel B.Z., S.M. Siegel and F. Thorarinsson (1973a) Icelandic geothermal activity and the mercury of the Greenland icecap. *Nature*, 241, 526
- Siegel S.M., B.Z. Siegel, A.M. Eshleman and K. Bachmann (1973b) Geothermal sources and distribution of mercury in Hawaii. *Environ. Biol. Med.*, 2, 81-89
- Skinner B.J. (1976) *Earth Resources*. 2nd ed'n., Prentice Hall, New Jersey, pp 75-102
- Steele J.H. (1974) *The structure of Marine Ecosystems*. Blackwell Scientific, Oxford, pp 74-96
- Strohal P., D. Huljev, S. Lulic and M. Picer (1975) Antimony in the coastal marine environment, North Atlantic. *Estuar. Coastal Mar. Sci.*, 3, 119-123
- Sugimae A. and T. Mizoguchi (1982) Atomic emission spectrometric analysis of airborne particulate matter by direct nebulization of suspensions into the inductively-coupled plasma. *Anal. Chim. Acta*, 144, 205-212
- Szekielda K.H., S.L. Kupferman, V. Klemas and D.F. Polis (1972) Element enrichment in organic films and foam associated with aquatic frontal systems. *J. Geophys. Res.*, 77, 5278-5282
- Takahashi K. and S. Honjo (1983) Radiolarian skeletons : size, weight, sinking speed and residence time in tropical pelagic oceans. *Deep Sea Res.*, 30, 543-568
- Tammes P.M. and M.M. de Lint (1969) Leaching of arsenic from soil. *Neth. J. Agric. Sci.*, 17, 128-132
- Thompson K.C. and D.R. Thomerson (1974) Atomic-absorption studies on the determination of antimony, arsenic, bismuth, germanium, lead, selenium, tellurium and tin by utilising the generation of covalent hydrides. *Analyst*, 99, 595-601
- Treanor C.E. (1966) A method for the numerical integration of coupled first-order differential equations with greatly differing time constants. *Math. Comput.*, 20, 39-45

- Trefry J.H, and B.J. Presley (1976) Heavy metal transport from the Mississippi River to the Gulf of Mexico. In "Marine Pollutant Transfer", Ed : H.L. Windom and R.A. Duce. Lexington Books, Massachusetts, pp 39-76
- Turekian K.K. (1969) The oceans, streams and atmosphere. In "Handbook of Geochemistry", Ed : K.H. Wedepohl. Vol. 1, Springer-Verlag, Berlin, pp 297-323
- Turekian K.K. (1976) Oceans. 2nd ed'n., Prentice Hall, New Jersey, p 142
- Turner D.R., M. Whitfield and A.G. Dickson (1981) The equilibrium speciation of dissolved components in freshwater and seawater at 25°C and 1 atm pressure. *Geochim. Cosmochim. Acta*, 45, 855-881
- Vijan P.N. and G.R. Wood (1974) An automated submicrogram determination of arsenic in atmospheric particulate matter by flameless atomic absorption spectrophotometry. *At. Absorpt. Newslett.*, 13, 33-37
- Vogel A.I. (1979) Textbook of Macro and Semimicro Qualitative Inorganic Analysis. 5th ed'n., Longman, London, pp 231-236
- Vonk H.J. (1960) Digestion and metabolism. In "The Physiology of Crustacea", Vol. 1, Ed : T.H. Waterman, Academic Press, New York, pp 291-316
- Wallace G.T. and R.A. Duce (1978) Open-ocean transport of particulate trace metals by bubbles. *Deep Sea Res.*, 25, 827-835
- Walsh P.R., J.L. Fasching and R.A. Duce (1976a) Losses of arsenic during the low temperature ashing of atmospheric particulate samples. *Anal. Chem.*, 48, 1012-1014
- Walsh P.R., J.L. Fasching and R.A. Duce (1976b) Matrix effects and their control during the flameless atomic absorption determination of arsenic. *Anal. Chem.*, 48, 1014-1016
- Walsh P.R., R.A. Duce and J.L. Fasching (1979a) Tropospheric arsenic over marine and continental regions. *J. Geophys. Res.*, 84, 1710-1718
- Walsh P.R., R.A. Duce and J.L. Fasching (1979b) Considerations of the enrichment, sources and flux and arsenic in the troposphere. *J. Geophys. Res.*, 84, 1719-1726
- Waslenchuk D.G. (1978) The budget and geochemistry of arsenic in a continental shelf environment. *Mar. Chem.*, 7, 36-52
- Waslenchuk D.G. (1979) The geochemical controls on arsenic concentrations in southeastern United States rivers. *Chem. Geol.*, 24, 315-325
- Waslenchuk D.G. and H.L. Windom (1978) Factors controlling the estuarine chemistry of arsenic. *Estuar. Coastal Mar. Sci.*, 7, 455-464
- Watling H.R. and R.J. Watling (1982) Comparative effects of metals on the filtering rate of the brown mussel (*Perna perna*). *Bull. Environ. Contam. Toxicol.*, 29, 651-657
- Wauchope R.D. (1975) Fixation of arsenical herbicides, phosphate and arsenate in alluvial soils. *J. Environ. Qual.*, 4, 355-358

- Wauchope R.D. and M. Yamamoto (1980) Extraction, speciation, and analysis of arsenical herbicides in runoff : Evaluation of simple methods at the ppb level. *J. Environ. Qual.*, 9, 597-601
- Weast R.C. (Ed.) (1980) *C.R.C. Handbook of Chemistry and Physics*. 61st ed'n., C.R.C. Press, Cleveland, Ohio
- Webster-Smith B. (1967) *The World's Great Copper Mines*. Hutchinson, London, 118 pp
- Weiss H., K. Bertine, M. Koide and E.D. Goldberg (1975) The chemical composition of a Greenland glacier. *Geochim. Cosmochim. Acta*, 39, 1-10
- Weiss H.V., M.M. Herron and C.C. Langway (1978) Natural enrichment of elements in snow. *Nature*, 274, 352-353
- Weiss H.V., M. Koide and E.D. Goldberg (1971) Mercury in a Greenland ice sheet : evidence of recent input by man. *Science*, 174, 692-694
- Welz B. and M. Melcher (1981) Mutual interactions of elements in the hydride technique in atomic absorption spectrometry. Part 1 : Influence of selenium on arsenic determination. *Anal. Chim. Acta*, 131, 17-25
- Whitfield M. (1979) The mean oceanic residence time (MORT) concept - a rationalisation. *Mar. Chem.*, 8, 101-123
- Whitfield M. and D.R. Turner (1979) Water-rock partition coefficients and the composition of seawater and riverwater. *Nature*, 278, 132-137
- Wiebe P.H., S.H. Boyd and C. Winget (1976) Particulate matter sinking to the deep sea floor at 2000 m in the Tongue of the Ocean, Bahamas, with a description of a new sediment trap. *J. Mar. Res.*, 34, 341-354
- Windom H.L. and F.E. Taylor (1979) The flux of mercury in the South Atlantic Bight. *Deep Sea Res.*, 26, 283-292
- Wishner K.F. (1980) The biomass of the deep-sea benthopelagic plankton. *Deep Sea Res.*, 27, 203-216
- Wood J.M. (1974) Biological cycles for toxic elements in the environment. *Science*, 183, 1049-1052
- Wood J.M., F.S. Kennedy and C.G. Rosen (1968) Synthesis of methylmercury compounds by extracts of a methanogenic bacterium. *Nature*, 220, 173-174
- Woodcock A.H. (1953) Salt nuclei in marine air as a function of altitude and wind force. *J. Meteor.*, 10, 362-371
- Woolson E.A. (1975) Bioaccumulation of arsenicals. In "Arsenical Pesticides", Ed : E.A. Woolson. ACS Symposium series 7, Washington DC, pp 97-107
- Woolson E.A., J.H. Axley and P.C. Kearney (1973) The chemistry and phytotoxicity of arsenic in soils : II Effects of time and phosphorus. *Soil Sci. Soc. Amer. Proc.*, 37, 254-259

- Wrench J.J. and R.F. Addison (1981) Reduction, methylation, and incorporation of arsenic into lipids by the marine phytoplankton Dunaliella tertiolecta. Can. J. Fish. Aquat. Sci., 38, 518-523
- Yamauchi H. and Y. Yamamura (1983) Concentration and chemical species of arsenic in human tissue. Bull. Environ. Contam. Toxicol., 31, 267-270
- Zoller W.H., E.S. Gladney and R.A. Duce (1974) Atmospheric concentrations and sources of trace metals at the South Pole. Science, 183, 198-200

APPENDICES

APPENDIX I

Integration Mathematics

When using the unmodified Runge-Kutta formula, terms higher than the 4th order in the Taylor's expansion are ignored. If these terms are significant, then spurious oscillations may occur. The Treanor (1966) modification allows for a closer approximation to the higher order terms. If the rate equation is expressed as a function of time (k) and reservoir mass (A), then :

$$\frac{dA}{dt} = f(t,A) \quad (A.1)$$

A(t) is expanded as a 4th order Taylor's series to be evaluated as a 4th order Runge-Kutta. Using an integration step of h, the four terms for t and A become :

$$\left. \begin{aligned} t_1 & ; A_1 \\ t_2 & = t_1 + \frac{h}{2} ; A_2 = A_1 + \frac{h}{2} f_1 \\ t_3 & = t_1 + \frac{h}{2} ; A_3 = A_1 + \frac{h}{2} f_2 \\ t_4 & = t_1 + h ; A_4 = A_1 + hf_3 \end{aligned} \right\} (A.2)$$

Where A is a function of t, i.e. $A_i = A(t_i)$, and f is a function of a and t, i.e. $f_i = f(t_i, A_i)$, the function being the first order rate equations operating on reservoir A.

The Runge-Kutta solution for the change in A over time interval h is then :

$$(\Delta A)_{RK} = \frac{h}{6} (f_1 + 2f_2 + 2f_3 + f_4) \quad (A.3)$$

This fails for large high order derivations because h must be kept very small, and A may then become oscillatory.

$$\frac{dA}{dt} = -P(A - \bar{A}) \quad (A.4)$$

where P is a large number, not yet determined, and \bar{A} is the equilibrium value of A. In this case, h must be restricted, so that Ph is less than unity. However, one may express \bar{A} as a power series in t, then integrate directly. Equation A.1 may be approximated by :

$$\begin{aligned} \frac{dA}{dt} = f(t,A) = & -P(A-A_1) + a + b(t - t_1) \\ & + \frac{c}{2} (t - t_1)^2 \end{aligned} \quad (A.5)$$

over the interval from t_1, A_1 to $t_1 + h, A_1 + \Delta A$. Equation A.5 may then be integrated to yield a value for ΔA of :

$$\Delta A = h \{ aF_1 + bhF_2 + ch^2F_3 \} \quad (A.6)$$

where the functions F_n are exponential functions of Ph :

$$\begin{aligned} F_0 &= e^{-Ph} ; \\ F_n &= \frac{F_{(n-1)} - \frac{1}{(n-1)!}}{(-Ph)} \\ &= \sum_{k=0}^{\infty} \frac{(-Ph)^k}{(n+k)!} \end{aligned} \quad (A.7)$$

The constants a,b,c and P can be evaluated by taking four points

(t_i, A_i) in the integration interval and solving equation A.5 for the unknowns. The chosen points are : (t_i, A_i) (the start of the interval), and three others as defined in equations A.2. Then :-

$$\left. \begin{aligned}
 P &= -\left(\frac{f_3 - f_2}{A_3 - A_2}\right) ; \\
 a &= f_1 ; \\
 bh &= [-3(f_1 + PA_1) + 2(f_2 + PA_2) \\
 &\quad + 2(f_3 + PA_3) - (f_4 + PA_4)] ; \\
 ch^2 &= 4 [(f_1 + PA_1) - (f_2 + PA_2) - (f_3 + PA_3) \\
 &\quad + (f_4 + PA_4)]
 \end{aligned} \right\} \text{(A.8)}$$

where $f_i = f(t_i, A_i)$

Equations A.6, A.7 and A.8 combine to form the Treanor integration formula :

$$\begin{aligned}
 A &= h \{ f_1 F_1 + [-3(f_1 + PA_1) + 2(f_2 + PA_2) + 2(f_3 + PA_3) \\
 &\quad - (f_4 + PA_4)] F_2 + 4 [(f_1 + PA_1) - (f_2 + PA_2) - (f_3 + PA_3) \\
 &\quad + (f_4 + PA_4)] F_3 \} \quad \text{(A.9)}
 \end{aligned}$$

Where P is as defined in equation A.8.

Where P tends to zero, equation A.9 reverts to the Runge-Kutta formula. For cases where Ph is very large, the Runge-Kutta formula for A_4 , in equations A.2, may prove to be imprecise. As P is determined from the second and third points in the interval, Ph may be evaluated before A_4 is considered. If Ph is large, a better approximation to A_4 may be obtained by omitting the quadratic term, and integrating equation A.5 :

$$A_4 = A_1 + h \{ 2f_3F_2 + f_1(F_1 - 2F_2) + f_2(Ph)F_2 \} \quad (A.10)$$

Equation A.10 then replaces the last of equations A.2.

In the evaluation of P to solve equation A.9, the difference between two values of f_1 is used. If both values of f_1 are large, and the difference is small, then many significant figures of P may be lost, and P may even be evaluated as negative. In such cases, P is set to zero, and the Runge-Kutta formula is used.

Adapted from Treanor C.E. (1966) Maths of Computation, 20, 39-45.

APPENDIX II

The Computer Programme

The mathematics from Appendix I has been incorporated into a computer programme written in FORTRAN 77. The integration method forms the main body of the programme, with two subroutines to determine the flux rates, and the pollutant rate constants. In addition to numerical output, solutions were output in graphical form. The graphics section of the programme has been omitted from the listing, as the HCBS library subroutines used to create the output might not be available on other machines. Only the code that will run on a machine equipped with a standard FORTRAN 77 compiler has been included.

PROGRAM GEOCYC

C GLOBAL GEOCHEMICAL CYCLES OF AS AND SB
 C PERTURBATION OF PRE-MAN STEADY STATE IS MODELLED BY INTRODUCING
 C POLLUTANT FLUXES TO GEOCHEMICAL CYCLES. THE RATE-CONSTANTS MAY BE
 C INCREASED TO SIMULATE GROWTH. HIGH TEMPERATURE POLLUTANT FLUXES
 C ARE MODELLED USING ECONOMIC GROWTH PRINCIPLES. LOW TEMPERATURE
 C POLLUTANT FLUXES ARE MODELLED USING LINEAR GROWTH, TO AVOID
 C EXCESSIVELY LARGE USAGE OF C. P. U. TIME. THE TIME-BASED
 C INTEGRATION USES A RUNGE-KUTTA FORMULA, OR TREANOR'S ADAPTATION TO
 C AVOID ARTEFACTUAL OSCILLATIONS.
 C SEE TREANOR (1966) MATHS OF COMPUTATION, VOL 20, PP 39-45.

C
 CHARACTER*8 TITLE(5), FLXTIT(5, 30), RESTIT(10)*4
 INTEGER COUNT
 DOUBLE PRECISION HMAX, HMIN, HINIT, TWRITE, TIMEO, TIME1, TIME2, TEND, H,
 *RATEK(30), A(10), A1(10), A2(10), A3(10), A4(10), DUMMY(10),
 *F1(10), F2(10), F3(10), F4(10), FF0, FF1, FF2, FF3, P, PH, B, C, DELTAA,
 *DELTAT, SEDALT, HNEGAT, MAGALT
 COMMON/RATES/RATEK, NRES, NRATE

C
 C INPUT NO. OF RESERVOIRS (NRES), NO. OF FLUXES (NRATE).

C
 READ(5, 10) NRES, NRATE
 10 FORMAT(2I2)

C
 C INPUT MAX. MIN. AND INITIAL INCREMENTS (HMAX, HMIN, HINIT), ELAPSE
 C TIME TO NEW DATA OUTPUT (TWRITE), AND START AND END TIMES (TIMEO, TEND)

C
 READ(5, 20) HMAX, HMIN, HINIT, TWRITE, TIMEO, TEND
 20 FORMAT(6D12. 5)

C
 C INPUT MODEL TITLE (TITLE), RESERVOIR TITLES (RESTIT), RESERVOIR
 C MASSES (A), FLUX TITLES (FLXTIT) AND RATE CONSTANTS (RATEK).
 C POLLUTANT RATE CONSTANTS ARE NOT INPUT, BUT CALCULATED AS A
 C FUNCTION OF TIME.

C
 READ(5, 30) (TITLE(J), J=1, 5)
 30 FORMAT(5A8)
 READ(5, 40) (RESTIT(J), A(J), J=1, NRES)
 40 FORMAT(A4, 6X, D12. 5)
 READ(5, 50) ((FLXTIT(I, J), I=1, 5), RATEK(J), J=1, (NRATE-4))
 50 FORMAT(5A8, D12. 5)

C
 C OUTPUT TITLE, FLUXES AND RATE-CONSTANTS

C
 WRITE(6, 70) (TITLE(J), J=1, 5)
 70 FORMAT(1H , 23X, 15('*'), 5A8, 2X, 15('*'))
 WRITE(6, 80)
 80 FORMAT(15X, 28('*'), ' MECHANISM AND RATE-CONSTANTS ', 28('*'), /15X,
 '**', 84X, '*')
 WRITE(6, 90) ((FLXTIT(I, J), I=1, 5), RATEK(J), J=1, (NRATE-4))
 WRITE(6, 91)
 91 FORMAT(15X, '*', 1X, 'PLUS FOUR POLLUTANT FLUXES, CALCULATED AS A FUNC
 TION OF TIME', 24X, '')
 90 FORMAT(15X, '*', 1X, 5A8, 30X, D12. 5, 1X, '*')
 WRITE(6, 100)
 100 FORMAT(15X, 86('*'), //)
 WRITE(6, 110) HINIT, HMAX, HMIN, TWRITE, TEND

```

110 FORMAT('INITIAL INCREMENT',D13.5/'MAX INCREMENT',D13.5/
  *'MIN INCREMENT',D13.5/'TIME BETWEEN DATA POINTS',D13.5/'DURATION O
  *F MODEL',D13.5)
  WRITE(6,115)A(NRES-2),A(NRES-1)
115 FORMAT('INITIAL SEDIMENT',2X,D12.5/'INITIAL MAGMA',2X,D12.5)
C
C CALCULATE AND OUTPUT INITIAL FLUX RATES. THESE ARE CALCULATED FROM
C THE INSTANTANEOUS RATE CONSTANT AND SOURCE RESERVOIR MASS.
C POLLUTANT RATE CONSTANTS MUST FIRST BE DETERMINED IN
C SUBROUTINE SETPOL, THEN THE FLUX RATES ARE DETERMINED IN
C SUBROUTINE SETRAT. IF THE FINAL VARIABLE ON THE CALL TO SETRAT
C IS -1, THEN THE FLUX RATES ARE OUTPUT.
C
  CALL SETPOL(TIME0,A(NRES),H)
  CALL SETRAT(A,DUMMY,-1)
C
C OUTPUT COLUMN HEADINGS FOR RESERVOIR MASSES TO ALLOW FOR 8-10
C RESERVOIRS. SEDIMENT AND MAGMA RESERVOIRS ARE SO LARGE THAT ONLY
C THE CHANGE IN THEIR MASS IS OUTPUT. THUS, SEDDIF AND MAGDIF, THE
C ORIGINAL SEDIMENT AND MAGMA MASSES, ARE SUBTRACTED FROM THE
C INSTANTANEOUS MASSES TO GIVE THE OUTPUT VARIABLES SEDALT AND
C MAGALT.
C
  SEDDIF=REAL(A(NRES-2))
  MAGDIF=REAL(A(NRES-1))
  SEDALT=A(NRES-2)-SEDDIF
  MAGALT=A(NRES-1)-MAGDIF
  WRITE(6,120)
120 FORMAT(/15X,85('*'))
  IF (NRES.EQ.8) THEN
    WRITE(6,130) (RESTIT(J),J=1,(NRES-3))
130   FORMAT(/5X,5(A4,10X),'DELTA-SEDI',1X,'DELTA-MAGMA'/)
    ELSE IF (NRES.EQ.9) THEN
    WRITE(6,140) (RESTIT(J),J=1,(NRES-3))
140   FORMAT(/5X,6(A4,10X),'DELTA-SEDI',1X,'DELTA-MAGMA'/)
    ELSE IF (NRES.EQ.10) THEN
    WRITE(6,150) (RESTIT(J),J=1,(NRES-3))
150   FORMAT(/5X,7(A4,10X),'DELTA-SEDI',1X,'DELTA-MAGMA'/)
  END IF
C
C OUTPUT START TIME AND INITIAL RESERVOIR MASSES. SET
C POLLUTION RATE-CONSTANTS FOR GROWTH CALCULATIONS.
C
  WRITE(6,160) TIME0,A(NRES),(A(J),J=1,(NRES-3)),SEDDIF,MAGDIF
160 FORMAT('TIME =',D12.5,2X,'POLLUTANT RESERVES =',D12.5/9(2X,D12.5))
C
C SET INITIAL MODEL CONDITIONS THEN START INTEGRATION. THE INTEGRATION
C LOOP IS INITIALISED AT LINE 190. COUNT IS THE COUNTER FOR THE
C NUMBER OF PASSES THROUGH THE INTEGRATION LOOP, IF IT EXCEEDS 8
C THEN THE CURRENT INTEGRATION STEP, H, IS INCREASED.
C
  COUNT=0
  TIME1=TIME0
  TIME2=TIME0
  H=HINIT
170 DO 180 J=1,NRES
180  A1(J)=A(J)
190  CONTINUE

```

```

C
C INITIAL CONDITIONS NOW SET. CHANGE POLLUTANT RATE CONSTANTS USING
C SUBROUTINE SETPOL, AND DETERMINE OVERALL RATE OF CHANGE OF RESERVOIR
C MASS USING SUBROUTINE SETRAT.
C
      CALL SETPOL(TIME2,A(NRES),H)
      CALL SETRAT(A1,F1,0)
C
C SET A2 AND A3 ACCORDING TO EQUATIONS A. 2, AND DETERMINE
C APPROPRIATE RATES USING SETRAT. EQUATION NUMBERS IN TEXT
C REFER TO EQUATIONS FROM APPENDIX I.
C
      DO 200 J=1,NRES
200  A2(J)=A1(J)+H*F1(J)/2.00D+00
      CALL SETRAT(A2,F2,0)
      DO 210 J=1,NRES
210  A3(J)=A1(J)+H*F2(J)/2.00D+00
      CALL SETRAT(A3,F3,0)
C
C SET A4 BY RUNGE-KUTTA FOR PH<0.3, OR BY TREANOR FOR PH>0.3. PH DERIVED
C FROM EQUATIONS A. 9 (CALCULATION OF P) AND A. 2. IF P<0.0, SET P=0 AND
C USE RUNGE-KUTTA. IF PH>75 OR A4 VERY SMALL HALVE H AND RESET EQNS.
C
      DO 240 J=1,NRES
      IF (A3(J).EQ.A2(J)) GOTO 220
      IF (F2(J).EQ.F1(J)) GOTO 220
      P=(F2(J)-F3(J))/(A3(J)-A2(J))
      PH=2.00D+00*(F2(J)-F3(J))/(F2(J)-F1(J))
      IF (P.LT.0.0D+00) GOTO 220
      IF (PH.LT.0.3D+00) GOTO 220
      IF (PH.GE.0.75D+02) GOTO 330
      GOTO 230
C
C CALCULATE A4 BY RUNGE-KUTTA USING EQUATIONS A. 2.
C
220  A4(J)=A1(J)+H*F3(J)
      GOTO 240
C
C CALCULATE A4 BY EQUATIONS A. 8 AND A. 10. FF IS AN EXPONENTIAL
C FUNCTION OF PH.
C
230  FF0=DEXP(-PH)
      FF1=(FF0-1.00D+00)/(-PH)
      FF2=(FF1-1.00D+00)/(-PH)
      FF3=(FF2-0.50D+00)/(-PH)
      A4(J)=A1(J)+H*(2.00D+00*FF2*(F3(J)-F1(J))+F1(J)*FF1+PH*F2(J)*FF2)
240  CONTINUE
C
C IF INTEGRATION STEP IS TOO LARGE, REDUCE IT.
C
      DO 250 J=1,(NRES-1)
250  IF (A4(J).LT.-1.0D-40) GOTO 330
C
C DETERMINE RATE FUNCTIONS, THEN THE CHANGE IN RESERVOIR MASSES BY
C THE TREANOR METHOD OR RUNGE-KUTTA AS APPROPRIATE. IF A3=A2 OR
C F2=F1 THEN THE TREANOR SOLUTION IS INCALCULABLE, AND THE RUNGE-
C KUTTA SOLUTION IS USED, WHICH ALSO APPLIES IF P IS NEGATIVE OR
C PH IS VERY SMALL.

```

```

C
CALL SETRAT(A4,F4,0)
DO 280 J=1,NRES
IF (A3(J).EQ.A2(J)) GOTO 260
IF (F2(J).EQ.F1(J)) GOTO 260
P=(F2(J)-F3(J))/(A3(J)-A2(J))
PH=2.00D+00*(F2(J)-F3(J))/(F2(J)-F1(J))
IF (P.LT.0.0D+00) GOTO 260
IF (PH.LT.0.3D+00) GOTO 260

C
C CALCULATE DELTAA BY TREANOR USING EQUATION A.9. DELTAA IS THE CHANGE
C RESERVOIR MASS OVER THE INTEGRATION STEP, H.
C
      B=(-3.00D+00)*(F1(J)+P*A1(J))+2.00D+00*((F2(J)+P*A2(J))+(F3(J)+P*A
      *3(J)))-(F4(J)+P*A4(J))
      C=(F1(J)+P*A1(J))-(F2(J)+P*A2(J))-(F3(J)+P*A3(J))+(F4(J)+P*A4(J))
      DELTAA=H*(F1(J)*FF1+B*FF2+4.00D+00*C*FF3)
      GOTO 270

C
C CALCULATE DELTAA USING RUNGE-KUTTA USING EQUATION A.3
C
260 DELTAA=H*(F1(J)+2.00D+00*(F2(J)+F3(J))+F4(J))/6.00D+00
C
C INCREASE A BY DELTAA. IF NEGATIVE, THEN A=0. THIS ONLY APPLIES TO THE
C POLLUTANT RESERVOIRS.
C
270 A1(J)=A1(J)+DELTAA
280 CONTINUE

C
C IF THE RESERVOIR MASSES ARE TOO SMALL, REDUCE THE INTEGRATION
C STEP, AND TRY AGAIN.
C
      DO 285 J=1,(NRES-1)
285 IF (A1(J).LT.-1.0D-40) GOTO 330

C
C INCREMENT A BY DELTAA, AND CHECK TEND HAS NOT BEEN EXCEEDED.
C
      DO 290 J=1,NRES
      A(J)=A1(J)
290 IF (A(J).LT.0.0) A(J)=0.0
      TIME2=TIME2+H
      IF (TIME2.GT.TEND) GOTO 310

C
C IF COUNT EXCEEDS 8, DOUBLE H TO ALLOW FOR RAPID STABLE INTEGRATION,
C BUT NOT EXCEEDING HMAX.
C
      COUNT=COUNT+1
      IF (COUNT.LT.8) GOTO 300
      H=2.00D+00*H
      COUNT=0
      IF (H.LT.HMAX) GOTO 300
      H=HMAX

C
C IF THE OUTPUT TIME HAS BEEN EXCEEDED, OUTPUT NEW DATA,
C OTHERWISE GO BACK THROUGH INTEGRATION LOOP.
C
300 DELTAT=TIME2-TIME1
      IF (DELTAT.LT.TWRITE) GOTO 190

```

```

    TIME1=TIME2
310 CONTINUE
    SEDALT=A(NRES-2)-SEDDIF
    MAGALT=A(NRES-1)-MAGDIF
    WRITE(6,320) TIME2,H,A(NRES),(A(J),J=1,(NRES-3)),SEDALT,MAGALT
320 FORMAT(/,'TIME=',D12.5,2X,'STEP-SIZE=',D12.5,2X,'POLLUTANT-RESERVE
    *S=',D12.5/9(2X,D12.5))
    IF (TIME2.LE.TEND) GOTO 190
    GOTO 350
C
C IF PH>75 HALVE H AND REDUCE POLLUTANT RATE CONSTANTS. IF H<HMIN
C ABANDON RUN.
C
330 HNEGAT=-H
    H=H/2.00D+00
    COUNT=0
    TIME2=TIME2+HNEGAT
    IF (H.GT.HMIN) GOTO 170
    WRITE(6,340) H,PH
340 FORMAT('STEP-SIZE IS TOO SMALL',5X,'H=',D12.5,'PH=',D12.5)
    GOTO 380
C
C CLOSE OUTPUT COLUMNS
C
350 IF (NRES.EQ.8) WRITE(6,130) (RESTIT(J),J=1,(NRES-3))
    IF (NRES.EQ.9) WRITE(6,140) (RESTIT(J),J=1,(NRES-3))
    IF (NRES.EQ.10) WRITE(6,150) (RESTIT(J),J=1,(NRES-3))
380 CONTINUE
    STOP
    END

```

SUBROUTINE SETRAT(A,F,NUM)
 C THIS DETERMINES THE OVERALL INFLUX OR OUTFLOW RATE, DA/DT, FOR EACH
 C RESERVOIR. FIRST THE FLUX RATES ARE CALCULATED, THEN THE OVERALL
 C RATES FOR EACH RESERVOIR. THIS EXAMPLE IS FOR AN 8-BOX
 C MODEL WITH 21 FLUXES.
 C

```

    DOUBLE PRECISION A(10),F(10),RATE(30),RATEK(30)
    COMMON/RATES/RATEK,NRES,NRATE
    DO 390 J=1,NRES
390 IF (A(J).LT.0.1D-01) A(J)=0.0D+00
    RATE(1)=RATEK(1)*A(1)
    RATE(2)=RATEK(2)*A(1)
    RATE(3)=RATEK(3)*A(1)
    RATE(4)=RATEK(4)*A(2)
    RATE(5)=RATEK(5)*A(2)
    RATE(6)=RATEK(6)*A(2)
    RATE(7)=RATEK(7)*A(3)
    RATE(8)=RATEK(8)*A(3)
    RATE(9)=RATEK(9)*A(4)
    RATE(10)=RATEK(10)*A(4)
    RATE(11)=RATEK(11)*A(4)
    RATE(12)=RATEK(12)*A(5)
    RATE(13)=RATEK(13)*A(5)
    RATE(14)=RATEK(14)*A(5)
    RATE(15)=RATEK(15)*A(6)
    RATE(16)=RATEK(16)*A(5)
    RATE(17)=RATEK(17)*A(7)
    RATE(18)=RATEK(18)*A(8)
    RATE(19)=RATEK(19)*A(8)
    RATE(20)=RATEK(20)*A(8)
    RATE(21)=RATEK(21)*A(8)
  
```

C
 C IF NUM = -1, OUTPUT INITIAL FLUX RATES THEN RETURN.
 C

```

    IF (NUM.EQ.-1) THEN
      WRITE(6,400) (RATE(J),J=1,NRATE)
400  FORMAT(/25X,'INITIAL FLUX RATES',6(/1X,5D15.5))
      RETURN
    END IF
  
```

C
 C SET OVERALL RATE OF CHANGE OF RESERVOIR MASSES (F1-F8).
 C

```

    F(1)=RATE(4)+RATE(12)+RATE(17)+RATE(18)-RATE(1)-RATE(2)-RATE(3)
    F(2)=RATE(1)+RATE(7)+RATE(9)+RATE(13)+RATE(19)-RATE(4)-RATE(5)
    *-RATE(6)
    F(3)=RATE(5)+RATE(10)-RATE(7)-RATE(8)
    F(4)=RATE(2)+RATE(6)+RATE(8)+RATE(14)+RATE(20)-RATE(9)-RATE(10)
    *-RATE(11)
    F(5)=RATE(3)+RATE(15)+RATE(21)-RATE(12)-RATE(13)-RATE(14)
    F(6)=RATE(11)-RATE(15)-RATE(16)
    F(7)=RATE(16)-RATE(17)
    F(8)=-RATE(18)-RATE(19)-RATE(20)-RATE(21)
    RETURN
    END
  
```

```

SUBROUTINE SETPOL(T,A,H)
C THIS SETS THE POLLUTION RATE CONSTANTS AS A FUNCTION OF THE DATE.
C FOR HIGH TEMPERATURE POLLUTANT FLUXES, THE INITIAL GROWTH RATE
C IS 3.6% (MATURE STAGE), WHICH DROPS TO A GERONTIC GROWTH RATE
C OF 5% IN 1982 AD, AND FINALLY TO A DECLINE RATE OF 5% IN 2008 AD,
C AS EACH THIRD OF THE POLLUTANT RESERVES ARE EXHAUSTED.
C

```

```

DOUBLE PRECISION T,RATEK(30),A,H
COMMON/RATES/RATEK,NRES,NRATE
IF (A.GT.0.0) THEN
  IF (T.GE.2008.0) THEN
    RATEK(NRATE-3)=DEXP(-(0.005)*T+3.54)
    RATEK(NRATE-2)=DEXP(-(0.005)*T-1.23)
    RATEK(NRATE-1)=DEXP(-(0.005)*T-1.23)
    RATEK(NRATE)=DEXP(-(0.005)*T+5.67)
  ELSE IF (T.GE.1982.0) THEN
    RATEK(NRATE-3)=DEXP(0.005*T-16.54)
    RATEK(NRATE-2)=DEXP(0.005*T-21.31)
    RATEK(NRATE-1)=DEXP(0.005*T-21.31)
    RATEK(NRATE)=DEXP(0.005*T-14.41)
  ELSE
    RATEK(NRATE-3)=DEXP(0.036*T-77.98)
    RATEK(NRATE-2)=DEXP(0.036*T-82.75)
    RATEK(NRATE-1)=DEXP(0.036*T-82.75)
    RATEK(NRATE)=DEXP(0.036*T-75.85)
  ENDIF
ELSE
  RATEK(NRATE-3)=0.0
  RATEK(NRATE-2)=0.0
  RATEK(NRATE-1)=0.0
  RATEK(NRATE)=0.0
ENDIF

```

```

C
C SET THE LOW TEMPERATURE PERTURBATION AS A LINEAR INCREASE OF
C THE LAND EFFLUX RATE. INCREASE AT A RATE OF 1.6D-07/YR/YR,
C STARTING IN 1750 AD, THE INDUSTRIAL REVOLUTION.
C

```

```

IF(T.GE.1750.0) RATEK(12)=RATEK(12)+H*1.6D-07
RETURN
END

```


To my parents for believing I would
finish the task.

The sky is darkening like a stain:
Something is going to fall like rain
And it won't be flowers.

W.H. Auden (1932) *The Witnesses*.

Attention is drawn to the fact that the copyright of this thesis rests with the author, and that no quotation from the thesis and no information derived from it may be published without the prior written consent of the author.

This thesis may be made available for consultation within the Plymouth Polytechnic Library and may be photocopied or lent to other libraries for the purposes of consultation.

Signed *L.S. Austen*

DECLARATIONS

At no time during the registration for the degree of Doctor of Philosophy has the author been registered for any other C.N.A.A. or University award. None of the material herein has been used in any other submission for an academic award. This study was financed with the aid of a Devon Education Authority Research Assistantship, and carried out in collaboration with the School of Environmental Sciences, University of East Anglia, Norwich.

A programme of advanced study was undertaken, which included an advanced course in scanning electron microscopy and development of techniques in analytical chemistry and programming in FORTRAN 77. Duties at Plymouth Polytechnic have also included teaching and examination of undergraduate courses in Chemistry and Oceanography.

External visits and conferences attended :

- April 1981 : Marine Chemistry Discussion Group meeting held at IMER, Plymouth
- April 1982 : Estuarine and Brackish Waters Sciences Association meeting, "The Tamar", held at IMER, Plymouth
- July 1982 : NATO Advanced Study Institute : Air-sea Exchange of Gases and Particles. Held at University of New Hampshire, Durham, USA. Poster presented entitled : "Geochemical Cycling of Arsenic". Holder of NATO travel award to attend the meeting.
- August 1983: CACGP Symposium on Troposphere Chemistry held at Christ Church College, Oxford University. Poster presented, entitled : "Temporal Variations in the tropospheric arsenic burden". L.S. Austin and G.E. Millward.
- April 1984 : Marine Chemistry Discussion Group meeting on Continental Shelf Chemistry held at University College, Swansea. Paper presented, entitled : "Deposition of As and Sb into coastal waters". L.S. Austin and G.E. Millward.
- July 1984 : Workshop on Research in Atmospheric Chemistry. Organised by the Coordinating Committee for Research in Atmospheric Chemistry and NERC, held at Department of Physical Chemistry, Oxford University.

Also meetings held with Dr. P.S. Liss of University of East Anglia, at Durham, USA, Oxford, and at UEA in Norwich.

Publications:

Austin L.S. and G.E. Millward. Modelling temporal variations in the tropospheric arsenic burden. Atmospheric Environment, In press.